University of Bath

UNIVERSITY OF BATH

PHD

Distribution and function of nematode glutamate-gated chloride channels

Portillo, Maria Virginia

Award date:
2003

Awarding institution:
University of Bath

Link to publication

Distribution and Function of Nematode Glutamate-Gated Chloride Channels

Submitted by

Maria Virginia Portillo

for the degree of PhD of the University of Bath

2003

UMI Number: U174779

Dissertation Publishing

ProQuest LLC
789 East Eisenhower Parkway
P.O. Box 1346
Ann Arbor, MI 48106-1346

Summary

Glutamate-gated chloride channels (GluCl) are related to GABA$_A$ receptors and are the target sites for the avermectin/milbemycin (AM) anthelmintics, drugs that cause paralysis of the somatic and pharyngeal muscles in nematodes. Four GluCl subunits: HcGluClα, HcGluClβ, HcGluClα3A & HcGluClα3B, have been previously identified from the sheep parasite *Haemonchus contortus*. In the present work, specific antisera were raised against all of these subunits and used in immunofluorescence experiments, to study their distribution on adult parasites. All of the subunits were expressed in the motor nervous system, especially motor neuron commissures. Double immunostaining experiments suggested that HcGluClα and HcGluClβ were expressed on the same commissures: these were also stained with an anti-GABA antibody, suggesting that they may correspond to inhibitory motor neurons. The HcGluClβ subunit was also detected in lateral and sub-lateral nerve cords. The HcGluClα3A & -B subunits, products of an alternatively spliced gene, were expressed in different neurons. In addition to the motor neuron commissures, the HcGluClαA was found in a pair of sensory, possibly amphid, neurons in the head. HcGluClα3B was detected in three cell bodies, probably of pharyngeal neurons, and in ventral and lateral cords. These results indicate that the GluCl are widely distributed in the *H. contortus* nervous system and suggest that they have critical roles controlling locomotion, pharyngeal function and possibly sensory processing in parasitic nematodes. These data were supported by behavioural studies carried out in the free-living nematode *Caenorhabditis elegans*. Ultimately, the present work provides an explanation for the observed effects of the AM anthelmintics, supporting the hypothesis that these receptors are the main drug targets in nematodes.

Acknowledgements

People love

to wonder,

and that...

is the

seed of

science

(anonymous)

To my parents

and

Federico

Publications and Communications resulting from this work

In refereed journals:

Portillo, V., Jagannathan, S. and Wolstenholme, A.J.

The distribution of glutamate-gated chloride channel subunits in the parasitic nematode, *Haemonchus contortus*.

The Journal of Comparative Neurology (in press).

Yates, D.M; Portillo, V. and Wolstenholme, A.J. **The avermectin receptors of *Haemonchus contortus* and *Caenorhabditis elegans*.**

Submitted to International Journal for Parasitology.

Communications:

Aptel, N., Portillo, V., Cook, A., Souter, P., Lambert, K., Holden-Dye, L., Wolstenholme, A.J. (2002). **The roles of the glutamate-gated chloride channels subunits in *C. elegans* behaviour.** European Journal of Neuroscience 14, 228.2.

Portillo, V., Harder, A. and Wolstenholme A.J. (2001) **Subunit composition of the avermectin receptor from the parasitic nematode *Haemonchus contortus*.** Society for Neuroscience, 27: 307.3. San Diego, California.

Cook A., Rakhra S., Aptel N., Pemberton D., Portillo V., Rogers C., Wolstenholme A.J. and Holden-Dye L. (2001). **Glutamate-gated chloride channels in the pharyngeal nervous system of *C. elegans*.** Society for Neuroscience, 27: 307.4. San Diego, California.

Aptel N., Cook A., Pemberton D., Portillo V., Rogers C., Holden-Dye L. and Wolstenholme A.J. (2001). **The physiological roles of AVR-14 in *C. elegans* and the parasite *H. contortus*.** 13th International *C. elegans* Meeting, University of California, Los Angeles.

Portillo V., Samson-Himmelstjerna G. and Wolstenholme A.J. (2001). **Immunolocalization of avermectin receptor subunits in *Haemonchus contortus*.** Keystone Symposia: Molecular Helminthology, Taos, New Mexico.

6

Portillo V., Jagannathan S., von Samson-Himmelstjerna G. and Wolstenholme A.J. (2000). **Expression pattern of avermectin receptor subunits in *Haemonchus contortus*.** New challenges in tropical medicine and Parasitology, Oxford.

TABLE OF CONTENTS

Abbreviations

Ab	antibody
AMs	avermectins/milbemycins
APS	ammonium persulphate
AVMs	avermectins
avr	avermectin resistance
bp	base pairs
BSA	bovine serum albumin
CI	chemotaxis index
cDNA	complementary deoxiribonucleic acid
ddH$_2$O	double distilled water
DMEM	Dulbecco's Modified Essential Medium
DMSO	dimethylsulfoxide
DNA	deoxyribonucleic acid
dNTP	deoxy ribonucleoside tri-phosphate
dsRNA	double-stranded RNA
DTT	dithiothreitol
DYT	Double Yeast Tryptone
EC$_{50}$	concentration of drug which gives half-maximal response (E: effective, C: concentration)
EDTA	ethylene diamine tetra acetate
ELISA	enzyme-linked immunosorbent assay
FITC	fluorescein iso thio cyanate
5-HT	5-hydroxy triptophan (serotonin)
GABA	γ-aminobutyric acid
GFP	green fluorescent protein
GluCl	glutamate-gated chloride channel
glr	glutamate receptor family
GST	glutathione S- transferase
IC$_{50}$	value that reduces functional response to half-maximum
IPTG	iso-propyl-β-D-thiogalactopyranoside
IVM	ivermectin
kDa	kilo Daltons
LB	Luria Bertani
mRNA	messenger ribonucleic acid

14

NGM	nematode growth medium
O.D.	optical density
PAGE	polyacrylamide gel electrophoresis
PBS	phosphate buffered saline
PCR	Polymerase Chain Reaction
Poly-E	Polyethylenimine
RNA	ribonucleic acid
RNAi	ribonucleic acid interference
RNase	ribonuclease
RT	room temperature
SDS	sodium dodecyl sulphate
SEM	standard error of the mean
Sulfo-MBS	m-Maleimidobenzoyl-N-hydroxysulfosuccinimidine ester
Sulfo-SMCC	Sulfosuccinimidyl-4-(N-maleimidomethyl) cyclohexane-1-carboxylate
TAE	tris acetate EDTA
TBE	tris borate EDTA
TBS	tris buffered saline
TBST	tris buffered saline tween
TEMED	N, N, N', N',-tetramethylene diamine
Tm	annealing temperature
TM	transmembrane domains
TMB	3, 3', 5, 5' tetramethyl benzidine
TRITC	tetramethylrhodamine isothiocyanate
UV	ultraviolet
unc	uncoordinated

CHAPTER 1

<u>GENERAL INTRODUCTION</u>

1.1 Nematodes

Members of the phylum Nematoda ('round worms') are numerous and diverse; of every five animals on the planet, four are nematodes (Platt, 1994). The vast majority are free-living microbivores, but many species include parasites of plants and animals mostly from terrestrial habitats (Smyth, 1994). The apparently basic anatomy of nematodes masks a complex pattern of diversity and estimates of species number within the phylum range from 40 000 to 100 million (Dorris et al., 1999). Nematodes, despite their diverse habitats and life-styles are consistent in their morphology and anatomy, which distinguish them easily from other helminths (derived from the Greek word helmins or herminthos, which means worm). They are vermiform, unsegmented and bilaterally symmetrical with two concentric tubes separated by a space, the pseudocoelom (Bird and Bird, 1991). In the adult, the pseudocoelomic space also contains one or two tubular gonads, which open through the vulva in the female and into the rectum in the male. The inner tube contains the intestine; the outer tube consists of cuticle, hypodermis, musculature and nerve cells. The cuticle is secreted by the hypodermis. In some members of the order Trichostrongyloidea, such as the parasitic nematode *Haemounchus contortus*, cuticle ridges running the length on the body on the sub-median as well as the lateral surface, are clearly observed. The hypodermis consists of a syncytium of cells with four longitudinal thick structures: the lateral, ventral and dorsal hypodermal ridges or lines. The lateral lines contain the excretory canals and lateral nerve cords and the dorsal and ventral hypodermal ridges carry the dorsal and ventral nerve cords, respectively (the nematode nervous system will be described in section 1.5).

The pharynx is one of the most characteristic features of nematode morphology. It varies considerably between orders and species, a diversity largely correlated with feeding habits. For example, in the free-living nematode *Caenorhabditis elegans*, the pharynx is swollen into two muscular bulbs (metacarpus and terminal bulb) and in the parasite *H. contortus* it has a conoid shape (Bird and Bird, 1991). Since nematodes generally have a high internal pressure, and because the nematode intestinal wall is only one cell thick (and therefore liable to collapse under turgor pressure), the intestine can only be filled by a pumping organ. The pharynx is a cellular structure with distinct cell types: muscular, supporting, neuronal and

glandular cells. When pharyngeal muscles contract, intrapharyngeal pressure builds up and food particles (normally semi-liquid contents) are propelled into the lumen. Upon muscle relaxation, the contents pass into the intestine through the pharyngeal intestinal valve. The intestine opens posteriorly through the anus.

1.2 Parasitic infections

It is believed that the reasons for the success of the phylum Nematoda as parasites probably include the presence of an environmentally protective cuticle, facultative diapause (like the dauer stage of *C. elegans*, section 1.4) and biochemical adaptations to existence in extreme conditions. The parasitic forms have substantial impact on human welfare, through diseases of both humans and domestic animals, and crop damage.

As far as human parasites are concerned, more than 1.5 billion people are infected with geohelminths such as *Ascaris lumbricoides* and hookworms (*Necator americanus* and *Ancylostoma duodenale*) (Crompton, 1999). These infections can interfere with appetite, growth, physical fitness, physical activity, work capacity, and cognitive development. Hookworm anaemia, if untreated, is especially pernicious during pregnancy and in young children can lead to a vicious cycle of low birth weight and malnutrition sequelae (Stephenson et al., 2000). Lymphatic filiariasis (LF) is also a major public health problem. Worldwide, 120 million people suffer from this disease caused by species such as *Wuchereria bancrofti* and *Brugia malayi* (Cox, 2000). Athough LF is rarely fatal in itself, 43 million of those infected are seriously incapacitated or disfigured due to the gross swellings of limbs, breasts and genitalia. Also, about 18 million are infected with *Onchocerca volvulus*, a filarial nematode that produces impaired sight or blindness (Foege, 1998).

Nematodes such as *H. contortus* and *Ostertagia ostertagi* are of veterinary importance. They are gastrointestinal parasites of ruminants which cause economically important losses to the livestock industry, such as meat and wool loss and animal mortality (McLeod, 1995).

Parasitic nematodes are the subject of extensive research efforts, often aimed to understand their lifestyle and ecology, so as to control or manage them better. The following sections will be mainly focused in *H. contortus* and the model nematode *C. elegans*, which are the organisms studied in this project.

1.3 *Haemonchus contortus*

Classification: Phylum, Nematoda; Order, Strongylida; Family, Trichostrongylidae.
H. contortus is one of the most common parasites of sheep and goats in both the southern and northern hemispheres. It is a dioecious haematophagous parasite whose adult stage is found in the fourth stomach (abomasum) of sheep, and other ruminants. Adult females are 18-30 mm in length and 0.55 mm diameter and males 10-20 mm and 0.4 mm respectively (Veglia, 1915). They present a clear sexual dimorphism. The female has a remarkable appearance of red and white stripes because of its white ovaries wrapped around the red blood filled intestine (Fig.1.1). The characteristic of the male is its external reproductive structure: copulatory bursa and brown spicules that form an umbrella-like expansion surrounding the cloaca.
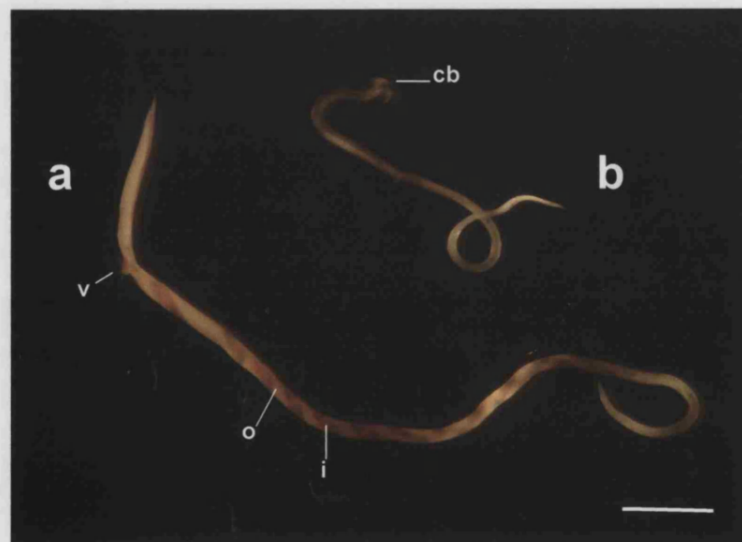
Fig. 1.1 Morphology of *Haemonchus contortus*

The anterior end of the worms are to the right. a: female; i: intestine; o: ovaries; v: vulva. b: male; cb: copulatory bursa. Scale bar, 2 mm.

The life cycle involves an external non-parasitic phase on the grass and soil, followed by a parasitic phase in the host (Smyth, 1994). A scheme of it is shown in figure 1.2. Adult worms mate in the abomasum producing fertile eggs that are released into the faeces. Females can lay up to 20,000 eggs per day. Eggs hatch to release first stage L1 larvae. After 14-17 hours they moult to give the second stage L2 larvae. L1 and L2 are both free-living microbivores. L2 larvae resume feeding for a further 40 hours and moult, but unlike the previous moults the L3 larvae retain their sheaths. Ensheathed L3 larvae, the non-feeding infective stage, survive by slow metabolism of stored reserves. L3 larvae are about 750 μm in length. They are unable to penetrate host skin, but they show positive geotrophism and climb up blades of grass, where they are accidentally ingested by ruminants.

In vertebrate   **Free-living**

| L4 moult to **adult** in the abomasum | → | **Eggs** passed in faeces |

| L3 larvae burrow into abomasum, moult to **L4 larvae** |

| **L1 larvae** feeding on faeces moult to **L2 larvae** |

| **Infection** upon direct ingestion of L3 larvae, followed by exsheathment in the rumen | ←   Blades of grass/soil | L2 larvae moult to **L3 larvae** but retain sheath (non-feeding infective stage) |
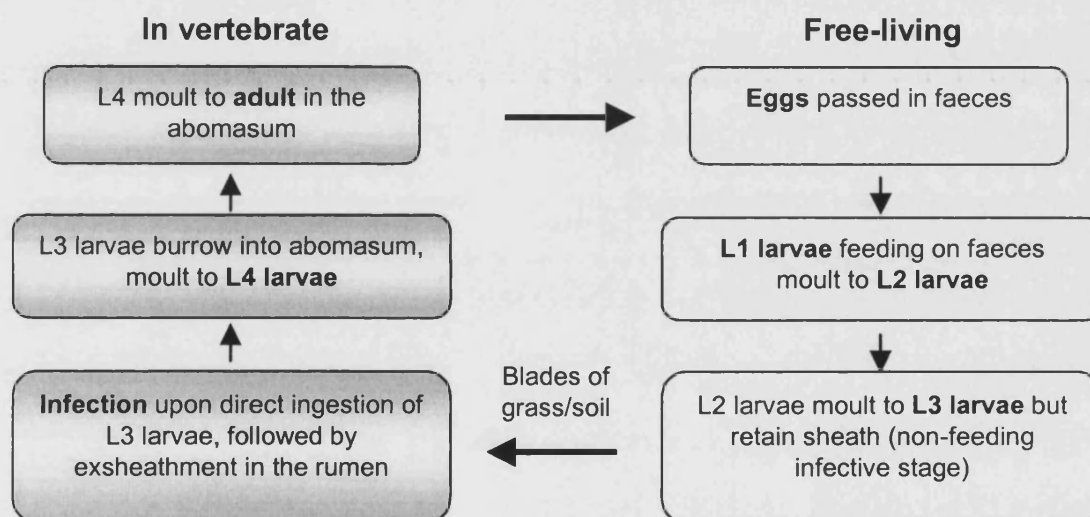
Fig. 1.2 Schematic representation of *H. contortus* life cycle

L3 exsheathment occurs during passage to the abomasum. In this organ, the L3 larvae burrow into gastric pits and start feeding. A third moult gives rise to the L4 larva. The early L4 larvae can arrest development in the host (Armour and Duncan, 1987). This diapause is induced by the onset of winter. The larvae must sense environmental cues in their host to allow then to re-enter the growth cycle after overwintering, and thus reinfect pasture and new lambs in the first flush of spring. Finally, a fourth moult is initiated and worms became sexually mature. Adults live buried in the host abomasum wall attached by their mouths to suck blood, but their bodies move actively, possibly to overcome the peristaltic action of the host

gastrointestinal tract. A single sheep may be infected with many thousands of *H. contortus* and it has been estimated that 4000 worms suck about 60 cm^3 of blood per day. This feeding can produce haemorrhaging of the abomasum and therefore blood plasma and proteins are lost in addition to the haemoglobin and iron from red blood cells. A loss of these components can cause anaemia and hypoalbuminaemia (Crompton and Joyner, 1980). As a result, production of milk, wool and meat becomes reduced, and in severe cases the sheep die.

1.4 *Caenorhabditis elegans*

Classification: Phylum, Nematoda; Order, Rhabditida; Family, Rhabditidae.

C. elegans is a small, free-living, soil nematode of 1 mm long. Hermaphrodites can be distinguished by the presence of a vulva, males by the fan-like tail (Fig. 1.3a). Hermaphrodites produce oocytes and sperm and can reproduce by self-fertilisation; they cannot fertilise each other. Males, which appear at a frequency of about 0.1 %, are capable of mating with hermaphrodites.

The *C. elegans* life cycle has a three-day generation time at 25°C. A single hermaphrodite can produce about 300-350 eggs. The embryo develops through a series of cell divisions that occur during the first 5 hours of embryonic development at 25°C (Fig. 1.3b). After about 14 hours of development in the case, the L1 larva hatches from the eggshell. The four larval stages (L1-L4) are each separated by a moult, during which the animal sheds its old cuticle. Under crowded conditions and with limited food, the L2 larva can enter an alternative developmental programme (dauer stage), in which the animal can survive long periods under harsh conditions. When those conditions improve and food becomes available, dauer larvae moult to L4 to later become adults.
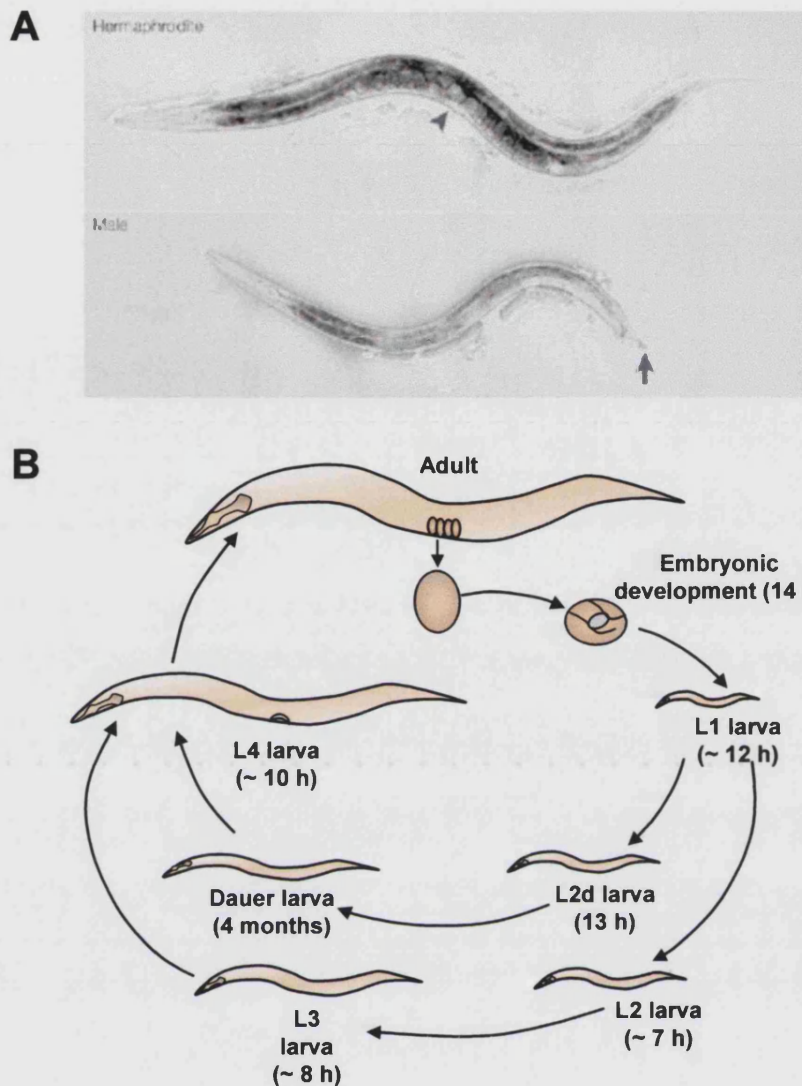
Fig. 1.3 Morphology and life cycle of *Caenorhabditis elegans*
A: Hermaphrodites can be distinguished by the presence of a vulva (arrowhead) and males by the fan-like tail (arrow). B: Schematic representation of the life cycle. d, dauer. Adapted from Jorgensen and Mango, 2002.

Since 1974, when Brenner published the first genetic screen in *C. elegans*, this worm has been a powerful model for the study of different biological process of multicellular organisms. Some of the features that have made of *C. elegans* such a good model include small size; rapid life-cycle; the choice of keeping strains as frozen stocks; transparent body and simple anatomy; identification of all somatic nuclei (959 in hermaphrodites); easy culturing and manipulation in the laboratory; the possibility of doing genetic analyses, molecular transfections and laser cell-ablation, and the completed genome sequence (The *C. elegans* Sequencing Consortium, 1998), etc. The choice of *C. elegans* as a model for metozoan biology has been fortunate for the study of parasitic nematodes. In particular, *C. elegans*

has served as a reasonable model for the discovery of anthelmintic drugs and for studying their mechanism of action (Geary and Thompson, 2001). Moreover, in the molecular phylogeny of nematodes (Blaxter et al., 1998), a study based on nucleotide sequence, the orders Rhabditida, which includes *C. elegans* and Strongylida, the order containing important trichostrongyloid parasites of ruminants such as *H. contortus*, are included in the same Clade V. The close association of these two nematodes supports the use of *C. elegans* as a model for the study of *H. contortus*.

1.5 *C. elegans* Nervous System

The most studied nematode nervous system is that of *C. elegans*. This nematode has only 302 neurons in the adult hermaphrodite, but despite this small number it has a rich variety of neuronal types. Regarding the nervous system anatomy, the most complete data has been obtained from reconstructions from electron micrographs (EM) of serial sections (White et al., 1986). It has been assumed, beyond possible ambiguities of the method, that the EM reconstructions showed all the neuronal connections in the hermaphrodite nervous system. Analysis of the wild-type circuitry, coupled with laser ablation and genetic tools that disrupt the function of a particular cell, have been used to identify the functional interactions between neurons in an identified circuit (Chalfie et al., 1985). For example, these approaches allowed the description of detailed models of how neurons function together to generate behaviour (Driscoll and Kaplan, 1997), and provided tools to interpret the spatial development and function of neurotransmitters (Rand and Nonet, 1997). Other approaches such as histochemistry and studies of the behavioural consequences of pharmacological agents have been used to investigate how this system works. Moreover, the recent development of electrophysiological techniques in *C. elegans*, such as patch clamping and voltage- and calcium-sensitive dyes, have contributed to the determination of the function of individual elements of a circuit (Kerr et al., 2000; Goodman et al., 1998).

C. elegans neurons differentiate, send out processes that migrate to their targets, form synapses with the correct targets and synthesize, package and release neurotransmitters. Synapses can be electrical (by gap junctions) or chemical.

Chemical synapses are *en passant* between adjacent processes within bundles, therefore no classic synaptic endings or synaptic terminals are present (White et al., 1986). Many synaptic contacts are multiple with two or more postsynaptic elements. Appropriate receptors on postsynaptic neurons directly or indirectly activate ion channels to transmit the signal to their terminals. Much of the cellular machinery used by *C. elegans* to carry out these processes is homologous to that known in other organisms (Kenyon, 1988). *C. elegans* uses acetylcholine, GABA (γ-aminobutyric acid), glutamate, 5-HT (serotonin), dopamine, the invertebrate catecholamine octopamine and neuropeptides as neurotransmitters (Bargmann and Kaplan, 1998; Brownlee and Fairweather, 1999). There are no predicted voltage-activated sodium channel genes in the *C. elegans* genome (Bargmann, 1998). However, *C. elegans* neurons have high membrane resistance, therefore they are able to propagate signals efficiently without the large-scale amplification provided by sodium channels (Davis and Stretton, 1989; Goodman et al., 1998). On the other hand, voltage-activated calcium channels and potassium channels participate on the regulation of nematode excitability.

1.5.1 Pharyngeal and Main Nervous System

The *C. elegans* nervous system (Chalfie and White, 1988) includes two almost independent units: the pharyngeal and the main nervous system that are only connected by a pair of ring interneurons (RIP). The processes of the RIP neurons penetrate the basement membrane in the anterior region of the pharynx (procorpus) and make gap junctions with two of the pharyngeal neurons (M1 and I1). In this case it seems that information flow runs from the sub-ventral nerve cords to the pharynx (Albertson and Thomson, 1976; White et al., 1986).

The *C. elegans* pharyngeal nervous system is composed of 20 cells: five classes of motor neurons (7 cells), six classes of interneurons (8 cells) and 5 other neurons (2 neurosecretory-motor neurons, 1 motor-interneuron and 2 marginal cells). The topography and connectivity of these cells were described by Albertson and Thomson (1976). Updated information about all *C. elegans* pharyngeal neurons which includes: description, location, lineage and neuronal function (if it is known) can be found on Leon Avery's web page: http://eatworms.swmed.edu

The main nervous system includes all the remaining neurons found throughout the animal. Most of *C. elegans* neurons have their cell bodies in the anterior end around the pharynx. Neuronal processes run in longitudinal or circumferential tracts adjacent to the hypodermis (the hypodermis is the external epithelium). The major areas of neuropil are the nerve ring and the ventral and dorsal cords (Figs. 1.4 and 1.5). The nerve ring encircles the centre region of the pharynx (isthmus) in an oblique disposition and consists of processes of sensory neurons, interneurons and motor neurons that innervate head muscles. In most of cases these processes are from neurons whose cell bodies lie in the head ganglia (the anterior, dorsal, lateral and ventral ganglions).
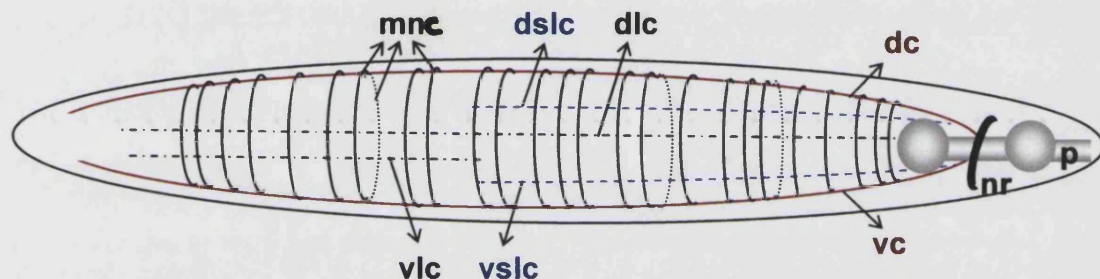
Fig 1.4 Schematic representation of *C. elegans* main nervous system
Lateral view of the right side of the worm; anterior is right. nr: nerve ring. Nerve cords: dc: dorsal; vc: ventral; dlc: dorsal lateral; vlc: ventral lateral; dslc: dorsal sub-lateral; vslc: ventral sub-lateral. p: pharynx. Note the sidedness of the motor neuron commissures (mnc); more are present on the right side than on the left (full and dotted circumferential lines, respectively).

The ventral nerve cord, the main process bundle, runs along the ventral mid-line extending from the ventral region of the nerve ring. This cord is made up of interneurons, and motor neurons that innervate body muscles. It is worth mentioning that all the cell bodies of these motor neurons lie on the ventral cord. Some motor neurons innervate ventral muscles and others dorsal muscles. This latter class send processes round to the dorsal mid-line via commissures, the motor neuron commissures. These then turn either anteriorly or posteriorly and together make up the dorsal nerve cord (Fig. 1.4). The nerve cords run adjacent to swellings of the hypodermis (hypodermal ridges). Because the hypodermal ridges are situated on the left of the process bundle, it may present a barrier on that side to commissures leaving the cord and might be the reason why most of the motor neuron commissures run round the right-hand side of the animal (Figs. 1.4 and 1.5).

25

In addition to the main cords, lateral cords (dorsal and ventral) and sub-lateral cords (dorsal and ventral) are present, containing nerve processes from nerve ring interneurons and some mechanosensory neurons. They are located in small hypodermal swellings, the lateral lines. The sub-lateral cords run along the anterior and middle portion of the worm. The dorsal lateral cord extends through the entire animal, but the ventral lateral cord is present only in the posterior region (Fig. 1.4)

1.5.2 Sensory organs

Sensory receptors are arranged in groups of sense organs, named sensilla. Each sensillum contains one or a number of ciliated nerve endings (cilia) and two non-neuronal cells: a sheath and a socket cell. A socket cell is an interfacial hypodermal cell that joins the sensillum to the hypodermis and a sheath cell is a glial-like cell that envelops the endings of neurons (Chalfie and White, 1988). Sensilla open through a hole in the overlying cuticle, giving the cilia access to the external environment. Such organs, generally considered to be chemosensory, include the two amphid sensilla and the six inner labial sensilla in the head, and the two phasmid sensilla in the tail. In contrast to *C. elegans*, the inner labial neurons of L3 larvae of the parasitic nematodes *Strongyloides stercoralis* and *Haemonchus contortus* end beneath the cuticle, and, consequently, are thought to be mechanosensory neurons (Fine et al., 1997; Li et al., 2000a). The amphid sensilla are described in section 1.5.2.1.

Some ciliated endings do not penetrate the cuticle and are, therefore, thought to mediate mechanosensation. These include the following sensilla: the six outer labial, the four cephalic, the two deirid sensilla and the two postdeirid sensilla. Other receptors with a characterised mechanosensory modality are the touch receptors: ALM, PLM, and AVM (Chalfie and Sulston, 1981). Their sensory processes are not organised as sensilla but are differentiated in prominent microtubules and extend along the length of the lateral lines and ventral midline.

The nerve ring receives sensory input from the anterior tip of the nematode through the anterior sensilla. The processes for the non-amphidial sensilla have their cell bodies in front of the nerve ring in the anterior ganglion, whereas fibres from the amphids run past the nerve ring to their bipolar cell bodies in the lateral ganglia

from which axonal processes turn back and enter the nerve ring (White et al., 1986).

1.5.2.1 Amphids

The amphid sensilla are the main chemoreceptive organs of the anterior end of the worm. They consist of two bilaterally symmetric sensilla (left and right) containing the ending of 12 types of sensory neurons. These neurons can be distinguished from each other by their morphology and by their connections to other neurons. Each neuron is bipolar, with one sensory process (dendrite) and one presynaptic process (axon) emerging from the cell body. The dendrites extend to the nose and terminate in sensory cilia. All the axons extend to the nerve ring, where they make connections with other neurons and each other. The amphidial process tracts are represented in the diagram of figure 1.5.
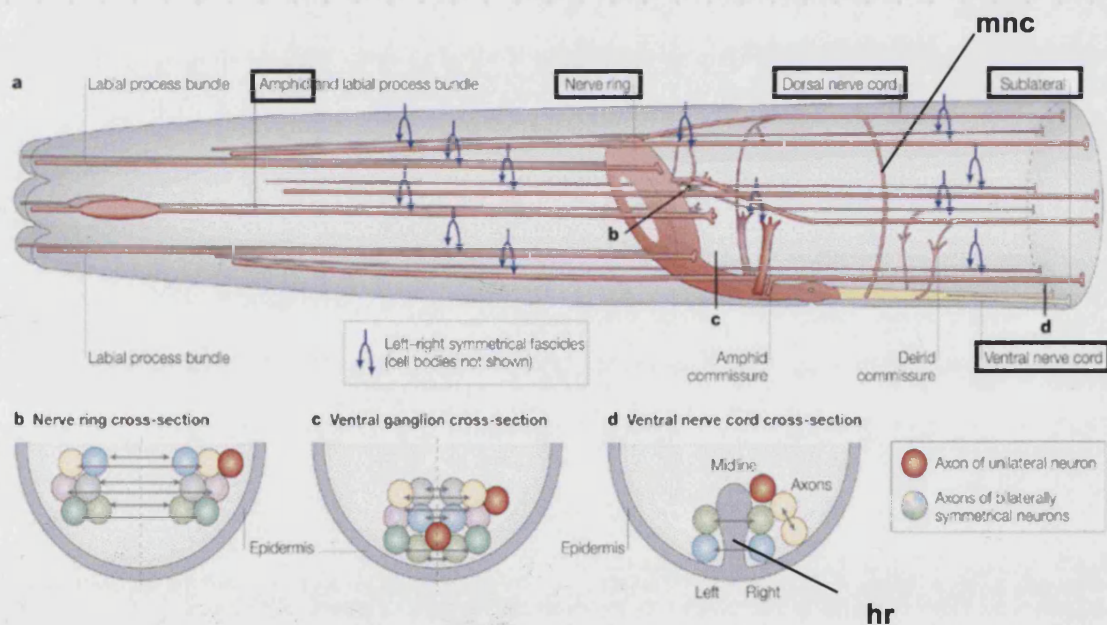
Fig. 1.5 *C. elegans* anterior nerve bundles.

a: left lateral view with the anterior of the worm towards the left. b-d: cross-sections at different regions, showing in circles axons of different neurons. Blue arrows indicate the bilateral symmetry of nerve processes. Notice amphidial nerves, nerve ring, the dorsal, ventral and sublateral nerve processes as a right-side motor neuron commissure (mnc). hr: hypodermal ridge. Adapted from Hobert et al., 2002.

Based on their dendritic morphology and function, amphidial neurons can be grouped into three classes: exposed, wing and finger cells (Ward et al., 1975). The

27

exposed cells have one or two long cilia open to the environment through the amphidial pore and include: ADF, ADL, ASE, ASG, ASH, ASI, ASJ and ASK neurons. These cells detect mostly water-soluble chemicals (Bargmann et al., 1990; Bargmann and Horvitz 1991 a,b; Kaplan and Horvitz 1993; Troemel et al., 1995). The wing cells have flattened branched cilia near the pore but enclosed by the sheath cell. They include the AWA, AWB and AWC neurons, which detect volatile odorants (Bargmann et al., 1993; Troemel et al., 1997). Finally the finger cell, AFD, has a complex brush-like dendritic membrane structure embedded in the sheath cell, and detects thermal cues (Mori and Ohshima, 1995). Neurons from different groups do not share sensory functions, excepting the ASH neurons which are particularly broad in their function. They detect water-soluble repellents: high osmotic strength (Bargmann et al., 1990), volatile repellents such as octanol (Troemel et al., 1995), and a mechanical repellent, light touch to the nose (Kaplan and Horvitz, 1993).

As far as *H. contortus* amphidial neurons are concerned, they do not take up fluorescent label fluorescein isothiocyanate (FITC), 1,1' dioctadecyl-3,3,3'-tetramethylindocarbocyanine perchlorate (DiI), or 3,3'-dioctadecyloxacarbocyanine perchlorate (DiO), as do those of *C. elegans* (Hedgecock et al., 1985); therefore dye filling cannot be used in the parasite as a tool to identify amphidial neurons (Li et al., 2000a). The sensory neuron anatomy of *H. contortus* first stage larva (L1), has been studied by neuronal laser microbeam ablation coupled to three-dimensional reconstructions from electron micrographs of serial transverse sections of the anterior sensilla (Ashton et al., 1999; Li et al., 2000a). On L1 and L3 larva, the stage-to-stage constancy of the amphidial neuronal number, position and structure in *H. contortus*, was confirmed (Li et al., 2000a). Amphidial structure in *H. contortus* is similar for the described on *C. elegans*, suggesting that the sensory functions controlled by these neurons might be also comparable. As in *C. elegans*, each amphid of *H. contortus* is innervated by 12 neurons. However, whereas the position of cell bodies is conserved between these nematodes, they differ on the number of neurons included in the amphid channel (ten in *H. contortus* instead of eight), and in that three of these neurons rather than two, end in double processes. Recently a comparison of amphidial structure between *H. contortus* ivermectin-resistant and susceptible strains, revealed a dramatic decrease in the length of sensory cilia in the resistant strains (Freeman et al., 2003). Whether such structural

modification of the dendrites facilitates survival of nematodes exposed to macrocyclic lactones remains unclear.

The structure of amphidial neurons has also been described for two other gastrointestinal nematode parasites: *Ancylostoma caninum*, the hookworm of dogs, and *Strongyloides stercoralis*, which normally parasitises humans, other primates and dogs (Ashton at al., 1999). Whereas in *A. caninum* the amphidial structure is very similar to that of *H. contortus*, in *S. stercoralis* is slightly different from that of *C. elegans*, *A. caninum* and *H. contortus* (Ashton et al., 1995 and 1999). Thirteen neurons instead of 12 are associated with the amphid. In each amphid, eleven neurons extend nearly to the amphidial pore as single ciliated dendritric processes. A twelfth dendrite terminates at the base of the amphidial channel. One specialised neuron (ALD) enters the base of the amphidial channel along with the other dendirtes, but leaves the channel and forms a complex of lamellae within the body of the amphidial sheath cell. The shape of it dendritic process is similar to the wing cell AWC in *C. elegans*, but it is much more complex. The large number of lamellae of ALD greatly increase the surface area of the process as do the microvilli of the *C. elegans* thermoreceptor neuron AFD, absent in *S. stercoralis*. It has been described that the neurons ALD mediate thermotaxis in this parasite, and would play an important role in host-finding behaviour (Lopez et al., 2000). Although some structural differences have been found between amphidial dendrites of *C. elegans* and parasitic nematodes, the position of the amphidial cell bodies are found to be quite similar (Ashton et al., 1999). Ashton et al (1998) demonstrated that *C. elegans* can serve as a model for predicting the function of amphidial neurons in *S. stercoralis*, based on similarities in the positions and morphological characteristics of the amphidial neurons of the two species. In *S. stercoralis* ASI and ASF (=ADF in *C. elegans*), two apparently *C. elegans* homologous amphidial neurons that control the process of becoming environmental resistant dauer larvae in the free-living nematode, also control the direction of larval development in the parasite.

The neurons of the amphid sensilla have synaptic outputs predominantly focused onto four nerve ring interneurons and the output of this circuit connects to ventral cord interneurons, providing a link to the motor nervous system (White et al., 1986).

1.5.3 Motor neurons and locomotion

In *C. elegans* and in *Ascaris suum*, a parasitic nematode whose motor nervous system has been widely studied (Stretton et al., 1978; Warlond et al., 1985; Johnson and Stretton, 1985 and 1987; Stretton et al., 1992), seven main classes of motor neurons are present along the ventral cord, arrayed in repeating units. *C. elegans* motor neurons VAn, VBn and VDn innervate ventral muscle and DAn, DBn, ASn and DDn, innervate dorsal muscle. The D-type of neurons and their analogous cells in *Ascaris* possess γ-aminobutyric acid (GABA)-like immunoreactivity and therefore, are thought to utilise GABA as their neurotransmitter (McIntire et al., 1993; Johnson and Stretton 1987). The other type of ventral cord motor neurons contains the vesicular acetylcholine transporters (VAChT) and choline acetyltransferase (ChAT), therefore use the neurotransmitter acetylcholine (Erickson et al., 1994; Johnson and Stretton, 1985).

Motor neurons innervate dorsal and ventral muscles. Body wall muscles are organised into two dorsal and two ventral rows. An unusual feature of nematode muscle is the manner in which it is innervated. Motor neurons do not extend axons peripherally to innervate muscles; instead, muscles send neuron-like processes (muscle arms) to the dorsal or ventral cords in which the axons of motor neurons reside (Chalfie and White, 1988). At neuromuscular junctions, motor neurons release either acetylcholine or GABA causing at a particular area and at the same time, contraction of muscle cells in one side of the animal and relaxation on the opposite side (Fig. 1.6). This model of cross-inhibition would prevent the simultaneous contraction of the dorsal and ventral muscles (White et al., 1986). This, coupled to the activation of cholinergic motor neurons by the command interneurons, drives worm locomotion.
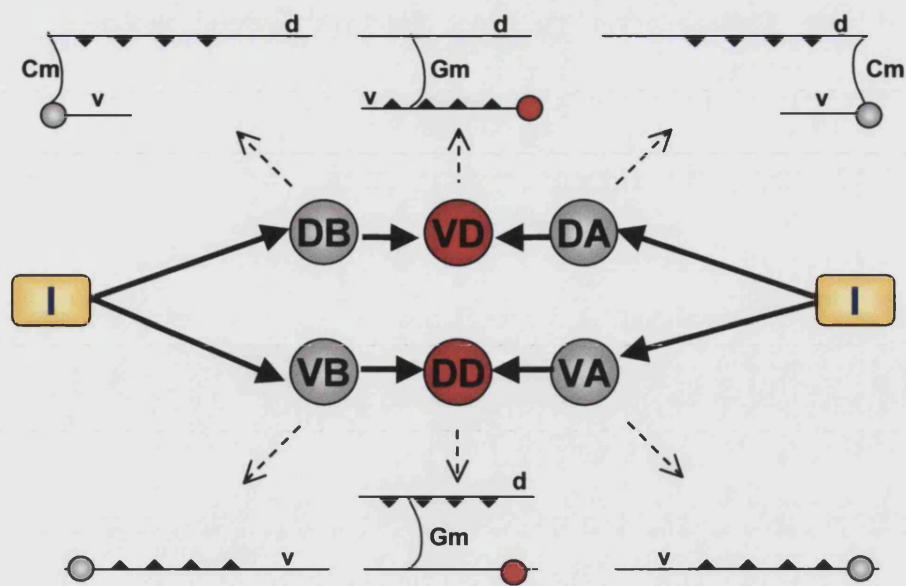
Fig. 1.6 Motor neurons and locomotory circuitry
The GABA-ergic motor neurons (red circles) synapse onto muscles situated opposite to those innervated by their presynaptic partners, the cholinergic motor neurons (grey circles), as indicated with triangles on the dorsal (d) and ventral (v) cords. The VB and VA motor neurons do not send processes to the dorsal cord. Cholinergic motor neuron commissures (Cm) emerge from motor neuron cell bodies, whereas the GABA-ergic motor neuron commissures (Gm) do not. The Gm are right handed but the Cm can be right or left handed. Command interneurons (I) synapse onto cholinergic motor neurons directing forward or backward movement. Full arrows indicate neuronal synapses (Adapted form Chalfie and White, 1988).

1.6 Control of *H. contortus* infection

1.6.1 Chemical control

The use of antiparasitic chemicals appears to be the most effective and is the most widely used method to tackle parasitic infections. Drugs isolated from natural botanic and microbiological resources or synthetic compounds have been applied (Thompson et al., 1996). However, there is a serious problem of anthelmintic resistance in nematode populations in the field. Up to date information on the chemotherapy used to treat nematode infections is reviewed by Harder (2002). The latest and most potent drugs to treat *H. contortus* infections belong to the family of avermectins and milbemicins (section 1.7).

1.6.2 Other methods

Alternative methods to chemotherapeutics include grazing management (Strong and Wall, 1990). Pasture resting counteracts the possibility of transmission by rotating livestock to clean pastures and by alternation grazing between species. Dung removal, by sweeping or vacuuming infected dung from the fields, is also recommended. Due to differences in management, pasture infectivity, climate, etc, it is difficult to establish which programme is to be preferred to control nematode infections in livestock. Grazing strategies, when possible, should be combined with drug treatment (Coop et al., 2002).

Biological control methods have also been implemented. They are based on the use of fungi with nematophagous activity, which are able to reduce the number of larvae of sheep and cattle nematodes while they are undergoing the free-living stages of their life cycle. Some fungal species are more efficient predators of infective larvae in sheep faeces (Waller and Larsen, 1993; Waller and Faedo, 1993). A disadvantage of this approach is that they mostly depend on climatic conditions. However, other fungal species have a greater capacity to survive passage through the gastrointestinal tract of ruminants and were used to feed nematode infected calves. Those assays showed a reduction on the levels of eggs from faecal deposits obtained from those calves (Gronvold et al., 1993).

Finally, vaccines could be another alternative used as a method of control. The development of vaccines has mainly depended on the identification of novel parasite antigen molecules able to elicit a protective immune response in the host (Meeusen, 1996). For *H. contortus* a vaccine based on an intestinal protein, contortin, showed a significant reduction in worm burden and egg count in sheep (Munn et al., 1987). Also *H. contortus* excretory-secretory products induced protective immunity against the parasite in the host (Schalling et al., 1997). However, no *H. contortus* vaccines are available. A commercially available vaccine must need to target multiple species of gastrointestinal nematodes, be cost-effective and be accepted into farm management strategies (Knox, 2000).

1.7 Ivermectin

The avermectins (AVMs) and milbemycins are structurally related classes of 16-membered macrocyclic lactones, a group of very hydrophobic compounds, which have potent anthelmintic, insecticide, and acaricide properties. Both were isolated in the 1970s from soil-dwelling *Streptomyces* species and remain at the forefront of control for a range of endo- and ecto-parasites, including nematodes. The first commercial member of the AVMs/milbemycins (AMs), ivermectin (IVM), was introduced in 1981. Ivermectin (22,23-dihydro-avermectin B_{1a}), is a semi-synthetic derivative of avermectin B_{1a}, the most potent of the 8 natural AVMs originally isolated, developed for use in animals (Chabala et al., 1980). The high potency of IVM against nematodes of sheep was first reported by Egerton et al (1980). They found that oral dosing of IVM to sheep at dosages almost 100 times less that thiabendazole (an anthelmintic drug that binds to β-tubulin and inhibits microtubule polymerisation (Lacey, 1990), eliminated nematode species from the gastrointestinal tract such as *H. contortus*, *Ostertagia circumcincta* and *Trichostrongylus* spp.

Other AMs anthelmintics used to control parasitic infections in small ruminants include doramectin, moxidectin and abamectin. All AMs are effective against the same spectrum of biologically diverse invertebrate parasites, they kill these organisms through hyperpolarisation and flaccid paralysis and they are efficacious at similar dosages (Shoop et al., 1995). Given the similarity in structure and action between the AVMs and milbemycins, it is often assumed that data obtained with one member of the family is generally applicable to all. Though this may be true, it is probably sensible to note that this may not always be the case and therefore it will be noted which compounds were actually used in the experiments reviewed here.

Like the other AMs, IVM has a broad spectrum of activity and has also been widely used to combat nematode parasitism of humans, other domesticated animals, and crops (Campbell, 1989). In man IVM has become the cornerstone of the mass drug administration program to eradicate onchocercasis (river blindness) (Dull and Meredith, 1998) and is used in part for a similar program to eliminate lymphatic filariasis (Brown et al., 2000).

1.7.1 Safety of AMs

The selective effect of action of AMs in the host, can be explained by their action on the glutamate-gated chloride channels (GluCls), present only in invertebrates (section 1.8). AMs generally show very low host toxicity. It is believed that the blood-brain barrier prevents access of IVM to the central nervous system (Fisher et al., 1992). Since at higher concentrations (100-fold more than therapeutic dosage) IVM can potentiate GABA-gated chloride channels and $\alpha 7$ nicotinic acetylcholine receptors (Adelsberger et al., 2000; Krause et al., 1998), it has been suggested that IVM and related drugs can be toxic for vertebrates that possess a deficiency in their blood barrier (Etter et al., 1999). This is supported by data from Kwei et al (1999) and Mealey et al (2001), which found that the side effects seen in vertebrates following IVM treatment may be due to the lack or functional deficiency of a P-glycoprotein membrane pump (mdr) in their blood barrier.

1.7.2 Ivermectin Resistance

In nematodes that infect small ruminants, particularly in *H. contortus*, anthelmintic resistance has reached enormous proportions in many parts of the world (Prichard, 1994; Sangster, 1999; Jackson and Coop, 2000). Genes involved in drug resistance may, but will not necessarily, be involved in the mechanism of action of an anthelmintic. Resistance mechanisms can broadly be considered as due to changes in the drug receptor, or modulation of drug concentration. However, genes that code for transport or metabolism, for example, can be involved in drug resistance but have no direct role in the mechanism of action. Population genetic studies have suggested that during the development of AMs resistance in *H. contortus*, there is selection at a P-glycoprotein (Pgp) gene (Blackhall et al.,1998a), at the *HcGluClα* (Blackhall et al., 1998b), which encodes a glutamate-gated chloride channel (section 1.8) and at *HG1* (Feng et al., 2002), a putative member of the amino acid-gated anion channel subunit family (Laughton et al., 1994). Studies from Le Jambre et al (1999) showed that the Pgp gene is not the major gene responsible for resistance, at least in the *H. contortus* CAVRS IVM-resistant strain. Further work is required to characterise whether the function of any of the other two is relevant for AM resistance. As far as *HcGluClα* is concerned, full-length cDNA

sequences from *H. contortus* IVM-resistant and IVM-sensitive isolates were analysed (Cheeseman et al., 2001). No consistent coding differences were found between both isolates, which led to the suggestion that if there are any changes in this gene associated with IVM resistance, they might be present in the non-coding regions and possibly result in alterations in the expression of the HcGluClα subunit rather than to its amino acid sequence.

C. elegans has been used to study the effects of gene knockouts and mutations on resistance to anthelmintics such as IVM. These studies have lead to the isolation of multiple IVM-resistant mutant strains. The genes known to be involved in IVM-resistance include genes encoding for GluCl subunits (*avr-15*, *avr-14* and *glc-1*), two innexin genes (subunits of invertebrate gap junctions) and dye filling defective (Dyf) genes (Dent et al., 2000). It seems that the development of resistance in *C. elegans* requires the simultaneous mutation of several of those genes to develop high level of resistance. IVM resistance in *C. elegans* does not necessary replicate the mechanisms of resistance in parasitic worms. However, *C. elegans* can help to identify orthologous genes in parasitic nematodes, which might provide insights into the possible mechanisms of resistance in parasitic nematodes.

1.7.3 Biological effects

A number of *in vitro* studies have shown that the AMs inhibit pharyngeal pumping (and hence feeding), motility and fecundity in susceptible nematodes. In *H. contortus,* pharyngeal pumping is the most sensitive of the processes affected by these anthelmintics (Gill et al, 1991, 1995; Geary et al., 1993; Paiement et al.,1999). IVM concentrations ≥ 0.1 nM paralyse the pharynx of adult *H. contortus*, whereas a reduction in motility leading to overall paralysis requires ≥ 10 nM IVM. Interestingly paralysis is confined to the mid-body region of the worm, with the head and tail regions still able to move normally (Geary et al., 1993). It is believed that inhibition of pharyngeal pumping would lead to a depletion of energy reserves as the parasite would no longer be feeding, while inhibition of motility would be expected to have a more immediate effect as gastrointestinal parasites would be swept away by digesta. AVMs exert similar effects at comparable concentrations on *H. contortus* larvae (Gill et al., 1991, 1995) and *C. elegans* (Kass et al., 1980; Avery and Horvitz, 1990; Arena et al., 1995). In some species, particularly the filaria, the

most important effect on the adult worm is to suppress new microfilariae production (Awadzi et al., 1985; Duke et al., 1991) without directly killing the resident macrofilariae; similar effects on fecundity are seen in *H. contortus* and *C. elegans* (Le Jambre et al., 1995; Grant, 2000). It remains unclear which mechanism is responsible for the overall potency of the AMs *in vivo* towards *H. contortus* and other parasitic nematodes. Since *H. contortus* and *Trichostrongylus colubriformis*, both gastrointestinal sheep parasites, may be expelled very rapidly after IVM treatment (within 8-10 hours), it has been suggested that parasite body wall paralysis rather than inhibition of feeding may be the crucial event for initial removal of those nematodes from the host (Gill and Lacey, 1998; Sangster and Gill, 1999). However, in *O. circumcincta* (a gastrointestinal cattle parasite) AMs effects on pharyngeal pumping may be crucial for the elimination of this nematode from the host. It seems likely that the relative importance of each of these major effects may differ between species and even developmental stages.

1.7.4 Molecular targets

It was apparent from early experiments that the AVMs interacted with ligand-gated chloride channels from both target and non-target species (Kass et al., 1980; Supavilai and Karobath 1981; Graham et al., 1982; Pong and Wang 1982) and so perhaps it was not surprising that it was thought that their main target could be the GABA receptor present at the nematode neuromuscular junction, though micromolar concentrations were required to elicit the blocking effects observed (Holden-Dye et al., 1988; Holden-Dye and Walker 1990). A patch-clamp study by Martin and Pennington (1989) on *A. suum* muscle also demonstrated that IVM antagonised GABA receptors, reducing the single-channel conductance and the frequency of channel openings. The same study showed that IVM activated both non-GABA chloride channels and cation-selective channels.

Older studies have also indicated that AVM B_{1a} could also block transmission between interneurons and excitatory motorneurons in the ventral cord and ventral inhibitory neuromuscular transmission (Kass et al., 1980, 1984). Delany et al (1998) proposed that this could be explained by the presence of glutamate-gated chloride channels (GluCls) on motor neurons innervating the somatic muscles. Today it is clear that the AMs can interact with a wide variety of channels, including

mammalian glycine and GABA$_A$ receptors (Adelsberger et al., 2000; Dawson et al., 2000; Shan et al., 2001), α7 nicotinic acetylcholine receptors (Krause et al., 1998) and P2X$_4$ receptors (Khakh et al., 1999).

The first direct evidence for an AM interaction with GluCls was revealed in insect muscle. IVM was shown to activate a chloride channel, which was sensitive to the glutamate analogue ibotenate but insensitive to GABA (Duce and Scott, 1985; Scott and Duce, 1985). In nematodes, IVM was shown to bind a site in membranes prepared from *C. elegans* with a 100-fold higher affinity than binding to membranes from rat brain. The relative binding affinities of IVM and a number of derivatives were shown to correlate well with their ability to inhibit motility in *C. elegans*, i.e. the higher the binding affinity the more potent the effect on motility (Schaeffer and Haines, 1989). High affinity binding by a series of AM analogues has also been demonstrated to membranes prepared from *H. contortus* (Rohrer et al., 1994; Hejmadi et al., 2000; Cheeseman et al., 2001). When avermectin-sensitive chloride currents were produced in *Xenopus* oocytes injected with *C. elegans* mRNA, they were found to be GABA-insensitive (Arena et al., 1991) but, later, to be sensitive to glutamate (Arena et al., 1992). This, and the subsequent cloning of cDNAs encoding avermectin sensitive GluCl subunits from *C. elegans*, parasitic nematodes and insects (Cully et al., 1994, 1996a; Dent et al. 1997, 2000; Laughton et al., 1997a; Forrester et al., 1999, 2002; Jagannathan et al., 1999; Cheeseman et al. 2001; Horoszok et al., 2001) has led to the belief that the GluCls are the principle targets through which the AMs exert their biological effects on nematodes.

Electrophysiological studies of pharyngeal preparations from both *C. elegans* and *A. suum* have shown that the AMs act on GluCls to inhibit pumping (Martin 1996; Adelsberger et al., 1997; Pemberton et al., 2001), though Brownlee et al (1997) also suggested a possible interaction with GABA receptors in the *A. suum* pharynx. In insects the situation has been recently complicated by the suggestion that the *Drosophila* avermectin receptor may contain both the GluCl subunit and the GABA receptor subunit, RDL (Ludmerer et al., 2002) and by the discovery of avermectin-sensitive histamine-gated chloride channels (HisCls) (Gisselmann et al., 2002; Zheng et al., 2002). Mutations in the *ort* gene, which encodes one of the HisCl subunits, alter the susceptibility of the flies to the avermectins (Georgiev et al., 2002; Iovchev et al., In Press) suggesting that these channels may be important

targets *in vivo*. In nematodes, where no HisCls have been demonstrated, the evidence remains strongly in favour of the GluCls as the clinically relevant AM target.

1.8 Glutamate-gated chloride channel (GluCl) subunits

The initial isolation of the *C. elegans* GluClα1 and GluClβ cDNAs by the Merck group, was carried out by subfractionation of clones from a cDNA library, screened by expression in *Xenopus* oocytes of mRNA pools that elicited responses to low concentrations of glutamate (1 mM) and/or IVM (1 μM) (Cully et al., 1994). Phylogenetic analyses indicated that these subunits belong to a discrete ligand-gated ion channel family that may represent genes orthologous to the vertebrate glycine channels (Vassilatis et al., 1997a). GluCl channels (GluCls) have been also described from neuronal and muscular tissues of insects (Cully-Candy and Usherwood, 1973), crustaceans (Cleland and Selverston, 1995) and molluscs (Ikemoto and Akaike, 1988).

The GluCl subunits share about 40 % and 30-35 % amino-acid identity with the vertebrate glycine and GABA$_A$ receptor subunits, respectively (reviewed by Cleland, 1996). The individual subunit sequences show all the characteristics of the ligand-gated ion channel family, with a long N-terminal extracellular domain followed by four membrane-spanning domains (Fig. 1.7). The N-terminal domain possesses a second pair of cysteine residues and carries the ligand-binding site. The intracellular loop between the third and fourth transmembrane domains contains consensus sequences for protein kinases: in other members of the family protein phosphorylation has been shown to affect the channel properties (Porter et al., 1990; Wafford and Whiting, 1992; Moss et al., 1995; Filippova et al., 2000). By analogy with other ligand-gated ion channels, the mature receptor is presumed to be a pentamer, made up of different types of subunit and with the second membrane-spanning domains lining the ion pore. To date there is no direct evidence on the subunit composition of any nematode GluCl. The 'α' subunits were named based on their ability to respond to IVM when expressed in a heterologous system, usually the *Xenopus* oocytes for *C. elegans* (Cully et al., 1994; Dent et al.,

1997; Vassilatis et al., 1997b; Dent et al., 2000; Horoszok et al., 2001). The 'β' subunit was defined by it ability to respond to glutamate, but not to IVM (Cully et al., 1994).
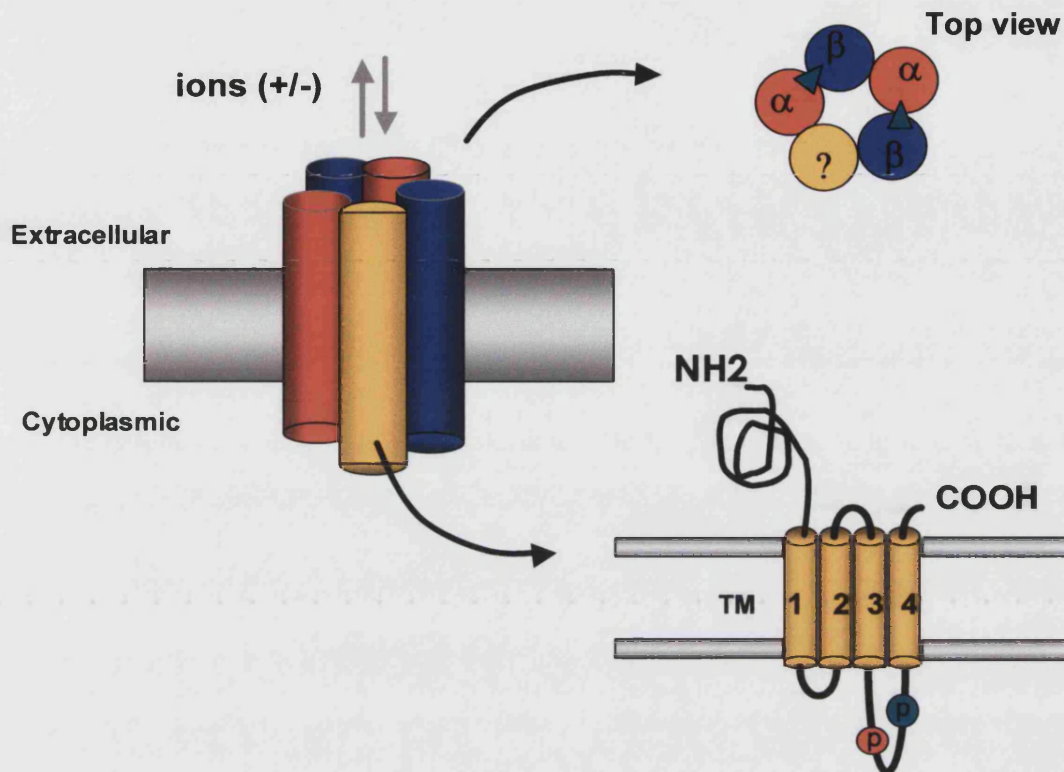
Fig. 1.7 Diagram of a putative GluCl receptor
Pentameric structure of the GluCl transmembrane channel. The subunits cluster around a central ion pore composed of their second transmembrane domains (TM), the TM2 regions. The lower panel ilustrates the composition of a single subunit showing a long N-terminal region, the four TM regions (TM1-TM4), and the cytoplasmic loop between TM3 and TM4 which contains consensus phosphorylation sites (P). The agonist binding sites are in the N-(t) domain and cross the interface between the β- subunit and the adjacent subunit (top view, green triangles). As the *C. elegans* GluClα and β subunits form heteromeric functional receptors when expressed in *Xenopus* oocytes (Cully et al., 1994), they were representatively chosen for this diagram.

Further cloning studies, together with the complete *C. elegans* genomic sequence, have led to the identification of a small family of six GluCl genes in this species (Table 1.1). At least two of these genes, *avr-14* and *avr-15*, are alternatively spliced (Dent et al., 1997, 2000; Laughton et al., 1997a; Vassilatis et al., 1997b) to yield at least eight possible subunits. Since the native GluCls are presumed to be pentamers, it is clear simply from the number of GluCl subunit genes that multiple forms of this channel must exist in worms, and there are therefore likely to be multiple AM target sites.

Table 1.1 GluCl genes and subunits

The current names used for genes and subunits are shown. Other names that have been used in the literature are given in brackets.

C. elegans gene	C. elegans subunit	H. contortus gene	H. contortus subunit
glc-1	GluClα1		
glc-2	GluClβ	Hcglc-2 (hg4)	HcGluClβ (HG4)
glc-3	GluClα4		
glc-4 (C27H5.8)	GLC-4		
avr-14 (gbr-2)	GluClα3A (GBR-2A)	Hcavr-14 (gbr-2)	HcGluClα3A (Hc-GBR2A)
	GluClα3B (GBR-2B)		HcGluClα3B (Hc-GBR2B)
avr-15	GluClα2A		
	GluClα2B		
		HcGluClα	HcGluClα

The alternative splicing of avr-14 is intriguing: both mRNAs encode the same N-terminal domain, which would include the glutamate binding site, but are attach to different membrane-spanning domains, which form the chloride ion channel (Laughton et al., 1997b). The parasitic species about which we have most information is H. contortus. So far, three genes encoding four GluCl subunits have been identified in this organism (Delany et al., 1998; Forrester et al. 1999; Jagannathan et al., 1999; Cheeseman et al., 2001) (Table 1.1). Figure 1.8 shows a neighbour-joining tree of the GluCl subunits so far identified in C. elegans, H. contortus and D. melanogaster. Three of the H. contortus subunits are clearly orthologues of ones in C. elegans, the HcGluClβ and α3 subunits; in the absence of a complete genome sequence it is impossible to know whether or not orthologues of the other C. elegans genes await discovery. Similar to C. elegans GluCls, HcGluClα was defined as an 'α' subunit based on it capability to bind IVM when expressed in cultured mammalian cells (Forrester et al., 1999; Cheeseman et al., 2001; Forrester et al., 2002). This subunit does not seem to be orthologous to any of the C. elegans genes (Cheeseman et al., 2001), indicating that there are differences in the genetics of the GluCls between even quite closely related

nematode species: *H. contortus* and *C. elegans* (Blaxter et al., 1998). Sequences corresponding to *avr-14* have also been isolated from *A. suum* and the filarial species *Onchocerca volvulus* and *Dirofilaria immitis* (Cully et al., 1996b; Jagannathan et al., 1999; Yates and Wolstenholme, pers. commun.): the alternative splicing of this gene is conserved in all the nematodes where this has been examined (Jagannathan et al., 1999; Yates and Wolstenholme, pers. commun.). The final member of the *C. elegans* GluCl family, *glc-4*, is somewhat divergent from
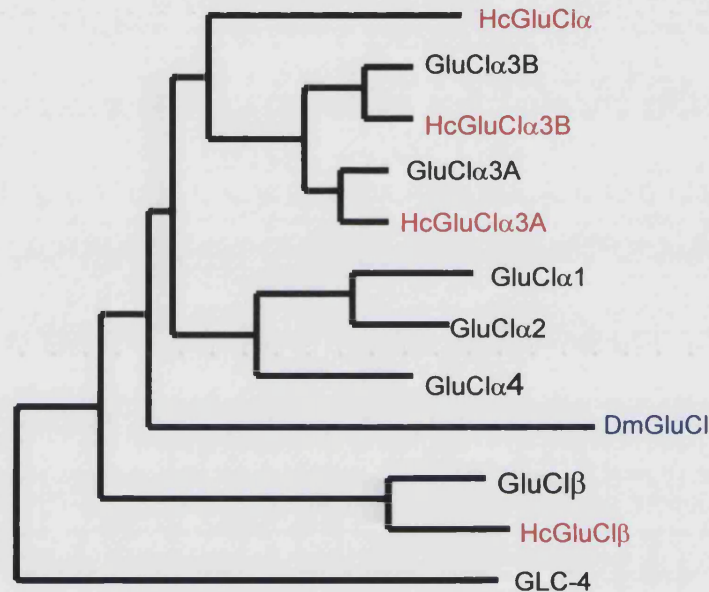
Fig 1.8 Neighbour-joining tree to illustrate the relationships between the identified *C. elegans*, *H. contortus* and *D. melanogaster* GluCl subunits
Amino-acid sequences were analysed. Taken from Yates et al., 2003.

the α and β subunits and may therefore represent a 'γ' subunit. Related sequences are present in the *Brugia malayi* genome, as yet we do not known whether this is also true for *H. contortus*.

The nomenclature of some of the GluCl genes and subunits is rather confusing, as may be obvious from Table 1.1. Some of this confusion stems from the original isolation of *C. elegans* avr-14 by both genetic (Dent et al., 2000) (*avr* = <u>a</u>vermectin <u>r</u>esistance) and molecular cloning (Laughton et al., 1997a) methods: originally *avr-14* was referred as *gbr* (<u>GA</u>BA-receptor <u>r</u>elated)-2 in the absence of any functional data and the name has continued to be used for the parasite orthologues. In *C. elegans* the subunits encoded by this gene have been referred to as GluClα3A & -B (Dent et al., 2000). A possible source of confusion in applying this nomenclature to the *H. contortus* subunits is that no 'α2' subunit has been identified to date and the

41

H. contortus α subunit is clearly different from *C. elegans* α1 (Cheeseman et al., 2001). In this work, and in order to clarify the present nomenclature, where clear orthologues of identified *C. elegans* genes are identified in parasites, equivalent names (*avr-14*, GluClα3) will be used. Where the evolutionary relationship between the genes is more uncertain (*HcGluClα*), we will use the names originally given in the literature.

1.8.1 Pharmacology of GluCl channels

The current understanding of nematode GluCl pharmacology has been derived from the following experimental approaches: two-electrode voltage clamp recordings from *Xenopus* oocytes expressing *C. elegans* GluCl subunits, radioligand binding studies on membranes from either whole worms or cell-lines expressing GluCl subunits, and electrophysiological assays using nematode tissue preparations. Pharmacological evidences suggest that the GluCls are the high-affinity binding sites for the AMs in nematodes. The current pharmacology data from all *C. elegans* GluCl subunits expressed in *X. laevis* oocytes, are summarised in table form in Pemberton et al (Pemberton et al., 2001).

Interestingly, the concentrations of IVM required to gate *C. elegans* GluCls expressed in *Xenopus* oocytes are high when compared to the concentrations able to paralyse pharyngeal pumping and motility in worms *in vitro*. Besides, a recent electrophysiological study on *C. elegans* pharynx, demonstrated that the native pharyngeal GluCls from *C. elegans* were considerably more sensitive to IVM than GluCls expressed in *Xenopus* oocytes (Pemberton et al., 2001). In this work the inhibitory response observed on the *C. elegans* pharynx was caused by a depolarisation of the membrane and not the previously suggested hyperpolarisation (Dent et al., 2000). IVM elicited a chloride-dependent depolarisation of the muscle: this response was typically irreversible and highly potent, with an $EC_{50}=2.7$ nM (Pemberton et al., 2001). The potency of the IVM response was comparable with concentrations shown to paralyse the pharynx *in vitro* (Avery and Horvitz, 1990; Geary et al., 1993). This could be explained by potentiation of the IVM response by endogenous glutamate (Pemberton et al., 2001). In support of this, a recent study has shown that glutamate potentiated AM binding to the *H. contortus* HcGluClα subunit (Forrester et al., 2002). Alternatively the observed differences of IVM

sensitivities could be explained by the native subunit composition of the IVM receptor. So far only a limited number of C. elegans GluCl subunit combinations have been successfully expressed in oocytes and none of these seemed to reflect the composition of native GluCls. Therefore, the elucidation of the subunits that form the native avermectin/GluCl receptor is vital to understand the pharmacology of AMs in this therapeutical relevant receptor.

Studies of H. contortus GluCl pharmacology have largely taken a radioligand binding assay approach. IVM has been shown to bind a high affinity site in H. contortus whole worm membrane preparations with a K_D ranging from 0.07-0.6 nM (Rohrer et al., 1994; Hejmadi et al., 2000; Cheeseman et al., 2001). This is comparable to the high affinity IVM binding site (K_D = 0.26 nM) described in C. elegans (Schaeffer and Haines, 1989) and to the concentrations of the drug that exhibit anthelmintic activity. Further binding studies were conducted with membranes prepared from COS-7 cells, a mammalian cell-line, expressing individual H. contortus GluCl subunits (Cheeseman et al., 2001; Forrester et al., 2002). As predicted by functional data from the C. elegans orthologues, the HcGluClα and HcGluClα3B subunits were shown to bind [^{3}H]-IVM with K_D values of 26-110 pM and 70 pM respectively. These data implicate the high-affinity IVM binding site to be a GluCl. Binding of [^{3}H]-IVM to the individual subunits and whole worm membranes was inhibited by a variety of AVMs, implying they all bound the same site. However glutamate, GABA and PTX failed to compete for the IVM binding site. The recombinant HcGluClα3A and HcGluClβ subunits exhibited no specific [^{3}H]-IVM binding, as predicted from the properties of their C. elegans orthologues expressed in Xenopus oocytes. Finally, radioligand binding assays indicate that glutamate and AMs do not share the same binding sites, as glutamate does not compete for IVM binding-sites in membrane preparations.

Table 1.2 summarises the pharmacology of the C. elegans and H. contortus GluCl subunits.

Table 1.2 Pharmacology of *C. elegans* and *H. contortus* GluCl subunits

C. elegans		*H. contortus*	
GluClα1 (*glc-1*)	Forms ivermectin-gated channels (Cully et al., 1994; Etter et al., 1996)		
GluClβ (*glc-2*)	Forms glutamate-gated channels (Cully et al., 1994)	HcGluClβ	Does not bind ivermectin (Cheeseman et al., 2001)
GluClα4 (*glc-3*)	Forms glutamate- and ivermectin- gated channels (Horoszok et al.,2001)		
GluClα2A/α2B (*avr-15*)	Forms glutamate- and ivermectin-gated channels (Dent et al., 1997; Vassilatis et al., 1997)	?	?
GluClα3A (*avr-14*)	Forms glutamate- and ivermectin- gated channels	HcGluClα3A	High affinity ivermectin binding (Cheeseman et al., 2001)
GluClα3B	Does not form functional channels (Dent et al., 2000)	HcGluClα3B	Does not bind ivermectin (Cheeseman et al., 2001)
X	x	HcGluClα	High affinity ivermectin binding (Cheeseman et al., 2001; Forrester et al., 2002)
GLC-4 (*glc-4*)	Does not form functional channels (Cully et al., 1996)		

1.8.2 Distribution of GluCl subunits

The expression patterns of the *C. elegans* GluCl genes have been studied using transformation techniques, where a putative promoter is fused to a reporter gene, either GFP or lacZ, and then microinjected into worms. Expression of the reporter gene in a cell indicates that the 'promoter' is active in that cell and the gene will be expressed there (Fire et al., 1990; Mello and Fire 1995). However, this technique presents some disadvantages such as, it may not indicate the intracellular location of the normal gene product and usually it is assume that the promoter used in those assays mimics the natural one. In parasitic nematodes, where transformation is much more difficult, the expression of the GluCl subunits has been studied using affinity-purified anti-subunit antibodies in immunofluorescence experiments.

In *C. elegans*, reporter gene constructs have shown that *avr-14* and *avr-15* are widely expressed in the nervous system (Dent et al. 1997, 2000) whereas *glc-2* expression is confined to pm4 pharyngeal muscle cells (Laughton et al., 1997b). *Avr-15* is also expressed in the pm4 and pm5 muscle cells of the pharynx (Dent et al., 1997). The relaxation of those muscles is triggered by the M3 pharyngeal motor neurons, a pair of fast inhibitory glutamatergic neurons. Also, the IVM effect observed in the pharynx of *C. elegans* was dependent on GluClα2 (Pemberton et al., 2001). Threfore, it is likely that the GluCl/IVM pharyngeal muscle receptor is a heteromer comprised of GluClα2, GluClβ and possibly one other GluCl subunit. To date, there have been no reported studies on the expression patterns of the *glc-1*, *glc-3* or *glc-4* genes.

In *H. contortus,* HcGluClβ was detected on motor neuron commissures but not on pharyngeal muscle (Delany et al., 1998). The HcGluClα3 subunits were detected in motor neuron commissures, nerve cords and the nerve ring (Jagannathan et al., 1999). In that work the same antibody, stained *A. suum* dorsal and ventral cords. As far as HcGluClα is concerned, no spatial data was described but RT-PCR studies showed the level of expression of this subunit was found to be adult > L_3 > eggs (Forrester et al., 1999).

The distribution of GluCl subunits from *C. elegans* and *H. contortus* known at the time I started this project is summarised in Table 1.3.

Table 1.3 Early data of the distribution of the GluCl subunits in *C. elegans* and their orthologous In *H. contortus*

	C. elegans		*H. contortus*	
GluClα1 (*glc-1*)	?	?		?
GluClβ (*glc-2*)	pharyngeal muscle[b]	HcGluClβ	motor neuron commissures[c]	
GluClα4 (*glc-3*)	?	?		?
GLC-4 (*glc-4*)	?	?		?
GluClα2 (*avr-15*)	pharyngeal muscle, some motor neurons in the head and ventral cord [a]	?		?
GluClα3 (*avr-14*)	extrapharyngeal neurons in the head, sensory neurons and ventral cord motor neurons[e]	HcGluClα3 (GluClα3A & GluClα3B)	motor neuron commissures, lateral and ventral nerve cords and nerve ring[d]	
x	x	HcGluClα	?	

[a] Dent et al., 1997. [b]Laughton et al., 1997a.[c] Delany et al, 1998.[d] Jagannathan et al, 1999. Note that the antibodies used in this work did not distinguish between the two alternative spliced variants HcGluClα3A and α3B. [e] Dent et al., personal communication (now Dent et al., 2000) ?=not yet identified; x=not present

As indicated by the number of question marks and crosses, a considerable amount remains to be discovered about the expression pattern of the *H. contortus* GluCl subunits. Besides, the antibody used to study the distribution of the HcGluClα3 subunits did not discriminate between the expression pattern of the alternatively-spliced products of the *H. contortus avr-14* gene, HcGluClα3A and HcGluClα3B.

1.9 Project Aims

A full understanding of the functions of the nematode glutamate-gated chloride channels (GluCls) and the effect of the avermectins/milbemycins (AMs), requires that we know where the receptors are expressed, their subunit composition and their physiological roles within the worm. Since the native GluCls are presumed to be pentamers, simply from the number of nematode GluCl subunit genes isolated so far, multiple forms of this channel must exist in worms. However, there was no direct evidence on the subunit composition of any nematode GluCl receptor. It was known that the GluCls are the target sites for the AMs, and that these drugs inhibit pharyngeal pumping (and hence feeding), motility and fecundity in nematodes. However, the nematocidal mechanism of the AMs still remained unknown.

The general aim of this project was to get insights into the composition and function of the native avermectin/GluCl receptor of *Haemonchus contortus*. In particular, I wished to map the distribution of all the GluCl subunits isolated for *H. contortus* and to study possible functions of GluCls using *Caenorhabditis elegans* as a model nematode.

The specific aims of the first part of the project included: the production of subunit-specific polyclonal antibodies raised against the HcGluClα, HcGluClβ, HcGluClα3A and HcGluClα3B subunits, and the immunolocalisation of these subunits in whole mount preparations of *H. contortus* adult worms. The results obtained from this work suggested that the *H. contortus* GluCls might have a role in locomotion and nematode sensory functions. This led to the second part of this project, which was to investigate possible roles of nematode GluCls, through behavioural assays conducted in *C. elegans* such as chemosensation and locomotion.

CHAPTER 2

PRODUCTION OF POLYCLONAL ANTIBODIES

2.1 Introduction

Most of the gene expression patterns described in *C. elegans* have been identified using promoter/reporter gene constructs. In contrast, no genetic transformation methods have been developed yet for *H. contortus* and the closest approach has been the use of *C. elegans* as an expression host for *H. contortus* genes (Britton et al., 1999). Thus, in *H. contortus* and other parasitic nematodes detection of gene expression has been mainly studied through immunocytochemistry (Keating et al., 1995; Delany et al., 1998; Jagannathan et al. 1999; Johnson and Stretton, 1987; Johnson et al., 1996; Maule et al., 1996).

In order to define the expression pattern of the GluCl receptor in *H. contortus*, specific antisera were raised against the currently known HcGluCl subunits. Two different approaches were used in this project to raise polyclonal antibodies. The first method consisted of the production of a recombinant protein expressed in a prokaryotic system, which once purified could be used to raise antibodies in rabbits, and the second method, of the use of synthetic peptides as antigens. In the following sections I will summarise the crutial steps to consider when producing antibodies.

2.1.1 Properties of antigens and antibodies

The term antigen refers to any molecule that can bind to an antibody, while the term immunogen is used when it induces an immune response mediated by lymphocytes. An immunocompetent animal can produce antibodies with well over 10^7 different antigen-combining sites (Harlow and Lane, 1988a). This represents a higher diversity of possible antibodies per antigen than using monoclonal antibodies where all of the descendants of one hybridoma cell line are identical, recognising hence only one epitope. Polyclonal mixtures of antibodies react with multiple epitopes on the surface of the antigen, being potentially more tolerant of minor changes in the antigen (e.g. heterogeneity of glycosylation, or slight denaturation) than will monoclonal antibodies. Although hybridoma cell lines provide an unlimited supply of homogeneous antibodies with a defined specificity, the production is time consuming and monoclonal antisera against peptide-antigens produce low titres

(Harlow and Lane, 1988a). For all the reasons mentioned above, polyclonal antibodies were preferred rather than producing monoclonal antibodies.

2.1.1.1 Immunogen properties

An ideal immunogen has to have three chemical features: 1) an epitope that can be recognised by the cell-surface antibody found on B cells, 2) it must be degradable, 3) the processed antigen fragments must bind simultaneously to both: the major histocompatibility complex (MHC class) II protein and the T-cell receptor to promote helper T cells-and B cells communication. This last requirement imposes a minimum size limit on an immunogen of M.W: 10 000 Da (Catty and Raykundalia, 1988). However, physical coupling of small molecules (haptens) to larger immunogenic ones (carriers) overcomes this problem (Erlanger, 1980). While the haptens serve as epitopes for binding to the antibodies on the B-cell surface, the carriers provide the MHC class II-T cell receptor binding sites.

2.1.1.2 Peptides vs. recombinant proteins

When a cloned DNA sequence is available, peptides or bacterially expressed proteins can be used as immunogens. Peptide antigens have advantages over whole protein antigens in that the antibodies generated may be targeted to unique sequence regions. The major disadvantage of anti-peptide antibodies is that because of peptide structural features, they may not recognize the native protein. In contrast, because of the larger size of the bacterially expressed protein, there is a better chance that the antibodies will bind to the native protein (Harlow and Lane, 1988a). However, because of possible toxic side effects of over-expression, some recombinant proteins are difficult to express in bacteria or, when expressed, they may result in inclusion bodies.

The successful production of anti-peptide antibodies often depends on the prediction of the peptide location within the proteins three-dimensional structure. Peptides with amino acids exposed on the surface of the native protein are more likely to be antigenic. When choosing the peptide sequence, the hydrophilicity value and the antigenic index for each amino acid should be considered (Kyte and Doolittle, 1982; Jameson and Wolf, 1988). Peptide hydrophilic regions are likely to be on the outside of the molecule and thus available for reaction. Besides,

50

hydrophilic peptides are more likely to be soluble for coupling reactions. Finally, the design of a peptide should take into consideration the method of coupling to the carrier protein.

2.1.1.3 Coupling of hapten to carrier protein

Most coupling methods depend on the presence of free amino, sulfhydryl, phenolic or carboxylic acid groups (Harlow and Lane, 1988a). Free amino groups used for coupling will be found on lysine side chains or on the amino-terminal residue. Sulfhydryl groups are found on cysteine side chains, phenolic groups on tyrosines and carboxylic acid groups on aspartic and glutamic acids and on the carboxy terminal residue. Peptides should preferably be linked to the carrier via the carboxy- or amino-terminal residue to avoid disruption of putative central epitopes. However, this depends on the peptide chosen and coupling through central epitopes can still produce good immunogens.

The cross-linkers used in this work were glutaraldehyde and the sulfhydryl-reactive cross-linking agents (maleimides): Sulfosuccinimidyl-4-(N-maleimidomethyl) cyclohexane-1-carboxylate (sulfo-SMCC) and m-Maleimidobenzoyl-N-hydroxysulfosuccinimidine ester (sulfo-MBS). Glutaraldehyde is a bifunctional cross-linker that reacts with free amino groups found on lysine side chains or on the amino-terminal residue. It is used when the synthetic peptide contains preferably only a single free amino group at its amino terminus (Reichlin, 1980). The maleimides (sulfo-SMCC and sulfo-MBS) are heterofunctional cross-linkers. The sulfosuccinimide group reacts with primary amines and the maleimide group reacts with free sulfhydryls present in cysteine residues. Since heteroreagents possess two selectively reactive groups that allow coupling to be carried out in a stepwise manner, better control of the conjugation chemistry is attainable, reducing the occurrence of unwanted side reactions such as homoprotein polymers (Peeters et al., 1989).

2.1.2 Immunisations

2.1.2.1 Adjuvants

Since soluble substances are readily cleared from circulation, either by some metabolic pathway or by excretion, through routes that largely by-pass reservoirs of immunopotent cells, they rarely stimulate the production of effective reagent antibodies. This problem is normally overcome by administering the antigen with some sort of adjuvant. Even then, they can vary widely in immunogenicity (Hurn and Chantler, 1980). Adjuvants provoke an immunogen depot effect protecting the antigen from rapid dispersal, making antibody responses more persistent. They also contain substances that stimulate the secretion of lymphokines, which recruit macrophages to the site of antigen deposition, increasing the local rate of antigen-processing cells and causing a local inflammatory reaction at the site of injection. Two methods of forming a deposit involve using mineral oils such as those present in Freund's or TiterMax® Gold adjuvants, or using aluminium hydroxide precipitates such as Imject® Alum. TiterMax® Gold adjuvant produce a more stable emulsion, easier to emulsify and is less viscous than Freund's adjuvant. However, side effects of water-in-oil formulations can invoke very aggressive and persistent granulomas in the host. This can be avoided by using aluminum hydroxide based adjuvants, instead. In this case, the immunogen is either allowed to adsorb to the preformed aluminium salt or can be trapped in the salt during precipitation. The final mixture is not viscous and is very simple to prepare.

2.1.2.2 Choice of animal, dose, and immunisation timing.

In most cases, rabbits represent the best choice of animals for producing polyclonal antibodies. They can yield up to 25 ml of serum from a single bleed and 150 ml from the final exanguination. They are also easy to immunise and bleed, giving good IgG responses to a variety of immunogens with long-term adjuvant-antigen mixtures. Because only small volumes of serum can be obtained from small animals such as rats, mice, hamsters and guinea pigs, these are not normally chosen for polyclonal antibody production. Although mice and rats are most commonly used for producing monoclonal antibodies, they can be very useful when polyclonal antibodies raised in different animal species rather than in rabbit are required, and when the volume of antiserum to be recover is not that critical.

Immunisations should be done in animals that are as far as possible, in evolutionary distance, from the source of the antigen. The use of chickens provides an alternative route when highly conserved mammalian antigens are weakly or not immunogenic in rabbits or rodents. The maximal yield of chicken serum is 500 ml. Only when large volumes of sera are needed, larger animals such as sheep, pigs, donkeys and horses are required. The best yields obtained form sheep antiserum are: 300-600 ml from individual bleeds and 5 litres from the final bleed. (Hurn and Chantler, 1980; Catty and Raykundalia, 1988).

The dose of antigen depends on the form and immunogenicity of the antigen. Suggested doses for rabbits, mice and rats vary from 10 to 100 μg. The dosage required for larger animals does not increase in proportion to body weight: 0.25-5 mg is satisfactory for sheep and 0.5-10 mg for donkeys. The choice of injection route may be influenced by the physical nature of the injection (e.g. immunogens in water in oil adjuvant formulations should be given intradermal or subcutaneously) and by the type of animal used (Catty and Raykundalia, 1988). Individual variation in response is often very striking; therefore groups of at least 2 animals should be started.

Primary immune responses are often very weak. When an animal is boosted, a much faster, more potent and more persistent secondary response occurs. A minimum of 2 weeks is advised before reintroducing the antigen to a primed animal. Because memory cells are long-lived, the secondary response can take place months or years after the primary response. The concentration of antibodies produced after the second injection increases exponentially and consists mainly of the high affinity IgG isotype. Antibody concentration and quality also increases in hyperimmunised aimals. As far as timing is concerned, to prevent rapid clearance of the newly injected antigen, the circulating level of antibody should be allowed to drop enough before injections.

The aim of the present study was to produce polyclonal antibodies against the *H. contortus* GluCl subunits. Two different approaches were assayed: the attempt to use a recombinant protein expressed into a prokaryotic system, and the use of synthetic peptides as antigens. The first part of this chapter includes the cloning of a HcGluClα3B cDNA fragment into an inducible expression vector, and its expression in *Escherichia coli*. Since the resulting protein was insoluble and once solubilised its purification was unsuccessful, subunit-specific synthetic peptides were preferred to produce polyclonal antibodies. Thus, the second part describes the production and purification of HcGluClα3A, α3B and HcGluClβ anti-peptide antibodies plus the purification of the anti-HcGluClα antibodies.

2.2 Materials and Methods

2.2.1 Biological materials

2.2.1.1 Bacterial strain genotypes

XL-1 Blue: *supE44 hsdR17 recA1 endA1 gyrA46 thi relA1 lac⁻* F' [*F' proAB lac^q lacZ* ΔM15 Tn10(tetR)]. Supplied by Stratagene Ltd (Cambridge, UK)

JM105: *supE endA sbcB15 hsdR4 rpsL thi* Δ(*lac-proAB*) F' [*traD36 proAB⁺lacI^q lacZ* ΔM15]. Supplied by New England Biolabs (Hitchin, UK)).

BL21: F⁻, *ompT*, hsdS (r_B⁻, m_B⁻), gal. Supplied by Amersham Biosciences (Little Chalfort, UK).

TOP10: F⁻ *mcrA* Δ(*mrr-hsd*RMS-*mcr*BC)φ*80lacZ*ΔM15 Δ*lac*X74 *deoR recA1 ara*D130 Δ(*ara-leu*)76797 *gal*U *gal*K *rpsL endA1 nupG*. Supplied by Invitrogen (Paisley, UK).

2.2.1.2 Laboratory animals

Rabbits and rats were obtained from the University of Bath, Animal House breeding colony.

2.2.2 Plasmid DNA

pCR®-Blunt II and pCR®-Blunt II TOPO vectors (Kan^r, Zeo^r): supplied by Invitrogen (Paisley, UK). Vector details can be downloaded from the company web site: http://ww.invitrogen.com.

pGEX-2T vector (Amp^r): obtained from Alison Bibbard, University of Bath. Vector details can be obtained from Amersham Biosciences web site: http://ww.amershambiosciences.com

2.2.3 Buffers & Media

2.2.3.1 Buffers

PBS (phosphate-buffered saline): 140 mM NaCl, 2.7 mM KCl, 10 mM Na_2HPO_4, 1.8 mM KH_2PO_4, pH 7.4). Autoclaved.

10 X TBE: 0.89 M Tris-Cl, 0.89 M boric acid, 20 mM EDTA, pH 8.0

50 X TAE: 2 M Tris Acetate, 50 mM EDTA, pH 8.0

2.2.3.2 Bacterial Media

LB: 10 g tryptone, 5 g yeast extract, 5 g NaCl, H_2O to 1 l. Autoclaved.

LB agar: 15 g agar per 1 l LB. Autoclaved.

SOC: Disolve 20 g tryptone, 5 g yeast extract and 0.5 g NaCl in 950 ml ddH_2O. Add 10 ml of 250 mM KCl, adjust pH to 7.5 with 5 M NaOH, and add ddH_2O to 1 l. Autoclave and add 10 ml sterile 1M $MgCl_2$.

2.2.4 Reagents and others materials

All chemicals used were of analytical grade and obtained from Sigma Chemical Company Ltd. (Poole, UK) and BDH chemicals (Poole, UK). Restriction enzymes were obtained from New England Biolabs ((NEB), Hitchin, UK)), Promega (Southampton, UK) or Amersham Biosciences (Little Chalfort, UK). DNA molecular weight markers were purchased from NEB, Promega and MBI Ferementas (Vilnius, Lithuania). Protein molecular weight markers were obtained from Amersham Biosciences and Bio-Rad (Cambridge, USA). DNA polymerase Expand ™ High Fidelity was obtained from Roche Molecular Biochemicals (Lewes, UK). T4 DNA Ligase was purchased from Promega. DNA gel extraction kit was obtained from QIAGEN (Crawley, UK) and the CONCERT™ plasmid preparation kit from GibcoBRL, now GIBCO-Invitrogen (Paisley, UK). Zero Blunt® PCR cloning kits were supplied by Invitrogen (Paisley, UK). Sources from other particular products will be indicated in the following sections.

Plasticware was Sterilin (Bibby Sterilin Ltd., Stone, UK), Nunc (Life Technologies Ltd), Paisley, UK) and Falcon (Falcon, New Jersey, USA).

General DNA Methods

2.2.5 The Polymerase Chain Reaction (PCR)

The polymerase used to amplify DNA by PCR was the Expand High Fidelity PCR system (Expand HF). This enzyme is composed of a mix containing thermostable Taq DNA and Pwo DNA polymerases. The advantage of this system is given by the 3'-5' exonuclease proofreading activity of the Pwo DNA polymerase, which increases the fidelity of DNA synthesis compared to Taq. Expand HF generates a mixture of 3' single A overhang and blunt ended PCR products, allowing direct ligation into 3'-T overhangs or Zero Blunt® (Invitrogen) cloning vectors. A typical PCR reaction contained 300 µM of each dNTP, 300 nM of each primer, 2.5 units (U) of the Expand HF enzyme, Expand HF buffer with 1.5 mM $MgCl_2$, 10 ng DNA and ddH_2O to 30 or 50 µl. A reaction where no template was added into the mixture was included as a negative control. Amplification conditions consisted of 2 min incubation at 94°C followed by the addition of the enzyme and then 35 cycles of denaturation at 94°C for 30 s, annealing for 30 s and extension at 72°C for 30 s, followed by a final extension of 72°C for 3 min. The annealing temperature (Tm) was set according to the primers used in the reaction. All amplifications were carried out on a PTC-150 hot-bonnet minicycler (GRI, Braintree, UK). PCR reactions were analysed by electrophoresis through a 1-1.5 % (w/v) agarose gel (section 2.2.6).

2.2.6 Agarose gel electrophoresis

Agarose gels were made by the addition of 1-1.5 % (w/v) agarose to 1 x TAE or TBE buffer. The agarose was dissolved by heating in a microwave oven at 40 % power. Visualisation of DNA was achieved by the addition of 5 µg/ml ethidium bromide to this solution. Gels were poured in a gel cast with comb and allowed to set before running in 1 X TAE or TBE in a horizontal gel apparatus at 100 V for 1-2 h. DNA samples were loaded with 6 X loading dye (15 % (w/v) Ficoll, 0.25 % (w/v) bromophenol blue, 0.25 % (w/v) xylene cyanol). Molecular weight markers 100 bp (NEB) and 1Kb (NEB or Promega) were used. DNA was visualised under UV illumination and photographs were taken using a Polaroid camera with a yellow filter and Polaroid 667 black and white ISO3000/36 film.

2.2.7 Purification of DNA from agarose gels

The protocol used was the one provided with the QIAquick Gel Extraction Kit. It allows the extraction and purification of DNA from 100 bp to 10 kb out of agarose gels in TAE or TBE buffer. DNA adsorbs to the silica-membrane contained on spin-columns in high salt conditions, while contaminants pass through the column. The buffers are a proprietary formulation. All the centrifugation steps were done at 12000 x g. The DNA band was excised and weighted in a 1.5 ml microfuge tube. Four volumes of buffer QX1 were added per volume of gel (100 mg correspond to 100 µl) and the tube was incubated at 50°C vortexing every 2-3 min. After the agarose was dissolved 1 gel volume of isopropanol was added. To bind DNA to the column membrane, the sample was applied in a QIAquick spin column placed into a 2-ml collection tube, and centrifuged for 1 min. To remove all traces of agarose, the column was washed with 0.5 ml of buffer QX1. A sample of 0.75 ml of PE buffer was added and then let to rest for 2-5 min before centrifugation. Residual ethanol from PE buffer was removed by an additional centrifugation step. The DNA was eluted in a 1.5 ml microfuge tube with 30-50 µl of ddH$_2$0 left standing for 1 min before centrifugation. DNA was stored at -20°C.

2.2.8 DNA quantification

Quantification of PCR products or linearised plasmid DNA, was estimated by comparison with a molecular weight DNA marker of known concentration (Gene Ruler^{TM} 100 bp or 1 kb, MBI Ferementas), analysed by agarose gel electrophoresis.

When required, the amount of DNA was estimated by determining the Absorbance at 260 nm of a 1:50 dilution of the sample in water. The concentration was calculated using the equation:

[DNA] µg/ml= Absorbance$_{260}$ x 50 x dilution factor

Absorbance at 280 nm was also determined to obtain a ratio for $O.D_{260}/O.D_{280}$ as an indication of DNA preparation purity.

2.2.9 DNA cloning

2.2.9.1 Preparation of *Escherichia coli* competent cells

REAGENTS	COMPONENTS
TSB medium	1 g Tryptone, 0.5 g Bacto-yeast extract, 0.5 g NaCl and 10 g Polyethylene Glycol (M.W: 3000) in 100 ml of ddH$_2$O, pH 6.1 adjusted with HCl 1N. Autoclaved for 1 hour. Added 5 % (v/v) DMSO, 10 mM MgSO$_4$, 10 mM MgCl$_2$. Adjusted to pH 6.1 with 3-5 drops of 1 mM HCl.

Ten ml of LB medium in a 100 ml flask were inoculated with 3-4 colonies of *Escherichia coli* XL1-Blue, JM105 or BL21 from LB plates and grew by shaking at 37°C to A$_{600}$= 0.5 O.D (4 hours aprox.). Upon reaching the required O.D, 1 ml of this culture was inoculated to 100 ml of fresh LB in 1 liter flask and grew in the same conditions as described above. The flask was chilled on ice and the cells were harvested by centrifugation in a Sorvall® RC-5B centrifuge at 4000 rpm in a SS-34 rotor for 10 min at 4°C. The pellet was resuspended in 10 ml of TSB medium and left on ice for 10 min. Aliquots of 500 µl were prepared and stored at -70°C.

2.2.9.2 Ligation

PCR products were cloned into pCR®-Blunt II or pCR®-Blunt II TOPO vectors using 50 ng of linearised plasmid. For the cloning into pGEX vector, 100 ng of plasmid and a 10:1 molar insert-to-vector ratio were used. Ligation was done in the presence of 0.1 volume of 10 X Ligation Buffer (Promega, supplied with 10 mM ATP) and 4 units of T4 DNA Ligase (Promega) in a final volume of 10 µl. The reaction was mixed gently and incubated overnight at 15°C.

2.2.9.3 Transformation of plasmid DNA into *E.coli* strains

A tube with 100 µl of *E. coli* XL1-Blue, JM105 or BL21 strains or 50 µl of One Shot™ TOP10 competent cells stored at -70°C, was thawed on ice for 5 min. An aliquot of 50-100 ng of plasmid DNA or 2 to 10 µl of the ligation mix was added and the tube was placed on ice for 30 min. Cells were heat shocked at 42°C for 30 sec

followed by immediate transfer to ice for 2min. A sample of 200 µl of SOC or LB media (pre-warmed to 37°C) was added and the mixture incubated in a shaker at 37°C for 1 h. Aliquots of 20, 50 and 100 µl of transformed cells were spread on LB agar containing plates in the presence of the selection antibiotic (Kanamycin, 50 µg/ml or Ampicillin 100 µg/ml). Plates were incubated at 37°C overnight.

2.2.9.4 Screening of transformants

Colonies were picked and grown for 12-16 hours in LB medium containing 50 µg/ml Kanamycin or 100 µg/ml of Ampicillin as required, and plasmid DNA was purified from bacteria (section 2.2.10). This DNA was analysed initially by restriction digestion (section 2.2.11) and then the clones that seemed to contain a DNA fragment of the expected size were sequenced (section 2.2.12).

2.2.10 Preparation of plasmid DNA

The alkaline lysis method from the CONCERT™ Rapid Plasmid Purification System (GibcoBRL) was used to isolate plasmid DNA from bacterial cultures. For small preparations, samples of 3 ml of an overnight bacteria culture were centrifuged at 14000 x g for 2 min and all medium removed. The resulting pellet was resuspended in 250 µl of G1 buffer (50 mM Tris-HCl, pH 8.0; 10 mM EDTA containing RNase A 20 mg/ml) by vortexing. Cells were lysed with 250 µl of G2 solution (200 mM NaOH, 1 % (w/v) SDS) and tubes were mixed by inversion before incubation at RT for 5 min to produce a clear solution. A sample of 350 µl of neutralization buffer (acetate and guanidine hydrochloride; proprietary formulation) was added and the solution mixed by inversion before centrifugation of samples at 14000 x g for 10 min. The resulting supernatant was placed into a spin cartridge, containing silica-based membranes where the plasmid DNA is selectively adsorbed, which was contained in a 2 ml wash tube. Following removal of the flow-through the column was washed with 500 µl of GX buffer (acetate, guanidine hydrochloride, EDTA, ethanol; proprietary formulation) followed by a wash with 700 µl of G4 buffer (NaCl, EDTA and Tris- HCl, pH 8.0, containing 95-100 % ethanol; proprietary formulation) at 14000 x g for 1 min. DNA was eluted from the column by the addition of 75 µl of TE buffer (10 mM Tris-HCl, pH 8.0; 0.1 mM EDTA) pre-warmed at 65-70°C, incubating for 1 min at RT and spinning down for 2 min. When higher concentrations and

higher purity of plasmid DNA were required, large-scale plasmid DNA preparations were obtained using either the High Purity CONCERT™ kit for maxipreps or the Qiagen Plasmid Maxikit (QUIAGEN), following the manufacturer instructions.

2.2.11 Endonuclease restriction assays

DNA samples of 1-5 µg were digested with 10 units of restriction enzymes in the presence of 0.1 volume of the reaction buffer recommended by the manufacturer. Sterile water was added to a volume of 30 µl and the reaction incubated at 37°C for 2 h. For double digestions, the enzymes that used the same reaction buffer were co-incubated into the reaction. When enzymes required different reaction buffers, the assay was first set for the one requiring low salt concentration in the reaction buffer, and after 1 h of incubation at 37°C, the second enzyme was added adjusting the salt concentration to the requirements of the second enzyme. Reaction was allowed to continue for 1 h at 37°C.

2.2.12 DNA sequencing and sequence analysis

Approximately 250 ng of DNA preparation was mixed with 10 pmol of primer in 6 µl of water and sent to sequence at the University of Bath DNA Autosequencing Service. The primers used for sequencing DNA cloned into pCR®-Blunt II or pCR®-Blunt II TOPO vectors, were the M13 forward and M13 reverse (Invitrogen) and the primers used for sequencing DNA cloned into the pGEX-2T vector were the 5' pGEX and 3' pGEX primers (GibcoBRL) (for primer sequences see table 2.1). Sequence analysis was carried out on the GCG (Genetic Computer group, Wisconsin, USA) suite of programs, accessible via the gnome workstation, for analysis and comparison with existing sequences in the database.

Table 2.1 Primers

Primer	Sequence	Tm (°C)	Suppliers
α3B 5'	5' NNNNNN<u>GGATCC</u>GAATTTCTTCGGAAG 3' ♣	55	GibcoBRL
α3B 3'	5' NNNNNN<u>GAATTC</u>*TTA*GTCCACCCTACG 3' ♦	55	GibcoBRL
pGEX 5'	5' GGGCTGGCAAGCCACGTTTGGTG 3'	57	GibcoBRL
pGEX 3'	5' CCGGGAGCTGCATGTGTCAGAGG 3'	57	GibcoBRL
M13 F(-20)	5' GTAAAACGACGGCCAG 3'	46	Invitrogen
M13 R	5' CAGGAAACAGCTATGAC 3'	52	Invitrogen

Restriction sites underlined: ♣ BamH I, ♦ EcoR I. The stop codon included in the α3B 3' primer is indicated in italics. All primers were ordered desalted and at 50 nmol scale.

2.2.13 Production of HcGluClα3B recombinant protein

2.2.13.1 Construction of the pGEX-GluClα3B plasmid

The pGEX expression system (Amersham Biosciences) was used to obtain a GluClα3B recombinant protein, which could then be used to raise polyclonal antibodies in rabbits. The DNA encoding the intracellular loop within the transmembrane domains III and IV of HcGluClα3B was amplified by PCR and cloned in frame into the pGEX-2T expression vector. Plasmid DNA containing the *Hcavr-14B* full-length sequence (obtained from C. Cheeseman, Univeristy of Bath) was used as template for PCR (PCR was described in section 2.2.5). Oligonucleotides α3B 5' and α3B 3' encode the 354-358 and 421-418 amino acids of the HcGluClα3B polypeptide sequence, respectively. In their 5' ends they possess 6 random nucleotides and specific restriction sites (Table 2.1) to ensure directional cloning into pGEX-2T vector, downstream and in frame with the *gst* gene. On the α3B 3' primer a stop codon followed the restriction site was also introduced.

Amplification conditions consisted of 2 min incubation at 94°C, followed by the addition of 2.5 units of the thermostable Expand ™ High Fidelity DNA polymerase and then 35 cycles of 94°C for 30 s, 55°C 30 s, 53°C for 30 s and 72°C for 30 s, followed by 72°C for 3 min. Amplification products were identified by

electrophoresis through a 1.5 % (w/v) agarose gel. The amplified DNA was purified from the gel, cloned into pCR®-Blunt vector (Invitrogen) and subcloned into pGEX-2T vector within the *Bam*H I and *Eco*R I sites of the vector polylinker.

2.2.13.2 Transformation of *E. coli* with pGEX plasmids

To get the recombinant plasmid pGEX:GluClα3B into *E. coli*, two transformation steps were required. The JM105 strain, with high transformation efficiency, was used first and the BL21 strain, required for the pGEX-2T expression, was used second. Therefore, the *Hcavr-14B* insert cloned into pCR®-Blunt vector was digested with *Bam*H I and *Eco*R I restriction enzymes and ligated into the pGEX-2T vector, previously linearised with the same enzymes. The ligation mix was used to transform *E. coli* JM105 cells. Screening of transformants was performed and the plasmid DNA isolated from one of these clones was used to transform the *E. coli* BL21 strain. The techniques mentioned above were described in sections 2.2.9 and 2.2.11.

2.2.13.3 Induction of fusion protein expression

E. coli BL21 cells containing the recombinant (pGEX-GST:GluClα3B) and the wild-type (pGEX-2T) plasmids were grown in LB medium containing Ampicillin (100 µg/ml) in an orbital shaker at 37°C. When the absorbance at 600 nm reached an O.D of 0.6, a sample of 1 ml (non-induced sample) was removed from the culture and the expression of the GST or GST:GluClα3B proteins was induced for 2 h by the addition of 0.1 mM iso-propyl-β-D-thiogalactopyranoside (IPTG) (final concentration) to the remaining culture. Induced and non-induced samples were precipitated and resuspended in PBS containing 1 mg/ml lysozyme and 1 mM PMSF. Finally, the cells were lysed by sonication on ice for 15 s and the debris precipitated by centrifugation at 4000 g for 15 min.

2.2.13.4 Detection of GST: GluClα3B recombinant protein

Aliquots of the IPTG non induced and induced insoluble and soluble material were analysed on a 12 % (w/v) SDS-PAGE (section 2.2.14). Proteins were transferred onto nitrocellulose membranes and probed with 1:1000, 1:2000 and 1:3000 antibody dilutions of goat anti-GST (Amersham Biosciences) antiserum and a

1:2000 dilution of a horseradish peroxidase (HRP)-conjugated rabbit anti-goat IgG secondary antiserum (section 2.2.15).

2.2.13.5 Solubilisation of inclusion bodies

Solubilisation of the GST:GluClα3B was carried out in the presence of a non-ionic detergent (NP-40). Bacteria were harvested by centrifugation at 7000 x g for 5 min and the cell pellet was resuspended in 100 mM NaCl, 1 mM EDTA, 50 mM Tris-HCl (pH 8.0) to a final concentration of 10 % (v/v). 1 mg/ml lysozyme and 1 mM PMSF were added and the mixture was incubated at RT for 20 min. Cells were collected by centrifugation at 5000 x g for 10 min, the supernatant was discarded and the pellet (spheroplasts) was resuspended in ice-cold 100 mM NaCl, 1mM EDTA, 0.1 % sodium deoxycholate (v/v), 50 mM Tris-HCl pH 8.0. The mixture was incubated on ice with occasional mixing for 10 min. Then, a final concentration of 8 mM $MgCl_2$ and 10 μg/ml DNase I were added and the solution was incubated at 4°C until the viscosity disappeared. Inclusion bodies were removed from suspension by centrifugation at 10000 x g during 10 min and solubilised by resuspending the pellet in 1 % NP-40, 100 mM NaCl, 1 mM EDTA, 50 mM Tris-HCl (pH 8.0). This final fraction was washed with 100 mM NaCl, 1 mM EDTA, 50 mM Tris-HCl (pH 8.0).

2.2.13.6 Purification of the GST:GluClα3B recombinant protein

The GST:GluClα3B protein was affinity-purified from solubilised bacterial protein extracts, prepared as described in section 2.2.13.5. Gutathione-agarose beads (Sigma) were swollen as recommended by the manufacturer and equilibrated with equilibration buffer: 100 mM NaCl, 1 mM EDTA, 50 mM Tris-HCl (pH 8.0) or PBS. A pilot purification assay was performed in 1.5 ml microcentrifuge tubes by mixing 100 μl of the slurry with 200 μl of protein extracts during 20 min at RT. Three washes of 1 ml of equilibration buffer or PBS were applied, centrifuging at 5000 x g to discard the supernatants. GST-recombinant proteins were eluted incubating the gel mixture with glutathione elution buffer (10 mM reduced glutathione (Sigma) prepared in 50 mM Tris-Cl (pH 8.0) or in PBS) during 15 min at RT. Eluted fractions were collected following centrifugations at 5000 x g and were analysed on a 12 % (w/v) SDS-PAGE. Finally, gel was washed with 10 V of equilibration buffer or PBS and stored at 4°C.

Protein Methods

2.2.14 Protein electrophoresis

Proteins were resolved through 12 % (w/v) sodium dodecyl sulphate polyacrylamide gel electrophoresis (SDS-PAGE). For the preparation of two 12% (w/v) separating gels, 6 ml of acrylamide solution (Sigma) (30% (w/v) acrylamide, 0.8% (w/v) N, N'-methylenebisacrylamide) were combined with 3.75 ml of 4X Tris-Cl/SDS pH 8.8 (1.5 M Tris-Cl pH 8.8, 0.4% (w/v) SDS; filtered through a 0.45-μm filter (Millipore, Bedford, USA) and stored at 4°C) and 5.25 ml of ddH$_2$O. The mixture was degassed under vacuum for 10 min and 100 μl of 10 % w/v ammonium persulfate (APS) (stored at 4°C for no more than 5 days) plus 10 μl of N, N, N', N'-tetramethylethylenediamine (TEMED) (Sigma) were added. The mixture was poured into assembled mini-gel glass plates (7 x 10 cm), overlaid with few drops of isopropanol to prevent contact with O$_2$ and allowed to polymerise. When gels were ready the solvent was removed and the gel interface rinsed with ddH$_2$O. A 4 % (w/v) stacking gel was prepared mixing 0.65 ml of acrylamide solution, 1.25 ml of 4X Tris-Cl/SDS pH 6.8 (0.5 M Tris-Cl, 0.4 % (w/v) SDS; filtered through a 0.45-μm filter and stored at 4°C) 3.05 ml of ddH$_2$O, 25 μl of 10 % (w/v) APS and 5 μl of TEMED. The solution was poured over the separating gels, the combs were inserted and they were allowed to set. After the stacking gel has polymerised, combs were removed and wells were rinsed with ddH$_2$O to remove unpolymerised acrylamide. Gels were placed into an electrophoretic chamber and 1 X running buffer (5 X stock: 3 g Tris-base, 14.4 g glycine and 0.5 g SDS in 100 ml of dd H$_2$O) was added.

Samples were resuspended in loading buffer (6 X stock: 0.35 M Tris-Cl, pH 6.8; 10 % (w/v) SDS, 36 % (v/v) glycerol, 5 % (v/v) β-mercaptoethanol, 0.012 % (w/v) bromophenol blue; store at -20°C) and denatured by incubation in a boiling water bath for 5 min. Finally, samples were centrifuged at 14000 x g for 3 min just prior to loading onto the gel. A rainbow molecular weight marker (10-250 kDa) (Amersham Biosciences) was also loaded.

Gels were run at 100 V until the dye front reached the bottom of the gel. They were stained by soaking and rotating in Coomasie Blue solution (50 % (v/v) methanol,

0.05 % (w/v) Coomasie Brillant Blue R, 10 % (v/v) acetic acid in ddH₂O). For the preparation of this solution, the Coomasie Brillant Blue R was first dissolved in methanol before adding the acetic acid and the water. Gels were destained with 50 % (v/v) methanol / 10 % (v/v) acetic acid in ddH₂O, until background staining was removed.

2.2.15 Western Blot

2.2.15.1 Blotting

A non-stained SDS-PAGE gel, two gel sized sets of 3 sheets of 3 MM Whatman filter paper (Whatman Ltd., Kent, UK) and a gel sized nitrocellulose membrane (Amersham Biosciences) (previously rinsed with ddH₂O), were soaked for 15 min in transfer buffer (25 mM Tris-HCl pH 8.3, 150 mM glycine, 0.037 % (w/v) SDS and 20 % ethanol (added immediately before using). One set of filter papers was aligned on the cathode plate of the graphite transfer electrode, followed by the nitrocellulose membrane and the gel rolled out on top of the membrane. This stack was overlaid with the second set of soaked filter papers and any air bubbles between layers were removed by rolling a glass pipette over the top of the "sandwich". The anode graphite plate was put on the top and it was connected to the power supply set at 0.8 mA/cm² of gel for 90 min.

2.2.15.2 Immunoprobing and detection

The nitrocellulose membrane was incubated overnight at 4°C in blocking solution (2 % (w/v) glycine, 5 % Marvel™ non-fat milk powder in TBST: 10 mM Tris-Cl pH 8.0, 150 mM NaCl, 0.1 % (v/v) Tween 20). The blot was briefly washed in TBST and incubated 1 hour at RT or overnight at 4°C with the first antibody diluted in blocking solution. The membrane was washed three times in TBST for 5, 10 and 15 min on a rotating table and incubated 1-2 hours at RT with a horseradish peroxidase-conjugated secondary antibody (Amersham Biosciences) diluted 1:1000 in TBST. The Electro Chemi- Luminescence (ECL) reagents (Amersham Biosciences) were used to detect immunoreactivity in the blot. An equal volume of detection solution 1 and 2 were mixed and poured onto the surface of the immunoprobed blot for 1 min. Excess fluid was drained off and the blot was wrapped in cling film. An X-ray film was placed in the dark on top of the blot inside a film cassette. Over a series of

exposure times (from 1 min to 5 min), films were developed using an X-Ograph Compact X2 processor.

2.2.16 Protein quantification

The Coomassie® Plus Protein Assay Reagent (PIERCE, Tattenhall, UK) was used for protein quantification. The method is based on the Bradford method (Bradford, 1976). The reagent contains: Coomasie® dye, methanol, phosphoric acid and solubilizing agents in water. Ninety-six well Nunc microtitre plates were used and either 10 or 15 µl of sample or standard protein (BSA) were added per well plus 300µl of the Coomassie® reagent. Plates were mix on a shaker for 30 sec and the absorbance was measured at 595 nm using a microtitre plate reader. A standard curve was prepared by plotting the average blank corrected 595 nm reading for each BSA standard, versus its concentration in µg/ml. This curve was used to determine the protein concentration of the unknown samples.

Anti-peptide antibodies

2.2.17 Production of polyclonal anti-peptide antibodies

2.2.17.1 Coupling of Peptides to Carrier Protein

The HcGluClβ, HcGluClα3A and HcGluClα3B peptides were synthesized on a Perseptive Biosystems 9050+ synthesizer and purified by HPLC by Dr. G. Bloomberg, Department of Biochemistry, University of Bristol. Peptides, stored at -20°C, were coupled to the carrier protein porcine thyroglobulin (Sigma, Poole, UK) using either glutaraldehyde (Grade 1, Sigma) or Sulfosuccincinimidyl-4-(N-maleidimidomethyl)-cyclohexane-1-carboxylate (sulfo-SMCC) (Calbiochem®, Beeston, UK) as crosslinkers.

2.2.17.1a HcGluClβ peptide

The peptide sequence used was the described by Delany et al (1998), designed in the N-terminus of the HcGluClβ mature polypeptide: RSTGGTQEQEILNELLSN, which corresponds to amino acids 24-41.

Two and a half mg of both freeze-dried porcine thyroglobulin (thyr) and HcGluClβ peptide were dissolved together in 0.1 M NaHCO₃ to give a final concentration of 2 mg/ml of thyr-peptide mixture. Glutaraldehyde (stored as a 25 % (w/v) aqueous solution at -20°C) from a fresh ampoule was added to a final concentration of 0.05 % (v/v). The mixture was inverted in a glass vial overnight at room temperature. A 0.1 volume of 1 M glycine ethyl ester (pH 8.0 with NaOH) was added and rotated as described before for 30 min to block unreacted gutaraldehyde. To remove the unbound peptide and excess of glutaraldehyde, the mixture was injected into a Slide-A-Lyzer® dialysis cassettes (PIERCE, Tattenhall, UK) of nominal molecular weight limit 10,000 Da and left to dialyse overnight in 1 l of PBS at 4°C. Finally the peptide conjugate solution was quantified using the Coomassie® Plus Protein Assay Reagent Kit (PIERCE) and stored in aliquots at -20°C.

2.2.17.1b HcGluClα3A and HcGluClα3B peptides

The HcGluClα3 peptide sequences used were, HcGluClα3A: CRIFVRRYKERSKRID and HcGluClα3B: CSERPALRLDLSNYRRRGWT. They correspond to amino acid residues 384-399 of GluClα3A and 373-391 of GluClα3B.

A sample of 3 mg of sulfo-SMCC was dissolved in 1 ml of 20 mM NaHCO₃. This solution was added to a 1.5 ml microcentrifuge tube containing 10 mg of thyroglobulin and was left at room temperature for 30 minutes. Unbound cross-linker was removed by gel filtration through a Sephadex G25 column of 10 ml (Amersham Biosciences), using 50 mM sodium phosphate buffer pH 7.0. The eluate was monitored at 220 nm, collecting fractions of 3 ml. The first peak, containing the SMCC-thyr conjugated, was stored at -20°C.

Samples of 8.6 and 10 mg of HcGluClα3A and 3B peptides were respectively activated with 1 mM DTT in sodium phosphate buffer pH 7.0 for 1 hour at room temperature. The excess of DTT was removed by gel filtration through a Sephadex G10 column of 10 ml (Amersham Biosciences), using 50 mM sodium phosphate buffer pH 7.0. The eluate was monitored at 280 nm. Peak fractions were collected immediately prior to the coupling reaction.

SMCC-thyr samples were mixed with half of the volume of the activated peptide fractions. The coupling was performed under argon (to prevent oxidation of sulfhydryl groups) at room temperature, stirring for 3 hours. The peptide conjugate solution was quantified using the Coomassie® Plus Protein Assay Reagent Kit (PIERCE) and stored in aliquots at -20°C.

For each peptide, a control coupling reaction using 5 mg of BSA (Sigma) as a carrier and 1.5 mg of m-Maleimidobenzoyl-N-hydroxysulfosuccinimidine ester (sulfo-MBS) (Calbiochem®) as a cross-linker, was carried out. The coupling reaction was performed as described above, using the remaining of the volume from the activation of the peptides.

2.2.17.2 Production of antisera

2.2.17.2a HcGluClβ rat antiserum

The antigen mixture was prepared adding dropwise one volume of the thyroglobulin-HcGluClβ conjugate to one volume of adjuvant (Imject® Alum, PIERCE), which was mixed by vortexing. The mixture was left at room temperature for 30 minutes, vortexing every 10 minutes for about 1 minute. Two anaesthetised male Wistar rats of 320 g were injected subcutaneously with 140 µg of the antigen mixture. Further immunisation timings were determined according to serum titres, and three doses of 70 µg were given two weeks, a month and four months after the first immunisation. A blood sample was taken day 0 (pre-immune serum). Test bleeds were done on anaesthetised animals by tail tip amputation.

2.2.17.2b HcGluClα3A and 3B rabbit antisera

For each peptide, two New Zealand white rabbits were immunised subcutaneously with thyroglobulin-peptide conjugates prepared as a water in oil emulsion with Titremax Gold™ (Sigma) as adjuvant, according to the manufacturer instructions. To prepare 1.0 ml of the antigen-adjuvant emulsion, 0.5 ml of antigen (volumen completed with PBS) and 0.5 ml of adjuvant were required. After the TiterMax Gold was vortexed and loaded in one syringe, two other syringes were loaded with 0.25 ml of aqueous antigen. The syringe containing the adjuvant and one of the loaded with the antigen solution, were connected via one 3-way stopcock. To obtain an adequate emulsion it was important to push the antigen into the adjuvant syringe

first and to push repeatedly the mixture between both syringes for approximately 2 min. Then, all the emulsion was pushed into one syringe and the empty one disconnected. The remaining syringe containing 0.25 ml of the aqueous antigen solution was connected end emlusified until a meringue-like emulsion was formed (aprox. 5 min).

The concentration of antigens used were 20 µg for the primings and 100 µg for the first second and third boosts given, according to serum titres, at weeks 2, 7 and 16 post-primings. A blood sample was taken the day 0 (pre-immune serum). To monitor sera titres, rabbits were preanaesthetised with Hypnorm 0,2 ml/Kg (Janssen Pharmaceutica (Beerse, Belgium)) and test bleeds were taken from the ear vein. When antibody titres reached a satisfactory level, animals were sacrificed by cardiac puncture under terminal anaesthetic. All animal handling was done by licensed staff.

2.2.17.3 Harvesting the sera

Collected blood was allowed to clot for 1 h at 37°C. The serum was separated from the clotted blood by centrifugation at 4°C, first at 2500 g for 30 min and then at 1500 g for 20 min. Purified supernatant was aliquoted and frozen at -20°C. Working aliquots were kept at 4°C in presence of 0.01 % (w/v) sodium azide.

2.2.17.4 Antibody quantification (ELISA)

Antibody production of isolated sera was assessed by performing enzyme linked immunoabsorbent assays (ELISAs).

Ninety-six well microtitre Falcon Pro-bind plates were coated with 10 µg/ml antigen in coating buffer (15 mM Na_2CO_3; 35 mM $NaHCO_3$, 0.01 % (w/v) NaN_3, pH 9.6). Plates were covered with foil paper and incubated overnight at 4°C. Unbound antigen was washed off the plates with wash buffer (PBS pH 7.0, 0.1 % (v/v) Tween-20) 3 times during 15 min each wash. The plates were drained of any residual solution by inverting and tapping on paper towels. Adsorption sites of the wells were blocked with 250µl of blocking buffer (PBS pH 7.0, 0.1 % (v/v) Tween 20, freshly prepared 1 % (w/v) casein) for 1h at RT. Plates were again washed

twice with wash buffer whereupon 100 μl/well of sera prediluted to 1/100 in wash buffer, was applied in duplicates in serial dilutions resulting in a 1/2 dilution in each well. Following an overnight incubation at 4°C, plates were washed four times with wash buffer before anti-rabbit Ig-peroxidase conjugated (Amersham Biosciences) or anti-rat Ig-peroxidase linked (Sigma) antibodies were applied at 1/1000 dilutions in wash buffer. Plates were incubated 1.5-2 hour at RT and washed again three times with wash buffer and two times with PBS. Then 100 μl of substrate solution (50 mM sodium acetate/citrate buffer pH 6.0, 0.1 mg/ml of 3, 3', 5, 5' tetramethyl benzidine (TMB), 0.006 % (v/v) H_2O_2) freshly prepared, was added and allowed to react in the dark for 10 min before being completed by the addition of 50 μl/well of 1.84 M H_2SO_4 (1:10 v/v dilution of concentrated stock). Absorbance was measured at 450 nm using a plate reader.

Antibody titre was determined by plotting absorbance against antiserum dilution, using the mean and standard error for each duplicate. The inflection point of the post-immune data when interpolated by drawing a line down to the X-axis, resulted in the Ab titre of the sera (http://www.perbio.com/pa/340913/html/chap6.html).

2.2.17.5 Antibody Purification

2.2.17.5a IgG isolation
Total IgG was first purified from the immune serum on Protein A Sepharose CL-4B columns (Sigma). A gram of the sepharose was swollen in 10 volumes (40 ml) of PBS pH 7.3. The slurry was packed into a column and washed with 10 volumes of PBS pH 7.3. Eight to 10 ml of antiserum were 1/10 diluted in PBS pH 7.3 and recycled through the column overnight at 4°C. Column was washed with PBS and IgG antibodies were eluted with 35 mM NaCl / 35 mM diethylamine pH 11.5 at 4°C. Eluted proteins were detected by absorbance at 280 nm, monitored by an uvicord (LKB-Optical Unit UV-1, Amersham Biosciences) and plotted on a chart recorder connected to the column. The eluants were neutralised by dialysis against PBS overnight at 4°C and stored at 4°C in presence of 0.01 % (w/v) sodium azide.

2.2.17.5b Peptide-Affinity Chromatography
Peptides were immobilised on cyanogen bromide (CNBr) -activated Sepharose 4B columns (Amersham Biosciences). A gram of CNBr-activated Sepharose 4B was

hydrated in 100 ml of 1 mM HCl pH 2.0. Swollen sepharose was poured on a sintered funnel connected to a vacuum pump and washed with 200 ml volumes of 1 mM HCl (pH 2.0-3.0), ddH$_2$O and 0.1 M NaHCO$_3$ pH 8.3 respectively. After the last wash, the swollen sepharose beads were mixed with 10 mg of peptide previously dissolved in 5 ml of 0.5 M NaCl / 0.1 M NaHCO$_3$ pH 8.3. The peptide-sepharose bead mixture was left to rotate end over end overnight at 4°C. Excess peptide was removed by washing with three gel volumes (about 15 ml) of 0.5 M NaCl / 0.1 M NaHCO$_3$ pH 8.3. Washes consisted of slow speed centrifugation of 2500 g for 2 min followed by removal of supernatants. The remaining active groups were blocked with 0.1 M Tris-HCl pH 8.0 rotating end over end overnight at 4°C. The peptide-coupled resin was washed with three cycles of alternating pH. Each one consisted of a wash with 0.5 M NaCl / 0.1 M sodium acetate/citrate buffer pH 4.0, followed by 0.5 M NaCl / 0.1 M Tris-HCl pH 8.3. Finally the resin was resuspended in 5 ml of 20 mM Na$_2$HPO$_4$ / 0.5 M NaCl containing 0.01 % (w/v) NaN$_3$.

The peptide-coupled sepharose was packed into a column. The beads were washed with PBS pH 7.3 and any unbound peptide was removed eluting with 50 mM diethylamine pH 11.5. The column was linked up to an uvicord (LKB-Optical Unit UV-1, Amersham Biosciences) and graph plotter at 4°C. Absorbance at 280 nm was monitored to detect peptides and or proteins passing through the column during all the purification steps. The resin was washed and purified IgGs (see section 2.2.17.5a) or antisera diluted 1/10 in PBS were recycled through the column overnight at 4°C. The column was washed with PBS until reaching the base level at 280 nm. Anti-peptide antibodies were eluted with 50 mM diethylamine pH 11.5. Samples corresponding to plotted peaks were dialysed against PBS overnight at 4°C and concentrated in centrifugal filter devices Centricon® Plus −20 (Millipore Bedford, USA) of nominal molecular weight limit of 30,000 Da. Antibody aliquots of 0.5 mg/ml were stored at -20°C in the presence of 0.01 % (w/v) sodium azide. The column was washed with PBS before regenerating with three alternating cycles of 0.5 M NaCl / 0.1 M Tris-HCl pH 8.3 and 0.5 M NaCl / 0.1 M sodium acetate/citrate buffer pH 4.0. Finally it was stored in 20 mM Na$_2$HPO$_4$ / 0.01 % (w/v) at 4°C.

2.3 Results

2.3.1 Production of HcGluClα3B recombinant protein

The Glutathione S-Trasferase (GST) gene fusion system (Smith and Johnson, 1988) was used to obtain a fragment of the HcGluClα3B subunit expressed in bacteria, which could then be used to raise polyclonal antibodies in rabbits. The pGEX plasmids provide an inducible and high-level intracellular expression of genes or genes fragments as fusions with *Schistosoma japonicum* GST protein. The GST-fusion proteins can be affinity purified from bacterial lysates using Glutathione-agarose beads. Cleavage of the desired protein from GST can be achieved using a site-specific protease whose recognition sequence is located immediately upstream from the multiple cloning site on the pGEX plasmids. Since GST is highly immunogenic, the whole purified fusion protein could also be used as antigen when small gene fragments are cloned into the pGEX vectors.

2.3.1.1 Construction of the pGEX:HcGluClα3B plasmid

The HcGluClα3B subunit was the first one selected to produce polyclonal antibodies. In order to obtain specific antibodies against it, a search for a non-conserved region in the predicted protein, which was also a putative antigenic peptide, was carried out. A sequence alignment between HcGluClα3B and α3A subunits showed an area of great diversity on the intracellular loop between the transmembrane domains III and IV (TM III-TM IV) of these subunits (Fig. 2.1). The predicted antigenicity of that region was also checked considering the following properties: hydrophilicity and antigenic index for each amino acid. The region selected comprises 58 amino acids and is indicated in figure 2.1. It has a mean hydrophilicity and antigenicity scores of 1.12 and 0.8 respectively. These values were obtained using the command peptidestructure in the GCG program suite, on the gnome workstation according to Kyte and Doolittle (1982) and Jameson and Wolf (1988). Good scores for antigenicity and hydrophilicity are around 1.3. Hydrophilicity scores of less than 1.3 mean that the peptide will be more hydrophobic, hence the amino acid residues will have less chances to be facing the outside of the molecule to be available for reaction.

```
        1                                                              ◆                        100
GluClα3A  MRNSVPLATR IGPMLALICT VSTIMSAVEA KRKLKEQEII QRILNNYDWR VRPRGLNASW PDTGGPVLVT VNIYLRSISK IDDVNMEYSA QFTFREEWVD
GluClα3B  MRNSVPLATR IGPMLALICT VSTIMSAVEA KRKLKEQEII QRILNNYDWR VRPRGLNASW PDTGGPVLVT VNIYLRSISK IDDVNMEYSA QFTFREEWVD

        101                                                                                                    200
GluClα3A  ARLAYGRFED .ESTEVPPFV VLATSENADQ SQQIWMPDTF FQNEKEARRH LIDKPNVLIR IHKDGSILYS VRLSLVLSCP MSLEFYPLDR QNCLIDLASY
GluClα3B  ARLAYGRFED .ESTEVPPFV VLATSENADQ SQQIWMPDTF FQNEKEARRH LIDKPNVLIR IHKDGSILYS VRLSLVLSCP MSLEFYPLDR QNCLIDLASY

        201                                                                         TM I                       300
GluClα3A  AYTTQDIKYE WKEQNPVQQK DGLRQSLPSF ELQDVVTKYC TSKTNTGEYS CLRTQMVLRR E.FSYYLLQL YIPSFMLVIV SWVSFWLDKD SVPARVTLGV
GluClα3B  AYTTQDIKYE WKEQNPVQQK DGLRQSLPSF ELQDVVTKYC TSKTNTGEYS CARVKLLLRR E.YSYYLIQL YIPCIMLLVV SWVSFWLDKD AVPARVSLGV

        301     TM II                                TM III                      ●                            400
GluClα3A  TTLLTMTTQS SGINANVPPV SYTKAIDVWI GVCLAFIFGA LLEFAWVNYA ARKDM..... .......... .......SCG QRMMKQLPQD GYRPLADSQP
GluClα3B  TTLLTMTTQA SGINSKLPPV SYIKAVDVWI GVCLAFIFGA LLEYAVVNYY GRKEFLRKEK KKKTRLDDCV CPSE...... .RPALRLDLS NYRRRGWTP.

        401              ■              TM IV          450
GluClα3A  RTSFCCRIFV RRYKERSKRI DVVSRLVFPI GYACFNVLYW AVYLM.....
GluClα3B  LNRL..LDML GRNADLSRRV DLMSRITFPS LFTAFLVFYY SVYVKQSNLD
```

Fig. 2.1 Alignment of *H. contortus* GluClα3A and GluClα3B subunit sequences.

Conserved residues are in bold and the predicted membrane-spanning domains (TM) boxed. The underlined region between TM III and TM IV of GluClα3B corresponds to the peptide selected for the construction of the recombinant protein. In colour, the peptides selected for synthesis. The putative glycosylation site is indicated by (◆) and the conserved PKC (■) and cAMP-dependent protein kinase (●) consensus sites are shown. Accession numbers: Y14233 and Y14234.

The corresponding DNA was amplified by PCR for cloning in frame into the pGEX-2T expression vector, downstream from the *gst* gene. Specific primers, α3B 5' and α3B 3', were designed to amplify the corresponding DNA of the intracellular TM III-TM IV region. The α3B 5' primer contained a *Bam*H I site and the α3B 3' an *Eco*R I site for directional cloning into the pGEX-2T vector (for details see methods 2.2.13).

A HcGluClα3B cDNA full-length clone was used as template for PCR and one band of the expected size (~200 bp) was obtained (Fig. 2.2 lane 3).
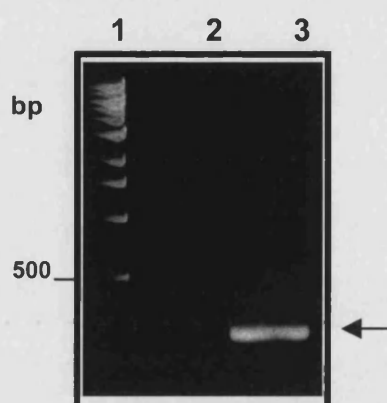
Fig. 2.2- PCR amplification of the intracellular TM III-TM IV region of HcGluClα3B
Lane 1, 1 Kb DNA ladder (NEB). Lane 2, no-template control PCR reaction. Lane 3, PCR product amplified from plasmid HcGluClα3B DNA. For the PCR mixture1μM of α3B 5' and 3' primers, 1.2 mM dNTP and 100 ng of template DNA were used in a 50 μl volume reaction. Cycling conditions: 94°C for 2 min, followed by the addition of 2.5 U DNA polymerase Expand ™ High Fidelity and then 35 cycles of 94°C for 30 s, 58°C for 30 s, 55°C for 30 s and 72°C for 30 s, terminating with 3 min at 72°C. 15 μl of PCR products were analysed by separation via electrophoresis on a 1.5% (w/v) agarose gel in 1X TAE. The arrow indicates the product of 200 bp.

The band was excised from the gel and the DNA extracted was cloned into the pCR®-Blunt vector. Five transformants were isolated and digested with *Eco*R I and *Bam*H I. The identity of one of these clones (number 1), was confirmed by sequencing. Clone 1 DNA was digested with *Eco*R I and *Bam*H I and the fragment obtained (~200 bps) was sub-cloned into the pGEX-2T vector. Attempts to ligate the HcGluClα3B DNA fragment to the pGEX vector and transform directly into *E. coli* BL21 (the bacteria strain suitable for pGEX fusion protein expression), were unsuccessful. Hence, the transformation of the recombinant plasmid was done in two steps. First, an alternate strain recommended by the manufacturer was used (*E. coli* JM105). Eleven transformants were isolated and their plasmid DNA assayed by restriction digestions with *Eco*R I and *Bam*H I enzymes. A fragment of the expected size (~200 bp) was released from all of the clones (Fig. 2.3).

75
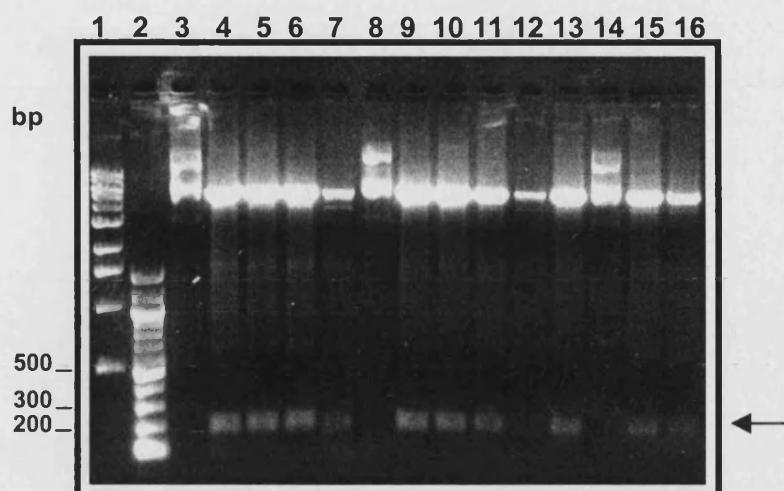
Fig. 2.3. Restriction analysis of plasmid DNA from *E. coli* JM105 transformed with pGEX:GluClα3B
1.5% (w/v) agarose gel in TBE. Lanes 1 and 2 DNA ladders 1 KB and 100 bp with relevant band sizes noted on the side. Lanes 3, 8 & 14, clones 1, 4 & 11 uncut. Lanes 4-7, 9-13 & 15-16 *Eco*R I- *Bam*H I digested DNA from clone 1 to 11. The arrow indicates the fragment of 200 bp released from the transformed clones.

The identity of two of these clones (1 and 2) as well as the conservation of the reading frame with the *gst* gene was confirmed by sequencing. Plasmid DNA from clone 1 was used to transform the strain required for the expression of the pGEX:GluClα3B plasmid. The *Eco*R I and *Bam*H I restriction analysis of six transformants is shown in the figure 2.4. The expected fragment of 200 bp was obtained in all of the clones. Clone number 2 was used for expression assays.
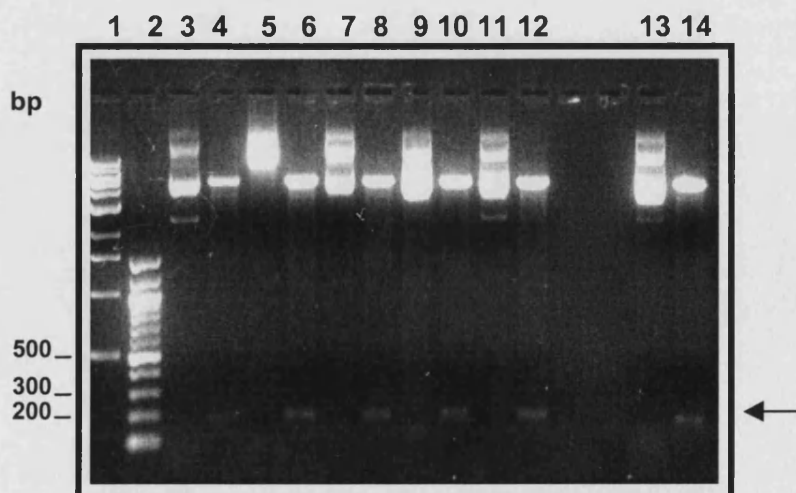
Fig. 2.4- Restriction analysis of plasmid DNA from transformed *E. coli* BL21
1.5% (w/v) agarose gel in TBE. Lane 1 and 2, 1 KB and 100 bp DNA ladders with relevant band sizes noted on the side. Lanes 3, 5, 7, 9, 11 & 13, uncut DNA from clones 1 to 6. Lanes 4, 6, 8, 10, 12 & 14, clones 1 to 6 digested with *Eco*R I- *Bam*H I. The arrow indicates the fragment of 200 bp released from the clones.

76

2.3.1.2 Expression, detection and purification of GST:GluClα3B

The HcGluClα3B intracellular TM III-TM IV region was expressed as a GST fusion protein designated GST:GluClα3B. A few colonies of *E. coli* transformed with the pGEX:GluClα3B or pGEX-2T plasmids (the last one used as the expression control), were grown into 3 ml of LB / Ampicillin broth to an A_{600} of 0.6. At this point a 1 ml sample was removed (uninduced cells) and the remaining culture was induced with IPTG. Following induction, cell lysates were separated by SDS-PAGE (Fig. 2.5A).
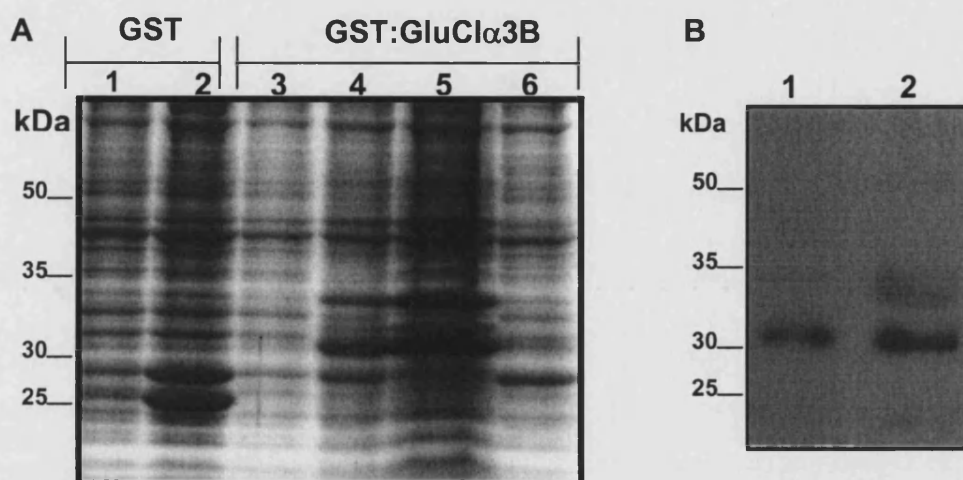
Fig. 2.5- Expression of GST fusion proteins
A: Cell lysates of *E. coli* BL21 transformed with pGEX-2T (1-2) and pGEX:GluClα3B (3-6) plasmids, separated on a 12% (w/v) SDS-PAGE and stained with Coomasie Blue solution. Lanes 1 & 3, soluble fraction of uninduced cells. Lanes 2 and 4-6, 0.1 mM IPTG-induced cells showing the pre-sonicated extract (4), the insoluble (5) and the soluble fractions (2 & 6). B: Western blot of the GST:GluClα3B pre-sonicated (1) and insoluble fractions (2) probed with 1:2000 dilution of a goat anti-GST serum, followed by incubation with a 1:2000 anti-goat horseradish peroxidase-conjugated antibody. Chemiluminescence was detected using the ECL reagents after 5 min of exposure on X-ray film. Relevant molecular weight marker bands are noted on the side of the gels.

Two major bands of 26 and 29 kDa were over-expressed on the pGEX IPTG-induced cell fraction (lane 2). The apparent molecular weight expected for GST is 26 kDa. Western blots assays using an anti-GST antibody showed immunoreactivity only for the 26 kDa band, confirming the identity of the lower band with the GST protein (data not shown). Two novel bands of approximately 32 kDa and 34 kDa appeared on the pGEX:GluClα3B induced lysate, on the pre-sonicated and insoluble fractions being the lower band more abundant that the upper one (lanes 4 and 5). As the expected size of the fusion protein is about 32 kDa (26000 Da of GST plus 6380 Da of the GluClα3B peptide), the lower band would

correspond to the GST: GluClα3B protein. To confirm this, the pre-sonicated and insoluble fractions of the GST:GluClα3B expressing cell extract were immunoprobed with an anti-GST antibody. At 1:2000 dilution of the antibody, the 32 kDa band was recognised on both extracts (Fig. 2.5B). When high amounts of proteins were loaded (see Fig. 2.5A lane 5), immunoreactivity against the 34 kDa band was also observed (Fig. 2.5B lane 2), suggesting a non-specific reaction of the antiserum.

As the GST:GluClα3B protein was found in the insoluble fraction, different induction conditions were tried to solubilise it such as decreasing the induction time and the temperature to 20°C, increasing aeration and changing the LB bacterial medium for minimal medium. All these attempts were unsuccessful. Finally and in order to prevent possible denaturation of the fusion protein, the non-ionic detergent NP-40 (1 % (v/v)) was used to solubilise it (for details see section 2.2.13.5).

A pilot affinity purification assay of the NP-40 solubilised extract was carried out using glutathione-agarose beads and reduced glutathione (10 mM) to elute the fusion protein. The analysis of the collected fractions is shown in the figure 2.6A.
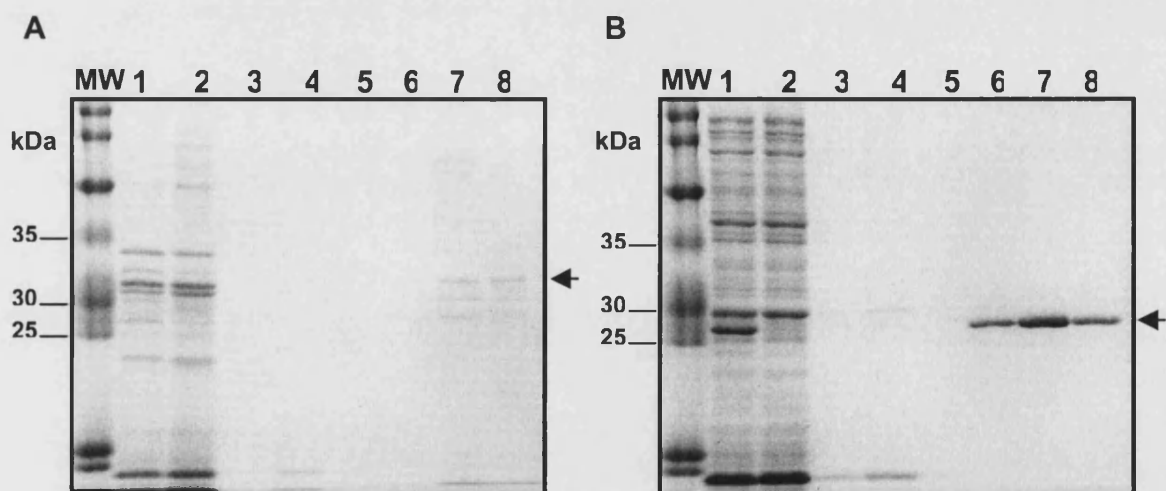
Fig. 2.6 Analysis of the purification of GST fusion proteins

12 % (w/v) SDS-PAGE stained with Coomasie Blue solution. A: Purification of GST:GluClα3B from a solubilised inclusion body extract. B: Purification of GST from a PBS soluble fraction. Lane 1, crude IPTG-induced extracts. Lane 2, proteins not adsorbed to the column. Lanes 3-5, PBS washes. Lanes 6-8, fractions eluted with 50 mM TrisCl (pH 8.0)/10 mM reduced glutathione. MW: Rainbow wide range molecular weight marker (Amersham) with relevant bands noted on the side. Arrows indicate the proteins of interest.

Most of the recombinant protein was not adsorbed to the beads (lane 2) and only a small fraction of the GST:GluClα3B protein was recovered on the elution steps (lanes 6-8), but contaminated with other proteins. As a control for the purification method, the same protocol was performed in parallel using bacterial extracts expressing the GST wild-type protein (Fig. 2.6B). In contrast, the GST protein was totally adsorbed to the agarose-beads (lane 2) and recovered pure (lanes 6-8).

In view of the difficulties encountered in preparing a suitable recombinant immunogen and the length of the procedures involved, the use of synthetic peptides was chosen as an alternative route for the production of polyclonal antibodies.

2.3.2 Production of anti-peptide antibodies

2.3.2.1 Peptide design

The ideal peptide antigen is 15-20 amino acids long and hydrophilic. Since most of the antigenic sites are located within surface exposed regions of a protein, hydrophilic peptides are more likely to be antigenic. Proline and/or tyrosine residues can induce structural motifs into the peptide that may mimic more closely the shape of the peptide in the naive protein. A cysteine residue should be present at the N- or C- terminus if a sulfhydryl-reactive cross-linker is to be used to couple the peptide to a carrier protein.

As it was mentioned above when selecting the peptide sequence for the GluClα3B recombinant protein, prediction programs suggest that good scores for antigenicity and hydrophilicity should be around 1.3. Scores of less than 1.3 for hydrophilicity mean that the peptide will be more hydrophobic and also possibly more difficult to solubilise it. Overall charges for ideal peptides should be neutral (+/-2); greater charges could result in charge interactions of the peptide that could alter conformation and affect solubility. To score peptide charges, Lys and Arg are score 1+; Asp, Gln and Glu 1− and His 1/2+ (Cambridge Research Biochemical http://www.crb.gb.com).

2.3.2.1a HcGluClα and β peptides

HcGluClα and HcGluClβ synthetic peptides were designed and used previously in our lab by S. Jagannathan and N. Delany to raise antibodies in rabbits. The 18

amino-acid length peptides (HcGluClβ: RSTGGTQEQEILNELLSN; HcGluClα: EKLLDEQKIIKHKKESPY) correspond to the predicted extreme N-terminus of the full-length mature proteins following the predicted signal peptide cleavage sites (Delany et al., 1998; Forrester et al., 1999; Cheeseman et al., 2001).

2.3.2.1b HcGluClα3A and 3B peptides

The alternatively spliced products of the *H. contortus gbr-2 (avr-14)* gene, HcGluClα3A and 3B, were previously shown to be widely distributed in the adult nervous system of *H. contortus* (Jagannathan et al., 1999). In order to distinguish between the expression patterns of HcGluClα3A and 3B, subunit-specific rabbit antisera were required. A search for the region of greatest sequence diversity between the two subunits was carried out and peptides corresponding to such sequences within the intracellular loop between transmembrane domains III and IV were selected (Fig. 2.1). Measures of hydrophilicity and antigenic index were calculated for each amino-acid, using the command "peptidestructure" in the GCG program suite according to Kyte and Doolittle (1982) and Jameson and Wolf (1988) prediction programs. Hydrophilicity plots for the GluClα3A & 3B full length sequences determined which parts of the proteins are likely to be on the outside of the molecule and thus available for reaction (Fig. 2.7).

The peptides finally chosen correspond to amino acids 384-399 for GluClα3A and 373-391 for GluClα3B.

GluClα3A peptide: *NH2*-CRIFVRRYKERSKRID-*COOH*   M.W: 2124.2

GluClα3B peptide: *NH2*-CSERPALRLDLSNYRRRGWT- *COOH*   M.W: 2449.4

A BLAST search for these peptide sequences was done and they only matched with their respective proteins. The mean hydrophilicity and antigenicity index scores for these peptides were 1.3 and 0.77 for GluClα3A and 1.32 and 0.95 for GluClα3B respectively. Also, an overall charge of +5 and +3 was scored for GluClα3A and 3B respectively. Notice that in the GluClα3B peptide a Cys residue was added at the amino terminal end. This was to allow the coupling to the sulfhydryl-reactive cross-linking agent sulfo-SMCC.
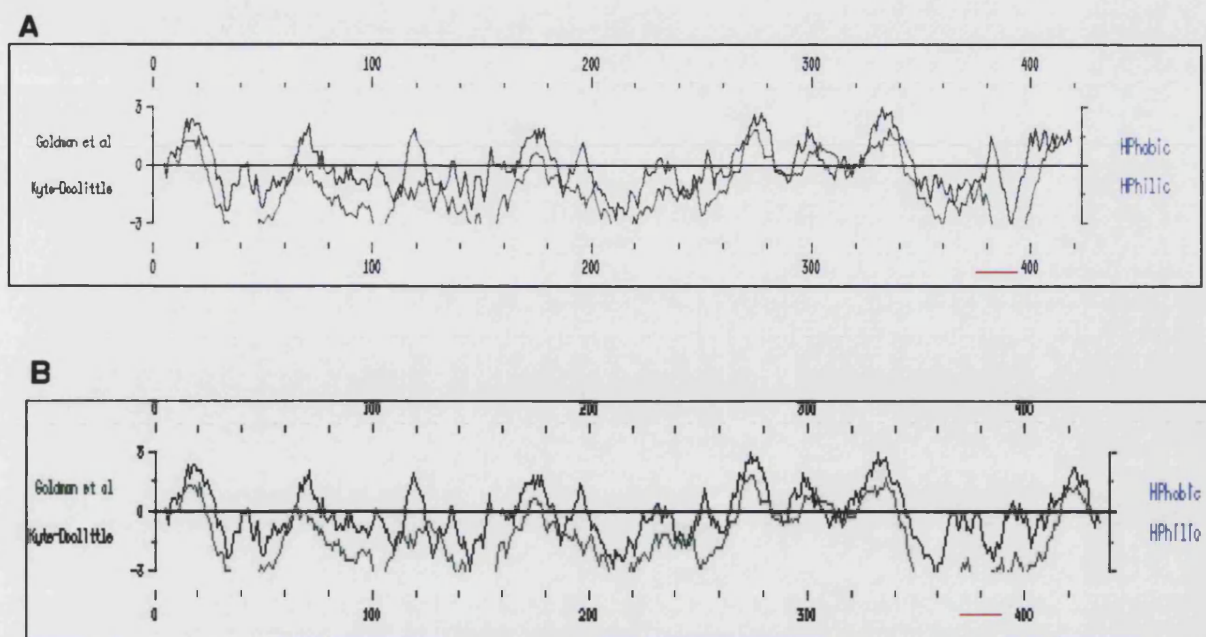
Fig. 3.7- Hydrophilicity profiles of GluClα3A and GluClα3A B proteins
The hydrophilicity plots for the amino-acid full-length sequences of GluClα3A (A) or 3B (B) proteins were obtained using the command peptidestructure in the GCG program suite, on the gnome workstation according to Kyte and Doolittle (1982) and Goldman et al. (1986). The numbers on the x axis represent each amino-acid in the sequences. The y axis represents the range of hydrophilicity/hydrophobicity values. The areas below the midpoint line indicate the regions predicted to be hydrophilic. The red bars denote the regions from which the peptides were chosen.

2.3.2.2 Coupling to carrier protein

In all cases thyroglobulin was selected as the carrier protein as it is not found in nematodes making any anti-thyroglobulin antibody less likely to cross-react with nematode proteins.

2.3.2.2a HcGluClβ

The HcGluClβ peptide was coupled to thyroglobulin using glutaraldehyde. The concentration of the final peptide-conjugated (Thyr-GluClβ) was 0.7 mg/ml.

Control coupling reactions included the peptides coupled to bovine serum albumin (BSA) by sulfo-MBS, cross-linker with the same chemistry of sulfo-SMCC. The use of sulfo-MBS to couple peptides to BSA was tested early in our lab, and showed a decreased migration of BSA conjugates when resolved on a 7.5% SDS-PAGE and a fuzzy doublet (J. Eastlake, pers. commun.). BSA control reactions were performed due to the large size (670 kDa) of the tetrameric thyroglobulin, which makes its migration on a 7.5% SDS-PAGE as well as the possibility of detecting variations on the apparent molecular weight upon peptide conjugation, very unpredictable. GluClα3B and 3A peptide coupling reactions were analysed by SDS-PAGE (Fig. 2.8).
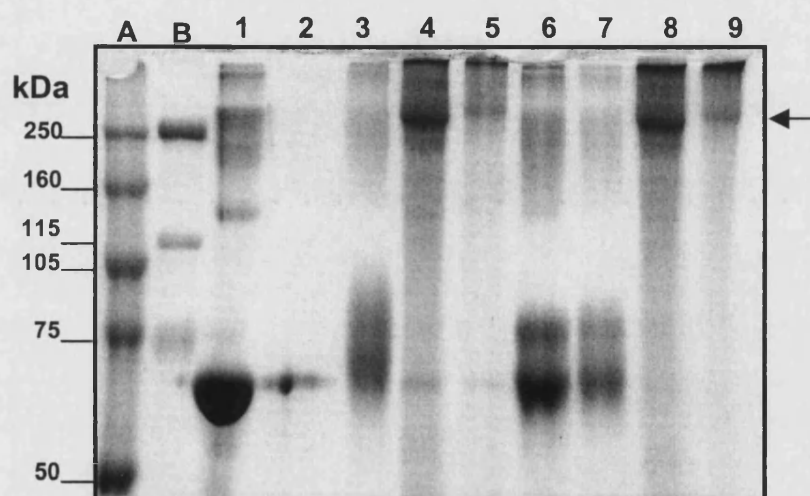
Fig. 2.8- Coupling analysis of GluClα3A and 3B peptides to thyroglobulin.
7.5% (w/v) SDS-PAGE stained with Coomasie Blue solution. Lane 1, BSA. Lanes 2 & 6 BSA cross-linked to MBS. Lanes 3 & 7, BSA-MBS-GluClα3B and BSA-MBS-GluClα3A conjugates, respectively. Lanes 4 & 8, thyroglobulin (Thyr) crosslinked to SMCC. Lanes 5 & 9, Thyr-SMCC-GluClα3B and Thyr-SMCC-GluClα3A conjugates, respectively. A: Rainbow (Amersham) and B: BioRad wide range molecular weight markers with relevant bands noted on the side. The arrow indicates the peptide-Thyr conjugates.

Both conjugates Thyr:GluClα3A and Thyr:GluClα3B showed a decrease in their migration profiles in comparison to Thyr-SMCC before being coupled, indicating that the reaction was successful (lanes 8 & 9 and 4 & 5 respectively). The difference in kDa was not estimated due to the molecular weight of these proteins were higher than the markers used in the SDS-PAGE. It is possible though that the band above 250 kDa corresponds to thyroglobulin. Of the control reactions only BSA coupled to the GluClα3B peptide showed a slightly decrease in the migration profile, which was difficult to estimate in kDa because of the characteristic fuzzy band obtained.

2.3.2.3 Immunisation and Determination of Antiserum Titres

For each antigen, two rabbits or rats were immunised with the thyroglobulin-peptide conjugates mixed with the adjuvants TiterMax® Gold (water in oil formulation) for the GluClα3A and α3B or Imject® Alum (aluminum hydroxide) for the GluClβ conjugates. Test bleeds were taken the day 0 (pre-immune serum) and 14 days after injections. Immunisation timings were determined according to serum titres measured by the enzyme linked immunosorbent assay (ELISA). Monitoring sera titres between injections prevented boosts from being given when sera titres were still high.

2.3.2.3a GluClα3A and 3B antisera

Rabbits injected with Thyr: GluClα3A and Thyr: GluClα3B conjugates were boosted 2 and 8 weeks after the primings. ELISA analyses of sera collected from the rabbits with the highest antisera titres (rabbits 264 and 263 respectively) are shown in figure 2.9. Antibody titre was determined by plotting absorbance at 450 nm (A_{450}) vs. antiserum dilution. The inflection point of the immune data when interpolated by drawing a line to the X-axis, resulted in the Ab titre of the sera.
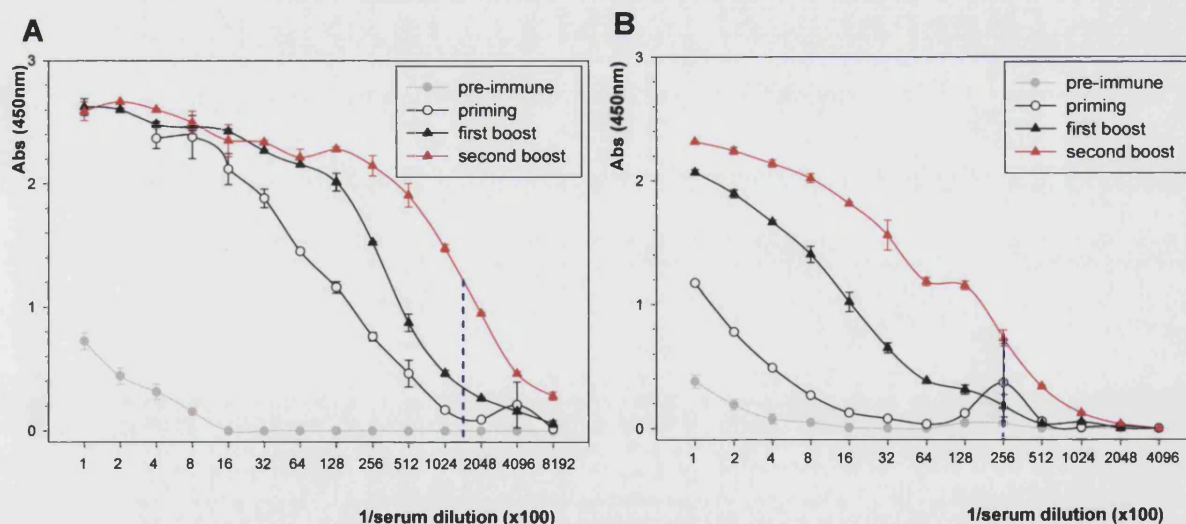
Fig. 2.9 Sera response to GluClα3A and GluClα3B peptides
ELISA readings on GluClα3A (A) and GluClα3B (B) peptide-coated plates analysing sera collected during the immunisation protocols with the GluClα3A and 3B antigens respectively. Data was ploted using the mean and standard error for duplicates. Dashed lines indicate the highest titres, achieved after the second boost: 1:153,600 in A and 1:25, 600 in B.

The antibody titre for both peptides reached the highest level after the second boost with a half-maximal response at 1:153,600 dilution for GluCl3A (rabbit 264) and 1:25,600 dilution for GluClα3B (rabbit 263) (Fig. 2.9, dashed lines). These rabbits

83

received a third and last boost 7 weeks later. In contrast to the GluClα3B antiserum which titre remained the same, the GluClα3A titre dropped to 1:51,200 after the third boost (Fig. 2.10), therefore rabbits were soon terminated. For each rabbit, 40 ml serum was extracted from the collected blood and aliquots of 7 ml were stored at −20 °C.

A

B
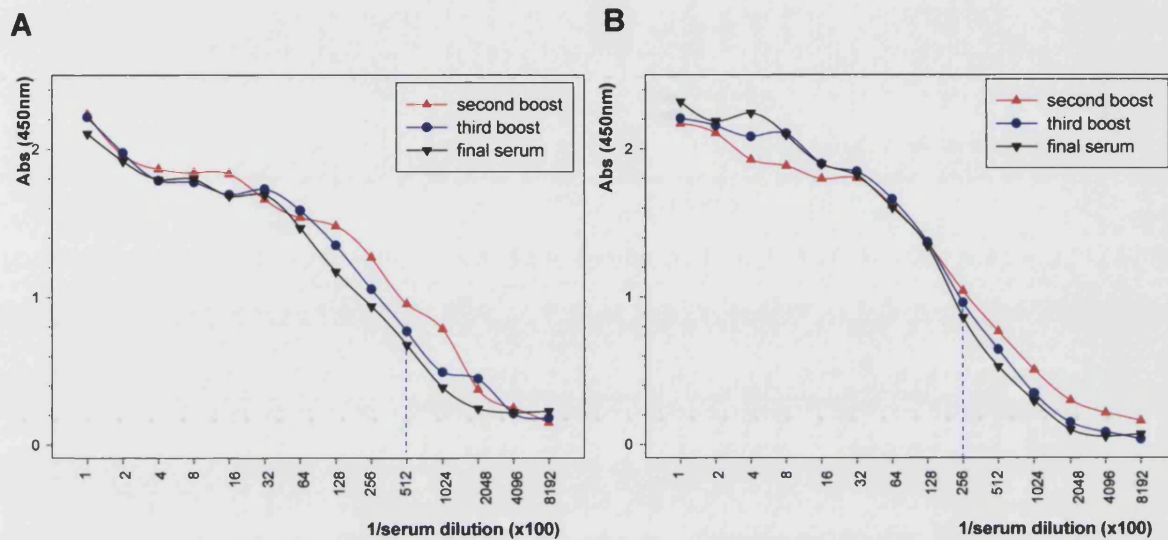
Fig. 2.10 Sera response to GluClα3A and GluClα3B peptides after the third boost. Comparison of GluClα3A (A) and GluClα3B (B) antisera titres measured by ELISA on GluClα3A (A) and GluClα3B (B) peptide-coated plates, collected after the second, third boost and just before the final bleed. Dashed lines indicate the titres achieved after the third boost: 1:51,200 in A and 1:25,600 in B.

2.3.2.3b HcGluClβ antiserum

As an anti-HcGluClα serum raised in rabbits was already available in our laboratory, producing an anti-HcGluClβ serum in a different animal species would allow to perform double labelling immunocytochemistry in *H. contortus*. Therefore, two rats were immunised with the Thyr-GluClβ mixture. After the first boost, only the serum of one animal showed immunoreactivity to GluClβ peptide. Hence, further boosts, monitored by ELISA, were given just to the immunoreactive rat two weeks, a month and four months after the priming. The ELISA analyses of the sera collected are shown in figure 2.11. The antibody titre for GluClβ peptide reached the highest level after the third boost with a half-maximal response at 1:6400 dilution. The animal was finally bled two weeks after this boost. Five ml of serum were extracted from the collected blood and used to purify anti-GluClβ antibodies.
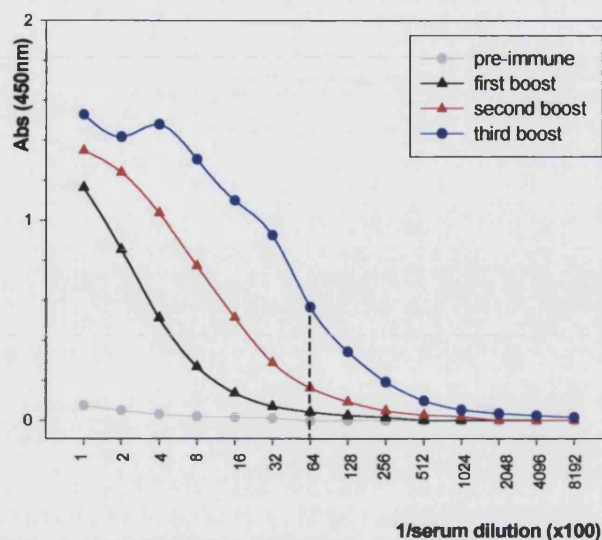
Fig. 2.11 Immune response to GluClβ peptide.
ELISA readings from sera collected during the immunisation protocol for the anti-GluClβ rat sera on a GluClβ peptide-coated plate. The dashed line indicates the highest titre (1:64,000), achieved after the third boost.

2.3.2.4 Antibody purification

Specific antibodies represent at most 20-30 % of the antisera immunoglobulins. Using total sera may reduce antibody efficiency and lead to high background in immunocytochemistry assays. To overcome these features, affinity purification of polyclonal antibodies was preformed. Anti-peptide antibody purification allows only the antibodies that bind to the antigen to be collected. In this work polyclonal antibodies were raised against thyroglobulin-peptides conjugates. Therefore, affinity purification of anti-peptide antibodies reduces the possibility of anti-thyroglobulin antibodies cross-reacting.

Anti-peptide antibodies can be purified straight from the immune sera or from total IgG. Isolation of IgG antibodies not only provides an enriched fraction of high affinity antibodies (IgG class), but also reduces the amount of non-specific serum proteins that would be recycled through the peptide-affinity column, which may interfere with the antibody binding to the column. However, antibody elution occurs at high pH and the more an antibody is exposed to high pH, the more it might be inactived. Therefore, both approaches were tried in this work. For the HcGluClα3A, 3B and HcGluClα immune sera, total IgG were firstly purified on Protein A Sepharose CL-4B columns. For the HcGluClβ rat antiserum, this additional step was not included.

85

Protein A, a constituent of the cell wall of the bacteria *Staphylococcus aureus*, binds to the Fc domain of IgG immunoglobulins with high affinity and this reaction is pH dependent.

2.3.2.4a HcGluClα3A and α3B anti-peptide antibodies

Five ml serum samples extracted soon after titres reached the highest levels (on the second boost for HcGluClα3A and 3B and third boost for the GluClα antisera), were diluted 1/10 in PBS and recycled through 5 ml Protein A Sepharose columns (one per antisera). IgG antibodies were eluted with 35 mM NaCl / 35 mM diethylamine pH 11.5 and neutralised by dialysis against PBS. Antisera were recycled and eluted three times. Eluted samples were pooled and recycled through the respective peptide-coupled Sepharose columns. Anti-peptide antibodies were then purified on peptide-affinity cyanogen bromide activated Sepharose 4B column with 50 mM diethylamine pH 11.5. Samples were neutralised in the same way as for the IgG and concentrated to 0.5 mg/ml. Affinity purified antibodies were tested by ELISA and the highest titres were: 1:4,800 for GluClα3A, obtained on the first elution and 1:3,200 for GluClα3B, obtained on the second peak of the first elution (Fig. 2.12, dashed lines).
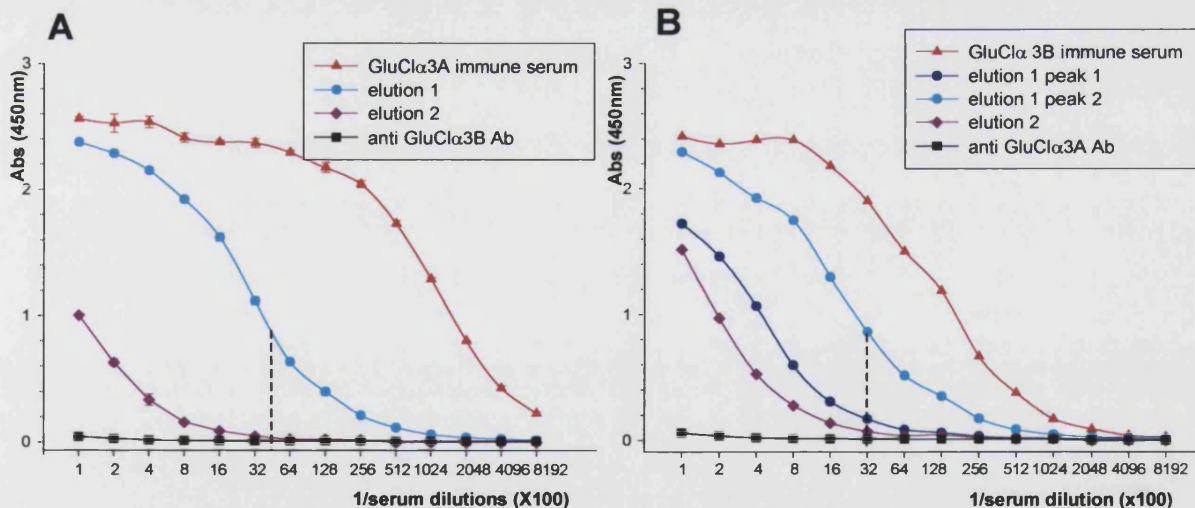
Fig. 2.12 Antibody titres from GluClα3A and GluClα3B affinity purified antibodies. Anti GluClα3A (A) and anti GluClα3B (B) affinity purified antibodies were analysed by ELISA on GluClα3A (A) and α3B (B) peptide-coated plates. The highest titres, indicated by a dashed line, were reached at elution 1 for both anti-peptide antibodies. Square symbol plots show non-cross reactivity of the anti GluClα3B Ab with the GluCα3A peptide or the anti GluClα3A Ab with the GluClα3B peptide.

These were the antibodies used in immunocytochemistry experiments (chapter 3). The anti-GluClα3B antibody showed no cross-reactivity with the GluClα3A peptide,

as assayed by ELISA, nor did the anti-GluClα3A antibody cross-react with the GluClα3B peptide (Fig. 2.12, plots on square symbols).

2.3.2.4b GluClα and GluClβ anti-peptide antibodies

An anti-GluClα immune serum obtained previously in our lab by S. Jagannathan was affinity purified. Serum titres against the GluClα peptide reached the highest level after the third boost (S. Jagannathan, personal communication) with a titre of 1:25,600 (Fig. 2.13A, red plot). Five ml of this antiserum were used to purify total IgG, in the same way as for the GluClα3 antisera (see above). GluClα anti-peptide antibodies were subsequently purified on a GluClα-affinity cyanogen bromide activated Sepharose 4B column with 50 mM diethylamine pH 11.5, neutralised on the same way than for the IgG and concentrated to 0.5 mg/ml. Anti-peptide antibodies were purified in just one elution step and the titre measured by ELISA was 1:12,800 (Fig. 2.13A).
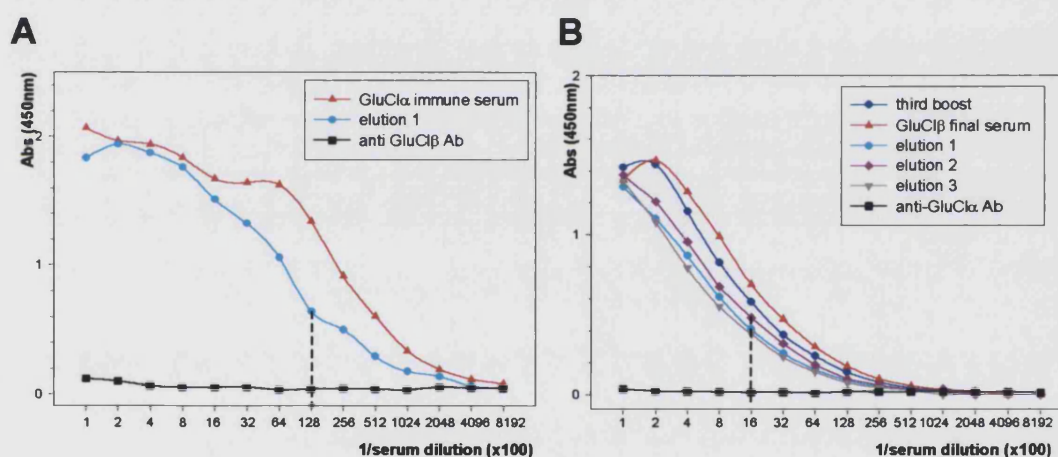
Fig. 2.13 Antibody titres from GluClα and GluClβ affinity purified antibodies.
Anti-GluClα (A) and anti-GluClβ (B) antibodies analysed by ELISA on GluClα (A) and GluClβ (B) peptide-coated plates. The anti-GluClα antibodies were eluted in one step but the anti-GluClβ in three cycles. The highest titres, indicated by a dashed line, were 1:12,800 and 1:1,600 respectively. Square symbol plots show non-cross reactivity of the anti GluClα Ab with the GluClβ peptide or the anti GluClβ Ab with the GluClα peptide.

The GluClβ rat antiserum achieved an acceptable high titre after the third boost (section 2.3.2.3b). Five ml of this serum diluted 1/10 in PBS were recycled through a GluClβ-affinity cyanogen bromide activated Sepharose 4B column. Affinity purified antibodies were obtained from three cycles of antisera recycling and were eluted with 50 mM diethylamine pH 11.5. Collected fractions were neutralised by

dialysis against PBS, concentrated to 0.5 mg/ml and tested by ELISA. Anti GluClβ antibodies were eluted in three steps and showed a titre of 1:1,600 (Fig. 2.13B).

The specificity of the HcGluClα and β antibodies was tested by ELISA. The HcGluClα antibodies did not show cross-reactivity with the GluClβ peptide nor did the rat anti HcGluClβ antibodies (elution 1 samples) cross-react with the GluClα peptide (Fig. 2.13, plots on square symbols). These antibodies were used in immunocytochemistry assays (chapter 3).

2.3.2.5 HcGluClα3B antibody recognition of the GST:GluClα3B protein

In order to demonstrate that anti GluClα3B antibodies would recognise the HcGluClα3B protein, a western blot assay against the recombinant protein GST:GluClα3B was performed (the production of the GST:GluClα3B protein was described in section 2.3.1). This protein consists of the GluClα3B intracellular loop between the transmembrane domains III and IV, the region where the GluClα3B peptide was designed to, expressed as a fusion protein with the S. japonicum GST. After induction with IPTG, bacteria transformed with the pGEX:GluClα3B plasmid were lysed, the proteins separated on a SDS-PAGE and blotted onto nitrocellulose. The affinity purified anti HcGluClα3B antibodies that reached the highest tires (Ab from elution 1 peak 2) were used at a 1:200 dilution in blocking solution. These antibodies recognised a 32 kDa protein on the IPTG induced extract, coinciding with the predicted size for the fusion protein (Fig. 2.14, lane 1). The antibodies did not react with the pGEX:GluClα3B transformed but uninduced cell lysate (lane 2).
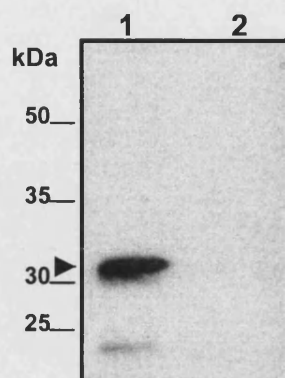
Fig. 2.14 Immunoreactivity of the anti-GluClα3B purified antibody to GST:GluClα3B
Cell lysates of *E.coli* BL21 transformed with pGEX:GluClα3B plasmid, separated on a 12% (w/v) SDS-PAGE and blotted on a nitrocellulose membrane. Lanes 1, pre-sonicated extract of 0.1 mM IPTG-induced cells. Lane 2, soluble fraction of uninduced cells. Blot probed with 1:200 dilution of the affinity purified anti GluClα3B antibody (elution 1 peak 2), followed by incubation with a 1:1000 goat anti-rabbit horseradish peroxidase-conjugated antibody. Chemiluminescence was detected using the ECL reagents after 5 min of exposure on X-ray film. The point arrow indicates the 32 kDa protein recognised by the antibody. Relevant molecular weight marker bands are noted on the side.

2.4 Conclusions

Specific polyclonal antibodies were produced to study the localisation of the GluCl subunits in *H. contortus*.

A recombinant protein consisting of the intracellular TM III-TM IV region of the HcGluClα3B subunit fused to the *S. japonicum* GST protein (GST:GluClα3B) was expressed in *E. coli*. The fusion protein resulting was insoluble, which is a possibility when overexpressing foreign proteins into a prokaryotic system. It was then solubilised using a non-ionic detergent. However, the purification of the protein was unsuccessful as the majority of the protein did not adsorb to the column and the small fraction that eluted was contaminated with other bacterial proteins. Although the non-denaturing method used to solubilise the recombinant protein should not interfere with the binding of the protein to the glutathione-agarose affinity column, this possibility cannot be ignored. Because of this, synthetic peptides were chosen to raise polyclonal antibodies against the GluClα3A, α3B, α and β subunits. The selected peptide sequences were specific to their respective subunits. Also, the predicted hydrophilicity and antigenic index gave good scores, predicting high chances for the peptides to be exposed on the native protein and hence available for antibody recognition.

Antisera produced against the HcGluClα3 peptides reached the highest titres after the second boost and for the GluClβ peptide, after the third boost. The GluClβ antiserum was raised in rats to allow purified antibodies to be used with the rabbit anti-GluClα antibodies in double labelling immunocytochemistry in *H. contortus*. Antibodies were purified on peptide-affinity columns. Titres of the immune sera and the purified antibodies dropped significantly for the anti GluClα3A and GluClα3B antibodies from 1:153,600 to 1:4,800 and from 1:25,600 to 1:3,200, respectively. However, when the GluClα and β antisera were affinity purified, only the titres for the GluClα antibodies showed a minor reduction from 1:25,600 on the immune serum to 1:12,000 on the purified fraction. In contrast, the titres for the GluClβ antibodies pre- and post-purification remained unchanged. A drop in antibody titres is normally expected during antibody purification procedures. One explanation for these low anti-peptide antibody titres is that the affinity of the antibodies for their

respective peptides is so high that with the elution conditions used, a vast majority of antibodies remain bound to the column. For testing this, different elution reagents such as low pH, high salt buffers, ionic detergents, dissociating agents or a combination of them could have been used to find out the better elution conditions for these antibodies. However, eluting antibodies with harsh treatments often denatures the antigen and the antibody leaving both inactive. It is also possible that anti-peptide antibodies had passed through the affinity column on the first column wash, before even interacting with the peptides or if they did, it is also possible that the antigen-antibody interactions were weak and the antibodies got detached during the column washes. Finally, other possibilities are that a large fraction of the GluClα3A and α3B anti-peptide antibodies might be wasted on the washes steps during the isolation of total IgG, previous to the antibodies affinity-purification. It is noteworthy that the calculation of the antibody titres was performed as an estimation of the inflexion point of the immune graphs. Therefore, intrinsic variations of the method might result in differences of Ab titres. Another possible way to calculate antibody-titres is using the IC_{50} value of the graphs. This method did not show significant differences with the employed in the present study (data not shown). On the ELISAs for the GluClα, α3A and α3B antibodies, the shift to the left observed between the immune sera and the affinity-purified antibody graphs, indicated a drop in the titre for the affinity-purified antibodies. Despite this drop, the levels reached post purification were satisfactory.

The peptide sequences chosen during the peptide design were subunit-specific and this was confirmed by a BLAST search. Cross-reactivity between the GluClα3 antibodies and between the GluClα and β antibodies was tested by ELISA. None of the affinity purified antibodies showed cross-reactivity with any of the peptides tested, reacting only with the peptide to which the antiserum was raised. This gave confidence that each antiserum would be specific when used in immunocytochemical assays.

Binding of peptides to microtiter plates could be a problem in ELISAs in that the peptide may not bind or may bind in a configuration that masks or distorts the epitopes so, they may not be recognised by the antibodies. However, all the anti-peptides antibodies in this work recognised their respective peptides by ELISA. Confirmation that the GluClα3B antibodies would recognise the intracellular TM III-

TM IV region of the HcGluClα3B subunit was achieved by Western blotting of the anti GluClα3B antibodies to the GST:GluClα3B recombinant protein.

CHAPTER 3

IMMUNOLOCALISATION OF GLUTAMATE-GATED CHLORIDE CHANNEL SUBUNITS IN *HAEMONCHUS CONTORTUS*

3.1 Introduction

The glutamate-gated chloride channels (GluCls) are the target sites for the avermectin/milbemycin (AMs) anthelmintics, drugs that cause paralysis of the somatic and pharyngeal muscles in nematodes. In order to study the composition of the avermectin receptor of *H. contortus* and to better understand the mechanism of action of the AMs, the distribution of all the currently known *H. contortus* GluCl subunits was studied in adult worms. This chapter introduces a brief review of the methods used, and describes the immunolocalisation of the HcGluClα, β, α3A and α3B subunits, using subunit-specific antibodies (see chapter 2).

3.1.1 Immunocytochemistry

Immunocytochemistry is the union of microscopy and immunology and exploits the very specific binding of an antibody for its antigen. Unlike promoter/reporter gene constructs and RNA *in-situ* hybridisation studies, which provide information on the transcription products and possibly transcriptional regulation of particular genes, the main advantage of protein immunocytochemistry is that it reveals where the majority of the protein is actually localised and presumably functions. In some cases, striking differences between the two patterns have been shown in *C. elegans* arising from post-transcriptional regulatory mechanisms (Evans et al., 1994) or secretion of the protein product (Sharrock, 1984). Immunocytochemistry is also a highly specific and relatively sensitive technique. In addition, it allows the detection of antigens at the cellular and subcellular levels and, when necessary, immuno-electron microscopy can provide additional resolution on the subcellular localisation of antigens.

3.1.1.1 Tissue fixation

The process of fixation is crucial to maintain the morphology of the tissue. The choice of fixation method represents a compromise between optimally preserving ultrastructural elements, while also allowing the antibody to penetrate the specimen and to bind to the fixed antigen.

Fixation methods fall generally into two classes: organic solvents and cross-linking reagents. Organic solvents such as alcohols and acetone remove lipids and dehydrate the cells, precipitating the proteins on the cellular architecture. Cross-linking reagents such as glutaraldehyde and paraformaldehyde form intermolecular bridges, normally through free amino groups, creating a network of linked antigens (Harlow and Lane, 1999). Choosing between these methods is empirical. Fixation of *H. contortus* works better with aldehydes, particularly with paraformaldehyde since glutaraldehyde causes a higher degree of auto-fluorescence in the worms (Skinner, 1997).

3.1.1.2 Permeabilisation

Staining worms can be a difficult procedure due to the surface cuticle, which is composed of covalently cross-linked soluble and insoluble structural proteins (collagens and cuticulins respectively), other minor proteins, lipids and carbohydrates. The major function of this structure is to act as a barrier to the environment. It also allows movement via opposed muscles, acts as a hydroskeleton, determines body shape and permits growth through the larval moults (Page, 2001).

Nematode cuticle varies throughout the developmental stages and also between free-living and parasitic species. A few methods have been developed in nematodes for gaining antibody access through the cuticle. In *C. elegans*, permeabilisation has been achieved by a freeze-crack approach whereby cuticles from specimens fixed to subbed slides are physically broken through the force of quickly popping off a frozen coverslip from the slide (Miller and Shakes, 1995). Cuticle permeabilisation has also been achieved by enzymatic treatment of nematode collagens combined with reduction of disulphide bonds, cross-linkers of collagen fibres. This latter approach potentially ensures uniform permeability of the cuticle and it has been used to study the distribution of neuronal proteins on whole mount preparations of *C. elegans* (Hekimi, 1990; McIntire et al., 1992) and *H. contortus* (Keating et al. 1995; Skinner et al., 1998, Delany et al., 1998, Jagannathan et al., 1999). Nematode body wall consists of the cuticle and the hypodermis in which the nervous system is embedded. In *A. suum* collagenase treatment has been used to dissociate the muscle cells, which then separate from

the body wall to expose the neurons (Johnson and Stretton, 1987; Skinner et al., 1998).

3.1.1.3 Antibody binding and detection: direct and indirect immunocytochemistry

Antibodies that are specific to the antigen of interest (primary antibodies) are purified and labelled with an easily detected label. In this work I used anti-peptide antibodies raised in rabbits and rats, purified by affinity chromatography (chapter 2). Primary antibodies are added to the fixed and permeabilised samples prepared as described above, and their localisation in the tissue is determined by detection of the label. The antibodies can be labelled directly or they can be detected indirectly by using a labelled secondary reagent. The indirect detection method is the most frequently used for several reasons: it is versatile, cost effective and saves the time to label each preparation of primary antibody. There are three labelled reagents: protein A, protein G and anti-immunoglobulin antibodies (secondary antibodies), available from commercial suppliers and all bind with high affinity and specificity to the primary antibodies. In this work, secondary antibodies were preferred because, in contrast to protein A and G that bind to only one site on the primary antibody, they can bind to multiple sites and thus would give a stronger signal.

As far as labelling is concerned, there is a wide choice of labelled reagents. The detection methods use enzymes or fluorochromes. Enzyme-linked detection works by modifying a chemical agent included in the reaction mixture so that it becomes coloured and insoluble. The insoluble product precipitates at the site of the antigen-antibody-secondary reagent complex (Nakane and Pierce, 1967). This method provide high sensitivity, only light microscope is needed and the staining is permanent. However, the resolution is low, endogenous enzyme activity might occur, some substrates are toxic and performing double staining is difficult. An alternative method is immunofluorescence microscopy.

3.1.1.4 Immunofluorescence microscopy

This method consists of the staining of a fixed tissue with a fluorescent-labelled antibody and visualisation by epifluorescence microscope. It became a widely used method for identifying the subcellular location of antigens in the early 1950s, when

the immunocytochemistry method was modified to include fluorochrome-linked secondary reagents to determine the site of antibody binding. For this method, samples are examined under light of a specific wavelength. Absorbing radiation of the appropriate wavelength causes the electrons of the fluorochrome to be raised to a higher energy level. As these electrons return to their ground state, light of a different wavelength is emitted forming the fluorescent image seen with the microscope (Harlow and Lane, 1999). Individual fluorochromes have discrete and characteristic excitation and emission spectra. Because some of them have emission spectra that do not overlap, multiple labelling is possible. Fluorescence detection also provides high-resolution power over the enzyme-linked method. When using conventional light microscopy, the resolution of immunofluorescent images is limited by stray light from fluorescent objects out of the plane of focus. In contrast, confocal scanning microscopy uses a laser to precisely scan a single optical section, increasing resolution in the z axis which eliminates out of focus fluorescence such that significantly crisper images can be obtained. Also, the confocal optical sections are ideal for three-dimensional reconstruction from a serie taken at successive focal levels. Since the images produced by the confocal system are held in a digital frame store, they are readily available for computer analysis.

Due to the relative transparency and small size of adult H. contortus (males ~ 15 mm, females ~ 27 mm), specimen anatomy can be clearly observed in whole mount preparations. As it was mentioned above, the coupling of immunofluorescence staining to confocal microscopy has been already used for detecting neuronal proteins in whole mount preparations of H. contortus. Therefore, it was chosen in this work to study the distribution of the HcGluClα, β, α3A and α3B subunits in adult worms, using subunit-specific antibodies (chapter 2). Secondary antibodies conjugated to the fluorescent probes tetramethylrhodamine isothiocyanate (TRITC) and fluorescein isothiocyanate (FITC) were chosen in the following set of experiments.

3.2 Materials and Methods

3.2.1 Materials

PBS tablets supplied by OXOID (Basingstoke, UK).

All chemicals used were of analytical grade and obtained from Sigma Chemical Company Ltd. (Poole, UK) and BDH chemicals (Poole, UK). Plasticware was Sterilin (Bibby Sterilin Ltd., Stone, UK), Nunc (Life Technologies Ltd), Paisley, UK) and Falcon (Falcon, New Jersey, USA). Sources from other products will be indicated in the following sections.

3.2.2 Adult Worm Collection

A sheep infected with 5000 L3 larvae of ivermectin-suceptible *Haemochus contortus* Weybridge strain, was slaughtered 3 weeks after infection. The abomasum was removed, rinsed with water, cut out and placed into an isolation apparatus in the presence of Dulbecco's Modified Eagle Medium (DMEM) (GIBCO, Paisley, UK) (Gerald Coles, School of Veterinary Science, University of Bristol, UK). Worms were kept at 37°C by a heat-emitting lamp in the isolation apparatus, which consists of a funnel connected by 20 cm tubing to a 50 ml centrifuge tube. Live worms attached to the abomasum wall were directly picked with forceps and fixed (see section 3.2.3), or allowed to detach from the organ and collected on the centrifuge tube. To remove residual debris, worms were washed with DMEM kept at 37°C before fixation.

3.2.3 Tissue Fixation and Permeabilisation

Adult *H. contortus* were incubated in freshly prepared fixative (4 % w/v paraformaldehyde in PBS) for 8 h at 4°C. Worms were washed three times in PBS and stored in 0.1 % w/v paraformaldehyde in PBS at 4°C for no more than 6 weeks. Worms were washed in PBS and the cuticle was permeabilised by incubating them in BME solution (5 % v/v 2-mercaptoethanol, 1 % v/v Triton X-100, 125 mM Tris-HCl pH 6.9) overnight at 37°C in a water bath. Finally, worms were briefly washed with PBS and transferred to Bijou tubes (Sterilin) where they were treated with 120 collagen digestion units/ml of collagenase type IA (Sigma) in collagenase buffer (1

mM $CaCl_2$, 100 mM Tris-HCl pH 7.5) for either 8, 10 to 24 h at 37°C in a water bath shaking at 100 rpm.

3.2.4 Immunofluorescence

Fixed and permeabilised worms were washed with PBS and four worms per Bijou tube (Sterilin) were incubated for 72 hours at 4°C with a 1:10 dilution of affinity purified antibodies in antibody diluent (0.1% (w/v) BSA, 0.5% (v/v) Triton X-100, 0.05% (w/v) sodium azide in PBS). For the mouse anti-γ-Aminobutyric Acid (GABA) monoclonal antibody (Sigma), dilutions of 1:10, 1:50 and 1:100 were used. Unbound antibodies were removed by three washes of one hour each with PBS and worms were treated overnight at 4°C with a 1:200 dilution of the appropriate secondary antibody: tetramethylrhodamine isothiocyanate (TRITC) -conjugated goat anti-rabbit IgG (Sigma), fluorescein isothiocyanate (FITC) -conjugated goat anti-mouse IgG (Jackson ImmunoResearch; West Grove, USA) or FITC-conjugated rabbit anti rat IgG (Vector Laboratories; Peterborough, UK). Worms were washed three times with PBS followed by a final overnight wash at 4°C with PBS / 0.1% (v/v) Triton X-100. They were mounted on microscope slides using Vectashield mounting media (Vector Laboratories), which reduces the effect of quenching of the fluorescence emission after exposure to excitation radiation and examined under a Zeiss LSM 510 confocal microscope (Zeiss, Germany). For the acquisition of images, filters and laser units were selected according to the fluorochrome used. FITC required a filter set 9 (blue excitation) and an argon laser (488 nm); TRITC a filter set 15 (green excitation) and a helium neon laser (543 nm). Transmitted-light observations were scanned using the argon laser (488 nm).

For each antibody, ten to twelve adult worms were treated on two or three different experiments. Controls included the omission of primary antibody and the use of peptide-adsorbed antibodies. In this case an excess of the appropriate peptide (20-40 µg/ml) was added to antibody working dilution and incubated at 37°C for 1 hour before been used for immunocytochemistry.

For double labelling of HcGluClα and GABA or HcGluClα and HcGluClβ, 12 worms were treated as described above but co-incubated with both primary antibodies and then both secondary antibodies as required. Omission of primary antibodies was

used as controls in these experiments. FITC and TRITC images were acquired separately and then the two scanned images were merged. All the antibodies used in double-labelling experiments were first tested in single labelling assays.

3.3 Results

3.3.1 General data

Whole mount adult *H. contortus* were immunostained with polyclonal anti-HcGluClα, -β, -α3A and -α3B subunit specific antibodies, obtained as described in chapter 2, and with an anti-GABA antibody.

Staining results did not show differences when incubating the worms for 6 or 8 h in the concentrated fixative (4 % (w/v) paraformaldehyde (PAF) in PBS). However, worms kept in the storage fixative (0.1 % (w/v) PAF in PBS) for more than 6 weeks did not immunostain. In this latter case it is possible that over-fixation or under fixation conditions have masked or eliminated the epitope(s), preventing the antibodies from interacting with their antigen(s). As far as tissue permeabilisation is concerned, worms were incubated for 8, 10 and 24 h in 120 collagen digestion units/ml of collagenase in collagenase buffer. Reactions were terminated when worms became fragile and showed signs of cuticle degradation. Although this varied between different batches of worms, in most cases the best immunostaining was obtained from specimens exposed for 10 h to the collagenase treatment. Longer incubations often damaged the worms, causing the "heads" to break-off from the rest of the body.

In all cases pre-adsortion of the affinity-purified antibodies with the appropriate synthetic peptide blocked all specific staining, consistent with the immunoreactivity being due to the presence of the relevant GluCl subunit. With all the anti-HcGluCl affinity-purified antibodies (section 2.3.2.4) presented in this work, specific staining was obtained using antibodies at a dilution of 1:10 (~50 μg/ml) in antibody dilutent, followed by incubations with TRITC- or FITC-conjugated secondary antibodies at a 1:200 dilutions. Similar staining was observed in female and male worms but the females seemed to stain better and therefore all the images are from females.

3.3.2 Immunolocalization of HcGluClα and HcGluClβ

3.3.2.1 HcGluClα

When the anti HcGluClα antibodies were used to immunostain adult worms, the HcGluClα subunit was found to be present on *H. contortus* motor neuron commissures (Fig. 3.1A). Specific staining was confined to the anterior part of the worm, below the pharynx to the anterior of the vulva. This result was very similar to that reported for the HcGluClβ subunit (Delany et al., 1998) and suggested that the α- and β-subunits are co-expressed in *H. contortus* and might co-assemble to form the native GluCl. Commissures projecting from nerve cords and passing through the lateral cord could be discerned (Fig. 3.1B).
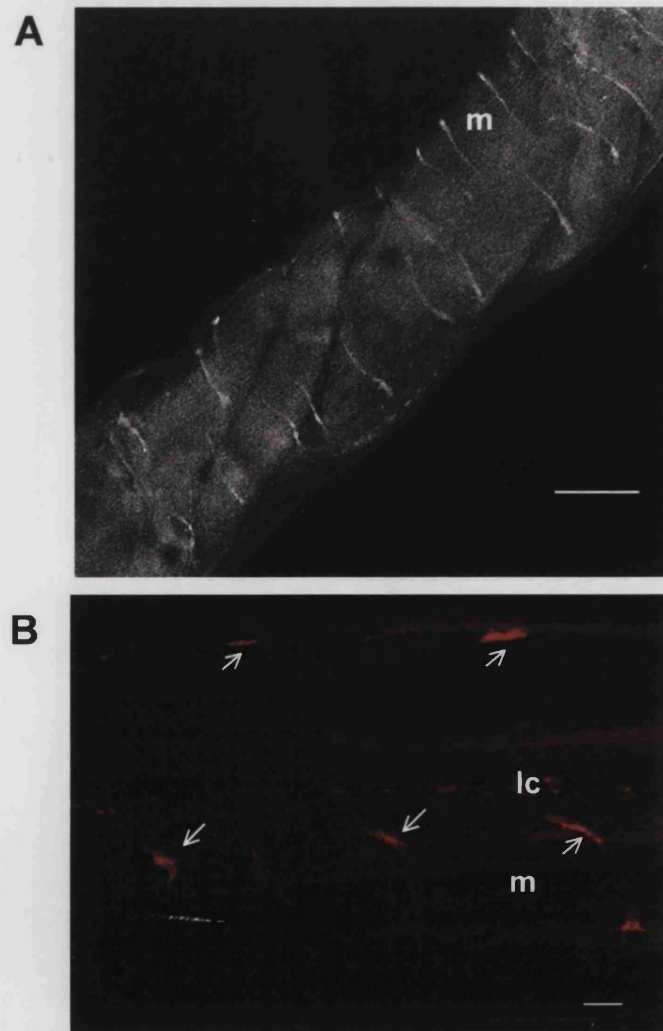
Figure 3.1 Confocal images of anti-HcGluClα antibody staining of *H. contortus*
Worms were incubated with 1:10 (v/v) dilution of anti-HcGluClα antibody followed by 1:200 (v/v) dilution of TRITC-conjugated secondary antibody. A: Lateral view from the anterior region of a female worm showing staining of motor neuron commissures (m). Orientation, anterior is top right. Scale bar 100 μm. B: High power magnification image of motor neuron commissures (m) projecting across the side of the worm (indicated by arrows) through the lateral cord (lc). Scale bar 20 μm.

In addition, the HcGluClα immunostaining was brighter where the motor neurons made contacts with nerve cords. No staining of pharyngeal muscle was observed. Motor neuron commissure staining was absent in worms incubated with peptide-adsorbed antibody, though non-specific staining was identified in the cuticle and in the intestine (Fig. 3.2A). Some general background fluorescence was observed in worms treated with pre-immune serum or with secondary antibody in the absence of primary antibody, as previously observed (Delany et al., 1998; Jagannathan et al.,1999). In these studies, pictures were obtained only from the anterior part of the worms but background fluorescence was observed all along the specimens (Fig. 3.2B and C). Incubations in the presence of 10 % (v/v) serum from the same species in which the secondary antibody was raised, did not reduce the background.
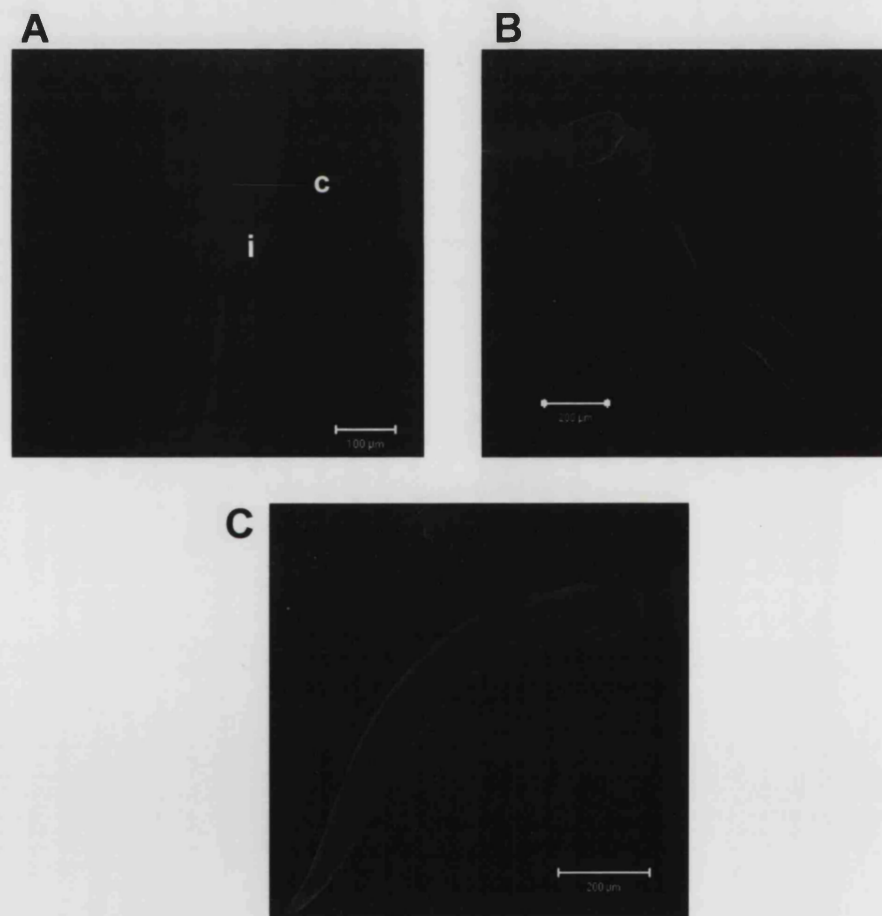
Figure 3.2 Negative controls of the HcGluClα immunostaining
Confocal images of nematodes probed with 1:10 dilutions of HcGluClα peptide (40 μg/ml) -adsorbed antibody (A), pre-immune HcGluClα serum (B) or in the absence of primary antibody (C). In all cases samples were incubated with 1:200 (v/v) dilution of dilution of TRITC-conjugated secondary antibody. A: lateral view of a mid-anterior region of a worm. B&C: head region. c: cuticle ridge; i: intestine.

3.3.2.2 HcGluClα and GABA

Nematodes posses distinct excitatory and inhibitory motor neurons that release acetylcholine or γ-Aminobutyric Acid (GABA), respectively, at neuromuscular junctions (Stretton et al., 1985; Walrond et al., 1985). In order to determine on which type the HcGluClα subunit is expressed, adult *H. contortus* were incubated with both anti-HcGluClα and anti-GABA antibodies. All the GABA-ergic neurons in the anterior and middle part of the worm were also stained by the antibody to HcGluClα (Fig. 3.3), which suggests that the HcGluClα subunit is expressed on inhibitory motor neurons.
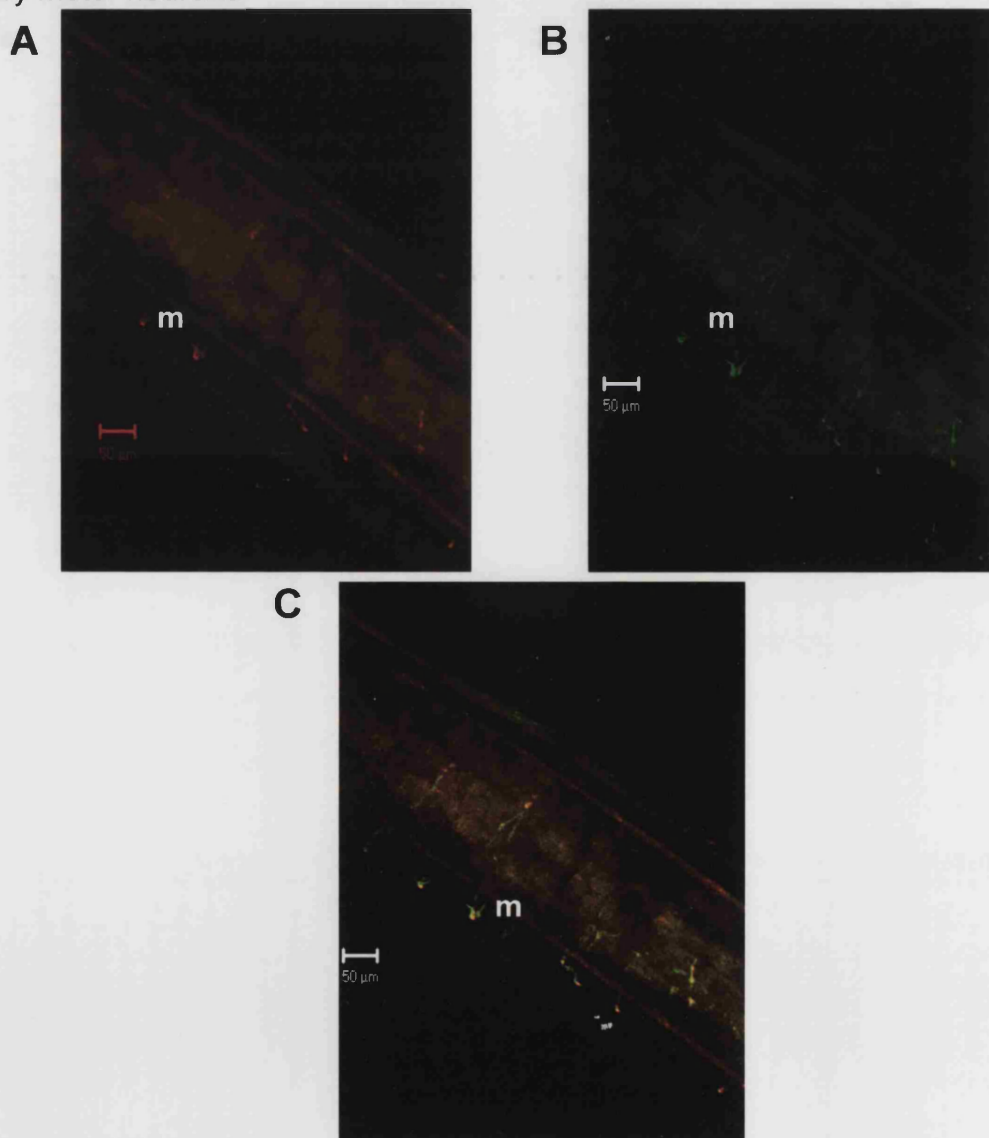
Figure 3.3 Confocal images of HcGluClα and GABA dual immunostaining Lateral view from an anterior region of a female worm probed with 1:10 (v/v) dilution of the HcGluClα antibody and 1:50 dilution (v/v) of an anti-GABA antibody, followed by incubation with 1/200 (v/v) dilution of TRITC- and FITC-conjugated secondary antibodies. A & B: Immunoreactivity to the HcGluClα subunit and to GABA, respectively. The expression of the HcGluClα subunit on GABA-ergic neurons is observed on the merged image (C). Note motor neuron commissures (m). Orientation, anterior is top left.

Is it also expressed on excitatory motor neurons? To date, none of the cholinergic marker genes, such as the vesicular acetylcholine transporter or choline acetyl transferase have been cloned from *H. contortus*. Attempts to immunostain *H. contortus* using polyclonal antibodies raised against *C. elegans* cholinergic markers were unsuccessful as these antibodies were incompatible with the fixation process used (data not shown). It is therefore not possible to determine whether or not excitatory motor neurons also express GluCl subunits.

3.3.2.3 HcGluClβ

The similar expression patterns of HcGluClα and HcGluClβ suggested that in the motor nervous system which innervates body wall muscles of *H. contortus*, avermectin receptors might contain both of these subunits. In order to demonstrate this directly, rat antibodies to HcGluClβ were produced (described in chapter 2). Immunofluorescence experiments showed that the rat HcGluClβ affinity-purified antibodies also stained motor neuron commissures in *H. contortus* (Fig. 3.4). Background staining of the two ovaries wrapping the intestine shows that the staining corresponds to the mid-anterior region of a female worm. Different planes of focusing allowed me to distinguish lateral commissures projecting across the worm via lateral and sub-lateral cords (Fig. 3.4A,B). As with the HcGluClα antibody, staining was brighter where the commissures made contact with nerve cords. In addition, the rat anti-HcGluClβ antibody showed staining on possible sub-lateral and lateral nerve cords in the mid-anterior region of the worm (Fig. 3.4A, B), and this coincided with the area where the antibody stained motor neuron commissures. A rabbit antibody to HcGluClβ has previously immunostained nerve cords in adult worms (Delany et al., 1998), however no distinction on the type of cord was described at that time.

The rat anti-HcGluClβ antibody showed no staining of pharyngeal muscle, nor did the rabbit anti-HcGluClβ antibody. Worms incubated only in the presence of secondary antibody, showed some fluorescence background in the ovaries and intestine (data not shown).
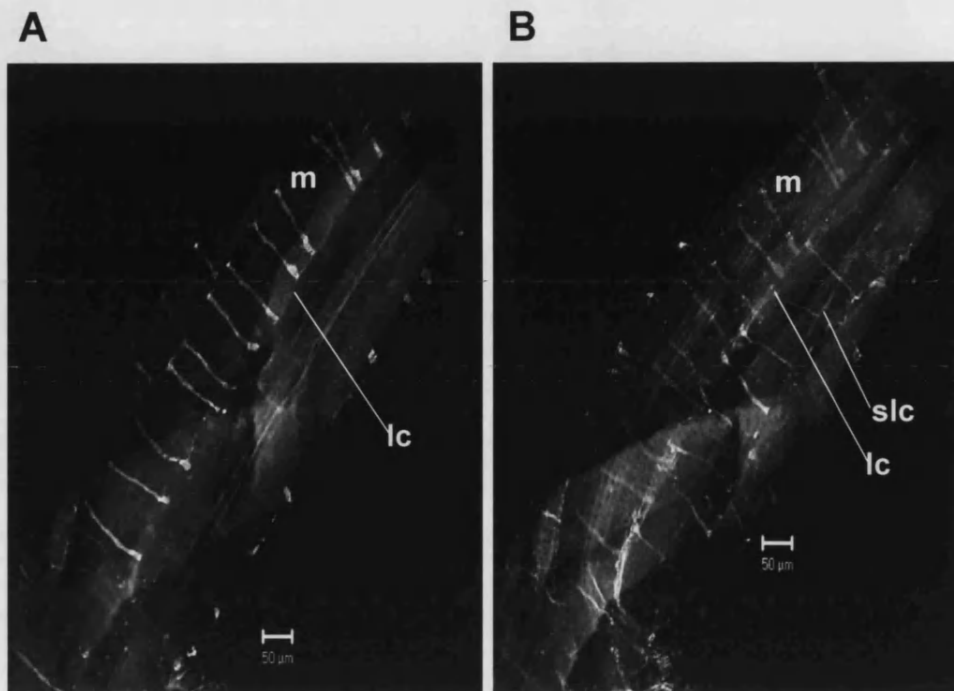
Figure 3.4 Immunolocalisation of HcGluClβ in *H. contortus*
Confocal images from the staining on the mid-anterior region of a female worm probed with 1:10 (v/v) dilution of the rat anti-HcGluClβ antibody and 1:200 dilution of a FITC-conjugated secondary antibody, scanned on different focal levels (A & B). Motor neuron commissures (m) project laterally via the lateral (lc) and sub-lateral nerve cords (slc). Orientation, right lateral side with the anterior towards the top right.

3.3.2.4 HcGluClα and HcGluClβ

Double labelling with the HcGluCl-α and β antibodies showed complete co-localisation in motor neuron commissures in the anterior and middle part of *H. contortus* (Fig. 3.5), suggesting that at this site the avermectin receptor does contain both of these subunits.
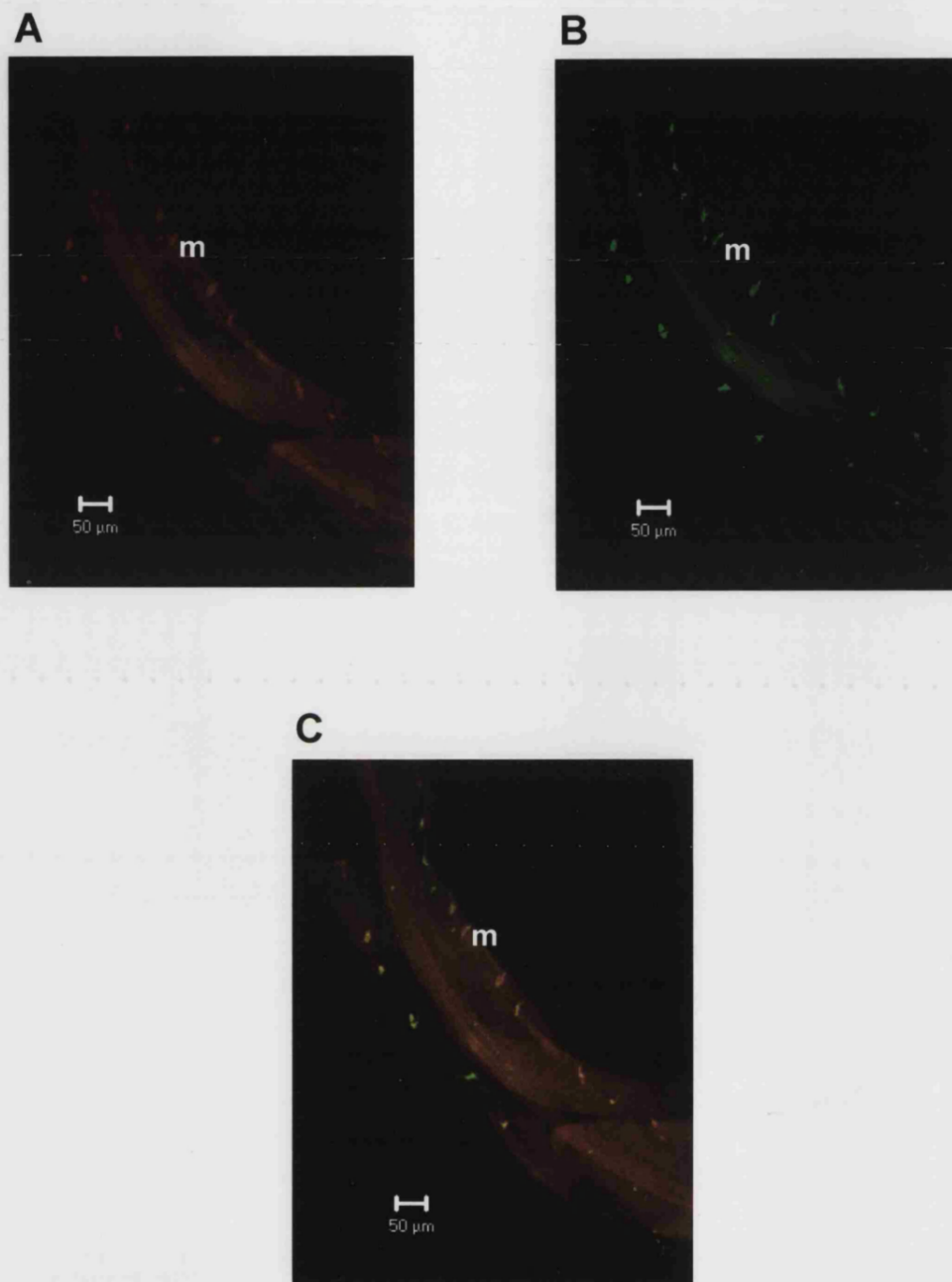
Figure 3.5 Confocal images of HcGluClα and β dual-immunolabelling
Lateral view of the mid-anterior region of a female worm probed with 1:10 (v/v) dilutions of the rabbit anti-HcGluClα and rat anti-HcGluClβ antibody followed by incubation with 1/200 (v/v) dilution of TRITC- and FITC-conjugated secondary antibodies. Immunoreactivity to the HcGluClα (A) and HcGluClβ (B) subunits was observed on motor neuron commissures (m). C: Overlay image of A and B. Orientation, anterior is top left.

3.3.3 Immunolocalisation of HcGluClα3A and HcGluClα3B

The alternatively-spliced products of the GluCl *H. contortus avr-14* (*gbr-2*) gene, HcGluClα3A and α3B, were previously shown to be widely distributed in the adult nervous system of *H. contortus* (Jagannathan et al., 1999). In order to distinguish between the expression patterns of HcGluClα3A & α3B, peptide-specific antisera were produced in rabbits and the antibodies purified by affinity chromatography (described in chapter 2). Antibody specificities were demonstrated by ELISA assays, where the anti-GluClα3A antibody did not show any cross-reactivity with the GluClα3B peptide, nor did the anti-GluClα3B antibody cross-react with the GluClα3A peptide (section 2.3.2.4a).

Immunofluorescence experiments showed that the HcGluClα3 subunits are both expressed in motor neuron commissures in the anterior and middle region of *H. contortus* (Fig. 3.6A, B). The anti-GluClα3A antibody seemed to stain fewer commissures than the anti-GluClα, β or GluClα3B antibodies did. Outside of these structures, the HcGluClα3A and 3B subunits are expressed in different regions of the worm nervous system. HcGluClα3B, but not α3A is expressed in nerve cords (Fig. 3.6B and C). Assuming that *H. contortus* neuroanatomy is similar to that described for *C. elegans*, the thick structure stained with the HcGluClα3B antibody in the figure 3.6B is probably the ventral nerve cord and the one parallel to it is the ventral sub-lateral cord. The punctate staining observed with the same antibody in the ventral nerve cord (Fig. 3.6C), suggests a synaptic localisation of the HcGluClα3B subunit.
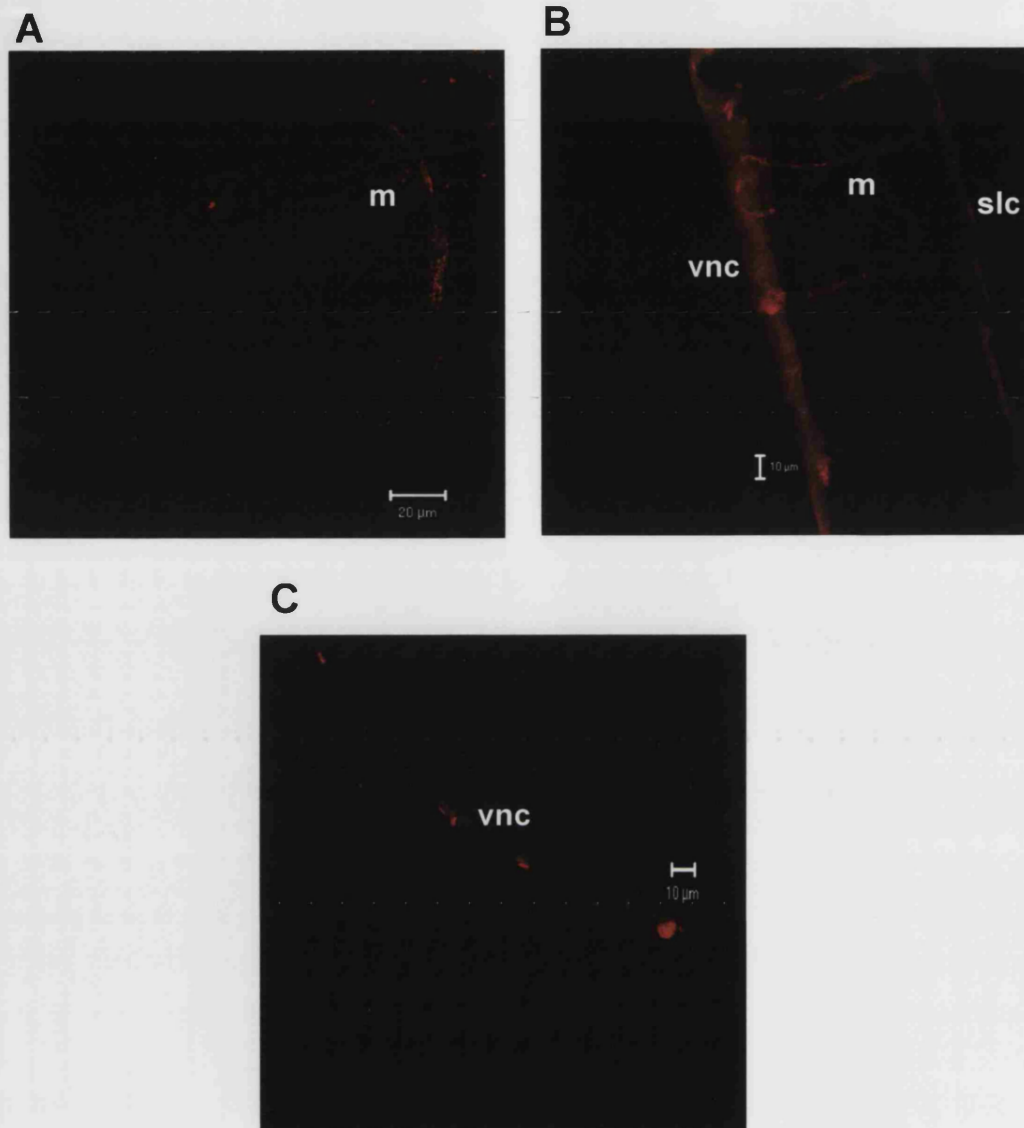
Figure 3.6 Distribution of HcGluClα3A and α3B subunits in the motor nervous system

Confocal images of lateral views from the middle region of worms probed with 1:10 (v/v) dilutions of the anti-HcGluClα3A (A) or anti-HcGluClα3B (B&C) antibodies, followed by incubation with 1:200 (v/v) of TRITC-conjugated secondary Ab. Both HcGluClα3A and α3B antibodies stained motor neuron commissures (m); but the HcGluClα3B also stained the ventral (vnc) and ventral sub-lateral (slc) nerve cords. Scale bars, A= 20 µM; B,C = 10 µM

In addition to the staining mentioned above, novel expression sites for the HcGluClα3A and -3B subunits were observed in the head of *H. contortus*. The anti-HcGluClα3A antibody stained a pair of lateral neurons in the anterior end (Fig. 3.7A). A pair of nerve processes, emanating from their cell bodies can be

distinguished. These may correspond to sensory neurons from the amphids, the large paired sensilla located on each side of the mouth.
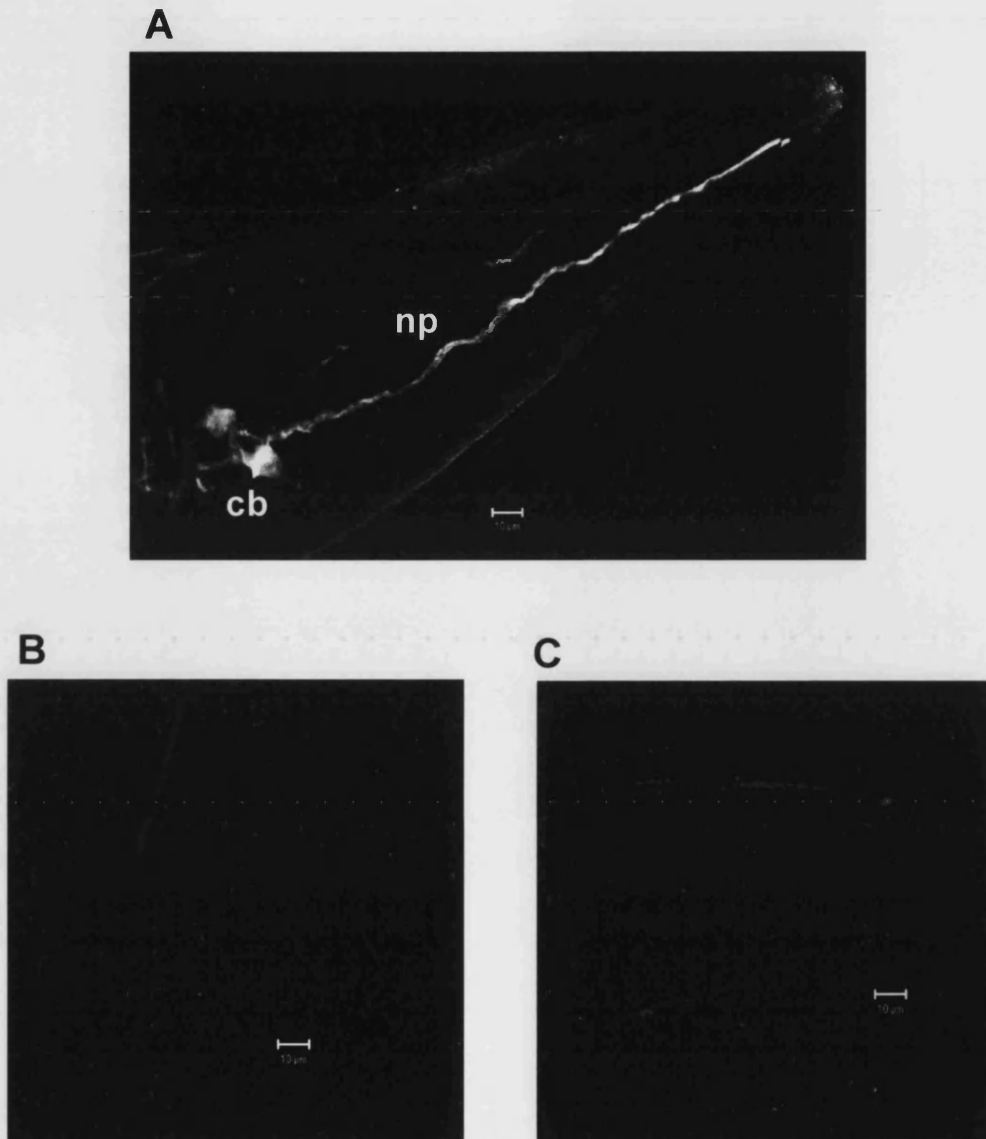
Figure 3.7 Immunolocalisation of HcGluClα3A in the head of *H. contortus*. Reconstruction from serial confocal sections of the staining on a female worm, probably on amphidial neurons. Worms were treated with 1:10 (v/v) dilutions of the anti-HcGluClα3A antibody (A), HcGluClα3A peptide (40 µg/ml)-adsorbed antibody (B) and pre-immune HcGluClα3A serum (C) followed by incubation with 1:200 (v/v) of TRITC-conjugated secondary antibody. Note nerve precesses (np) and cell bodies (cb). Orientations: the worm anterior end is top right in A, left bottom in B and right in C. A-C images were scanned keeping the same confocal settings. Scale bars, 10 µM.

The stained cell bodies were ~ 300 µm from the anterior tip of the worm. Since in *H. contortus* adult females the nerve ring has been located ~ 285 µm from the anterior end of the body (Veglia, 1915), it seems that the cell bodies stained with the HcGluClα3A antibody are located just behind the nerve ring, possibly in the lateral

ganglion. In *H.contortus* L1 and L3 larva as in *C. elegans,* all receptor neurons of the amphid sensilla have their cell bodies in the lateral ganglia (Li et al., 2000 a & b). This specific neuronal staining was absent after treatment with HcGluClα3A peptide-adsorbed antibody or pre-immune sera, which detected only some non-specific cuticle staining in both cases (Fig. 3.7B and C).

In the head, the anti-HcGluClα3B antibodies reacted with three possible neuronal cell bodies situated ~ 500 μm from the anterior tip. These structures, arranged in a triangular disposition, one in one plane and two in a different focal plane, were in the region of the pharynx (Fig. 3.8A,B). They might correspond to pharyngeal motor neuron cell bodies, possibly the equivalents of the two M2 and single M1 neurons found in *C. elegans* (Albertson and Thomson 1976). The staining was absent in worms incubated with HcGluClα3B peptide-adsorbed antibody or pre-immune sera, which again gave rise to non-specific staining of the cuticle (Fig. 3.8D, E).
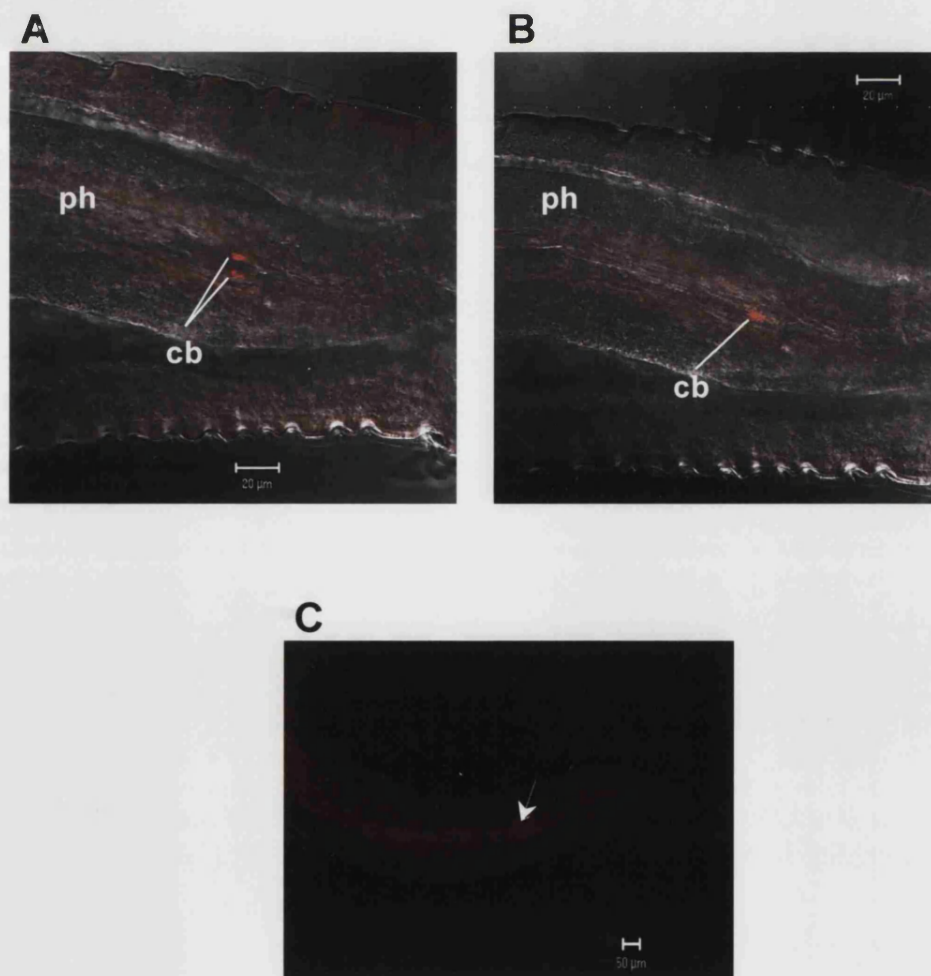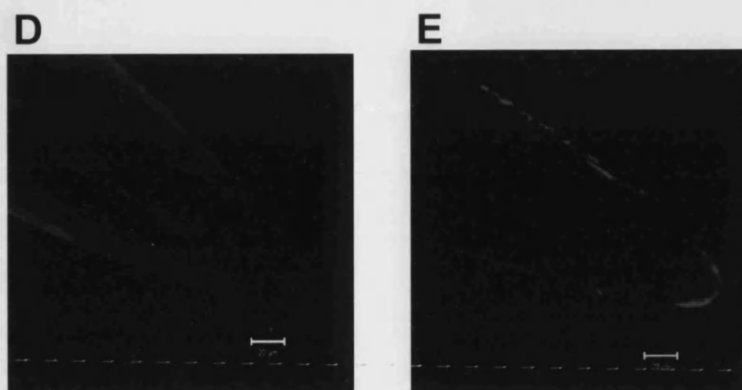
Figure 3.8 Immunolocalisation of HcGluClα3B in the pharynx of *H. contortus*. Worms were probed with 1:10 (v/v) dilutions of the anti-HcGluClα3B antibody (A-C), HcGluClα3B peptide (40 μg/ml)-adsorbed antibody (D) and pre-immune HcGluClα3B serum (E) followed by incubation with 1:200 (v/v) of TRITC-conjugated secondary antibody. A&B: Confocal images scanned in two different planes of focusing, merged with their DIC images. Note three cell bodies (cb) stained on the pharynx (ph). C: Low power magnification image; the arrow indicates the staining observed in A and B. Orientation, anterior is right. A-E images were scanned keeping the same confocal settings. Scale bars, panels A, B, D, E = 20 μM; C = 50 μM.

Taken together, these data allowed the description of the expression pattern of all the currently identified GluCl subunits in *H. contortus* (Table 3.1) and to draw some preliminary conclusions about the subunit compositions of the avermectin receptors in this organism.

Table 3.1. Location of avermectin subunits in *H. contortus*

GluClα	motor neuron commissures[a] (Fig. 3.1, 3.3 & 3.5)
GluClβ	motor neuron commissures[b, a] (Fig. 3.4 & 3.5) and lateral and sub-lateral nerve cords[a] (Fig. 3.4)
GluClα3A	amphidial neurons[a] (Fig. 3.7) and motor neuron commissures[c, a] (Fig. 3.6A), nerve cords and nerve ring[c]
GluClα3B	pharyngeal neurons[a] (Fig. 3.8), motor neuron commissures[c, a] (Fig. 3.6B), lateral and ventral nerve cords[c,a] (Fig. 3.6B,C) , nerve ring[c]

[a] current study; [b] Delany et al, 1998; [c] Jagannathan et al, 1999. Note that the antibodies used in this work did not distinguished between the two alternative spliced variants GluClα3A and 3B.

112

3.4 Discussion

Specific antisera raised against the HcGluClα, β, α3A and α3B subunits were used to study the distribution of the *H. contortus* avermectin receptor in adult worms. The data presented provide the first immunocytochemical evidence for the possible association of α and β subunits in native nematode GluCls and reveal different expression sites for the alternatively spliced gene products of *Hcgbr-2*.

In general, good reproducibility of the results was seen between preparations and between individual worms within a preparation. However, some variation was seen. It is difficult to assess the biological significance of this, as it is necessary to almost completely destroy the cuticle in order to permit penetration of antibodies. Under-digestion with collagenase results in no specific staining, whereas over-digestion produces extremely fragile worms that do not survive the antibody treatment and washes intact. The best results were obtained by halting the digestion just as the worms were about to disintegrate. Given the inherent biological variation in populations this inevitably means that some worms will be slightly over- or under-digested in each preparation. In fact, the reason for obtaining better results with female worms is possibly due to a slightly different cuticle structure. Certain sites of expression may therefore not be available for detection using this protocol and for that reason, though the presence of specific immunoreactivity certainly implies expression of a particular subunit at a site, the absence of reactivity does not necessarily imply the absence of expression.

HcGluClα and β

The expression pattern obtained for the HcGluClα and β subunits shows that both co-localise in motor neuron commissures in adult *H. contortus,* strongly suggesting that these subunits are part of the same receptor. This expression of GluCls in motor neurons is consistent with the paralysing effect of ivermectin on *H. contortus* somatic musculature (Gill et al., 1991; Geary et al., 1993). Since the HcGluClα subunit binds ivermectin (IVM) with high affinity (Cheeseman et al., 2001; Forrester et al., 2002), it is possible that a HcGluClα- and HcGluClβ-containing receptor is responsible for at least part of the paralysing effects of the drug.

The presence of GABA in the nematode motor nervous system has been demonstrated for both *C. elegans* and *Ascaris suum*, a large parasite of pigs (Johnson and Stretton 1987; McIntire et al., 1993). The use of anti-HcGluClα and anti-GABA antibodies showed that the HcGluClα subunit, and therefore the 'α + β' receptor, is expressed on GABA-ergic motor neurons. This conclusion is supported by the data of Kass et al (1980) who found that avermectin inhibits transmission between inhibitory (VI) motor neurons and muscle in *A. suum*. Moreover, Davies (1998) showed that, in this parasite, the dorsal inhibitory motor neuron (DI) exhibits a reversible glutamate-induced hyperpolarisation, an observation which could be explained by the presence of GluCls on the GABA-ergic motor neurons.

The GluClα and β immunostaining revealed commissures crossing lateral and sub-lateral cords, as previously reported (Delany et al., 1998). GluCl immunoreactivity was stronger where the commissures make contacts with these nerve cords, suggesting a concentration of receptors at possible synaptic areas. Johnson and Stretton (1987) suggested that motor neurons may receive inputs from neurons in the lateral cords that are important for the control of movement in the right-left plane. GluCl subunits staining was found in motor neurons between the pharynx and the vulva, consistent with the IVM-induced paralysis of the mid-body region of adult *H. contortus* (Geary et al., 1993). In *C. elegans* this area contains neurons running in sub-lateral nerves as well as the ALM and AVM touch receptor neurons running in the lateral and ventral nerve cords, respectively (White et al., 1986). The expresssion of *eat-4* (a glutamate transporter gene) in ALM and AVM suggested that these neurons are glutamatergic (Lee et al., 1999). Thus, it is tempting to speculate that the GluCl could be target sites for glutamatergic transmission from those neurons.

HcGluClα3A and α3B

Specific antibodies to HcGluClα3A and α3B allowed the distinction between the expression patterns of these subunits. This work confirmed that both subunits are expressed in motor neuron commissures, and, excluding this location, it does suggest that the HcGluClα3A and α3B subunits are expressed in different regions of the worm nervous system. HcGluClα3B, but not HcGluClα3A is expressed in nerve cords. Indeed, ventral cord staining has already been described for the HcGluClα3 subunits in *H. contortus* and for *avr-14* in *C. elegans* (Jagannathan et

al., 1999; Dent et al., 2000). However, neither the antibody used earlier in *H. contortus* nor the reporter gene construct used in *C. elegans* distinguished between the two gene products. More recently the HcGluClα3B antibody was used to immunostain *C. elegans* and in agreement with the data presented here, it showed immunoreactivity in the *C. elegans* motor nervous system (A. Cook and L. Holden–Dye, pers. commun.). Expression of HcGluClα3B in lateral cords might correspond to the touch receptor neuron ALM or interneurons, both with axons running laterally. In *C. elegans* the lateral interneuron SIADL receives in the nerve ring a synapse from the glutamatergic neuron ALM. It is possible that the SIADL or other(s) lateral interneurons express GluCls and receive glutamatergic inputs, such as from ALM, not yet characterised. HcGluClβ was also present on lateral cords but whether HcGluClα3B and HcGluClβ are part of the same GluCl channel in the cords, is still unclear. In the present study, double labelling assays with both anti-peptide antibodies were inconclusive.

In the ventral cord, the anti-HcGluClα3B antibody might be staining motor neurons and or command interneurons. The punctate pattern obtained with this antibody suggests a post-synaptic role for the HcGluClα3B-containing GluCl in the ventral cord. *C. elegans* command interneurons control locomotion by receiving inputs from sensory neurons and synapsing onto motor neurons and other command interneurons along the ventral cord. Recently, a GFP-tagged version of the *C. elegans* GluClα3 was expressed in interneurons and localised to distinct synapses along the ventral nerve cord (Grunwalnd, 2001). In addition, indirect evidence from the sensory response to anterior touch behaviour in *C. elegans*, suggested the presence of the GluClα2 subunit in the AVB and PVC command interneurons (Lee et al., 1999). These interneurons control *C. elegans* forward locomotion and the AVA, AVD and AVE command interneurons backward movement (Chalfie and White, 1988). Very recently, a glutamate-gated chloride current has been detected in the AVA neuron, being suggested that the GluCls may help to reestablish forward movement following a backwards one (Mellem et al., 2002). Therefore, the expression of GluCls in possibly lateral and ventral cord interneurons may further contribute to the function of the GluCl receptor expressed in motor neuron commissures on the locomotory control in *H. contortus*.

In the head, HcGluClα3A was found in a pair of probable sensory neurons. The distance from their cell bodies to the tip of the worm and the bilateral disposition of the neuronal processes suggested that they were amphidial neurons. Amphids, the main chemoreceptor sense organs from the anterior end of nematodes, are the largest sensilla located on each side of the mouth. The amphidial structure of the first stage larva of *H. contortus* has been described and is very similar to their counterparts in *C. elegans* (Li et al., 2000a). However, there is no information about the amphids in adult *H. contortus* making it difficult to determine which neurons are stained with the anti-HcGluClα3A antibody. In *C. elegans*, the orthologous *avr-14* gene is also expressed in extrapharyngeal neurons in the head of the worm as well as in other sensory neurons (Dent et al., 2000). Expression of GluCl subunits in these neurons has not been reported before and their function here is uncertain. It has been shown that HcGluClα3A, when expressed alone in a heterologous system, failed to form IVM binding sites and, presumably, functional receptors (Cheeseman et al., 2001). This suggests that other, as yet unidentified, GluCl subunits are likely to be expressed in *H. contortus* amphidial neurons.

The connectivity of *C. elegans* nervous system has been studied by electron microscopy reconstructions (White et al., 1986). As far as amphid neurons is concerned, there are several instances of neurons synapsing directly onto others, such as those of ASH onto ASK and ASK onto ASJ. Also, some of them synapse onto more than one other type of neuron, such as ASE onto AWC and AFD. Interestingly, the two pairs of ASH and ASK neurons (left and right) express the *eat-4* glutamate transporter and hence, supposed to be glutamatergic (Lee, et al.1999). If this was the case for *H. contortus*, it is possible that the GluClα3A- containing receptor expressed in the amphids was the synaptic target for the ASH or ASK glutamatergic amphidial neurons. Chemical synapses in *C. elegans* and probably in *H. contortus*, occur *en passant* between neighbouring parallel processes. Since amphidial neurons run parallel into the amphidial channel, apart from the well-characterised outputs of those neurons described on the nerve ring area, synapses onto the distal nerve processes cannot be ruled out. This would explain the expression of GluClα3A in the anterior processes of *H. contortus* amphid neurons. It seems likely that amphid receptor-receptor connections facilitate the modulation of the activity of one receptor by another (White et al., 1986). GluCl channels have been implicated in the formation of inhibitory synapses (Dent et al., 1997). In this

case amphid neurons expressing HcGluClα3A-containing receptors might modulate sensory modality inactivating chemical transmission.

Interestingly, a direct role for ligand-gated ion channels in chemosensation has been already reported for a nicotinic acetylcholine receptor in *C. elegans* (Yassin et al., 2001). This receptor (DEG-3/DES-2) was localised to sensory neurons in the head, probably IL2s and FLPs, and was preferentially activated by choline. Unlike the punctate staining typical of nematode synaptic proteins (Nonet et al., 1993), the antibody staining for the DEG-3 subunit was diffuse. The HcGluClα3A amphidial staining was also diffuse. This may be a result of receptor translocation intermediates. Alternatively, the glutamate HcGluClα3A-containing receptor might have a non-synaptic role in the amphids. It is tempting to speculate that expression of HcGluClα3A in amphidial neurons might modulate sensory signals; these neurons are very likely to play an important role in mediating the infective process, including host contact, host recognition, and initiation of parasitic growth and development (Ashton et al., 1999; Li et al., 2000b; Lopez et al., 2000). IVM would therefore be predicted to interfere with these processes and studies on *Brugia pahangi* (a filarial nematode) have indeed shown that the drug can block physiological responses to chemical stimuli (Perry, 2001; Rolfe et al., 2001). Interestingly, in *C. elegans* the entry of IVM into the nematode seems to be facilitated by amphidial neurons (Dent et al., 2000). This might also be the case in *H. contortus* but the link of this, if it is any, with the expression of HcGluClα3A is unclear.

Previous reports have shown that a major effect of the avermectin/mylbemycin (AM) anthelmintics on parasitic nematodes is the paralysis of pharyngeal muscle (Geary et al. 1993; Martin, 1996). Results presented here have now demonstrated the expression of the HcGluClα3B subunit in pharyngeal cells. Expression of the subunit was restricted to three cell bodies situated about 500 μm from the anterior tip of the worm. The identity of these cells is still unknown. However, due to their position in the pharynx, and assuming that the localisation of the cell bodies is similar to that seen in *C. elegans*, the staining might correspond to pharyngeal neurons M2 (right and left) and M1. This presynaptic localisation in pharyngeal neurons suggests a modulatory effect of *H. contortus* GluCl on nematode feeding and might explain the paralysing effect of IVM on this process. In *C. elegans* the

HcGluClα3B antibody also stained pharyngeal neurons (A. Cook and L. Holden-Dye, pers. commun). Although the immunostaing appeared more widespread than observed in *H. contortus,* a triplet of neurons identified as M1 and M2 in the terminal bulb of the pharynx (Fig. 3.9), resembles the staining here reported in *H. contortus*. In *C. elegans* the M1 is a single motor neuron with unknown function whose cell body is in the anterior terminal bulb. It synapses to pharyngeal muscle (pm) 1, pm2 and pm3. The M2 motor neuron innervates pm4 and pm5 pharyngeal muscles. Interestingly, the GluCl genes *glc-2* and *avr-15* were expressed in the pm4 and the *avr-15* was also expressed in the pm5 (Laughton et al., 1997b and Dent et al., 2000) (Fig. 3.9). Expression of GluCl subunits in nematode pharyngeal system, either in pharyngeal muscles for *C. elegans* or in pharyngeal neurons in both *C. elegans* and *H. contortus*, suggests an important role for GluCls in controlling nematode feeding.
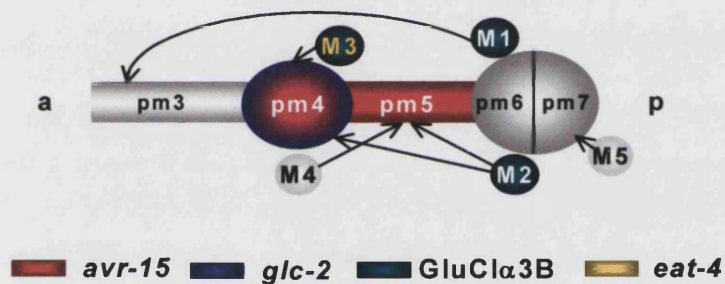
Fig. 3.9 *C. elegans* GluCl subunit staining in the pharynx

Lateral view of the pharynx showing in colour the muscles expressing reporter gene constructs for the *avr-15* and *glc-2* genes. In red, expression of the GluClα2A::GFP promoter fusion in the pharyngeal muscle cells 4 (pm4) and 5 (pm5) and in blue, the GluClβ::lacZ construct expressed in the pm4. Small circles correspond to the cell bodies of pharyngeal motorneurons that synapse onto pharyngeal muscle. Notice the GluClα3B subunit expressed in M1, M2 and M3. Chemical synapses are indicated by arrows. Notice that the glutamatergic M3 motorneuron (which expresses *eat-4*) synapses onto pm4. References are mentioned in the discussion. a, anterior. p,posterior.

In contrast to early results obtained with the anti-HcGluClα3 antibodies (Jagannathan et al., 1999); none of the subunit-specific anti-HcGluClα3A or α3B antibodies stained the *H. contortus* nerve ring in the present work. This might be explained by differences in the affinities of the antibodies used or variation in tissue fixation and/or permeabilisation conditions.

It is noteworthy that the results presented confirmed that the expression pattern of orthologous GluCl subunits is not conserved between *C. elegans* and *H. contortus*, as demonstrated earlier for the β-subunits (Laughton et al., 1997b; Delany et al., 1998), though we have not yet identified the parasite orthologues, if any, of *C. elegans glc-1* or *avr-15* genes. There is, however, a strong correlation between the biological activity of IVM on *C. elegans* and *H. contortus*, with both pharyngeal pumping and motility being inhibited in both species (Bernt et al., 1989; Avery et al., 1990; Geary et al., 1993; Arena et al., 1995). It seems that nematodes contain more than one type of GluCl, and it is possible that differences in the expression of individual subunit genes between nematode species reflect their adaptation to different life-styles. This would predict that the effects of the AM anthelmintics would vary in different species, reflecting the varying roles and subunit composition of the GluCl. A number of observations support this prediction; the avermectins (AVMs) have different effects on the development, fertility and somatic and pharyngeal musculature of different parasitic nematodes (Gill et al., 1998; Grant 2000). AVM effects on motility are critical for efficacy against *H. contortus* and *Trichostrongylus colubriformis*, whereas its effects on pharyngeal pumping are crucial for the elimination of *Ostertagia circumcinta* (Gill et al., 1998).

In summary, it was shown that *H. contortus* GluClα and β subunits co-localise and probably co-assemble in motor neuron commissures in native glutamate gated-chloride channels. The expression of HcGluClα3 subunits in motor neurons was confirmed and their expression in nerve cords was dissected, identifying only the HcGluClα3B subunit in the sub-lateral and ventral cords. New expression sites for the HcGluClα3A and α3B subunits were detected in sensory and possibly pharyngeal neurons, respectively. These expression patterns suggest that the GluCls have critical roles controlling locomotion, pharyngeal function and possibly sensory processing in parasitic nematodes. They also provide an explanation for the observed effects of the AMs anthelmintics on *H. contortus* and the different effects that are observed on different nematode species.

CHAPTER 4

STUDY OF THE ROLES OF GLUTAMATE-GATED CHLORIDE CHANNEL SUBUNITS IN *C. ELEGANS* BEHAVIOUR

4.1 Introduction

4.1.1 *C. elegans* behaviour

Behavioural studies have been important screening tools for the isolation of mutations in *C. elegans* (Brenner, 1974; Wood, 1988; Bargmann, 1993). The study of behavioural genetics in *C. elegans*, an organism in which the nervous system is small enough (302 neurons in the adult hermaphrodite) to theoretically allow the role of every neuron in a given behaviour to be known, has given unique insights into how genes contribute to behaviour in general. Laser ablation of identified neurons has allowed researchers to investigate the role of single neurons in specific behaviours (Chalfie et al., 1985), and once determined, the neuronal circuit can be used to explore the roles of other neurons that connect to the circuit in the same behaviour.

Naturally occurring behaviours in *C. elegans* can be divided into four classes: 1) sensory input: chemosensation, thermosensation and mechanosensation; 2) locomotion; 3) survival: foraging, feeding, defaecation and dauer larva formation, and 4) reproduction: egg laying and male mating. Other complex behaviours include: social behaviour, learning and memory (Rankin, 2002). General descriptions of the behaviours studied in the present work are described below.

4.1.1.1 Chemosensation

C. elegans sense different stimuli detected by the amphids and the inner labial sensilla in the anterior tip of the worm and by the phasmid sensilla at the posterior end of the animal (Bargmann and Horvitz, 1991a). The amphids and phasmids are considered to be the main chemoreceptive organs in *C. elegans* because their structure permits a group of nerve endings to be exposed to the external environment of the animal (White et al., 1986). Chemosensory functions have been identified for 11 pairs of amphid neurons. Each type of neuron has a particular sensory specificity and most of them recognise several different chemical cues. The chemical specificities of different neurons can overlap; for example: two types of neurons sense thiazole and four types sense salts. Also, some neurons respond to more than one type of stimulus (Bargmann and Mori, 1997). It is believed that behavioural specificity is probably encoded by synaptic connections between

sensory neurons and their partners (interneurons) in the nerve ring. In brief, the stimuli detected by the sensory neurons are transmitted to interneurons, which synapse onto motor neurons such as those responsible for driving locomotion in the worm.

Although many genetic screens for *C. elegans* mutants unable to respond to chemicals have been conducted, they have generally not led to the identification of the receptors, with the exception of *odr-10* (Sengupta et al., 1996). ODR-10, the receptor for diacetyl, is a G protein-coupled 7-transmembrane domain protein that localises to the cilia of the AWA neurons, where diacetyl detection is believed to occur. Identification of other chemosensory receptors as well as the events that occur downstream of the sensory neurons remain largely unsolved.

Chemotaxis

Chemotaxis represents a complex response of the animal to its environment. The animal must sense continuous changes in external conditions and convert sensory information into movement in a particular direction. *C. elegans* moves up gradients of attractive stimuli and moves down gradients of repellent stimuli. The *C. elegans* sensory neurons required for normal responses to a number of chemical attractans or repellents have been identified by laser ablation of particular cell types. In this way, Bargmann and Horvitz (1991a) found that the amphidial neuron ASE is the single most important chemosensory neuron for chemotactic responses to cAMP, biotin, Cl⁻ and Na⁺. Chemical attractants and repellents for *C. elegans* have been identified by screening large numbers of volatile and non-volatile chemicals. Salts, some amino acids, some nucleotides and some vitamins act as water-soluble attractants (Ward, 1973; Dusenbery 1974; Bargmann and Horvitz, 1991a) as do many different volatile organic molecules (Bargmann et al., 1993). Although mutants worms that have specific chemotaxis defects have been isolated (Culotti and Rusell, 1978), the mechanism by which chemotaxis is accomplished is only partly understood. Chemotaxis towards water-soluble attractants requires the cyclic nucleotide-gated channel encoded by *tax-2* and *tax-4*. TAX-2 and TAX-4 form a putative sensory transduction channel gated by cGMP, which is permeable to Na^+ and Ca^{2+} (Komatsu et al., 1999). Recently, Yassin et al (2001) showed for first time that a *C. elegans* nicotinic receptor DEG-3/DES-2, is involved in chemotaxis, in this case towards choline.

Osmosensation

High osmotic strength is repulsive to *C. elegans*. Detection of a high osmotic strength, low pH or octanol induces a rapid reversal response, which is followed by a change in direction (Culotti and Russell 1978; Troemel et al., 1995). The polymodal sensory neuron ASH seems to play the predominant role in detecting hyperosmolarity (Hart et al., 1999). It also mediates the responses to nose touch, volatile and water-soluble repellents (such as octanol and sodium dodecyl sulphate, respectively), with each of the three stimuli evoking backward locomotion (Bargmann et al., 1990; Kaplan and Horvitz, 1993; Troemel et al, 1995; Hilliard et al., 2002). It is believed that hyperosmolarity and touch are both detected by mechanically gated ion channels. In mammals, ubiquitous stretch-activated channels mediate osmosensation (Oliet and Bourque, 1993; 1996). However, it is unclear in *C. elegans* which receptor(s) respond(s) directly to the osmotic modality. The search for mutants defective only in ASH-mediated osmotic avoidance but normal for ASH-mediated nose touch sensitivity, resulted in the isolation of OSM-10 (Hart et al., 1999). This is a cytosolic protein expressed in ASH, and in three other classes of sensory neurons required for osmosensory signalling. Recently, Mellem et al (2002) showed that ASH polymodal signalling in *C. elegans* occurs via differential activation of postsynaptic glutamate receptors. Particularly, osmotic signals activate non-NMDA (GLR-1 and GLR-2)- and NMDA (NMR-1)- dependent glutamate currents.

In this chapter, a new osmotic avoidance assay described by Hilliard et al (2002) was used in preference to the standard ring assay described by Culotti and Russell (1978). The reason for this, as recently suggested by Mellem et al (2002), is that the ring assay does not measure the immediate avoidance response to an osmotic stimulus and may reflect a variety of signalling processes including desensitization and adaptation. In this way, the drop assay described by Hilliard has just revealed that *glr-1* mutant worms with a normal osmotic avoidance response assayed by the osmotic ring method (Maricq et al., 1995), were in fact defective compared to wild-type worms. These worms, showed a significant increase in the delay to the withdrawal response (Mellem et al., 2002).

4.1.1.2 Locomotion

Locomotion in *C. elegans* is achieved by moving the body in sinusoidal waves. To generate this pattern, the contraction of the dorsal and ventral body muscles must be out of phase: to turn the body dorsally, the dorsal muscles contract while the ventral muscles relax. A pattern of altering dorsal and ventral contractions is produced by interactions between excitatory and inhibitory motor neurons (for details see chapter 1, section 1.5.3).

Circuit for forward and backward locomotion

In *C. elegans* the locomotory control circuit regulates movement in response to environmental stimuli. Forward and backward locomotion are regulated by several pairs of command interneurons (Chalfie et al., 1985). These are bilaterally symmetrical ventral cord neurons, whose axons run the entire length of the cord providing inputs to the ventral cord motor neurons: VA, VB, DA and DB. The command interneurons AVB and PVC activate forward movement and the AVA, AVD and probably AVE, backward movement (see figure 4.1). The command interneurons receive extensive input from sensory circuits, both directly from sensory neurons and indirectly through amphid interneurons and other nerve-ring interneurons. It is likely that the command interneurons integrate complex sensory information and direct appropriate locomotory responses. Also, the forward and backward interneurons have reciprocal connections, which could mediate coordination of opposing circuits (White et al., 1986).
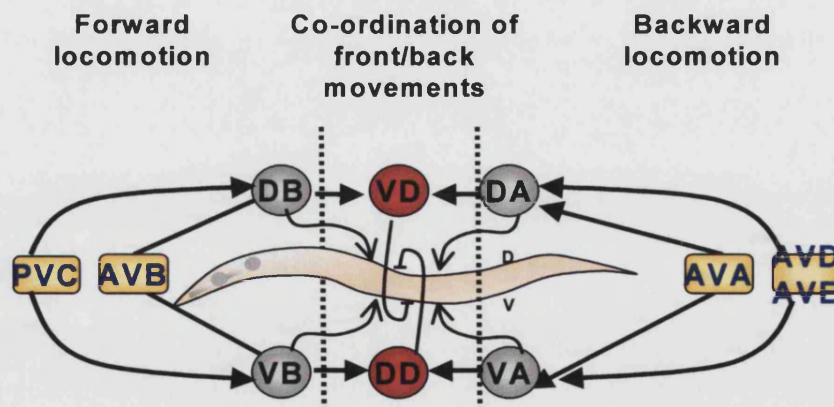
Fig. 4.1 *C. elegans* motor circuitry
Backward and forward movement is mediated by the activation of excitatory motor neurons (grey circles) by their associated command interneurons (yellow rectangles). The GABA-ergic inhibitory motor neurons (red circles) receive their synaptic input from the other motor neuron classes. They coordinate the front and back movements synapsing onto muscles situated on the opposite side of those that are innervated by their presynaptic partners (indicated by capped lines). Cholinergic neuromuscular synapses are indicated by thin arrows. D: dorsal, V: ventral. Thick arrows: neuronal chemical synapses; straight connecting lines: gap junctions. Adapted from Chalfie and White, 1988.

4.1.2 Double strand RNA interference in *C. elegans*

RNA-mediated interference (RNAi) transiently inhibits or knocks-down the activity of a gene by the introduction of double-stranded RNA (dsRNA) sequences specific to the targeted gene (Fire et al., 1998). The specificity, potency and relatively easy methodology of RNAi, make it ideal for investigating gene function in *C. elegans*. RNAi is transmitted to the first generation (F1) progeny but in most cases complete recovery of wild-type gene activity occurs in the second (F2) generation (Fire et al., 1998; Tabara et al., 1998; Timmons and Fire, 1998; Fraser et al., 2000). Although the mechanism of RNAi is not completely understood, current evidence favours a model in which RNAi blocks a posttranscriptional step in gene expression. It has been described that when dsRNAs enter the cell, they are cut up into short double stranded fragments during at least two steps of RNA silencing. First, dsRNA is processed into many short pieces of 21-22 nucleotides by a specific RNaseIII-like nuclease. These fragments are then incorporated into a multi-subunit complex, which carries out the second RNA-degradation reaction. Apparently, the role of the 22-nucleotide RNAs generated in the first step is to interact, by base pairing, with the target mRNA in which the sequence of nucleotides is the same as in the dsRNA. The short RNA molecules thus guide the RNases of the multi-subunit complex, ensuring specific degradation of those mRNA species related to the dsRNA (Baulcombe, 2001).

Initially, the introduction of dsRNA into *C. elegans* has been assayed by microinjection into the gonad of an adult hermaphrodite (Fire et al., 1998). Since RNA can be absorbed through the gut and distributed to somatic tissue and the germ line, it has also been possible to initiate RNAi by soaking worms in a solution of dsRNA (Tabara et al., 1998) or by feeding nematode larvae with *E. coli* expressing target gene dsRNA (Timmons and Fire, 1998). *C. elegans* normally feed on bacteria, ingesting and grinding them in the pharynx and subsequently absorbing bacterial contents in the gut. RNAi by feeding has been more used than the dsRNA soaking method and has several advantages over microinjection. It is less labour-intensive, is more convenient for performing RNAi on a large number of worms, and is less expensive than injection resulting in a durable reagent (a bacterial strain expressing dsRNA corresponding to a gene of interest) which can be reused to reproduce an RNAi phenotype easily (Kamath et al., 2000). For all these reasons, the RNAi method by feeding was the one used in this work.

4.1.3 GluCl subunits and behaviour studies

Previous data from our group suggested that *C. elegans* GluCl subunits participate in locomotion, egg laying and feeding behaviours (Aptel et al., 2002). Studies on *avr-14* and *avr-15* mutant worms showed a 50 % decrease in the duration of forward movement and about 60 % reduction in the progeny in these mutants, compared to wild-type worms. RNA interference experiments with *avr-14* or *avr-15* in wild-type worms showed a similar reduction in the duration of the forward movements, confirming that this method can be used to study the effect of reducing the expression of GluCl genes for which no mutant alleles are yet available. As far as feeding is concerned, the *avr-15* mutant but not the *avr-14*, showed a reduction in the pumping rate. The phenotypes observed in *avr-14* and *avr-15* mutant worms are in agreement with the biological effects of ivermectin in susceptible nematodes, such as the inhibition of: pharyngeal pumping, motility and fecundity. Also, and although no GluCl subunits have been found in the *C. elegans* reproductive system yet, there is a good correlation between the presence of GluCl subunits on neurons and muscle cells and the behavioural phenotypes found in GluCl mutant worms. Therefore, behavioural assays would also allow identify possible roles for the GluCl subunits whose expression patterns have not been described yet, such as the *C. elegans* GluClα1 encoded by the *glc-1* gene. Besides, disrupting the expression of particular GluCl subunits, for example through RNAi assays in a wild- type and in a GluCl mutant background strain, might also help to dissect the contribution of different subunits to the function of the native GluCl receptor in *C. elegans*.

When considering that the biological effects of ivermctin on *C. elegans* and *H. contortus* are conserved between the two species and that the drug target sites, the GluCls, are mainly expressed in the nervous system of these worms, studies in *C. elegans* could be used as a model to find out possible functions of the GluCl receptors in the parasitic nematode. Table 4.1 shows a comparison of the expression pattern between *C. elegans* and *H. contortus*. In particular, the distribution for the orthologous GluClα3 subunits is very similar in both nematodes, as indicated in Table 4.1 by the same font colours. Expression on the neuronal structures responsible for movement, nerve cords and motor neurons, correlates with the locomotion defects described for the *avr-14* mutants, as mentioned above.

Table 4.1. Comparison of the known expression patterns of the GluCl subunits in *C. elegans* and *H. contortus*

	C. elegans		*H. contortus*
GluClα2 (*avr-15*)	pharyngeal muscle, some motor neurons in the head and ventral nerve cord [a]	?	?
GluClα3 (*avr-14*)	extrapharyngeal neurons in the head, sensory neurons and ventral nerve cord motor neurons[e]	HcGluClα3A	amphidial neurons[f] and motor neuron commissures[d,f], nerve cords and nerve ring[d]
	and interneurons[g]	HcGluClα3B	pharyngeal neurons[f], motor neuron commissures[d,f], lateral and ventral nerve cords[d,f], nerve ring[d]
GluClβ (*glc-2*)	pharyngeal muscle[b]	HcGluClβ	motor neuron commissures[c,f] and lateral and sub-lateral nerve cords[f]
X	x	HcGluClα	motor neuron commissures[f]

[a] Dent et al., 1997. [b]Laughton et al., 1997a.[c] Delany et al, 1998.[d] Jagannathan et al, 1999. Note that the antibodies used in this work did not distinguish between the two alternative spliced variants HcGluClα3A and α3B. [e] Dent et al., 2000.[f] this project (Figs. from chapter 3), [g]Grunwald and Kaplan, 2001. ?=not yet identified; x=not present

The extrapharyngeal neurons expressing the *C. elegans* GluClα3 subunits correspond to neurons from the ring ganglia of the head (Dent et al., 2000), which contains cell bodies of sensory neurons, motor neurons and interneurons. Moreover, the *H. contortus* GluClα3A subunit was localised to possible amphidial neurons (sensory neurons in the head) (chapter 3, Fig. 3. 7). However to date, no data have been published linking nematode GluCl subunits to a chemosensory function.

The aim of the experiments described in this chapter was to further characterise the contribution of GluCl receptors into *C. elegans* behaviour. So far, the roles of GluCls in locomotion have been analysed for all the *C. elegans* GluCl subunits except for the GluClα1. Besides, the results obtained in chapter 3 showed that the *H. contortus* GluClα3A subunit is expressed in a pair of sensory neurons in the head and in motor neuron commissures. Therefore, the particular interest of this work was to investigate whether the GluClα1 subunit (*glc-1*) participates in *C. elegans* locomotion and to find out whether GluClα3 (*avr-14*), orthologous to HcGluClα3A in *H. contortus*, and GluClα2 (*avr-15*) have a role in the sensory behaviours, chemotaxis and osmosensation. This could then be used as an approach in the understanding of the function of these channels in *H. contortus*.

4.2 Materials and Methods

4.2.1 *C. elegans* strains

<u>Wild-type</u>: N2, Bristol strain

<u>Mutant strains</u>:

glr-1 (n2461): nonsense mutation in codon 807

avr-14 (ad1302): missense V60E mutation in an exon common to both transcripts of
$\qquad$ *avr-14*

avr-15 (ad1051): molecular null for *avr-15*

avr-14/avr-15 (ad1302/ad1051): *avr-14* and *15* double mutant

Wild-type and *glr-1* mutant stocks were obtained from the <u>C</u>aenorhabditis <u>G</u>enetics <u>C</u>enter (CGC) (University of Minnesota, USA). *avr-14*, *avr-15* and *avr14/avr15* mutant stocks were provided by Leon Avery (Southwestern Medical Center, University of Texas, Dallas).

4.2.2 Bacterial strain genotypes

E. coli OP50: *RecA1 endA1 gyr96 thi-1 hsdR17 (r_k-m_k^+) supE44 relA1 lac* [F' *proAB*
$\qquad$ *lac^{Z}ΔM15* Tn*10*]. Obtained from CGC

E. coli HT$_{115}$: F⁻, *mcrA, mcrB, IN(rrnD-rrnE)1, λ-, rnc14::Tn10(DE$_3$ lysogen:lacUV$_5$
$\qquad$ promoter-T7 polymerase)*. Obtained from L. Holden-Dye (University of
$\qquad$ Southampton, UK)

4.2.3 Plasmids and clones

L4440, provided by L. Holden-Dye (University of Southampton, UK). This plasmid is designed for bi-directional transcription of the gene of interest by bacteriophage T7 RNA polymerase; it has two T7 promoters in inverted orientation flanking the multiple cloning site. It also contains the β-lactamase gene, which confers the Amp^r phenotype (Timmons and Fire, 1998).

L4440-*unc22* clone, provided by L. Holden-Dye (University of Southampton, UK).

L4440-*glc-1* clone, obtained from N. Aptel (University of Bath, UK). The *glc-1* insert is a 200 bp DNA, corresponding to the sequence encoding the intracellular loop between the transmembrane domains III and IV of the GluClα1 subunit.

4.2.4 Media

NGM (Nematode Growth Medium) agar: 3 g NaCl, 17 g agar, 2.5 g peptone, H_2O 975 ml. Autoclaved; then 1 ml cholesterol (5 mg/ml in EtOH), 1 ml $CaCl_2$ 1 M, 1 ml $MgSO_4$ 1 M and 25 ml potassium phosphate 1M (pH 6.0) were added.

LB agar: 10 g tryptone, 5 g yeast, 5 g NaCl, 15 g agar, H_2O to 1 l. Autoclaved.

DYT broth: 20 g Bacto-yeast, 10 g Bacto-tryptone, 5 g NaCl, H_2O to 1 l. Autoclaved.

4.2.5 Reagents

L-glutamate USB (Ohio, USA)

All other chemicals used were of analytical grade and obtained from standard commercial sources such as Sigma Chemical Company Ltd. (Poole, UK), Difco laboratories (East Molesey, UK) and BDH chemicals (Poole, UK).

C.elegans Methods

4.2.6 *C. elegans* culture

C. elegans was fed with *E. coli* OP50 grown on NGM agar plates. To prepare the bacterial food source, OP50 was streaked from a OP50-LB agar plate to generate single bacterial colonies. A single colony was used to inoculate a flask containing 5 ml sterile DYT broth. This was incubated at 37°C overnight. The resulting culture was kept at 4°C for 2-3 weeks.

Nematode culturing was performed on Petri plates. The NGM agar was poured into 60 mm or 90 mm diameter plates. The NGM agar OP50 plates were prepared using 100 or 200 μl of *E. coli* OP50 liquid culture, respectively. Bacteria were spread creating a square lawn leaving the edges of the plate clear of bacteria. Plates were incubated overnight at 37°C and stored at 4°C. Nematodes were maintained at

20°C on NGM OP50 plates by transferring them to new plates before they became starved, normally every 3-4 days. A wire bacteriological loop was used to pick worms under a dissecting inverted microscope (Zeiss, Germany). Normal bacterial sterile precautions at the open bench were adequate for these procedures. Worms were maintained as self-fertilising hermaphrodites.

4.2.7 Behavioural assays

4.2.7.1 Chemotaxis

Chemotaxis assays were based on those described by Bargmann and Horvitz (1991a) with some modifications. Assay plates (90 mm diameter) contained 5 mM potassium phosphate (pH 6.0), 1 mM $CaCl_2$, 1 mM $MgSO_4$, and 2 % (w/v) agar. Agar plugs of about 6 mm diameter cut with a 200 µl yellow pipet tip a were soaked for 1 h in 50 µl of attractant (1M NaCl or 100 mM L-glutamate) or ddH_2O. The gradient was produced by placing the plug saturated in attractant on the right side of an assay plate, 5-10 mm from the edge. A plug soaked in ddH_2O was positioned at a point diametrically opposite the peak of the gradient (Fig. 4.2, step 1). Plates with both plugs soaked in ddH_2O were included (negative control). Plates were left overnight (14-20 h) at 20°C. Shortly before the chemotaxis assay, the plugs were removed and 1 µl of 0.5 M NaN_3 was spotted onto the same position to anaesthetise the animals on the peak of the gradient (Fig 4.2, step 2).

Non-starved *C. elegans* adults were washed twice with wash buffer (5 mM potassium phosphate (pH 6.0), 1 mM $CaCl_2$, 1 mM $MgSO_4$) in 15 ml centrifuge tubes. Worms were allowed to decant and the supernatant, containing bacteria debris, was removed. After the second wash and just before starting the chemotaxis assay, a brief 120 xg spin was done. Approximately 100 worms were placed equidistant to the two plugs (start) and left to move freely on the assay plate for 40-50 min at room temperature (Fig 4.2, step 3). The assay plates were chilled to 4°C, and the chemotaxis index (CI) determined. CI was calculated as CI=(N^+-N^-)/(total number of animals on the plate), where N^+ is the number of animals on the quadrant where the attractant was placed and N^- on the control quadrant.
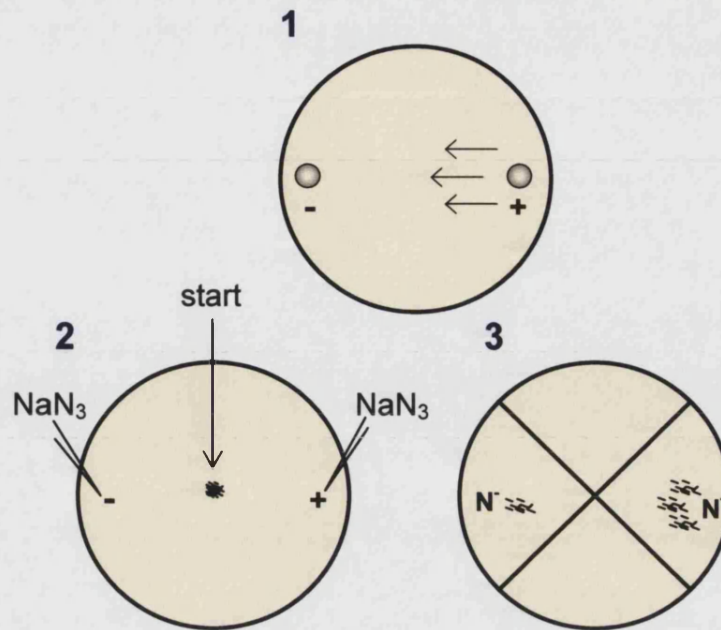
Fig. 4.2 Configuration of the chemotaxis assay

4.2.7.2 Osmotic avoidance

The osmotic avoidance assay was based on the method described by Hilliard et al (2002). A young adult or adult worm was transferred without food to a 60 mm NGM agar plate and allowed to recover for 1 min. A ~ 5 nl drop of control buffer (30 mM Tris, pH 7.5, 100 mM NaCl, 10 mM KCl) or 1M fructose in control buffer, was placed in the path of the worm as it moved forward. Drops were delivered using glass capillaries (3.5 inches Drummond glass capillary tubes, Drummond Scientific Company, USA). To reduce the diameter of the tip, capillaries were pulled on a stationary coil Narishige microelectrode puller (Stutter Instrument Co., USA) and then the needle was gently broken with a pair of forceps under a binocular microscope. The capillaries were back filled with sterile mineral oil, attached to the plunger of a Drummond "Nanoject" microinjector (Broomhall, PA, USA) set up to inject ~ 5 nl drops, and front filled with 2 μl of the solution to be tested (control buffer or 1 M fructose). The response was analysed under a dissecting microscope and the time interval (delay) between the initial contact with the solution and the response (backward movement) was determined using a stopwatch. Individual tests were performed on 12 worms per experiment.

4.2.7.3 RNA-mediated interference

RNA-mediated interference (RNAi) assays were based on those described by Kamath et al (2000). NGM agar plates (60 mm diameter) were prepared with 1 mM IPTG (IPTG stock: 100 mM in H_2O, sterilised by filtration through a 0.22 μm filter and stored at -20°C). Single colonies of HT_{115} bacteria transformed with the L4440 plasmids (empty, or containing *unc-22* or *glc-1* DNA inserts), were picked and grown in culture in LB with 100 μg/ml Ampicillin. The HT_{115} strain expresses the T7 polymerase gene from an inducible (Lac) promoter and is RNAase III-deficient, beneficial for RNAi by feeding. NGM IPTG agar plates were seeded in triplicates with the different bacterial cultures and incubated overnight at 37°C. L2-stage worms were placed onto these plates (5 per plate) and incubated for 48 h at 20°C. Once the twitching phenotype appeared on the *unc-22* RNAi treated worms (positive control), L4 individuals but not the *unc-22* dsRNA fed worms, were transferred to NGM off-food plates. Locomotion behaviour was assessed 12 or 24 h later. Twelve worms were analysed per condition, in each experiment.

4.2.7.4 Locomotion assays

The movement of RNAi treated worms was analysed on NGM agar off-food plates. Two different aspects of locomotion were quantified: the number of reversals and the duration of backward movements carried out per worm in 5 min. A reversal was measured each time a worm moving forward, stopped, went backwards and moved forward again but in a new direction. Backward locomotion was measured from the time a worm started a backward movement until it re-started moving forward. For a given experiment, in order to reduce possible variability in the data as a consequence of room temperature, humidity, dryness of plates, etc., all RNAi treated worms were scored on the same day.

4.2.7.5 Statistical analysis

Data represent the mean ± standard error of the mean (S.E.M), indicated by error bars, of at least 3 independent experiments. Statistical significance was determined using Mann-Whitney Rank Sum test or one-way ANOVA plus post hoc Tukey's test, as stated in the figure leyends. Values of $p < 0.05$ were taken to be statistically significant.

4.3 Results

4.3.1 Chemotaxis to water-soluble chemicals

Chemotaxis towards NaCl and L-glutamate was assayed in *C. elegans* wild-type and *avr-14/avr-15* mutant worms. Pictures taken from the NaCl and water (negative control) assay plates were used as examples to show typical chemoattraction behaviour (Fig. 4.3A). Figure 4.3B shows that both *C. elegans* strains chemotax towards NaCl and L-glutamate, but no differences in the responses were found between wild-type and *avr-14/avr-15* mutant worms. Worms on the water plates, where water was used as substitute for the attractants, moved randomly showing no preference for the right or left side of the plates. Chemotaxis towards the attractants was evident 30 minutes after starting the experiments. The chemotaxis index (CI) obtained to NaCl was 0.6 ± 0.12 for wild-type and 0.82 ± 0.05 for *avr-14/avr-15* worms. These values are similar to the CI described for *C. elegans* wild-type worms and some mutant strains that chemotax towards NaCl (Saeki et al., 2001; Yassin et al., 2001). The CI found for L-glutamate was 0.23 ± 0.04 for wild-type and 0.27 ± 0.06 for *avr-14/avr-15* worms. These figures were not as high as the CI for NaCl, but were significantly increased compared to the CI obtained on the negative controls (0.03 ± 0.03 for wild-type and 0.06 ± 0.05 for *avr-14/avr-15* worms). Since the worms are exposed to a gradient of an attractant, the only concentration of the attractant that is known is the one at the peak of the gradient (100 mM for L-glutamate and 1 M of NaCl).

These results show that the *avr-14/avr-15* mutant worms are not deficient to chemotax towards the compounds tested, suggesting that the GluCl subunits encoded by *avr-14* and *avr-15* are not involved in detecting NaCl or glutamate in *C. elegans*. These experiments were performed in collaboration with N. Aptel.
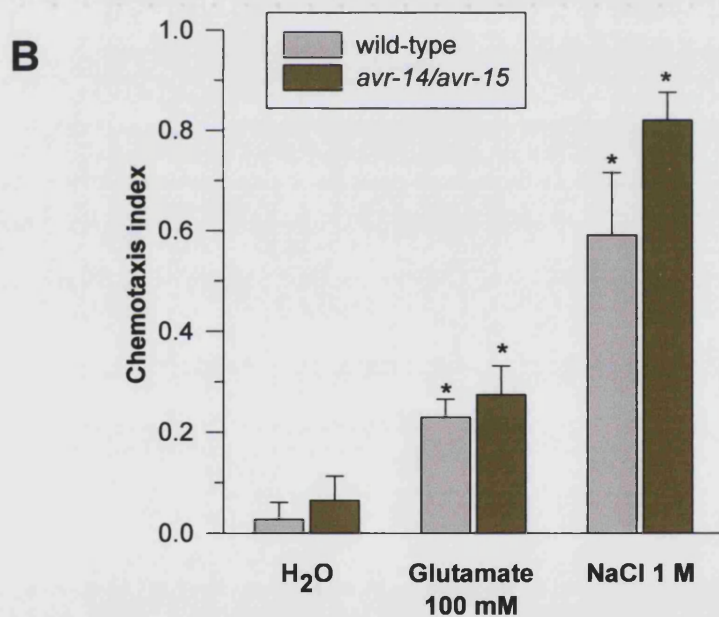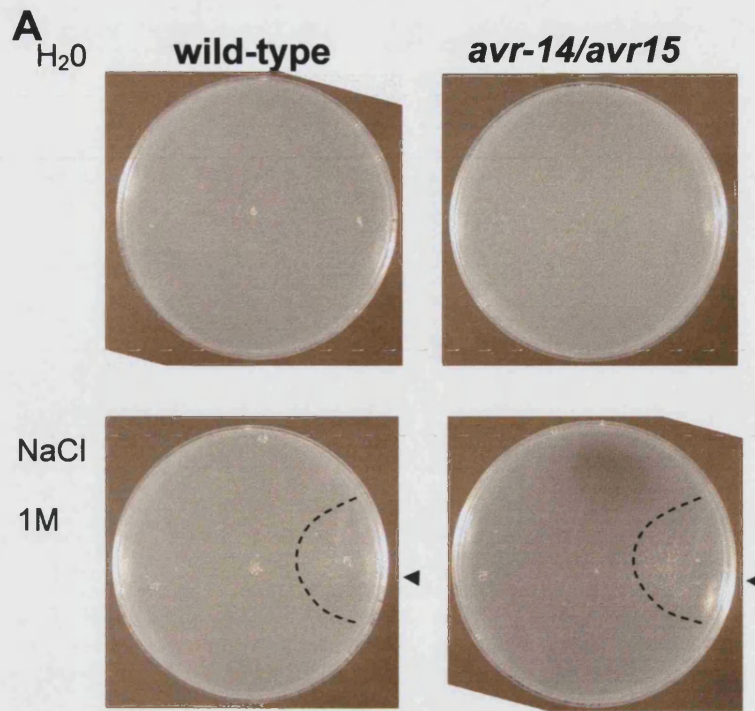
Fig. 4.3 Chemotaxis response of wild-type and *avr-14/avr-15* worms to NaCl and L-glutamate

Adult worms were collected, washed and assayed for 1M NaCl or 100 mM L-glutamate chemotaxis. Two agar plugs soaked in H_2O or attractant, were placed on the surface of an assay plate; the plug with attractant was placed on the right. For the H_2O plates, both plugs were soaked in H_2O (negative control). The gradient was allowed to form for 20 h at 20°C, the plugs were removed and 1μl of 0.5M NaN_3 was spotted onto the place occupied for the plugs, as anaesthetic. A: Pictures from the H_2O and NaCl plates, taken 40 min after placing ~100 animals at the starting position (centre of the plate). Arrow heads indicate chemotaxis towards NaCl. B: Chemotaxis index (CI) towards H_2O, 100 mM L-glutamate and 1M NaCl. The three conditions were tested in parallel. Values are means ± S.E.M of 3 independent experiments, each carried out in triplicate. Significantly different from the control, *$p < 0.05$, one-way ANOVA and post huc Tukey's test.

4.3.2 Osmotic avoidance

By placing a small drop of control buffer or buffer with the osmotic repellent (1 M fructose) in the path of a worm moving forward, it was possible to test the osmotic avoidance response (Fig. 4.4A). Wild-type and mutant worms that encountered the control buffer moved through the drop with no change in velocity or direction of movement (data not shown). In contrast, worms that encountered the fructose drop stopped their movement and initiated, after a brief delay, a backing response (Fig. 4.4B). *glr-1* and *avr-14* mutants displayed defects in the osmotic avoidance behaviour. Both mutants showed an increase in the response delay after contacting 1 M fructose compared to wild-type worms (*glr-1*: 1.58 ± 0.097 s; *avr-14*: 2.42 ± 0.15 s and wild-type: 0.36 ± 0.016 s). Interestingly, the delay in the response observed in the *avr-14* mutant was more severe than the observed in *glr-1* mutants (*p*<0.01). *glr-1* encodes an ionotropic glutamate receptor subunit, GLR-1, similar to the vertebrate non-NMDA glutamate subunits (Maricq et al., 1995). The response delay showed in the figure 4.4B for the *glr-1* (*n2461*) mutant and wild-type worms is very similar to the data described by Mellem et al (2002) using the same osmotic avoidance method described here, but testing the *glr-1* (*ky176*) mutant. Both mutant alleles (n2461 and ky176) cause loss of receptor function in *glr-1* mutant animals. The *glr-1* (*ky176*) mutants were also defective for osmotic avoidance and displayed a delay in the withdrawal response significantly increased compared to wild-type worms (~ 1.2 s and ~ 0.3 s, respectively). These results showed that the osmotic assay is working under the conditions set in the laboratory and validates the use of *glr-1* (*n2461*) mutant worms as a positive control for the osmotic avoidance experiments.

Osmotic avoidance was also assessed in *avr-15* mutants. Unlike *avr-14* mutants, these mutants showed a normal response to osmotic stimuli (Fig. 4.4B), suggesting that *avr-14* but not *avr-15* GluCl containing receptor might be required for the osmotic avoidance response in *C. elegans*.
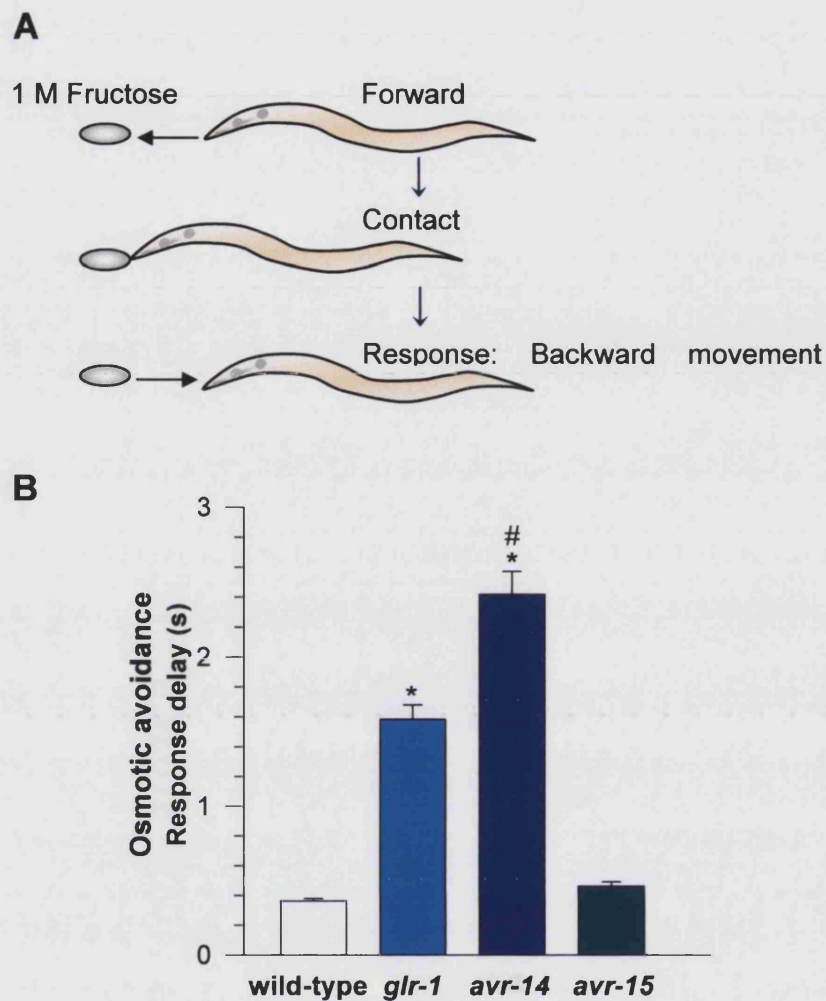
Fig. 4.4 *C. elegans avr-14* but not *avr-15* mutants are defective in osmotic avoidance

A: Diagram of the osmotic avoidance assay. A drop of 1 M fructose is placed in the path of a worm moving forward on an off-food NGM agar plate. B: Time taken (response delay) for wild-type, *glr-1* (n2461), *avr-14* and *avr-15* mutant worms to go backwards after contacting the fructose. s: seconds. Values are means ± S.E.M of 3 independent experiments. In each assay, individual tests were carried out in 12 worms. Statistically different from wild-type, *p<0.001 and from *glr-1*, # p<0.01, Mann-Whitney Rank Sum test.

4.3.3 Locomotion behaviour

The expression of *glc-1*, which encodes the *C. elegans* GluClα1 subunit, was disrupted in wild-type and *avr-14* mutant worms through RNAi assays. In all the experiments the following controls were included: L4440 (negative control) and *unc-22* (positive control). The first one corresponds to worms fed from *E. coli* HT$_{115}$ (a RNAi feeding strain) carrying the L4440 empty vector. The *unc-22* controls,

corresponds to worms fed from *E. coli* HT$_{115}$ transformed with a L4440-*unc22* clone. *unc-22* (unc: uncoordinated movement) encodes an abundant muscle filament protein (Benian et al., 1993). All worms treated with *unc-22* RNAi produced a characteristic and uniform twitching phenotype, observed 40 hours post-feeding L2 larvae.

In order to study whether silencing the GluClα1 subunit affects *C. elegans* locomotion, movement was assessed by quantifying the number of reversals performed per individual in 5 minutes. This approach was preferred to the quantification of the duration of forward locomotion, solely for the simplicity of the measurements. When searching for food, worms move in a regulated manner with fairly long forward runs interspersed with shorter periods of backward locomotion and turns. Reversals were considered when a worm moving forwards went backwards and moved forward again changing direction. In wild-type worms, *glc-1* RNAi showed a 92.6 % increase in the number of reversals compared to the L4440 wild-type control (10 ± 0.57 and 5.4 ± 0.5, respectively) (Fig. 4.5A). Since previous studies showed no differences in locomotion between L4440 controls and animals from the same strain non-assayed for RNAi (N. Aptel, pers. commun.), it was assumed that the results obtained for the L4440 controls represent the regular phenotype of the assayed strains.

avr-14 mutants treated with the L4440 empty vector (negative control), showed an increase of reversals compared to wild-type, which was not significantly different from *glc-1* RNAi treated wild-type worms (Fig. 4.5A). However, *avr-14* mutants treated with *glc-1* RNAi showed a 43 % reduction in the number of reversals compared to the L4440 *avr-14* controls (4.9 ± 0.6 and 8.6 ± 0.6, respectively), reaching similar values to the wild-type L4440 control worms (4.9 ± 0.6 and 5.4 ± 0.5 reversals in 5 minutes, respectively).

Qualitative observations showed that *avr-14* mutant worms treated with *glc-1* RNAi had a tendency for long backward movements, being defective in re-starting forward locomotion. These worms made a few attempts to go forward before actually achieving it. This phenotype was thus called hesitation. To further characterise this behaviour, the duration of backward movement was quantified in these worms.
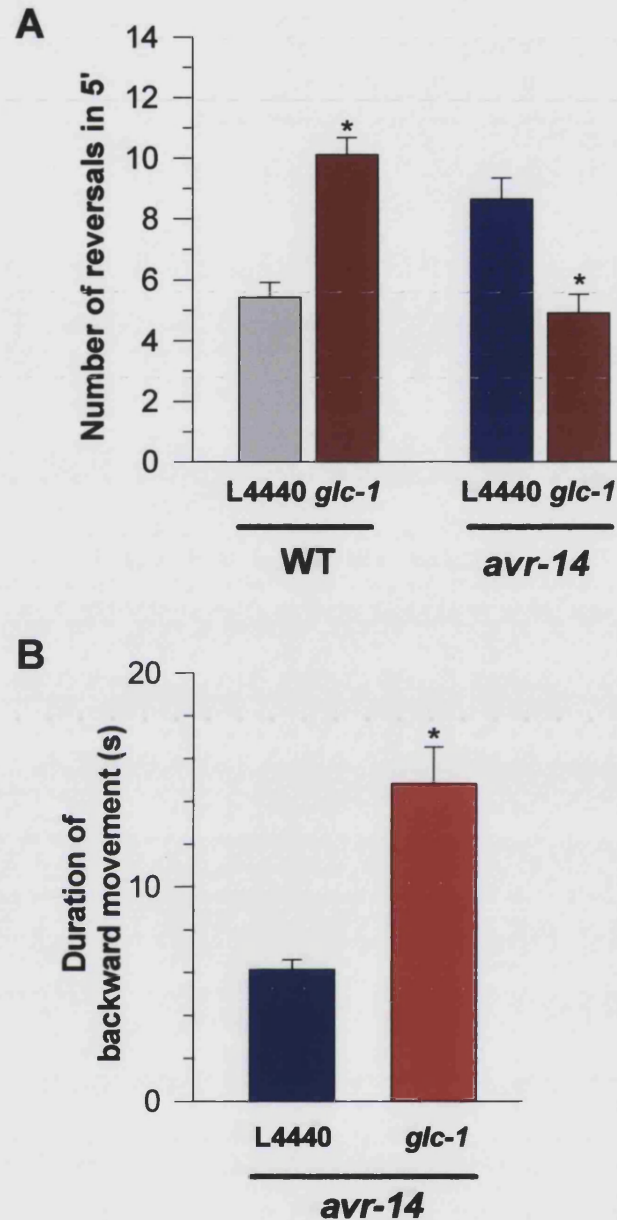
Fig. 4.5 Effects of *glc-1* RNAi on the locomotion of wild-type and *avr-14* worms
RNAi was carried out by feeding *C. elegans* L2 larvae with *E. coli* HT_{115} transformed with the control plasmid (L4440) or with the same vector containing a DNA fragment of *glc-1* (construct obtained by N. Aptel), for 48 h. L4 worms were transferred to NGM off-food plates and locomotion phenotypes were assessed 24 h later. At all times, *unc-22* RNAi of wild-type worms was included as positive control and worms showed the twitching phenotype 40 h post-feeding. Locomotion behaviour was not assayed on these worms. A: *glc-1* RNAi in wild-type and *avr-14* worms. Data represent the number of times worms reverse direction in 5 minutes. B: *glc-1* RNAi in *avr-14* worms. The duration of the backward movement was measured as the time since a worm started a backward movement until it re-started moving forwards. s:seconds. Values are means ± S.E.M of 3 independent experiments, each carried out on 10-12 individuals. Significantly different from L4440 control, *$p<0.001$, Mann-Whitney Rank Sum test.

The effect of *glc-1* RNAi on *avr-14* mutants showed about a 140 % increase in the duration of backward movement compared to control worms (14.8 ± 1.7 s and 6.1 ± 0.48 s, respectively) (Fig. 4.5B). This suggests that the reduction in the number of reversals found with these worms, might be the result of an impediment in re-starting a forward movement.

4.4 Discussion

Sensory and locomotion studies allowed the definition of possible functions of some of the GluCl subunits in *C. elegans* behaviour.

Chemotaxis

The chemotaxis response to NaCl and L-glutamate is not deficient in *avr-14/avr-15* mutants, suggesting that neither *avr-14* nor *avr-15* gene products are involved in detecting those attractants, or at least none of them seem to be crucial for that function. Preliminary results showed that the *avr-14/avr-15* mutants also chemotax towards other water-soluble substances such as sodium acetate and ammonium chloride (N. Aptel, pers. commun.), in agreement with the results presented in this work. However, no final conclusion can be draw at this stage, as chemotaxis towards more water-soluble compounds and volatile attractants and/or repellents should be tested.

Although *C. elegans* chemotaxis to NaCl has been previously described (Saeki et al., 2001; Yassin et al., 2001) there was no previous data on the chemoattraction to glutamate. Since *C. elegans* chemotax towards other amino acids such as: lysine, cysteine and histidine (Ward, 1973; Dusenbery, 1974) and towards serotonin (Bargmann and Horvitz, 1991a), is not surprising that worms detect glutamate. However, the biological relevance of chemotaxis towards glutamate is unclear. In the soil, *C. elegans* lives at the air-water interface and is exposed to both liquid and airborne chemicals (Bargmann and Mori, 1997). Many of the attractants are by-products of bacterial metabolism, so glutamate might be one of those chemicals present in the animal's natural environment.

Osmotic avoidance

The sensory response to osmolarity is defective in *avr-14* but seems normal in *avr-15* mutant worms, which suggests a role for the *avr-14* but not the *avr-15* containing receptor in osmosensation. It is very unlikely that the avoidance behaviour observed in this work reflects a mechanosensory response to contact with the solution for the following reasons: first, wild-type worms did not respond to the drop of control buffer and second, worms that encountered the stimulus after the drop of

fructose has been absorbed into the agar showed an avoidance response comparable to worms that contacted the fructose on the agar surface.

Excluding the expression in the ventral cord, *avr-14* and *avr-15* localised to different regions of the worm. *avr-15* is expressed in pharyngeal muscle and head motor neurons (Dent et al., 1997), whereas *avr-14* is expressed in extrapharyngeal neurons (which may be amphidial neurons) and mechanosensory neurons (Dent et al., 2000). *avr-14* expression in extrapharyngeal neurons correlates with the possibility of having a role in a sensory function mediated, for example, by amphidial neurons, such as osmosensation. However, the way a GluClα3 subunit (encoded by *avr-14*) containing receptor might accomplish this function is unclear. A simple explanation would be that this receptor had a direct role in osmosensation through the amphids. However, this is improbable since the response to hyperosmolarity is thought to be mediated by mechanically gated ion channels. Alternatively, GluCls might indirectly regulate high osmolarity responses in the amphids, through the activation of amphidial neurons that respond to osmotic avoidance. Interestingly, the delay in the response to fructose obtained in this work for the *avr-14* mutants (~ 2.4 seconds) was very similar to that observed by Mellem et al (2002) in *eat-4* mutants (~ 2.7 seconds). The mutant used was a null allele for the EAT-4, the *C. elegans* vesicular glutamate transporter (Lee et al., 1999). It seems that in the osmotic avoidance response, the absence of one of the GluCl genes, *avr-14*, is as severe as the lack of glutamatergic transmission. The amphidial neuron ASH seems to play the major role in hyperosmolarity (Hart et al., 1999). ASH expresses *eat-4* and is therefore supposed to be glutamatergic (Lee et al., 1999). It is possible then that *avr-14* regulates the function of ASH in the osmotic avoidance function. If this is true, a GluClα3 containing receptor might act as an autoreceptor regulating glutamate release on the pre-synaptic ASH neuron. The fact that GluCls might function as autoreceptors was suggested for *avr-14* expressed on the glutamatergic sensory neurons for the tap-withdrawal response in *C. elegans:* ALM, PLM and AVM (Steidl et al., 2002).

Interestingly, the fact that *C. elegans* GluClα3 seems to participate in osmosensation correlates with the presence of the orthologous *H. contortus* subunit (HcGluClα3A) in a pair of sensory neurons in the head of the worm, possibly amphidial neurons (chapter 3, figure 3.7). As it was discussed in chapter 3, the

function of GluCls in those neurons is uncertain. The results obtained on the present work for *C. elegans*, strongly suggest a sensory role for the HcGluClα3A containing receptor in *H. contortus*, possibly in osmosensation, though other roles cannot be ruled out.

Locomotion

The disruption of *glc-1* expression through RNAi produced a locomotion defective phenotype. Previous data obtained in our group showed that RNAi can phenocopy the phenotype of *avr-15* and *avr-14* mutants. This gave us confidence that the phenotype obtained on the *glc-1* RNAi experiments represented a specific effect of *glc-1* RNAi in *C. elegans*.

Since a 50 % decrease on the duration of the forward movement has been described for GluCl *avr-14*, *avr-15*, *glc-3* and *glc-4* mutant worms compared to wild-type animals (Aptel et al., 2002), it is not surprising that wild-type *glc-1* RNAi treated worms showed a 100 % increase in the number of reversals. Expression of *avr-14* and *avr-15* in the ventral cord, which possesses motor neurons and interneurons responsible for driving nematode locomotion (for references see table 4.2), correlates with the movement defects previously observed on those mutants. Therefore, the results obtained in this work for *glc-1* suggests that this GluCl gene might also be expressed in the neuronal tissue that controls *C. elegans* locomotion. As far as knocking-down *glc-1* expression in *avr-14* mutants is concerned, the *glc-1* RNAi worms were more defective in locomotion than the single knockouts. The observed increase in the duration of backward locomotion was the result of the 'hesitation' phenotype detected in those worms for re-starting a forward movement. Therefore, the decrease in the number of reversals to values similar to wild-type worms seems to be a consequence of the long backward movements rather than a wild-type phenotype rescue. Finally, the additive defect in locomotion obtained with worms lacking the GluClα1 and GluClα3 subunits (encoded by *glc-1* and *avr-14*, respectively), suggests that at least in some neurons responsible for nematode movement, these GluCl subunits might not be part of the same receptor.

The work presented in this section showed that the absence or disruption of GluCl subunit expression produces locomotion defects in *C. elegans*. How might this phenotype be achieved? As already mentioned in the discussion of chapter 3, an

inhibitory glutamate-gated chloride current has been recently detected in the AVA neuron (a command interneuron that controls backward movement) and it was suggested that the GluCls may help to reestablish forward movement following backwards locomotion (Mellem et al., 2002). This would explain why in the absence of *avr-14* or *glc-1*, worms tend to increase the number of reversals or the duration of backward locomotion.

Finally, it seems that three different $GluCl\alpha3$ subunit-containing receptors might be present in *C. elegans*: one regulating sensory behaviour, one modulating locomotion and a third one controlling feeding (the feeding behaviour was studied by Aptel et al (2002). This agrees with the expression pattern found in *C. elegans* for *avr-14* and in *H. contortus* for the orthologous $HcGluCl\alpha3A$ and $\alpha3B$ subunits (discussed in chapter 3). The behavioural phenotypes found in this work for the GluCl mutant or RNAi treated *C. elegans*, support the possible roles of *H. contortus* GluCls in motor and sensory behaviours, as discussed in chapter 3.

CHAPTER 5

<u>FINAL DISCUSSION</u>

Antibodies raised against all the currently known *H. contortus* glutamate-gated chloride channel (GluCl) subunits allowed the mapping of their distribution in adult worms. The anti-HcGluClβ antibody produced in this work confirmed the expression of this subunit in motor neuron commissures, as reported previously (Delany et al. (1998), but also detected expression in the lateral and sub-lateral nerve cords. HcGluClα was localised to motor neuron commissures and double immunolabelling experiments showed that the α- and β-subunits co-localise to the same commissures in adult worms, suggesting that these subunits are part of the same receptor. Nematodes possess distinct excitatory and inhibitory motor neurons that release acetylcholine or GABA, respectively, at neuromuscular junctions (Stretton et al., 1985; Walrond et al., 1985). The anti-HcGluClα subunit fluorescence overlapped with that produced by an anti-GABA antibody, suggesting that an 'α+β' containing receptor is expressed on GABA-ergic motor neurons.

Specific anti-peptide antibodies designed to HcGluClα3A and α3B allowed us to distinguish between the expression patterns of these subunits. They were previously shown to be localised to motor neuron commissures, nerve cords and the nerve ring of *H. contortus* (Jagannathan et al., 1999), but the antibody used in those experiments did not discriminate between the two subunits. The results presented in this project confirmed that the HcGluClα3A and α3B subunits are expressed in motor neuron commissures but that, outside of these cells, they were expressed in different regions of the worm nervous system. HcGluClα3B, but not HcGluClα3A, is expressed in nerve cords, in agreement with the results obtained with the HcGluClα3B antibody in *C. elegans*, which showed immunoreactivity in the worm motor nervous system (A. Cook and L. Holden-Dye, pers. commun.). New expression sites were also detected for both subunits in the head of *H. contortus*. HcGluClα3A was found in a pair of putative sensory amphid neurons and HcGluClα3B in three probable pharyngeal neurons, which may correspond to the M1 and M2 motor neurons. In *C. elegans*, *avr-14* is also expressed in extrapharyngeal neurons in the head of the worm, in other sensory neurons and in the ventral cord (Dent et al., 2000). Recently, the HcGluClα3B antibody also seemed to stain the M1 and M2 pharyngeal neurons in *C. elegans* (A. Cook and L. Holden-Dye, pers. commun.), further supporting the results obtained in *H. contortus*.

The expression pattern obtained in this study for all the currently identified GluCl subunits of *H. contortus*, was presented in a table format in chapter 4 (table 4.1), and is now summarised in the figure 5.1.
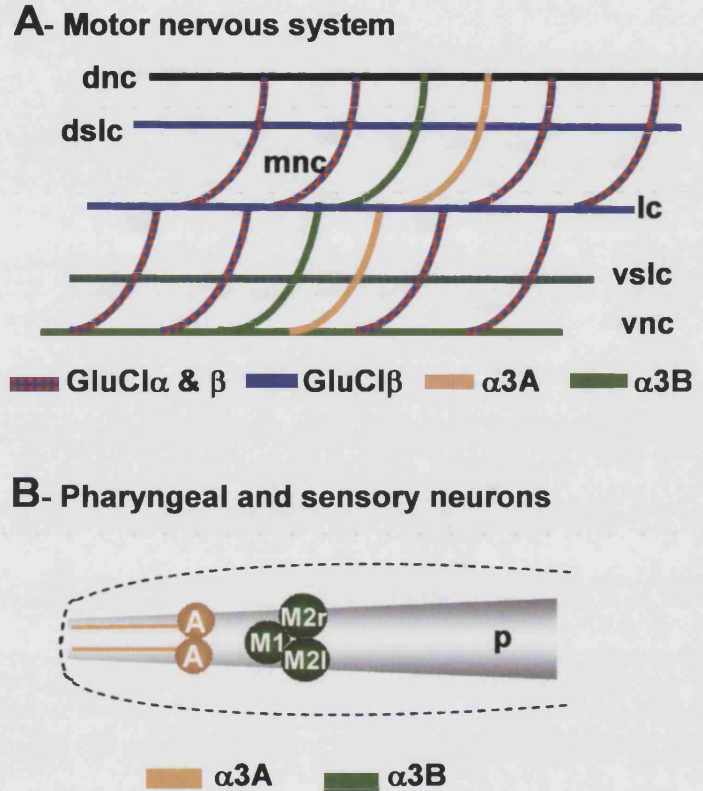

A- Motor nervous system

B- Pharyngeal and sensory neurons

Fig 5.1 Distribution of *H. contortus* GluCl subunits
A: Schematic representation of a mid-anterior portion of the right lateral side of a worm showing structures from the motor nervous system expressing HcGluCl subunits. Anterior is left. See key boxes to identify the location of each subunit. dnc: dorsal nerve cord; dslc: dorsal sub-lateral cord; mnc: motor neuron commissure; lc: lateral cord; vslc: ventral sub-lateral cord and vnc: ventral nerve cord. B: Top view of the head showing the expression of the HcGluClα3 subunits. Green circles: cell bodies of 3 possible pharyngeal motorneurons that may correspond to *C. elegans* M1 and M2 left (l) and right (r). Yellow circles: cell bodies of possible amphidial neurons (A). Notice the anterior nerve processes (yellow lines) also containing this subunit. p, pharynx.

These results strongly suggest that *H. contortus* contains more than one type of GluCl, distributed in distinct regions in the worm nervous system: 1) in the motor nervous system (motor neuron commissures and nerve cords); 2) in the pharyngeal nervous system and 3) in a pair of sensory, possibly amphid, neurons in the head. As the HcGluClα and -β subunits showed complete co-localisation in motor neuron commissures, it is very tempting to think that these subunits probably co-assemble in motor neuron commissures in native GluCl receptors. It would obviously have

147

been interesting to determine whether these motor neurons were the same as those expressing the HcGluClα3A and α3β subunits. Attempts to double-label adult *H. contortus* with the rat anti-HcGluClβ and rabbit anti-HcGluClα3A or α3B antibodies showed some indications of co-localisation. However, the data were not conclusive and it does remain an obvious possibility that the native GluCl contains the α, one or both α3, and β-subunits. The same thought can be applied to the HcGluClβ and α3B subunits, which are both expressed in the ventral sub-lateral cord. The present data suggest that the HcGluClα3-contaning receptors are the GluCl subunits most widely distributed in the *H. contortus* nervous system. Since the α3A and α3B are alternative spliced products from the *avr-14* (*gbr-2*) gene, it is not surprising that they may contribute to increase the number of subunit combinations available to the worm and therefore, the diversity of GluCl receptors. Besides, the HcGluClα3B and α3A subunits seem also to be part of GluCls expressed in pharyngeal neurons and in a pair of putative amphidial neurons, respectively. Considering that the GluCls are thought to be heteromeric channels, the expression of the GluClα3 subunits in those structures suggest that other, as yet unidentified, GluCl subunits are likely to be expressed in *H. contortus* pharyngeal and sensory neurons.

The distribution of the *H. contortus* GluCl subunits suggests that the GluCls have critical roles controlling pharyngeal function, locomotion, and possibly sensory perception and processing in the nematode. Does this distribution explain the mode of action of the AM anthelmintics? The observed inhibition of pharyngeal pumping may be explained by the presence of the AM-sensitive GluCls on motor neurons innervating pharyngeal muscle in *H. contortus*. Based on the *C. elegans* motor circuitry (Chalfie and White, 1988), the expression of the *H. contortus* GluClα, α3A, α3B and β subunits in motor neurons which innervate somatic muscle, strongly suggests that the GluCls contribute to the control of movement. The presence of *H. contortus* GluCls in GABA-ergic motor neurons also suggests that these receptors are involved in the co-ordination of forward and backward movements. This leads to a model for the paralysing effects of ivermectin and related drugs shown in figure 5.2, where the drug inhibits the control interneurons and/or the inhibitory motor neurons, leading to a cessation of movement. This model predicts that the AMs have no direct effect on the muscle, but disrupt neuronal signalling to it. The results

obtained in *C. elegans* from behavioural assays, together with previous studies (Aptel et al., 2002), further support the role of GluCls in regulating locomotion. Knocking-out or knocking-down the expression of GluCl genes leads to changes in nematode locomotion, specifically an increased frequency of backward movements.
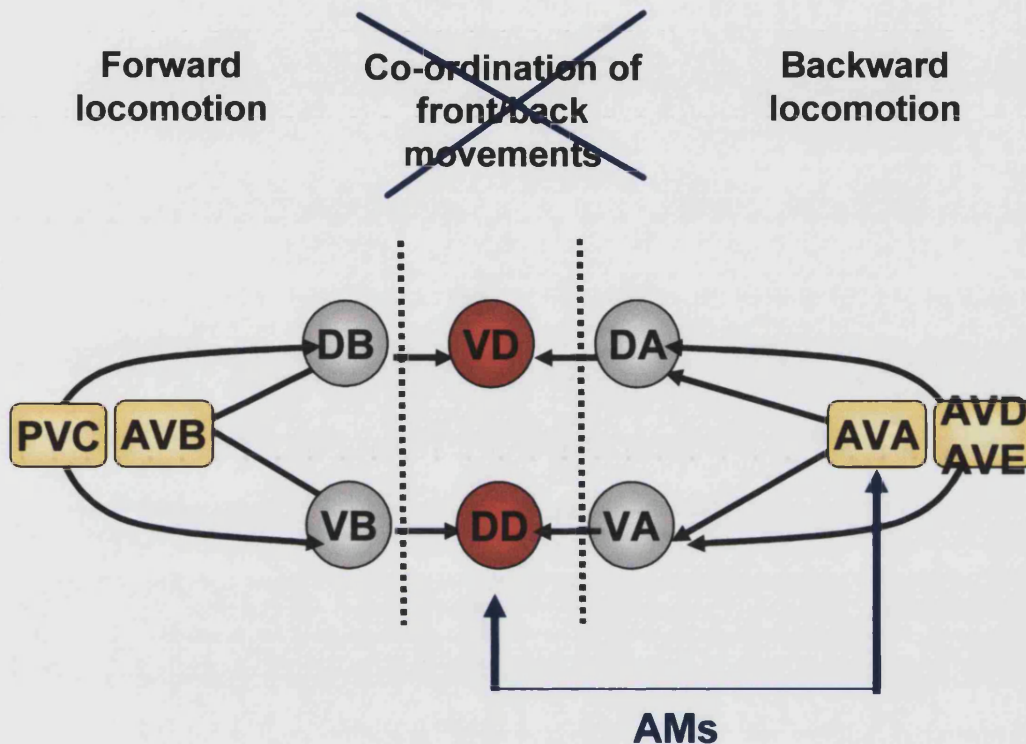

Fig 5.2 Model for the effect of the AMs on locomotion in nematodes
GluCls are expressed in the inhibitory motor neurons (red circles) and may also be present in the command interneurons (yellow octagons). Application of avermectin/milbemycin (blue arrows) will 'irreversibly' open these channels, preventing neurotransmission and hence inhibiting muscle contraction/relaxation. Grey circles represent excitatory motor neurons, black arrows indicate chemical synapses and straight connecting lines gap junctions. Diagram based on the circuitry described by Chalfie and White (1988).

As far as sensory perception is concerned, chemosensory assays performed in this work showed that neither the *avr-14* nor *avr-15* genes are involved in chemotaxis, at least for the chemicals tested. However, an $\alpha 3$- but not $\alpha 2$- containing receptor seems to have a role in osmosensation. Preliminary data from dye-filling assays with DiO (a fluorescent lipophilic dye), showed no clear differences between *avr-14* or *avr-15* mutants compared to wild-type worms (Victoria Lumby, pers. commun.), suggesting that amphidial neuron structure is not altered in either of these mutants. Therefore, it is possible that the *C. elegans* GluCl$\alpha 3$ subunits (encoded by *avr-14*)

149

might regulate osmotic avoidance, functioning as autoreceptors on the glutamatergic ASH amphidial neurons, as discussed in chapter 4. What is the relevance of this result, if any, to *H. contortus*? Aspects of the biology of parasitic species are completely different to the free-living nematode *C. elegans*, making it difficult to correlate functions directly. However, it is tempting to speculate that *H. contortus* might sense osmolarity and or other stimuli in the host, and that HcGluClα3A-containing receptors expressed in putative amphidial neurons, might have a role in that sensory behaviour, but other roles cannot be ruled out. Alternatively, it seems likely that amphid receptor-receptor connections facilitate the modulation of the activity of one receptor (sensory neuron) by another (White et al., 1986). GluCl channels have been implicated in the formation of inhibitory synapses (Dent et al., 1997). In this case, amphid neurons expressing GluClα3A containing receptors might modulate sensory modality by inactivating chemical transmission.

In summary, the distribution of the known GluCl subunits in *H. contortus* seems to correlate well with the observed actions of the AMs, providing further evidence that these receptors are the main drug targets in nematodes. One exception to this may be the effects of the anthelmintics on fecundity, as there is as yet no direct evidence for any role for the GluCls in the reproductive system. The exact effect that the AMs have on the channels is still somewhat uncertain, as there are clear quantitative differences between the concentrations of drug required to eliminate parasites and those that directly activate recombinant *C. elegans* GluCls expressed in *Xenopus* oocytes. The genetic molecular complexity and distribution of the GluCl family clearly indicates that there are multiple forms of the channel, and thus multiple AM targets, in these organisms. There are differences in the genetic make-up of the GluCl family between the two nematode species considered here, as well as in the expression patterns of some particular subunits. Given the close phylogenetic relationship between *C. elegans* and *H. contortus* (Blaxter et al., 1998), it would not be surprising if more extensive differences in the composition and function of the GluCl exist in more diverse species, such as the filaria. Such differences may well underlie the different effects the AM anthelmintics have on different parasites.

Future directions

Studies using techniques such as co-immunoprecipitation, might help to further elucidate the composition of the *H. contortus* native GluCls. Expression of the GluClα and β subunits, as well as all the other GluCl subunits in the combinations mentioned above, and new ones, could be assessed in *Xenopus* oocytes and the relevant pharmacology carried out to prove that these subunits do form functional glutamate-gated chloride channels. However, this expression system has proved quite difficult to express for nematode GluCls (D. Yates, pers. commun). In addition, attempts to establish *H. contortus* GluCl stable cell lines in a mammalian cell line (L929) proved unsuccessful (Cheeseman, 2001). Appendix 1 describes the results obtained from transient expressions of the HcGluClα and HcGluClβ subunits in mammalian (COS-7 and HEK-293) and insect cells (S2).

It would be of interest to find out whether there is any difference in the expression pattern found between IVM-sensitive and IVM-resistant worms. Previous studies have shown no differences either in the predicted amino-acid sequence of HcGluClα, β or α3 subunits (Chesseman et al., 2001; Hejmadi et at., 2000), or on the expression pattern of the β and α3 between *H. contortus* IVM-sensitive and IVM-resistant isolates.

Finally, behavioural studies mentioned in this work could also be performed in the triple *avr-14*, *-15* and *glc-1* mutant worms. In addition, chemotaxis to other attractants and repellents could be assessed in *avr-14/avr-15* mutant worms, as well as avoidance response assays to other high osmotic solutions in *avr-14* and *avr-15* mutant *C. elegans*.

The results shown in the present work provide additional evidence for the understanding of the action of the AMs, suggesting that the native avermectin/GluCl receptor seems to be composed of different types of GluCl subunits, which might form different types of receptors in different areas of the worm nervous system. Considering the therapeutic relevance of the GluCls, this could help to develop a combination of novel, receptor-type specific AMs.

APPENDIX 1

TRANSIENT EXPRESION OF *H. CONTORTUS* GLUCL SUBUNITS IN CELL LINES

A1.1 Introduction

Heterologous expression of nematode GluCl subunits has been studied in expression systems such as *Xenopus* oocytes and mammalian cell lines. In particular, *Haemonchus contortus* GluCl subunits have been transiently expressed in the COS-7 mammalian cell lines (Cheeseman et al., 2001; Forrester et al., 2002). The expression of HcGluClα in the mammalian COS-7 expression system produced high affinity binding for [^{3}H]-ivermectin (IVM), suggesting that this subunit can form homomeric receptors in COS-7 cells. In contrast, the HcGluClβ subunit expressed in the same system failed to bind [^{3}H]-IVM, as predicted by functional data from the *Caenorhabditis elegans* orthologue. Radioligand binding data does not prove receptor functionality but provides an approach to study the receptor pharmacology. Considering that GluCls belong to the superfamily of ligand-gated ion channels (LGIC), it is probable that they act as heteropentamers. Despite the progress in identifying individual HcGluCl subunits that bind [^{3}H]-IVM, such as the HcGluClα and HcGluClα3B, so far no combinations of putative subunits have been expressed in an *in vitro* system. Pharmacological studies on cell lines expressing homomeric and heteromeric GluCls might also be used as a tool to investigate possible receptor-subunit combinations. Thus, this might provide an idea of the putative composition of the GluCl receptors.

It was described in chapter 3 that the HcGluClα and β subunits co-localised in *H. contortus* motor neuron commissures. The aim of this part of the project was to find out whether the HcGluClα and β subunits co-express in an *in vitro* system. If they do, they could then be used to assess the pharmacology of these receptors *in vitro*. This appendix describes the cloning of HcGluClα and β into two different expression vectors required for gene expression into mammalian or insect cell lines, and the results obtained from transient expression of those constructs in the mammalian COS-7 and HEK-293 cells and in the *Drosophila* S2.

A1.2 Materials and Methods

A1.2.1 Cells

Mammalian: COS-7: monkey kidney cell line, supplied by the European Collection of Cell Cultures (ECACC) Salisbury, UK. HEK293: Human embryonic kidney cell-line, supplied by the American Type Culture Collection (ATCC), USA.

Insect: *Drosophila* Schneider 2 Cells (S2 cells) (Invitrogen, Paisley, UK). Many features of the S2 cell line suggest that it is derived from a macrophage-like lineage (Schneider, 1972).

Bacteria: *Escherichia coli* TOP10 competent cells (Invitrogen)

A1.2.2 Plasmid DNA

Vectors: pCR®-Blunt II TOPO (Invitrogen); pCMV/myc (Invitrogen); pFLAG-CMV-5a (Sigma); pMetSV and pActSV obtained from M. Kapsetaki (IMBB, Iraklion, Greece). For restriction maps of the pMetSV and pActSV vectors see appendix 1.1.

Clones: pcDNA3(-)HcGluClα and pcDNAHcGluClβ obtained in our group by C. Cheeseman; pActSV-EGFP obtained from M. Kapsetaki (IMBB, Iraklion, Greece) (for restriction map see appendix 1.1); GFP-CD36, obtained from B.J Reaves (University of Bath); hTRPC3-c-myc and hTRPC1-FLAG, obtained from I. Franklin (University of Bath).

A1.2.3 Primers

All the primers were ordered from Life technologies Gibco BRL® (Paisley, UK) desalted and 50 nmol scale. Those used to sequence pCMV/myc and pFLAG-CMV vectors were the commercial ones recommended by the supplies.

Primers used for cloning the HcGluClα and β subunits into pCMV/myc and pFLAG vectors

αfull 5'	5' NNNNNN<u>CTGCAG</u>ATGTTCGCCTTAATTC 3' ♣
αfull 3'	5' NNNNNN<u>CTCGAG</u>TTCCAACTGCGCTTG 3' ♠
βfull 5'	5' NNNNNN<u>AAGCTT</u>ATGTCACAGTATATG 3' ♦
βfull 3'	5' NNNNNN<u>CTGCAG</u>GACTAGTCTTGAC 3' ♣

Restriction sites underlined: ♣ *Pst* I, ♠ *Xho* I, ♦ *Hind* III.

Primers used for cloning HcGluClα and β subunits into the pMet vector

αNhe 5'	5' NAA<u>GCTAGC</u>ATGTTCGCCTTAATTC 3' ♣
αPac 3'	5' NN<u>TTAATTAA</u>*TCA*CCCATTCAGATCC 3' ♠
βMet 5'	5' NNN<u>GTCGAC</u>ATGTCACAGTATATGATGG 3' ◊
βFlagNot 3'	5' NN<u>GCGGCCGC</u>*CTA*CTTGTCATCGTCG 3' *
PMet 5'	5' GCATCTGGCCAATGTG 3'
PMet 3'	5' TATGTTTCAGGTTCAGGGG 3'
PAct 5'	5' GCTGTGTGGATACTCCTCCC 3'
PAct 3'	5' TTATGTTTCAGGTTCAGGGG 3'

Restriction sites underlined: ♣ *Nhe* I, ♠ *Pac* I, ◊ *Sal* I, * *Not* I. In italic, stop codons. In bold, primers used to sequence DNA cloned into the pMet and pAct vectors.

A1.2.4 Antibodies

<u>Primaries</u>: Anti-Tags: anti c-myc: mouse anti-c-*myc* monoclonal antibody (CHEMICON International, Inc, Harrow, UK). anti FLAG: mouse anti-FLAG monoclonal antibody (Sigma) and chicken anti-DYKDDDDK polyclonal antibody (Aves Labs, Inc; Oregon , USA). Anti-HcGluClα (obtained as described in chapter 2).

<u>Secondaries</u>: anti-mouse FITC- and TRITC-conjugated antibodies and anti-rabbit TRITC-conjugated antibody purchased from by Jackson ImmunoResearch Lab. (West Grove, USA).

A1.2.5 Others

Cell culture reagents were purchased from Sigma Chemical Company Ltd. (Poole, UK). FuGENE™6 transfection reagent was purchased from Roche (Lewes, UK). PBS tables were supplied by OXOID (Basingstoke, UK). General chemicals were of analytical grade and obtained from Sigma Chemical Company Ltd. (Poole, UK) and BDH chemicals (Poole, UK). Plasticware was Sterilin (Bibby Sterilin Ltd., Stone, UK), Nunc (Life Technologies Ltd), Paisley, UK) Falcon (Falcon, New Jersey, USA) and Greiner Labortechnik Ltd. (Stonehouse, UK).

A1.2.6 Expression constructs

PCR and DNA cloning were performed as described in chapter 2 (sections 2.2.5 & 2.2.9). For preparing the HcGluClα-c-myc and HcGluClβ-FLAG constructs, HcGluClα and β cDNA full-length clones were used as templates for PCR. The resultant constructs were later used as templates for PCR to clone the tagged α and β subunits into the pMet vector. PCR cycling conditions consisted of 94°C for 3 min, followed by 35 cycles of 94°C for 1 min, 55°C for 1 min and 72°C for 1 min, terminating with 5 min at 72°C. A first step cloning in pCR®-Blunt II TOPO vector (Invitrogen) was done following the manufacturer instructions recommendations. Then the HcGluClα cloned product was sub-cloned into PCMV/myc vector linearised with *Pst* I and *Xho* I and the HcGluClβ into pFLAG linearised with *Hind* III and *Pst* I enzymes. The HcGluClα-cmyc and HcGluClβ-FLAG subunits were cloned into the multiple cloning site of the pMet expression vector between the following restriction sites: *Nhe* I and *Pac* I for the α, and *Sal* I and *Not* I for the β subunit. *E. coli* TOP 10 competent cells were used for transformations.

A1.2.7 Cell culture

A1.2.7.1 Mammalian cell culture

COS-7 or HEK-293 cells were cultured in 75 cm^2 vented flasks containing 12 ml of DMEM (Dulbecco's Modified Eagle's Medium) supplemented with 2 mM L-glutamine, 10 % (v/v) heat inactivated foetal bovine serum (treated for 30 min at 56°C) and 1 % (v/v) penicillin-streptomycin stabilised solution. Cells were incubated at 37°C with 5 % CO_2. At approximately 80 % confluence cells were washed with PBS and harvested with 1 ml 10 X trypsin-EDTA for 10 minutes at 37°C. Cells were split 1:10 to reach 80% confluency after 48-72 hours. HEK-293 cells used had 19-22 passages.

A1.2.7.2 Insect cell culture

S2 cells grow at room temperature without CO_2 as a loose, semi-adherent monolayer in tissue culture flasks and in suspension in spinners and shake flask. In this work cells were incubated in a 22-24°C incubator. They were cultured in 75 cm^2 screw capped flasks (Greiner Labortechnik Ltd.) containing 12 ml of Shields and

Sang M3 insect medium (Sigma; Cat. N° S-8398). This is a powdered M3 medium that was prepared in Milli-Q water following the manufacturer instructions with the exception that only 0.5 g/l and not extra NaCl, were added during its preparation. The optimal pH is 6.5 but as it increases slightly with sterilisation by filtration, the pH was adjusted to 0.2-0.5 units below the optimum. Medium was supplemented with 12.5 % (v/v) heat inactivated foetal bovine serum and 50 µg/ml gentamycin. For general maintenance, cells were passed when cell density was about 6 to 20×10^6 cells/ml and split at a 1:2 to 1:5 dilution. Cells were collected by centrifugation at 1000 x g for 4 min., the medium was removed and cells were washed in PBS centrifuged as above, and then resuspended in fresh medium.

A1.2.8 Transient expression in cell lines

A1.2.8.1 Preparation of cell cultures for trasfection

Mammalian cells

Prior to transfection a 80-90 % confluency cell culture was split 1:10 in DMEM and about 6 drops of the diluted culture were then plated drop-wise onto coverslips in 6 well plates. Cells were allowed to adhere to the coverslip for 90 min before 2 ml of DMEM were added to each well. Cells were incubated at 37°C with 5 % CO_2 until they reached 20-30 % confluency for the HEK-293 cells (normally 24h) and 40-50 % confluency for the COS-7 cells (overnight), before transfection. Coverslips used for growing HEK-293 cells were pre-treated with Polyethylenimine (see below).

Treatment of coverslips with Polyethylenimine (Poly-E)

One gram of Poly-E (50 % (w/v) aqueous solution) was diluted in 9 ml of ddH_2O and sterilised with a 0.22µM filter (stock solution). A 1:100 dilution from the stock was prepared in sterile 0.1 M Borax and 2ml were added on to coverslips in 6 well plates. Plates were incubated for at least 2h at 37°C. Finally the Poly-E solution was removed and the dishes were washed 2 or 3 times with PBS. HEK-293 cells were plated onto the coverslips as described above.

Insect cells

Cell were transfected at a density of 2 to 4×10^6 cells/ml in 2 ml of M3 medium in 6 well plates.

A1.2.8.2 Transfection methods

COS-7 and HEK-293 cells were transiently transfected using a lipophilic transfection reagent, FuGENE™6, or calcium phosphate. FuGENE™6 was used at a ratio of 3µl of reagent / µg of DNA, following the manufacturer instructions. Cells were incubated for 48 hours and assayed for gene expression.

The Calcium Phosphate transfection methodology was used to introduce DNA into COS-7, HEK-293 and S2 cells.

Calcium Phosphate transfection of COS-7 and HEK-293 cells

The medium was changed 3 to 4 hours prior to transfection. For transfecting cells on coverslips, 2-4 µg DNA were thoroughly mixed with 12 µl 2M $CaCl_2$ in a 1.5 ml microcentrifuge and sterile H_2O was added up to 100 µl total volume. In co-transfections, half of the DNA used for single transfections was used for each DNA assessed. The DNA solution was added dropwise to 100 µl 2X HEPES Buffered Saline (HBS; 140 mM NaCl, 1.5 mM $Na_2HPO_4 \cdot$ $2H_2O$, 50 mM HEPES, pH 7.05) shaking the tube vigorously between additions for 1-2 min to maximise aeration, promoting the formation of a calcium phosphate-DNA precipitate. The mixture was left for 30-40 min at RT to allow DNA precipitation to occur. For combined volumes of over 500 µl, 15 ml centrifuge tubes were used. Following this time the precipitate was added drop-wise to the cells. The final volume of DNA-$CaCl_2$ did not exceed 1/10 of the volume of medium in which the cells were plated. The cells were then left to incubate overnight at 37°C with 5 % CO_2. The following day the cells were washed twice with 1X PBS in order to remove the precipitate and 2 ml of fresh medium were added. The cells were incubated for a further 24-48 hours at 37°C with 5 % CO_2 and assayed for gene expression (section A1.2.8.3).

To monitor expression conditions and levels, the following control samples were included. COS-7 cells were transfected with a GFP-CD36 construct, and HEK-293 cells were transfected with hTRPC3-c-myc and hTRPC1-FLAG constructs. These myc- and FLAG- tagged constructs also allowed for the monitoring of immunodetection conditions. As in HcGluClα-myc and β-FLAG, expression of the mentioned constructs was driven by a constitutive promoter (CMV).

<u>Calcium Phosphate transfection of S2 cells</u>

The procedure described above for the mammalian cells was used in S2 with some modifications based on the Invitrogen protocol (see http://www.invitrogen.com). Ten to 19 µg of DNA were used per well in a 6 well plate. Expression driven under the methallothionein (Met) promoter was induced 3 days after transfection, using 0.5 mM $CuSO_4$. Transient expression was analysed by immunofluorescence detection, 3 days after induction. At this step, cells were placed onto a PE-treated coverslip, cells were allowed to set for 1 hour and immunostaining was carried out as described in section A1.2.8.3. Transfections in S2 cells were monitored for efficiency by investigating the expression of a costitutive pActGFP construct in control samples.

A1.2.8.3 Immunofluorescence

Cells cultured on coverslips in 6 well plates were washed 3 times in PBS and fixed in 2 ml of 4 % (v/v) paraformaldehyde in PBS for 20 minutes at room temperature (RT). After 3 washes in PBS, cells were permeabilised with 0.1 % (v/v) Triton X-100 in PBS for 5 minutes at RT (in some experiments this step was omitted). After one wash with PBS cells were incubated in blocking solution (0.2 % (w/v) BSA in PBS) for 30 minutes at RT. Coverslips were inverted first onto 70 µl of primary Ab and then onto the same volume of secondary Ab for 1 hour and 20 minutes respectively. Antibody dilutions were carried out in blocking solution. Two washes of 5 minutes each with blocking solution and PBS were carried out after antibody incubations. Cells were placed back into the dishes and washed twice with blocking solution and twice with PBS. Incubations and washes with the secondary antibody were performed in the dark. Coverslips were mounted onto a drop of Mowiol mounting medium (prepared as described by Harlow and Lane, 1988b) on a coverslide and dried overnight at RT. Results were analysed under a Zeiss LSM 510 confocal microscope using the settings according to the fluorochrome-conjugated secondary antibody used in the assay. Images obtained for the negative controls (untransfected cells incubated only with the secondary antibody) were scanned under the same confocal settings used for the cells incubated with primary and secondary antibodies.

A1.3Results

A1.3.1 Expression of HcGluClα and β in mammalian cells

A1.3.1.1 Cloning of the α and β subunits into expression vectors

The HcGluClα and β subunits were C-terminal tagged with the c-myc and FLAG epitopes respectively. Full-length HcGluClα and HcGluClβ subunit cDNAs, with the exception of their stop codons, were amplified by PCR and cloned into pCMV/myc and pFLAG vectors respectively. Endonuclease restriction of all the transformants analysed shown a fragment of the expected size (1.3 Kb) (Fig. 1). The sequence of clones N°1 from the HcGluClα and β constructs confirmed the identity of the sequences with the expected ones as well as the conservation of their open reading frames with the tag protein's sequences. These clones were used for transfections.
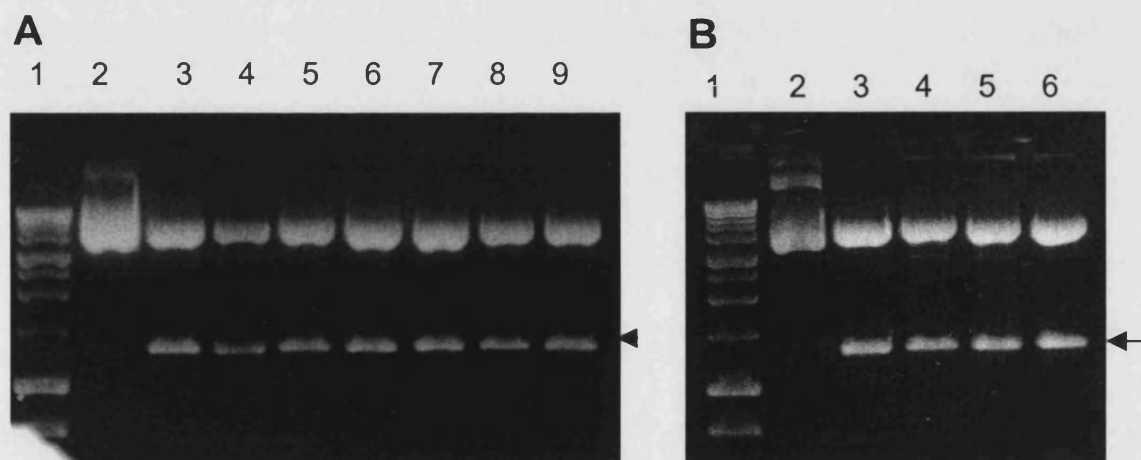

Fig. 1 Restriction analysis of plasmid DNA from HcGluClα-myc (A) and HcGluClβ-FLAG (B) mammalian expression constructs
1 % (w/v) agarose gel in TBE. Lane 1, 1Kb DNA ladder (Promega). Lane 2, uncut DNA from clone 1. Lane 3, clone 1 digested. Lanes 4-9 clones 2 to 7. Clones in A were digested with *Pst* I and *Xho* I; in B with *Hind* III and *Pst* I. The arrows indicate the fragment of about 1.3 Kb released from the clones.

A1.3.1.2 Transfection and immunodetection

Receptor subunits were then transiently expressed in COS-7 and HEK-293 cells and any expression analysed by immunofluorescence. COS-7 cells were also transfected with pcDNA3-HcGluClα construct, obtained by C. Cheeseman (University of Bath). The results described below were achieved using the calcium phosphate transfection method, which gave me better results than using the FuGENE™ reagent.

Immunostaining for the α subunit was detected using the anti-HcGluClα and an anti-c-myc antibody. The two antibodies showed cytoplasmic staining in permeabilised cells (Fig. 2). The staining seemed to be located possibly in the endoplasmic reticulum (ER) and in cytoplasmic vesicules. Intracellular staining was also detected in non-permeabilised cells and rarely expression was detected in the plasma membrane (data not shown). The staining observed in COS-7 or HEK-293 cells was very bright, but the expression level in terms of the proportion of cells that stained was very low (about 10 cells were stained on a coverslip of about 80 % confluency of cells). The high proportion of stained cells showed in figure 2.A, was very rare to obtain. From here onwards, the term 'expression level' will be considered in terms of percentage and not intensity of staining, which will be mentioned separately. No staining was detected either in COS-7 untransfected cells probed only with the TRITC- or FITC-conjugated secondary antibodies (Fig. 2E,F) nor in HEK-293 untransfected cells probed only with the FITC-conjugated antibody (Fig. 3E).
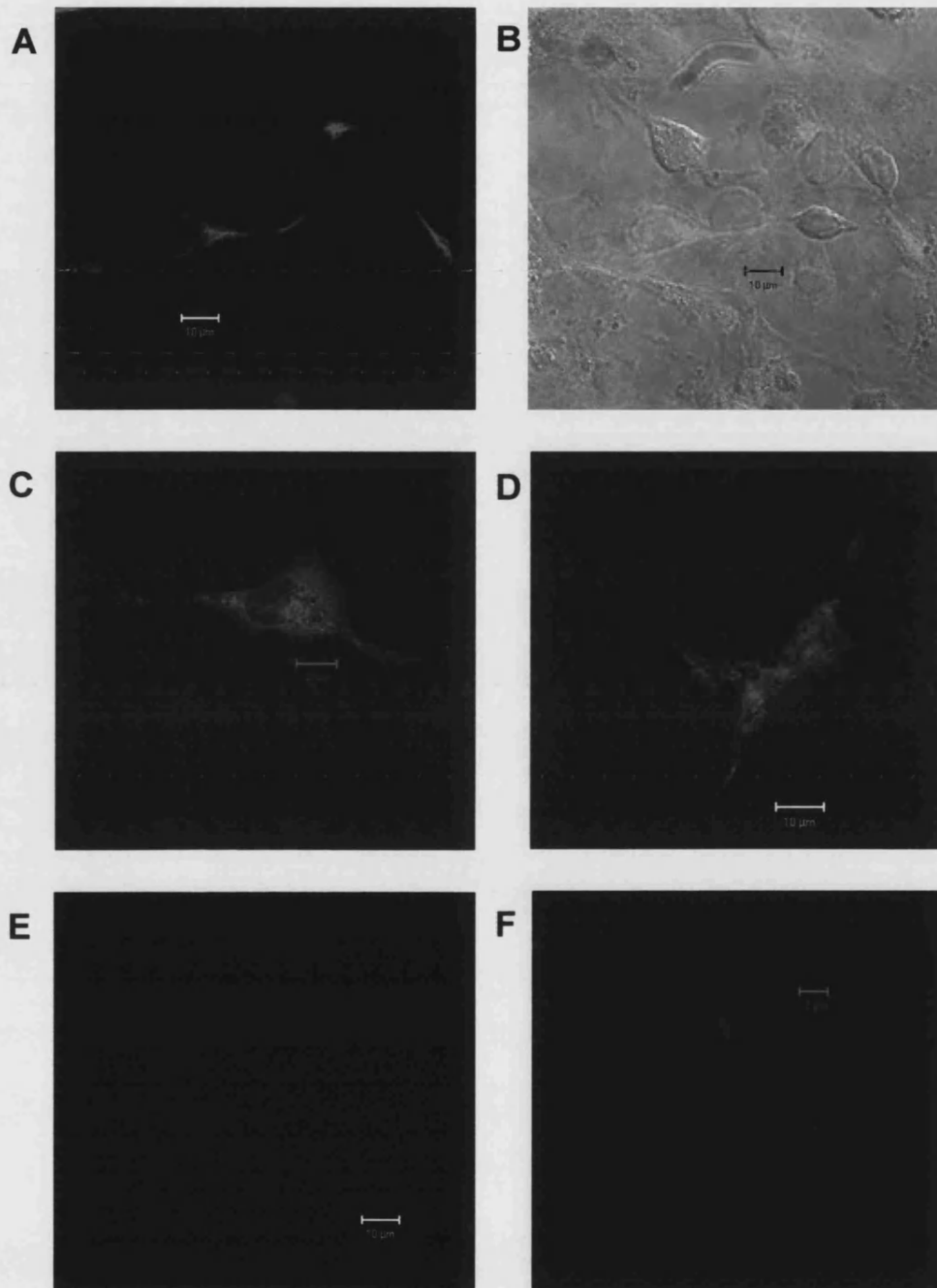
Fig. 2 Expression of HcGluClα in COS-7 and HEK-293 cells

Confocal images of transient expression of HcGluClα in COS-7 cells (A, B), myc-tagged HcGluClα in COS-7 (C) and HEK-293 cells (D) probed with 1:10 dilution of anti-HcGluClα Ab (A, B) and 1:200 dilution of mouse anti-c-myc Ab (C, D), followed by 1:200 dilution of TRITC- (in red) and FITC- (in green) conjugated secondary Abs. B: fluorescence obtained in A merged with it transmitted image. E & F: non-transfected COS-7 cells probed with TRITC- and FITC-conjugated secondary, respectively. Immunostaining was carried out in cells permeabilised with 0.1 % (v/v) Triton X-100 in PBS. Scale bars, panels A, B, D, E, F = 10 μm, panel C = 20 μm.

Expression of the GluClβ subunit was studied in COS-7 (Fig. 3A) and in HEK-293 cells (Fig. 3B-E). Staining, using a mouse anti-FLAG antibody, was detected in the cytoplasm for both cell types in permeabilised cells (Fig. 3A,B) and also at the plasma membrane under non-permeable staining conditions (Fig. 3C,D). The best expression level for the β subunit was about 30 % reached in HEK-293 cells 48h post transfection with 7 μg of DNA per coverslip. No staining was detected in non-transfected cells probed only with the secondary antibody (Fig. 3E).

Co-transfection experiments with the α and β subunits did not produce any cells expressing both in the same cell. Different transfection conditions were assayed such as varying the concentration of DNA and the expression timing, but they did not make any difference. It was then decided to test a different expression system, the *Drosophila* S2 cell line. Since in mammalian cells the GluClα and β proteins were expressed mainly in the cytoplasm, which could be a side effect of constitutive expression driven by the CMV promoter, this time the α and β subunits were cloned under an inducible promoter (methallothionein (Met) promoter) (section A1.3.2).
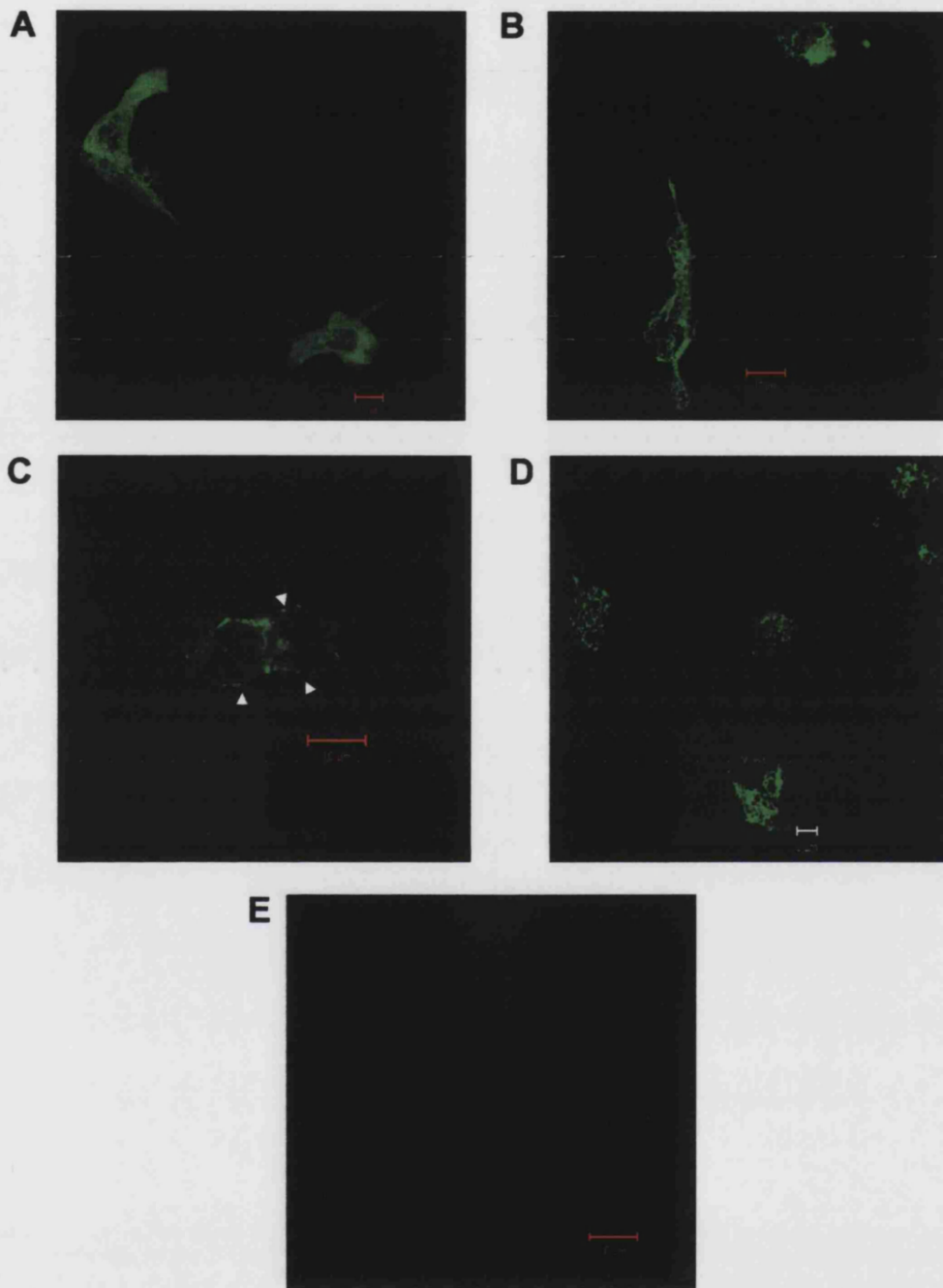
Fig. 3 Expression of HcGluClβ in COS-7 and HEK-293 cells

Confocal images of transient expression of HcGluClβ-FLAG in COS-7 (A) and HEK-293 (B-D) cells probed with 1:1000 dilution of mouse anti-FLAG Ab followed by 1:200 dilution of FITC-conjugated secondary Ab. A, B, E : cells permeabilised with 0.1 % (v/v) Triton X-100 in PBS. C-D, non-permeabilised cells. E : non-transfected HEK-293 cells probed with FITC-conjugated secondary. In C, arrows indicate plasma membrane staining. Scale bars, panels A-C, E = 10 μm, panel D = 5 μm.

A1.3.2 Expression of HcGluClα and β in S2 insect cells

A1.3.2.1 Cloning of the α and β subunits into an inducible expression vector

The GluClα-myc and GluClβ-FLAG sequences were amplified by PCR using as templates plasmid DNA from the clones used for transient expression in mammalian cell lines described above. Bands of the expected size (about 1.3 Kb) were obtained (Fig. 4 lanes 1 & 3).
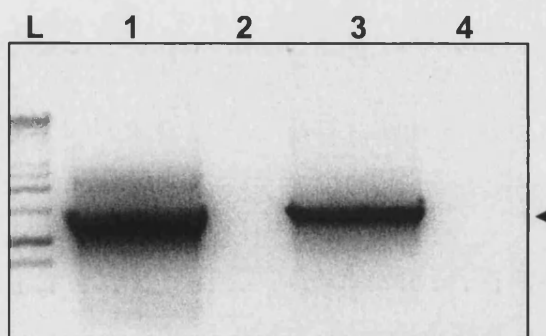

Fig. 4 PCR amplification of GluClαc-myc and GluClβFLAG DNA
1 % (w/v) agarose gel in TBE. L, 1Kb DNA ladder (Promega). Lanes 1 & 3, PCR products for GluClβ-FLAG & GluClα-myc DNAs respectively. Lane 2 & 4, no template controls. The arrow indicates the products of about 1.3 Kb.

The excised bands were cloned separately into the pCR®-BluntII TOPO® vector as a previous step before the cloning into the insect expression vector pMet (vector map is shown in Appendix 2). HcGluClα-c-myc was cloned into the *Nhe* I and *Pac* I sites of the pMet vector and HcGluClβ-FLAG into *Sal* I and *Not* I. Seven pMet transformants were isolated per construct type and digested with the relevant enzymes (Fig. 5B). The sequence from clone N°1 & 7 for HcGluClα-c-myc and N°1 and 2 for HcGluClβ-FLAG constructs was confirmed as well as the conservation of the open reading frame with the tagged sequences. From those, clone 7 and 2 were the ones used for transfections.
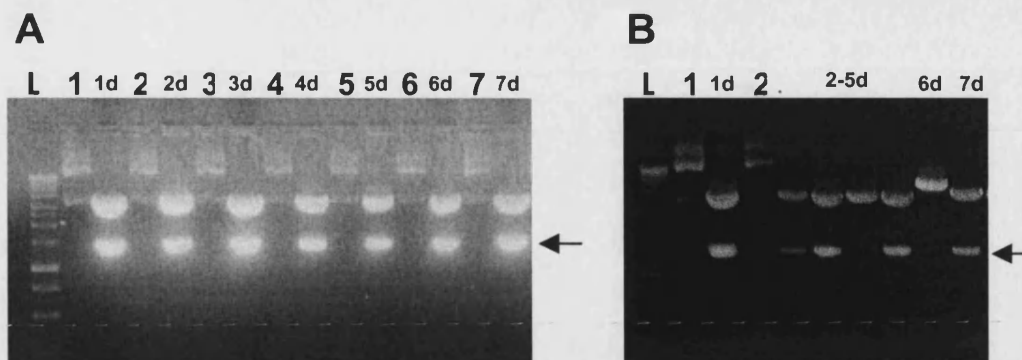
Fig. 5 Restriction analysis of plasmid DNA from HcGluClα-myc (A) and HcGluClβ-FLAG (B) insect expression constructs. 1 % (w/v) agarose gel in TBE. L, 1Kb DNA ladder. 1-7, different clones digested (d) in A with *Nhe* I and *Pac* I and in B with *Sal* I and *Not* I. The arrows indicate the fragment of about 1.3 Kb released from the clones.

A1.3.2.2 Transfection and immunodetection

HcGluClα and β, c-myc and FLAG tagged respectively, were transiently expressed in S2 cells and expression was analysed by immunofluorescence. Mouse antibodies to the c-myc and FLAG proteins showed cytoplasmic staining in permeabilised cells (Fig. 6A-E). Immunostaining under non-permeable conditions was hardly observed (not shown). No staining was detected in untransfected cells probed with the TRITC- conjugated antibodies (Fig. 6F,G). The expression levels obtained for the α or β subunits were about 10 %. Besides, within the same preparation fluorescence detected in some cells was brighter than others. Co-transfection experiments with these subunits did not show cells expressing both proteins in the same cell. Different rations of DNA such as 1:1, 1:5 and 1:10 were assayed but still no co-expression was detected.

166
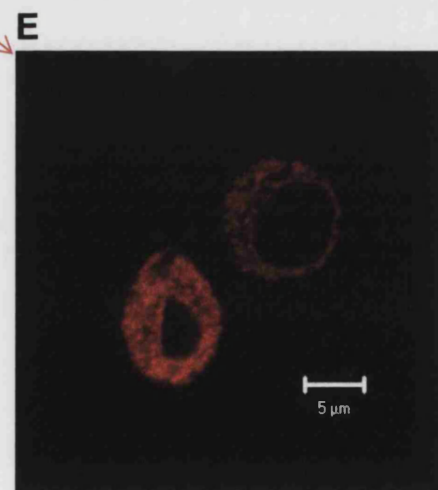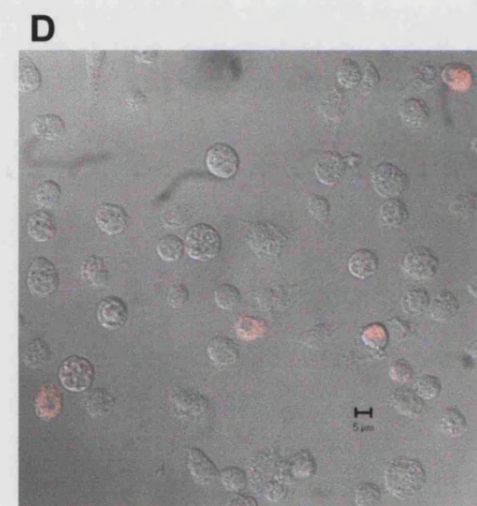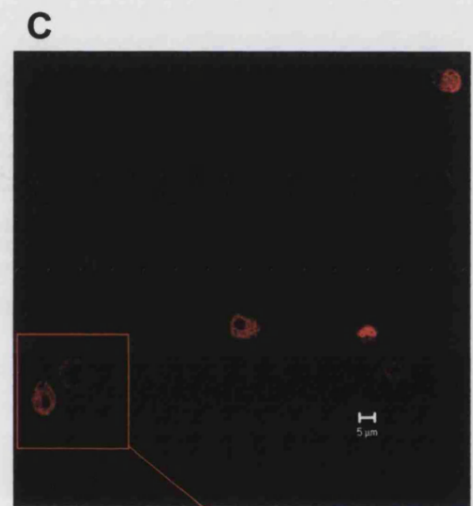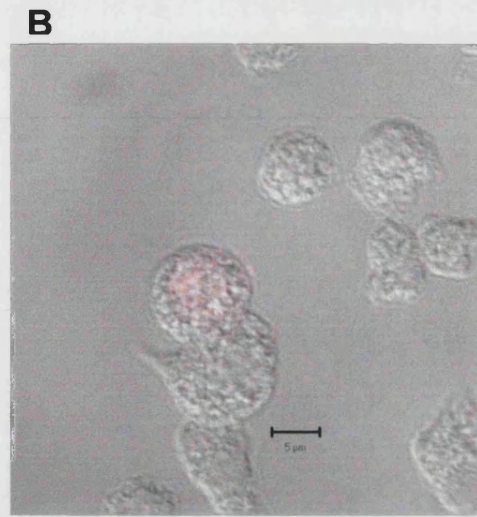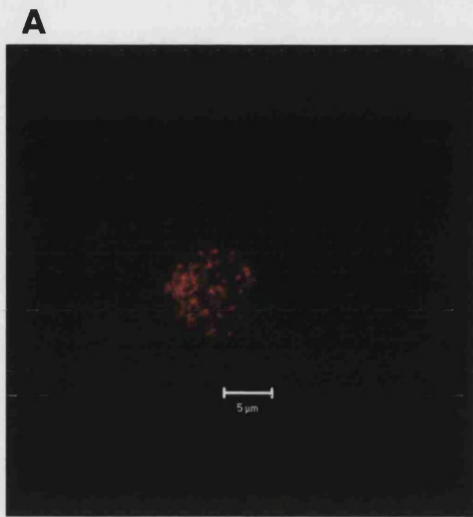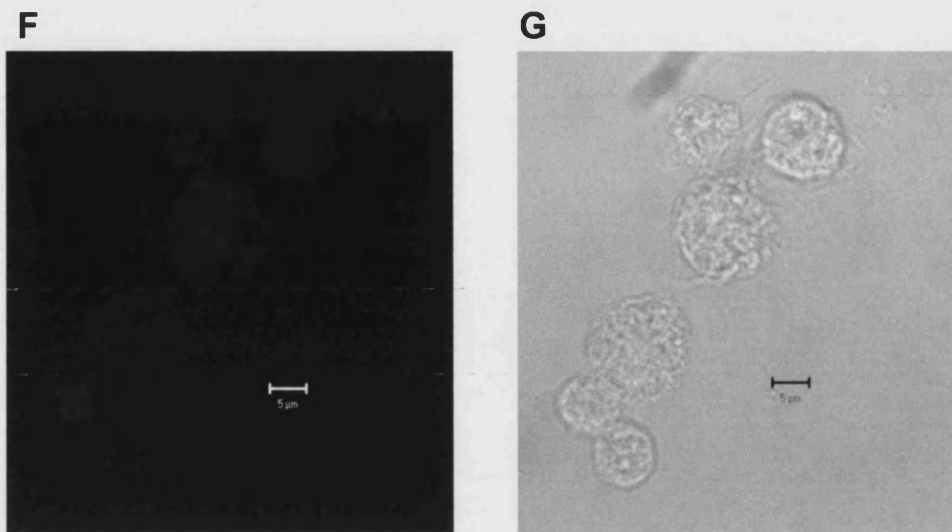
Fig. 6 Expression of HcGluClα and HcGluClβ in S2 cells

Confocal images of transient expression of HcGluClα-c-myc (A, B) and HcGluClβ-FLAG (C-E) induced with 0.5 mM $CuSO_4$. Cells were probed with 1:200 dilution of anti-c-myc Ab (A,B) or 1:1000 dilution of anti-FLAG Ab (C-E), followed by 1:200 dilution of TRITC-conjugated secondary Ab. B & D: fluorescence obtained in A & C merged with their respective transmitted images. E: zoom-in image of a section from C. F & G: non-transfected S2 cells probed with TRITC-conjugated secondary Ab. G is the transmitted image of F. Scale bars, 5 μm.

168

A.1.4 Discussion

Two different expression systems were assessed to transiently express the HcGluClα and HcGluClβ subunits *in vitro*. These subunits were c-myc and FLAG-tagged and successfully expressed in mammalian and insect cells. COS-7 and HEK-293 were used to express the α and β subunits under a constitutive promoter (CMV) whereas a *Drosophila* S2 cell line was used to express these subunits under an inducible promoter (methallothionein promoter).

In mammalian cells, with the exception of the β subunit which was also localised at the plasma membrane, the α and β subunits were expressed intracellularly. As far as the α subunit is concerned, the incorporation of the c-myc tag peptide at the C-terminus of the protein seemed not to interfere with the expression pattern of this subunit in COS-7 cells. The expression detected using two different constructs (c-myc tagged and a non-tagged) and two different antibodies (anti-c-myc and anti HcGluClα), was very similar and showed cytoplasmic and perinuclear staining. As expression was only analysed 48 hours after transfection some of the intracellular staining might be explained by over-expression of those subunits. Hence, they might be stacked in the cytoplasm either during protein synthesis pathways and/or recycling endosome pathways. Alternatively, as has been described for other members of the LGIC superfamily (Gorrie et al., 1997; Taylor et al., 2000; Kittler et al., 2000), GluCl subunit co-assembly and receptor targeting to the plasma membrane may require the presence of multiple subunits. This theory together with the putative staining of the ER detected for the HcGluClα subunit in mammalian cells, are supported by studies carried out by Connolly et al (1999) who showed that GABA$_A$ receptor subunits expressed alone are ER retained. In contrast, when α1β2 subunits are co-expressed they co-assemble, localise on the cell surface and form functional receptors. If this were the situation for the HcGluClα and β subunits, co-expressing both might result in functional receptors expressed on the cell surface. Unfortunately, co-expression experiments did not show cells expressing both subunits in the same. This could be explained simply because they may not co-express *in vitro*, at least under the conditions used in these experiments. Also, it may be the result of the low expression levels obtained for these proteins, particularly for the α subunit in mammalian cells, which may reduce the chances of

finding α and β co-expression. Alternatively, these two subunits might require additional(s) GluCl subunits (s) for α and β co-expression. Ultimately, absence of staining cannot be considered lack of expression. It is possible then that the method used in this work was not sensitivity enough to detect lower protein concentration.

Inducible expression of HcGluClα and β subunits in S2 cells also showed a cytoplasmic distribution of the proteins, supporting the idea discussed above about the necessity of additional GluCl subunits to target the receptor to the plasma membrane. The same theories about the lack of α and β co-expression discussed for the expression in mammalian cells could be applied to the S2 cells. It is worth mentioning that, although the expression levels, as counted by the number of immunolabelled cells, for the α subunit in S2 was about 10 % this figure is much higher than that detected in mammalian cells where no more than 10 cells per coverslip expressed the α subunit. Moreover, preliminary data obtained from the expression of HcGluClα-GFP in S2 cells driven by the constitutive insect promoter Act5c, resulted in about 15-20 % level of expression 48 h post trasfection. The expression pattern for this GFP-tagged α subunit was cytoplasmic (Fig. 7), very similar to the observed with the c-myc tagged α subunit under the inducible promoter (Fig. 6A,B). Considering that the level of expression detected for the control vector (pActSV-EGFP) was about 30 %, the constitutive expression of HcGluClα-GFP in S2 seems to be the better choice to express this subunit in vitro for future studies.
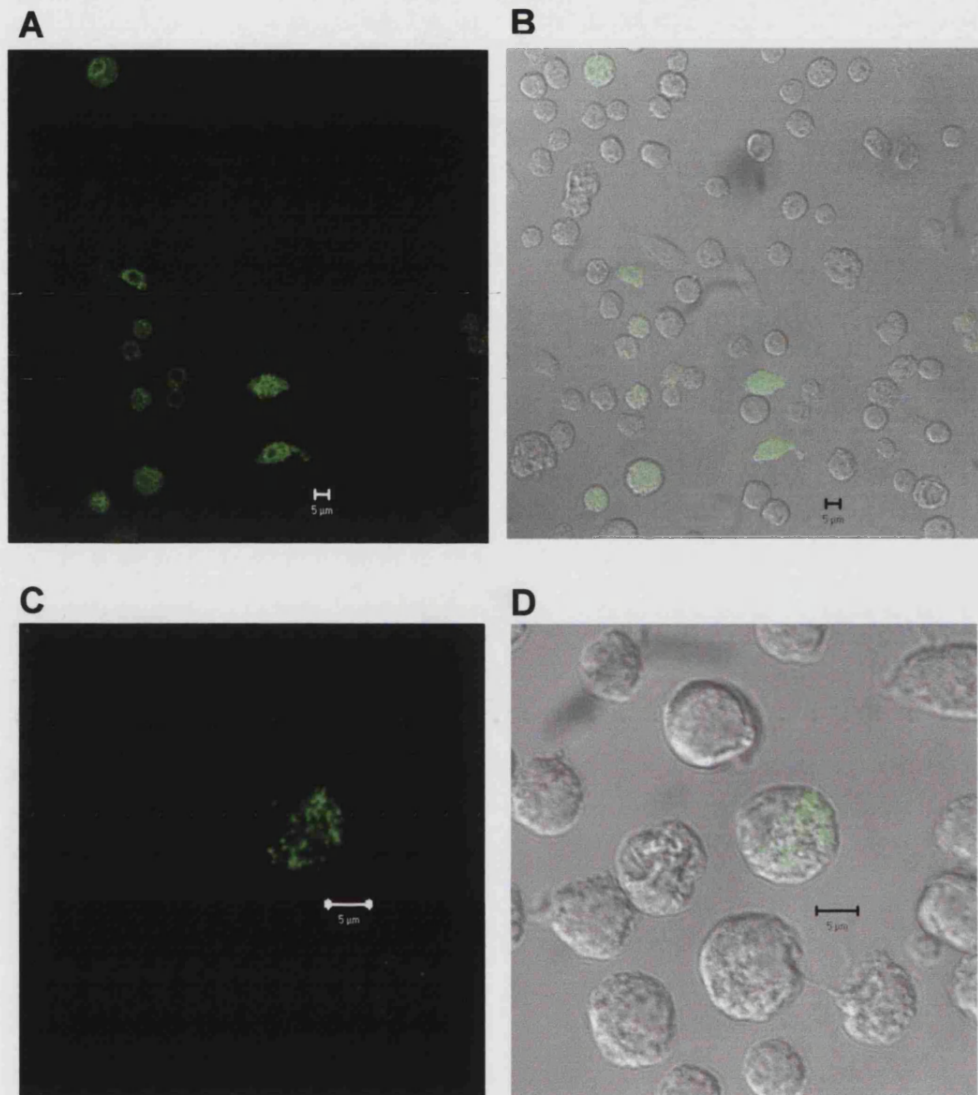
Fig. 7 Expression of HcGluClα-GFP in S2 cells
Confocal images of transient expression of HcGluClα-GFP cloned into the pActSV insect vector for constitutive expression in S2 cells. B & D: fluorescence obtained in A & C respectively, merged with their transmitted images. Scale bars, 5 μm

APPENDIX 1.1

RESTRICTION MAPS

This section includes the restriction maps of the vectors used for transient expression of in *Drosophila* S2 cells, supplied by M. Kapsetaki (IMBB, Iraklion, Greece). Single restriction sites are indicated in brown and enzymes that cut twice are indicated in black. These vectors derive from the LITMUS 28 cloning vector, supplied by NEB (Hitchin, UK). The polylinker was modified and the promoters and SV40 polyA termination signal were added. The SV40 signal was cloned between the *Xba* I (77) and *Afl* II (305) restriction sites.
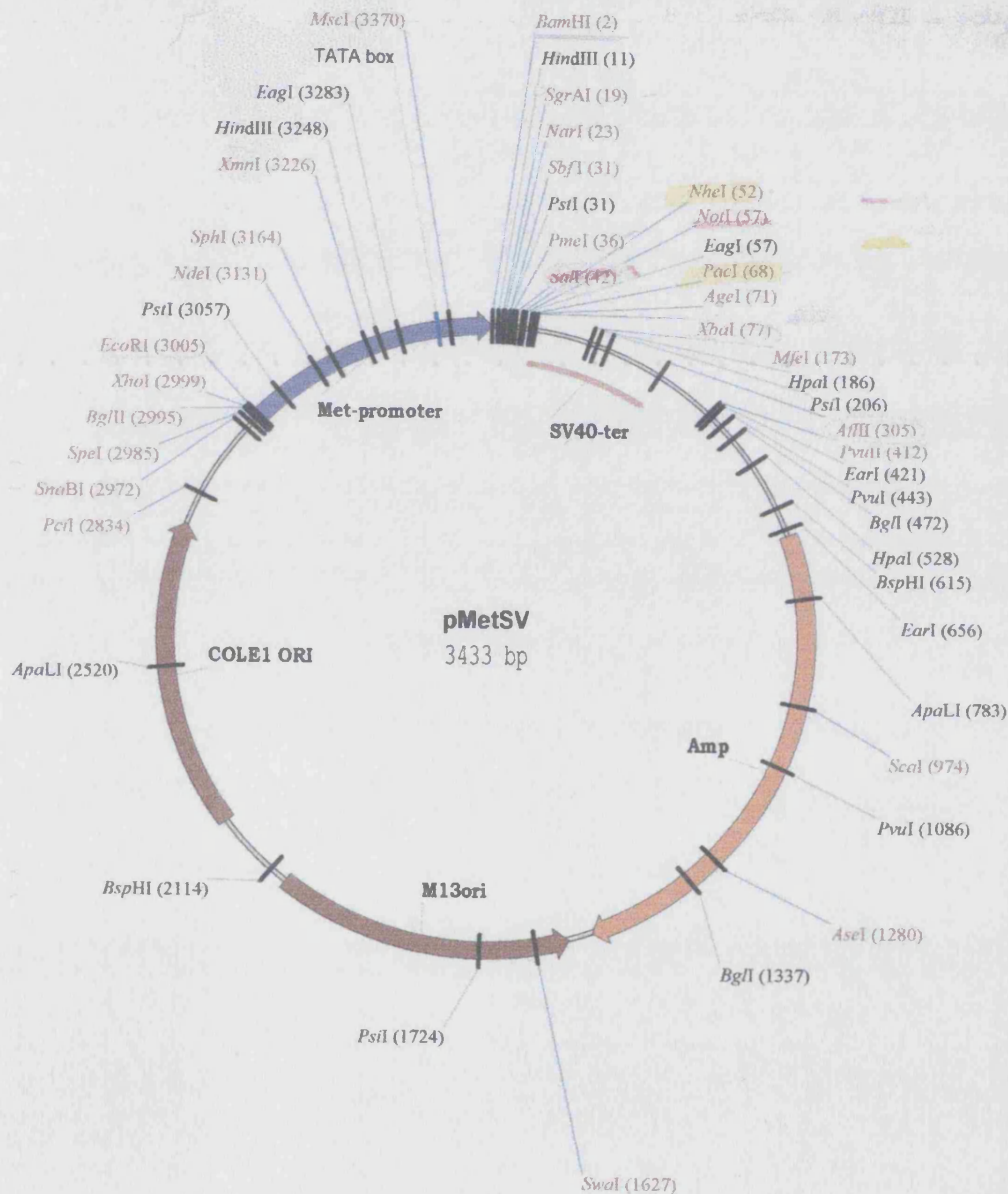
Fig. A1.1 1 Restriction map of pMetSV vector
This vector contains a methallothionein (Met) promoter, cloned between *EcoR* I and *BamH* I sites as indicated in purple. It gets induced with 0.5 mM $CuSO_4$ in cell culture medium. The *Xba* I (77) site is methylated. Restriction sites highlighted in yellow were the selected for HcGluClα-cmyc cloning and in pink for HcGluClβ-FLAG cloning as described in appendix 1.
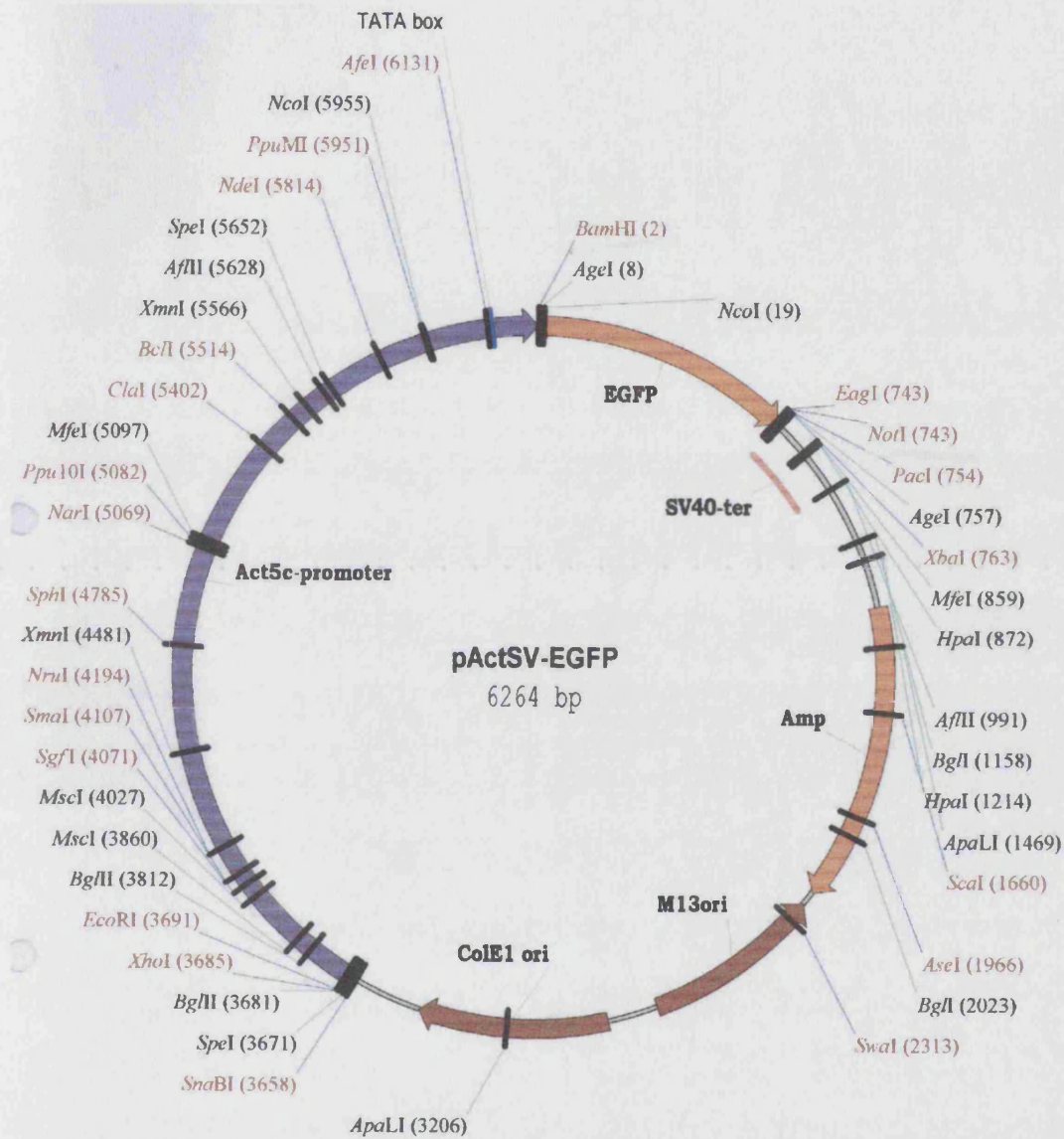
Fig. A1.1 2 Restriction map of pActSV-EGFP vector

This vector contains a constitutive (Act5c) promoter, as indicated in purple. The EGFP sequence was cut from the pEGFP-1 vector (CLONTECH, Palo Alto, USA) and cloned into the *BamH* I and *Not* I restriction sites. This vector was used to monitor transfection efficiency in S2 cells.

Fig. A1.1 3 Restriction map of pActSV vector

It contains a constitutive (Act5c) promoter, as indicated in purple.

REFERENCES

Adelsberger, H., Lepier, A., & Dudel, J. (2000) Activation of rat recombinant $\alpha(1)\beta(2)\gamma(2S)$ GABA(A) receptor by the insecticide ivermectin. Eur.J.Pharmacol. 394: 163-170.

Adelsberger, H., Scheuer, T., & Dudel, J. (1997) A patch clamp study of a glutamatergic chloride channel on pharyngeal muscle of the nematode *Ascaris suum*. Neurosci.Lett. 230: 183-186.
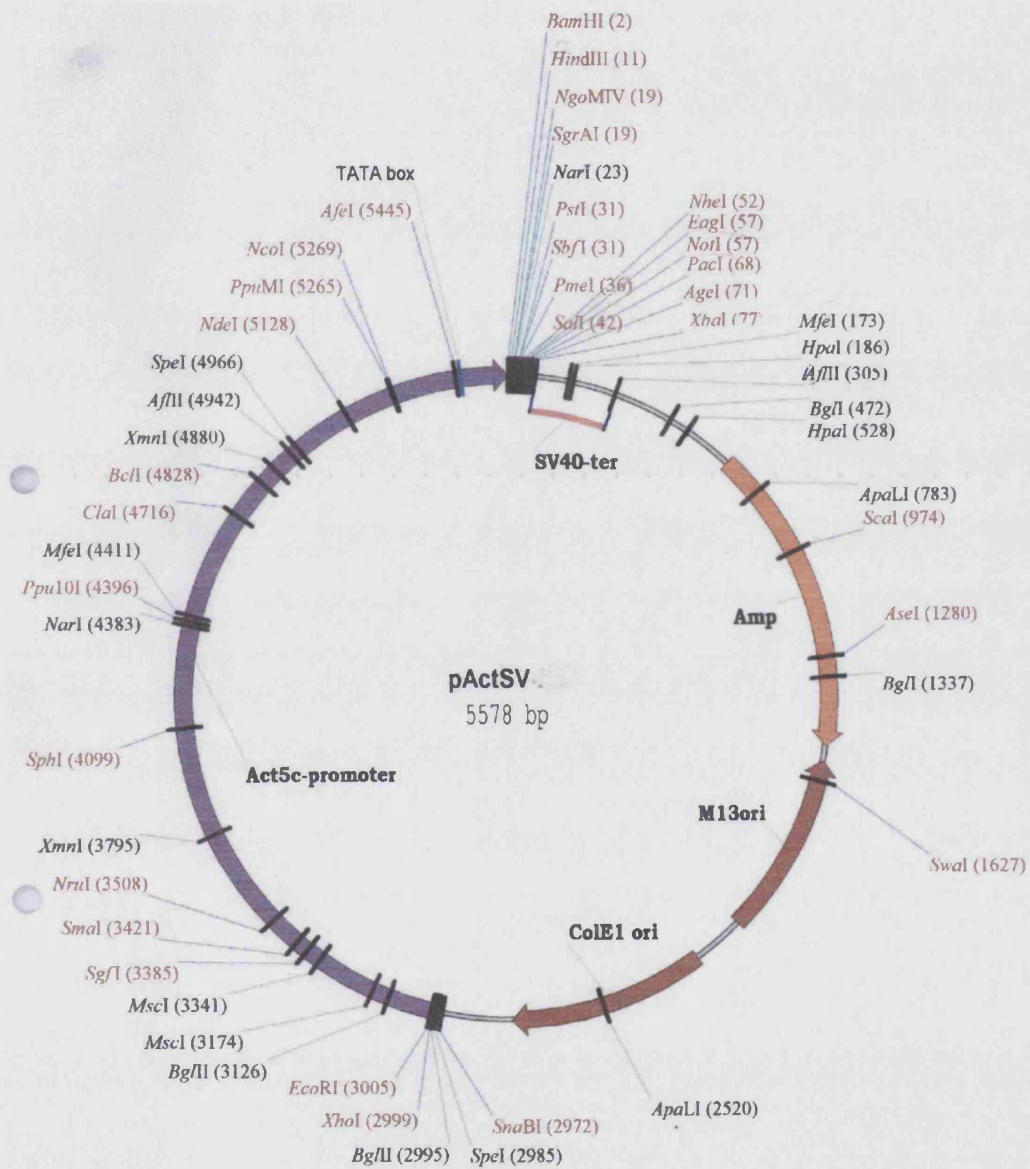
Albertson, D. G., & Thomson, J. N. (1976) The pharynx of *Caenorhabditis elegans*. Philos.Trans.R.Soc.Lond B Biol.Sci. 275: 299-325.

Aptel, N., Portillo, V., Cook, A., Souter, P., Lambert, K., Holden-Dye, L., & Wolstenholme, A. (2002) The roles of the glutamate-gated chloride channels subunits in *Caenorhabditis elegans* behaviour. Eur.J.Neurosci. 14, 228.2.

Arena, J. P., Liu, K. K., Paress, P. S., & Cully, D. F. (1991) Avermectin-sensitive chloride currents induced by *Caenorhabditis elegans* RNA in *Xenopus* oocytes. Mol.Pharmacol. 40: 368-374.

Arena, J. P., Liu, K. K., Paress, P. S., Schaeffer, J. M., & Cully, D. F. (1992) Expression of a glutamate-activated chloride current in *Xenopus* oocytes injected with *Caenorhabditis elegans* RNA: evidence for modulation by avermectin. Brain Res.Mol.Brain Res. 15: 339-348.

Arena, J. P., Liu, K. K., Paress, P. S., Frazier, E. G., Cully, D. F., Mrozik, H., & Schaeffer, J. M. (1995) The mechanism of action of avermectins in *Caenorhabditis elegans*: correlation between activation of glutamate-sensitive chloride current, membrane binding, and biological activity. J.Parasitol. 81: 286-294.

Armour, J., & Duncan, M. (1987) Arrested larval development in cattle nematodes. Parasitol. Today 3: 171-176.

Ashton, F. T., Bhopale, V. M., Fine, A. E., & Schad, G. A. (1995) Skin-penetrating nematode parasite: *Strongyloides stercoralis*. I. Amphidial neurons. J. Comp. Neurol. 357: 281-295.

Ashton, F. T., Bhopale, V. M., Holt, D., Smith, G., & Schad, G. A. (1998) Developmental switching in the parasitic nematode *Strongyloides stercoralis* is controlled by the ASF and ASI amphidial neurons. J. Parasitol. 84: 691-695.

Ashton, F. T., Li, J. & Schad, G. A. (1999) Chemo- and thermosensory neurons: structure and function in animal parasitic nematodes. Vet.Parasitol. 84: 297-316.

Avery, L. & Horvitz, H. R. (1990) Effects of starvation and neuroactive drugs on feeding in *Caenorhabditis elegans*. J.Exp.Zool. 253: 263-270.

Awadzi, K., Dadzie, K. Y., Shulz-Key, H., Haddock, D. R., Gilles, H. M., & Aziz, M. A. (1985) The chemotherapy of onchocerciasis X. An assessment of four single dose treatment regimes of MK-933 (ivermectin) in human onchocerciasis. Ann.Trop.Med.Parasitol. 79: 63-78.

Bargmann, C. I., Thomas, J. H., & Horvitz, H. R. (1990) Chemosensory cell function in the behavior and development of *Caenorhabditis elegans*. Cold Spring Harb.Symp.Quant.Biol. 55: 529-538.

Bargmann, C. I., & Horvitz, H. R. (1991a) Chemosensory neurons with overlapping functions direct chemotaxis to multiple chemicals in *Caenorhabditis elegans*. Neuron 7: 729-742.

Bargman, C. I., & Horvitz, H. R. (1991b) Control of larval development by chemosensory neurons in *C. elegans*. Science 251:1243-1246.

Bargmann, C. I., Hartwieg, E., & Horvitz, H. R. (1993) Odorant-selective genes and neurons mediate olfaction in *C. elegans*. Cell 74: 515-527.

Bargmann, C. I., & Mori, I. (1997) Chemotaxis and thermotaxis. In, *C. elegans* II (Eds. Riddle, D., Blumenthal, T., Meyer, B., Priess, J.), pp. 717-737. Cold Spring Harbor Laboratory Press, New York.

Bargmann, C. I. (1998) Neurobiology of the *Caenorhabditis elegans* genome. Science 282: 2028-2033.

Bargmann, C. I., & Kaplan, J. M. (1998) Signal transduction in the *Caenorhabditis elegans* nervous system. Annu.Rev.Neurosci. 21: 279-308.

Baulcombe, D. (2001) RNA silencing. Diced defence. Nature 409: 295-296.

Benian, G., L'Hernault, S., & Morris, M. E. (1993) Additional sequence complexity in the muscle gene, *unc-22*, and its encoded protein, twitching, of *C. elegans*. Genetics 134: 1097-1104.

Bernt, U. M., Junkesdorf, M., Londenshausen, M., Harder, A., & Schiesenberg, E. (1989) Effects of anthelmintics and different modes of action on the behavior and development of *C. elegans*. Fundament. Appl. Nematol. 21: 251-263.

Bird, A. F., & Bird, J. (1991) The structure of nematodes. 2nd Ed. Academic Press, New York.

Blackhall, W. J., Liu, H. Y., Xu, M., Prichard, R. K., & Beech, R. N. (1998a) Selection at a P-glycoprotein gene in ivermectin- and moxidectin-selected strains of *Haemonchus contortus*. Mol.Biochem.Parasitol. 95: 193-201.

Blackhall, W. J., Pouliot, J. F., Prichard, R. K., & Beech, R. N. (1998b) *Haemonchus contortus*: selection at a glutamate-gated chloride channel gene in ivermectin- and moxidectin-selected strains. Exp.Parasitol. 90: 42-48.

Blaxter, M., De Ley, P., Garey, J. R., Liu, L. X., Scheldeman, P., Vierstraete, A., Vanfleteren, J., Mackey, L., Dorris, M., Frisse, L., Vida, J. T., & Thomas, W. K. (1998) A molecular evolutionary framework for the phylum Nematoda. Nature 392: 71-75.

Bradford, M. M. (1976) A rapid and sensitive method for the quantitation of microgram quantities of protein utilizing the principle of protein-dye binding. Anal Biochem. 72: 248-254.

Brenner, S. (1974) The genetics of C. elegans. Genetics 77: 71-94.

Britton, C., Redmond, D. L., Knox, D. P., McKerrow, J. H., & Barry, J. D. (1999) Identification of promoter elements of parasite nematode genes in transgenic *Caenorhabditis elegans*. Mol.Biochem.Parasitol. 103: 171-181.

Brockie, P. J., Mellem, J. E., Hills, T., Madsen, D. M., & Maricq, A. V. (2001) The *C. elegans* glutamate receptor subunit NMR-1 is required for slow NMDA-activated currents that regulate reversal frequency during locomotion. Neuron 31: 617-630.

Brown, K. R., Ricci, F. M., & Ottesen, E. A. (2000) Ivermectin: effectiveness in lymphatic filariasis. Parasitology 121 Suppl: S133-S146.

Brownlee, D. J., & Fairweather, I. (1999) Exploring the neurotransmitter labyrinth in nematodes. Trends Neurosci. 22: 16-24.

Brownlee, D. J., Holden-Dye, L., & Walker, R. J. (1997) Actions of the anthelmintic ivermectin on the pharyngeal muscle of the parasitic nematode, *Ascaris suum*. Parasitology 115: 553-561.

Campbell, W. C. (1989) Ivermectin and abamectin. Springer-Verlag, New York.

Catty, D. & Raykundalia, C. (1988) Production and quality control of polyclonal antibodies. In, Antibodies, Vol I, A practical approach (Ed. Catty, D.), pp. 19-79. IRL Press, Oxford, UK.

Chabala, J. C., Mrozik, H., Tolman, R. L., Eskola, P., Lusi, A., Peterson, L. H., Woods, M. F., Fisher, M. H., Campbell, W. C., Egerton, J. R., & Ostlind, D. A. (1980) Ivermectin, a new broad-spectrum antiparasitic agent. J.Med.Chem. 23: 1134-1136.

Chalfie, M., & Sulston, J. (1981) Developmental genetics of the mechanosensory neurons of *Caenorhabditis elegans*. Dev.Biol. 82: 358-370.

Chalfie, M., Sulston, J. E., White, J. G., Southgate, E., Thomson, J. N., & Brenner, S. (1985) The neural circuit for touch sensitivity in *Caenorhabditis elegans*. J.Neurosci. 5: 956-964.

Chalfie, M., & White, J. (1988) The Nervous System. In: The nematode *C. elegans* (Eds. Wood, W. B., and the Community of *C. elegans* Researchers), pp. 337-391. Cold Spring Harbor Laboratory Press, New York.

Cheeseman, C. L., Delany, N. S., Woods, D. J., & Wolstenholme, A. J. (2001) High-affinity ivermectin binding to recombinant subunits of the *Haemonchus contortus* glutamate-gated chloride channel. Mol.Biochem.Parasitol. 114: 161-168.

Cheeseman, C. L. (2001) Characterisation of glutamate-gated chloride channel receptors in the parasitic nematode *Haemonchus contortus*. PhD Thesis, University of Bath.

Cleland, T. A. (1996) Inhibitory glutamate receptor channels. Mol.Neurobiol. 13: 97-136.

Cleland, T. A., & Selverston, A. I. (1995) Glutamate-gated inhibitory currents of central pattern generator neurons in the lobster stomatogastric ganglion. J.Neurosci. 15: 6631-6639.

Connolly, C. N., Kittler, J. T., Thomas, P., Uren, J. M., Brandon, N. J., Smart, T. G., & Moss, S. J. (1999) Cell surface stability of γ-aminobutyric acid type A receptors. Dependence on protein kinase C activity and subunit composition. J.Biol.Chem. 274: 36565-36572.

Coop, R., Barger, I. A., Jackson, F. (2002) The use of macrocyclic lactones to control parasites of sheep and goats. In, Macrocyclic Lactones in Antiparasitic Therapy (Eds. Vercruysse, J., Rew, R. S.), pp. 303-321. CABI Publishing.

Cox, F. E. (2000) Elimination of lymphatic filariasis as a public health problem. Parasitol.Today 16: 135.

Crompton, D. W., & Joyner, S. M. (1980) Parasitic Worms. Wykeham Publications, Oxford, UK.

Crompton, D. W. (1999) How much human helminthiasis is there in the world? J.Parasitol. 85: 397-403.

Cull-Candy, S. G., & Usherwood, P. N. (1973) Two populations of L-glutamate receptors on locust muscle fibres. Nat.New Biol. 246: 62-64.

Cully, D. F., Vassilatis, D. K., Liu, K. K., Paress, P. S., Van der Ploeg, L. H., Schaeffer, J. M., & Arena, J. P. (1994) Cloning of an avermectin-sensitive glutamate-gated chloride channel from *Caenorhabditis elegans*. Nature 371: 707-711.

Cully, D. F., Paress, P. S., Liu, K. K., Schaeffer, J. M., & Arena, J. P. (1996a) Identification of a *Drosophila melanogaster* glutamate gated chloride channel sensitive to the antiparasite agent avermectin. J. Biol. Chem. 271: 20187-20191.

Cully, D. F., Wilkinson, H., Vassilatis, D. K., Etter, A., & Arena, J. P. (1996b) Molecular biology and electrophysiology of glutamate-gated chloride channels of invertebrates. Parasitology 113 Suppl: S191-S200.

Culotti, J. G., & Russell, R. L. (1978) Osmotic avoidance defective mutants of the nematode *C. elegans*. Genetics 90: 243-256.

Davis, R. E., & Stretton, A. O. (1989) Passive membrane properties of motorneurons and their role in long-distance signaling in the nematode *Ascaris*. J.Neurosci. 9: 403-414.

Davies, R. E. (1998) Neurophysiology of glutamatergic signalling and anthelmintic action in *Ascaris suum*: pharmacological evidence for a kainate receptor. Parasitology. 116: 471-486.

Dawson, G. R., Wafford, K. A., Smith, A., Marshall, G. R., Bayley, P. J., Schaeffer, J. M., & Meinke, P. T., & McKernan, R. M. (2000) Anticonvulsant and adverse effects of avermectin analogs in mice are mediated through the γ-aminobutyric acid(A) receptor. J.Pharmacol.Exp.Ther. 295: 1051-1060.

Delany, N. S., Laughton, D. L., & Wolstenholme, A. J. (1998) Cloning and localisation of an avermectin receptor-related subunit from *Haemonchus contortus*. Mol.Biochem.Parasitol. 97: 177-187.

Dent, J. A., Davis, M. W., & Avery, L. (1997) *avr-15* encodes a chloride channel subunit that mediates inhibitory glutamatergic neurotransmission and ivermectin sensitivity in *Caenorhabditis elegans*. EMBO J. 16: 5867-5879.

Dent, J. A., Smith, M. M., Vassilatis, D. K., & Avery, L. (2000) The genetics of ivermectin resistance in *Caenorhabditis elegans*. Proc.Natl.Acad.Sci.U.S.A 97: 2674-2679.

Dorris, M., De Ley, P., & Blaxter, M. L. (1999) Molecular analysis of nematode diversity and the evolution of parasitism. Parasitol.Today 15: 188-193.

Driscoll, M., & Kaplan, J. (1997) Mechanotransduction. In: *C. elegans* II (Eds. Riddle, D., Blumenthal, T., Meyer, & B., Priess, J.), pp. 645-678. Cold Spring Harbor Laboratory Press, New York.

Duce, I. R., & Scott, R. H. (1985) Actions of dihydroavermectin B1a on insect muscle. Br.J.Pharmacol. 85: 395-401.

Duke, B. O., Zea-Flores, G., & Munoz, B. (1991) The embryogenesis of *Onchocerca volvulus* over the first year after a single dose of ivermectin. Trop.Med.Parasitol. 42: 175-180.

Dull, H. B., & Meredith, S. E. (1998) The Mectizan Donation Programme: a 10-year report. Ann.Trop.Med.Parasitol. 92 Suppl 1: S69-S71.

Dusenbery, D. B. (1974) Analysis of chemotaxis in the nematode *Caenorhabditis elegans* by countercurrent separation. J.Exp.Zool. 188: 41-47.

Egerton, J. R., Birnbaum, J., Blair, L. S., Chabala, J. C., Conroy, J., Fisher, M. H., Mrozik, H., Ostlind, D. A., Wilkins, C. A., & Campbell, W. C. (1980) 22, 23--dihydroavermectin B1, a new broad-spectrum antiparasitic agent. Br.Vet.J. 136: 88-97.

Erickson, J. D., Varoqui, H., Schafer, M. K., Modi, W., Diebler, M. F., Weihe, E., Rand, J., Eiden, L. E., Bonner, T. I., & Usdin, T. B. (1994) Functional identification of a vesicular acetylcholine transporter and its expression from a "cholinergic" gene locus. J.Biol.Chem. 269: 21929-21932.

Erlanger, B. F. (1980) The preparation of antigenic hapten-carrier conjugates: a survey. Methods Enzymol. 70: 85-104.

Etter, A., Cully, D. F., Liu, K. K., Reiss, B., Vassilatis, D. K., Schaeffer, J. M., & Arena, J. P. (1999) Picrotoxin blockade of invertebrate glutamate-gated chloride channels: subunit dependence and evidence for binding within the pore. J.Neurochem. 72: 318-326.

Evans, T. C., Crittenden, S. L., Kodoyianni, V., & Kimble, J. (1994) Translational control of maternal glp-1 mRNA establishes an asymmetry in the *C. elegans* embryo. Cell 77: 183-194.

Feng, X. P., Hayashi, J., Beech, R. N., & Prichard, R. K. (2002) Study of the nematode putative GABA type-A receptor subunits: evidence for modulation by ivermectin. J.Neurochem. 83: 870-878.

Filippova, N., Sedelnikova, A., Zong, Y., Fortinberry, H., & Weiss, D. S. (2000) Regulation of recombinant γ-aminobutyric acid (GABA)(A) and GABA(C) receptors by protein kinase C. Mol.Pharmacol. 57: 847-856.

Fine, A. E., Ashton, V. M., Bhopale, V. M., & Schad, G. A. (1997) Sensory neuroanatomy of a skin-penetrating nematode parasite *Strongyloides stercoralis*. II. Labial and cephalic neurons. J. Comp. Neurol. 389:212-223.

Fire, A., Harrison, S., & Dixon, D. (1990) A modular set of lacZ fusion vectors for studying gene expression in *C. elegans*. Gene 93: 189-198.

Fire, A., Xu, S., Montgomery, M. K., Kostas, S. A., Driver, S. E., & Mello, C. C. (1998) Potent and specific genetic interference by double-stranded RNA in Caenorhabditis elegans. Nature 391: 806-811.

Fisher, M. H., & Mrozik, H. (1992) The chemistry and pharmacology of avermectins. Annu.Rev.Pharmacol.Toxicol. 32: 537-553.

Foege, W. H. (1998) 10 years of Mectizan. Ann.Trop.Med.Parasitol. 92 Suppl 1: S7-10.

Forrester, S. G., Hamdan, F. F., Prichard, R. K., & Beech, R. N. (1999) Cloning, sequencing, and developmental expression levels of a novel glutamate-gated chloride channel homologue in the parasitic nematode *Haemonchus contortus*. Biochem.Biophys.Res.Commun. 254: 529-534.

Forrester, S. G., Prichard, R. K., & Beech, R. N. (2002) A glutamate-gated chloride channel subunit from *Haemonchus contortus*: expression in a mammalian cell line, ligand binding, and modulation of anthelmintic binding by glutamate. Biochem.Pharmacol. 63: 1061-1068.

Fraser, A. G., Kamath, R. S., Zipperlen, P., Martinez-Campos, M., Sohrmann, M., & Ahringer, J. (2000) Functional genomic analysis of *C. elegans* chromosome I by systematic RNA interference. Nature 408: 325-330.

Freeman, A. S., Nghiem, C., Li, J., Ashton, F. T., Guerrero, J., Shoop, W. L., & Schad, G. A. (2003) Amphidial structure of ivermectin-resistant and suceptible laboratory and field strains of *Haemonchus contortus*. Vet.Parasitol. 110: 217-226.

Geary, T. G., Sims, S. M., Thomas, E. M., Vanover, L., Davis, J. P., Winterrowd, C. A., Klein, R. D., Ho, N. F., & Thompson, D. P. (1993) *Haemonchus contortus*: ivermectin-induced paralysis of the pharynx. Exp.Parasitol. 77: 88-96.

Geary, T. G., & Thompson, D. P. (2001) *Caenorhabditis elegans*: how good a model for veterinary parasites? Vet.Parasitol. 101: 371-386.

Georgiev, P. G., Wolstenholme, A. J., Pak, W. L., & Semenov, E. P. (2002) Differential responses to avermectins in ort mutants of *Drosophila melanogaster*. Pestic. Biochem. Physiol. 72: 65-71.

Gill, J. H., & Lacey, E. (1998) Avermectin/milbemycin resistance in trichostrongyloid nematodes. Int.J.Parasitol. 28: 863-877.

Gill, J. H., & Redwin, J. M. (1995) Cryopreservation of the first-stage larvae of trichostrongylid nematode parasites. Int.J.Parasitol. 25: 1421-1426.

Gill, J. H., Redwin, J. M., van Wyk, J. A., & Lacey, E. (1991) Detection of resistance to ivermectin in *Haemonchus contortus*. Int.J.Parasitol. 21: 771-776.

Gisselmann, G., Pusch, H., Hovemann, B. T., & Hatt, H. (2002) Two cDNAs coding for histamine-gated ion channels in *D. melanogaster*. Nat.Neurosci. 5: 11-12.

Goodman, M. B., Hall, D. H., Avery, L., & Lockery, S. R. (1998) Active currents regulate sensitivity and dynamic range in *C. elegans* neurons. Neuron 20: 763-772.

Gorrie, G. H., Vallis, Y., Stephenson, A., Whitfield, J., Browning, B., Smart, T. G., & Moss, S. J. (1997) Assembly of GABA-A receptors composed of α1 and β2 subunits in both cultured neurons and fibroblasts. J.Neurosci. 17: 6587-6596.

Graham, D., Pfeiffer, F., & Betz, H. (1982) Avermectin B1a inhibits the binding of strychnine to the glycine receptor of rat spinal cord. Neurosci.Lett. 29: 173-176.

Grant, W. (2000) What is the real target for ivermectin resistance selection in *Onchocerca volvulus*? Parasitol.Today 16: 458-459.

Gronvold, J., Wolstrup, J., Nansen, P., Henriksen, S. A., Larsen, M., & Bresciani, J. (1993) Biological control of nematode parasites in cattle with nematode-trapping fungi: a survey of Danish studies. Vet. Parasitol., 48: 311-325.

Grunwald, M. E., & Kaplan, J. M. (2001) Differential targeting of glutamate receptors in *C. elegans*. Soc. Neurosci. Abstr. 27, 252.16.

Harder, A. (2002) Chemotherapeutic approaches to nematodes: current knowledge and outlook. Parasitol.Res. 88: 272-277.

Harlow & Lane (1988a) Immunisation. In, Antibodies, a Laboratory Manual, pp. 53-138. Cold Spring Harbor Press, New York.

Harlow & Lane (1988b) Cell Staining. In, Antibodies, a Laboratory Manual, pp. 418-512. Cold Spring Harbor Press, New York.

Harlow and Lane (1999) Staining Cells. In, Using Antibodies, a Laboratory Manual, pp. 103-145. Cold Spring Harbor Press, New York.

Hart, A. C., Kass, J., Shapiro, J. E., & Kaplan, J. M. (1999) Distinct signaling pathways mediate touch and osmosensory responses in a polymodal sensory neuron. J.Neurosci. 19: 1952-1958.

Hartman, D., Donald, D. R., Nikolaou, S., Savin, K. W., Hasse, D., Presidente, P. J., & Newton, S. E. (2001) Analysis of developmentally regulated genes of the parasite *Haemonchus contortus*. Int.J.Parasitol. 31: 1236-1245.

Hedgecock, E. M., Culotti, J. G., Thomson, J. N., & Perkins, L. A. (1985) Axonal guidance mutants of *Caenorhabditis elegans* identified by filling sensory neurons with fluorescein dyes. Dev.Biol. 111: 158-170.

Hejmadi, M. V., Jagannathan, S., Delany, N. S., Coles, G. C., & Wolstenholme, A. J. (2000) L-glutamate binding sites of parasitic nematodes: an association with ivermectin resistance? Parasitology 120 (Pt 5): 535-545.

Hekimi, S. (1990) A neuron-specific antigen in *C. elegans* allows visualization of the entire nervous system. Neuron 4: 855-865.

Higazi, T. B., Merriweather, A., Shu, L., Davis, R., & Unnasch, T. R. (2002) *Brugia malayi*: transient transfection by microinjection and particle bombardment. Exp.Parasitol. 100: 95-102.

Hilliard, M. A., Bargmann, C. I., & Bazzicalupo, P. (2002) *C. elegans* responds to chemical repellents by integrating sensory inputs from the head and the tail. Curr.Biol. 12: 730-734.

Hobert, O., Johnston, R. J., Jr., & Chang, S. (2002) Left-right asymmetry in the nervous system: the *Caenorhabditis elegans* model. Nat.Rev.Neurosci. 3: 629-640.

Holden-Dye, L., Hewitt, G. M., Wann, K. T., Krogsgaardlarsen, P., & Walker, R. J. (1988) Studies involving avermectin and the γ-aminobutyric acid (GABA) receptor of *Ascaris suum* muscle. Pestic. Sci. 24: 231-245.

Holden-Dye, L. & Walker, R. J. (1990) Avermectin and avermectin derivatives are antagonists at the γ-aminobutyric acid (GABA) receptor on the somatic muscle cells of *Ascaris*; is this the site of anthelmintic action? Parasitology 101 Pt 2: 265-271.

Horoszok, L., Raymond, V., Sattelle, D. B., & Wolstenholme, A. J. (2001) GLC-3: a novel fipronil and BIDN-sensitive, but picrotoxinin-insensitive, L-glutamate-gated chloride channel subunit from *Caenorhabditis elegans*. Br.J.Pharmacol. 132: 1247-1254.

Hurn, B. A., & Chantler, S. M. (1980) Production of reagent antibodies. Methods Enzymol. 70: 104-142.

Iovchev, M. I., Kodrov, P., Wolstenholme, A. J., Pak, W. L., & Semenov, E. P. Altered drug resistance and recovery from paralysis in *Drosophila melanogaster*. J. Neurogenet. In press.

Ikemoto, Y., & Akaike, N. (1988) The glutamate-induced chloride current in *Aplysia* neurones lacks pharmacological properties seen for excitatory responses to glutamate. Eur.J.Pharmacol. 150: 313-318.

Jackson, F., & Coop, R. L. (2000) The development of anthelmintic resistance in sheep nematodes. Parasitology 120 Suppl: S95-107.

Jackstadt, P., Wilm, T. P., Zahner, H., & Hobom, G. (1999) Transformation of nematodes via ballistic DNA transfer. Mol.Biochem.Parasitol. 103: 261-266.

Jagannathan, S., Laughton, D. L., Critten, C. L., Skinner, T. M., Horoszok, L., & Wolstenholme, A. J. (1999) Ligand-gated chloride channel subunits encoded by the *Haemonchus contortus* and *Ascaris suum* orthologues of the *Caenorhabditis elegans gbr-2* (*avr-14*) gene. Mol.Biochem.Parasitol. 103: 129-140.

Jameson, B. A., & Wolf, H. (1988) The antigenic index: a novel algorithm for predicting antigenic determinants. Cabios 4: 181-186.

Johnson, C. D., & Stretton, A. O. (1985) Localization of choline acetyltransferase within identified motoneurons of the nematode *Ascaris*. J.Neurosci. 5: 1984-1992.

Johnson, C. D., & Stretton, A. O. (1987) GABA-immunoreactivity in inhibitory motor neurons of the nematode *Ascaris*. J.Neurosci. 7: 223-235.

Johnson, C. D., Reinitz, C. A., Sithigorngul, P., & Stretton, A. O. (1996) Neuronal localisation of serotonin in the nematode *Ascaris suum*. J. Comp. Neurol. 367: 352-360.

Jorgensen, E. M., & Mango, S. E. (2002) The art and design of genetic screens: *C. elegans*. Nat. Rev. Gen. 3: 356-369.

Kamath, R. S., Martinez-Campos, M., Zipperlen, P., Fraser, A. G. & Ahringer, J. (2000) Effectiveness of specific RNA-mediated interference through ingested double-stranded RNA in *C. elegans*. Genome Biology 2: 1-10.

Kaplan, J. M. & Horvitz, H. R. (1993) A dual mechanosensory and chemosensory neuron in *Caenorhabditis elegans*. Proc.Natl.Acad.Sci.U.S.A 90: 2227-2231.

Kass, I. S., Stretton, A. O., & Wang, C. C. (1984) The effects of avermectin and drugs related to acetylcholine and γ-aminobutyric acid on neurotransmission in *Ascaris suum*. Mol.Biochem.Parasitol. 13: 213-225.

Kass, I. S., Wang, C. C., Walrond, J. P., & Stretton, A. O. (1980) Avermectin B1a, a paralyzing anthelmintic that affects interneurons and inhibitory motoneurons in *Ascaris*. Proc.Natl.Acad.Sci.U.S.A 77: 6211-6215.

Keating, C. D., Holden-Dye, L., Thorndyke, M. C., Williams, R. G., Mallett, A., & Walker, R. J. (1995) The FMRFamide-like neuropeptide AF2 is present in the parasitic nematode *Haemonchus contortus*. Parasitology 111: 515-521.

Kenyon, C. (1988) The nematode *C. elegans*. Science 240: 1448-1453.

Kerr, R., Lev-Ram, V., Baird, G., Vincent, P., Tsien, R. Y., & Schafer, W. R. (2000) Optical imaging of calcium transients in neurons and pharyngeal muscle of *C. elegans*. Neuron 26: 583-594.

Khakh, B. S., Proctor, W. R., Dunwiddie, T. V., Labarca, C., & Lester, H. A. (1999) Allosteric control of gating and kinetics at P2X(4) receptor channels. J.Neurosci. 19: 7289-7299.

Kittler, J. T., Wang, J., Connolly, C. N., Vicini, S., Smart, T. G., & Moss, S. J. (2000) Analysis of GABA-A receptor assembly in mammalian cell lines and hippocampal neurons using γ2 subunit green fluorescent protein chimeras. Mol.Cell Neurosci. 16: 440-452.

Knox, D. P. (2000) Development of vaccines against gastrointestinal nematodes. Parasitology 120 Suppl: S43-S61.

Komatsu, H., Jin, Y. H., L'Etoile, N., Mori, I., Bargmann, C. I., Akaike, N., & Ohshima, Y. (1999) Functional reconstitution of a heteromeric cyclic nucleotide-gated channel of Caenorhabditis elegans in cultured cells. Brain Res. 821: 160-168.

Krause, R. M., Buisson, B., Bertrand, S., Corringer, P. J., Galzi, J. L., Changeux, J. P., & Bertrand, D. (1998) Ivermectin: a positive allosteric effector of the α7 neuronal nicotinic acetylcholine receptor. Mol.Pharmacol. 53: 283-294.

Kwa, M. S., Veenstra, J. G., Van Dijk, M., & Roos, M. H. (1995) β-tubulin genes from the parasitic nematode Haemonchus contortus modulate drug resistance in Caenorhabditis elegans. J.Mol.Biol. 246: 500-510.

Kwei, G. Y., Alvaro, R. F., Chen, Q., Jenkins, H. J., Hop, C. E., Keohane, C. A., Ly, V. T., Strauss, J. R., Wang, R. W., Wang, Z., Pippert, T. R., & Umbenhauer, D. R. (1999) Disposition of ivermectin and cyclosporin A in CF-1 mice deficient in mdr1 a P-glycoprotein. Drug Metab Dispos. 27: 581-587.

Kyte, J., & Doolittle, R. F. (1982) A simple method for displaying the hydropathic character of a protein. J.Mol.Biol. 157: 105-132.

Lacey, E. (1990) Mode of action of benzamidazoles. Parasitology Today. 6: 115-116.

Laughton, D. L., Amar, M., Thomas, P., Towner, P., Harris, P., Lunt, G. G., & Wolstenholme, A. J. (1994) Cloning of a putative inhibitory aminoacid receptor subunit from the parasitic nematode Haemonchus contortus. Receptors Channels 2: 155-163.

Laughton, D. L., Lunt, G. G., & Wolstenholme, A. J. (1997a) Alternative splicing of a Caenorhabditis elegans gene produces two novel inhibitory amino acid receptor subunits with identical ligand binding domains but different ion channels. Gene 201: 119-125.

Laughton, D. L., Lunt, G. G., & Wolstenholme, A. J. (1997b) Reporter gene constructs suggest the *C. elegans* avermectin receptor β-subunit is expressed solely in the pharynx. J. Exp. Biol. 200: 1509-1514.

Le Jambre, L. F., Gill, J. H., Lenane, I. J., & Lacey, E. (1995) Characterisation of an avermectin resistant strain of Australian *Haemonchus contortus*. Int.J.Parasitol. 25: 691-698.

Le Jambre, L. F., Lenane, I. J., & Wardrop, A. J. (1999) A hybridisation technique to identify anthelmintic resistance genes in *Haemonchus*. Int.J.Parasitol. 29: 1979-1985.

Lee, R. Y., Sawin, E. R., Chalfie, M., Horvitz, H. R., & Avery, L. (1999) EAT-4, a homolog of a mammalian sodium-dependent inorganic phosphate cotransporter, is necessary for glutamatergic neurotransmission in *Caenorhabditis elegans*. J.Neurosci. 19: 159-167.

Li, J., Ashton, F. T., Gamble, H. R., & Schad, G. A. (2000a) Sensory neuroanatomy of a passively ingested nematode parasite, *Haemonchus contortus*: amphidial neurons of the first stage larva. J.Comp Neurol. 417: 299-314.

Li, J., Zhu, X., Boston, R., Ashton, F. T., Gamble, H. R., & Schad, G. A. (2000b) Thermotaxis and thermosensory neurons in infective larvae of *Haemonchus contortus*, a passively ingested nematode parasite. J.Comp Neurol. 424: 58-73.

Lopez, P. M., Boston, R., Ashton, F. T., & Schad, G. A. (2000) The neurons of class ALD mediate thermotaxis in the parasitic nematode, *Strongyloides stercoralis*. Int.J.Parasitol. 30: 1115-1121.

Ludmerer, S. W., Warren, V. A., Williams, B. S., Zheng, Y., Hunt, D. C., Ayer, M. B., Wallace, M. A., Chaudhary, A. G., Egan, M. A., Meinke, P. T., Dean, D. C., Garcia, M. L., Cully, D. F., & Smith, M. M. (2002) Ivermectin and nodulisporic acid receptors in *Drosophila melanogaster* contain both γ-aminobutyric acid-gated Rdl and glutamate-gated GluClα chloride channel subunits. Biochemistry 41: 6548-6560.

Maricq, A. V., Peckol, E., Driscoll, M., & Bargmann, C. I. (1995) Mechanosensory signalling in *C. elegans* mediated by the GLR-1 glutamate receptor. Nature 378: 78-81.

Martin, R. J. (1996) An electrophysiological preparation of *Ascaris suum* pharyngeal muscle reveals a glutamate-gated chloride channel sensitive to the avermectin analogue, milbemycin D. Parasitology 112: 247-252.

Martin, R. J., & Pennington, A. J. (1989) A patch-clamp study of effects of dihydroavermectin on *Ascaris* muscle. Br.J.Pharmacol. 98: 747-756.

Maule, A. G., Bowman, J. W., Thompson, D. P., Marks, N. J., Friedman, A. R., & Geary, T. G. (1996) FMRFamide-related peptides (FaRPs) in nematodes: occurrence and neuromuscular physiology. Parasitology 113 Suppl: S119-135.

McIntire, S. L., Garriga, G., White, J., Jacobson, D., & Horvitz, H. R. (1992) Genes necessary for directed axonal elongation or fasciculation in *C. elegans*. Neuron 8: 307-322.

McIntire, S. L., Jorgensen, E., Kaplan, J., & Horvitz, H. R. (1993) The GABAergic nervous system of *Caenorhabditis elegans*. Nature 364: 337-341.

McLeod, R. S. (1995) Costs of major parasites to the Australian livestock industries. Int.J.Parasitol. 25: 1363-1367.

Mealey, K. L., Bentjen, S. A., Gay, J. M., & Cantor, G. H. (2001) Ivermectin sensitivity in collies is associated with a deletion mutation of the mdr1 gene. Pharmacogenetics 11: 727-733.

Meeusen, E. N. (1996) Rational design of nematode vaccines; natural antigens. Int.J.Parasitol. 26: 813-818.

Mellem, J. E., Brockie, P. J., Zheng, Y., Madsen, D. M., & Maricq, A. V. (2002) Decoding of polymodal sensory stimuli by postsynaptic glutamate receptors in *C. elegans*. Neuron 36: 933-944.

Mello, C. C., & Fire, A. (1995) DNA transformation. In: *C. elegans*: Modern biological analysis of an organism (Eds. Epstein, H. F., and Shakes, D. C.), pp. 452-482. Academic Press, San Diego.

Miller, D. M., & Shakes, D. C. (1995) Immunofluorescence microscopy. Methods Cell Biol. 48: 365-394.

Mori, I., & Ohshima, Y. (1995) Neural regulation of thermotaxis in *Caenorhabditis elegans*. Nature 376: 344-348.

Moss, S. J., Gorrie, G. H., Amato, A., & Smart, T. G. (1995) Modulation of GABA-A receptors by tyrosine phosphorylation. Nature 377: 344-348.

Munn, E. A., Greenwood, C. A., & Coadwell, W. J. (1987) Vaccination of young lambs by means of a protein fraction extracted from adult *Haemonchus contortus*. Parasitology 94: 385-397.

Nakane, P. K., & Pierce, G. B., Jr. (1967) Enzyme-labeled antibodies for the light and electron microscopic localization of tissue antigens. J.Cell Biol. 33: 307-318.

Nonet, M. L., Grundahl, K., Meyer, B. J., & Rand, J. B. (1993) Synaptic function is impaired but not eliminated in *C. elegans* mutants lacking synaptotagmin. Cell 73: 1291-1305.

Oliet, S. H., & Bourque, C. W. (1993) Mechanosensitive channels transduce osmosensitivity in supraoptic neurons. Nature 364: 341-343.

Oliet, S. H., & Bourque, C. W. (1996) Gadolinium uncouples mechanical detection and osmoreceptor potential in supraoptic neurons. Neuron 16: 175-181.

Page, A. P. (2001) The nematode cuticle: synthesis, modification and mutants. In, Parasitic Nematodes: Molecular Biology, Biochemistry and Immunology (Eds. Kennedy, M. W. and Harnett, W.), pp. 167-193. CABI Publishing, New York.

Paiement, J., Prichard, R. K., & Ribeiro, P. (1999) *Haemonchus contortus*: characterization of a glutamate binding site in unselected and ivermectin-selected larvae and adults. Exp.Parasitol. 92: 32-39.

Peeters, J. M., Hazendonk, T. G., Beuvery, E. C., & Tesser, G. I. (1989) Comparison of four bifunctional reagents for coupling peptides to proteins and the effect of the three moieties on the immunogenicity of the conjugates. J.Immunol.Methods 120: 133-143.

Pemberton, D. J., Franks, C. J., Walker, R. J., & Holden-Dye, L. (2001) Characterization of glutamate-gated chloride channels in the pharynx of wild-type and mutant *Caenorhabditis elegans* delineates the role of the subunit GluCl-α2 in the function of the native receptor. Mol.Pharmacol. 59: 1037-1043.

Perry, R. N. (2001) Analysis of the sensory responses of parasitic nematodes using electrophysiology. Int.J.Parasitol. 31: 909-918.

Platt, H. M. (1994) The phylogenetic systematics of free-living nematodes (Eds. S. Lorenzen). The Ray Society, London.

Pong, S. S., & Wang, C. C. (1982) Avermectin B1a modulation of γ-aminobutyric acid receptors in rat brain membranes. J.Neurochem. 38: 375-379.

Porter, N. M., Twyman, R. E., Uhler, M. D., & Macdonald, R. L. (1990) Cyclic AMP-dependent protein kinase decreases GABA-A receptor current in mouse spinal neurons. Neuron 5: 789-796.

Prichard, R. (1994) Anthelmintic resistance. Vet.Parasitol. 54: 259-268.

Rand, J. B., & Nonet, M. L. (1997) Synaptic Transmission. In: *C. elegans* II (Eds. Riddle, D., Blumenthal, T., Meyer, B., & Priess, J.), pp. 611-644. Cold Spring Harbor Laboratory Press, New York.

Rankin, C. H. (2002) From gene to identified neuron to behaviour in *Caenorhabditis elegans*. Nat.Rev.Genet. 3: 622-630.

Reichlin, M. (1980) Use of glutaraldehyde as a coupling agent for proteins and peptides. Methods Enzymol. 70: 159-165.

Rohrer, S. P., Birzin, E. T., Eary, C. H., Schaeffer, J. M., & Shoop, W. L. (1994) Ivermectin binding sites in sensitive and resistant *Haemonchus contortus*. J.Parasitol. 80: 493-497.

Rolfe, R. N., Barrett, J., & Perry, R. N. (2001) Electrophysiological analysis of responses of adult females of *Brugia pahangi* to some chemicals. Parasitology 122: 347-357.

Saeki, S., Yamamoto, M., & Lino, Y. (2001) Plasticity of chemotaxis revealed by paired presentation of a chemoattractant and starvation in the nematode *C. elegans*. J. Exp. Biol. 204: 1757-1764.

Sangster, N. C. (1999) Anthelmintic resistance: past, present and future. Int.J.Parasitol. 29: 115-124.

Sangster, N. C., & Gill, J. (1999) Pharmacology of anthelmintic resistance. Parasitol.Today 15: 141-146.

Schaeffer, J. M., & Haines, H. W. (1989) Avermectin binding in *Caenorhabditis elegans*. A two-state model for the avermectin binding site. Biochem.Pharmacol. 38: 2329-2338.

Schallig, H. D. F. H., Van Leeuwen, M. A. W., & Cornelisen, A. W. C. A. (1997) Protective immunity induced by vaccination with two *Haemonchus contortus* excretory secretory proteins in sheep. Parasite Immunology, 19: 447-453.

Sengupta, P., Chou, J. H., & Bargmann, C. I. (1996) *odr-10* encodes a seven transmembrane domain olfactory receptor required for responses to the odorant diacetyl. Cell 84: 899-909.

Schneider, I. (1972). Cell lines derived from late embryonic stages of *Drosophila melanogaster*. J. Embryol. Exp. Morph. 27, 363-365.

Scott, R. H., & Duce, I. R. (1985) Effects of 22,23-dihydroavermectin B_{1A} on locust (*Schistocerca gregaria*) muscles may involve several sites of action. Pestic. Sci. 16: 599-604.

Shan, Q., Haddrill, J. L., & Lynch, J. W. (2001) Ivermectin, an unconventional agonist of the glycine receptor chloride channel. J.Biol.Chem. 276: 12556-12564.

Sharrock, W. J. (1984) Cleavage of two yolk proteins from a precursor in *C. elegans*. J. Mol. Biol. 174: 419-431.

Shoop, W. L., Mrozik, H., & Fisher, M. H. (1995) Structure and activity of avermectins and milbemycins in animal health. Vet.Parasitol. 59: 139-156.

Skinner, T. M. (1997) Cloning and localisation of nematode inhibitory aminoacid receptors. PhD Thesis, University of Bath.

Skinner, T. M., Bascal, Z. A., Holden-Dye, L., Lunt, G. G., & Wolstenholme, A. J. (1998) Immunocytochemical localization of a putative inhibitory amino acid receptor subunit in the parasitic nematodes *Haemonchus contortus* and *Ascaris suum*. Parasitology 117: 89-96.

Smith, D. B., & Johnson, K. S. (1988) Single-step purification of polypeptides expressed in *Escherichia coli* as fusions with gluthatione S-transferase. Gene 67: 31-40.

Smyth, J. D. (1994) Introduction to animal parasitology. 3rd Ed. Cambridge University Press, New York.

Steidl, S., Dube, N., Rose, J. K., & Rankin, C. H. (2002) Mutations of a glutamate-gated chloride channel in *C. elegans* affect short-term memory in a isi dependant manner, long term memory and foraging behavior. Soc. Neurosci. Abstr. 28, 377.3.

Stephenson, I., & Wiselka, M. (2000) Drug treatment of tropical parasitic infections: recent achievements and developments. Drugs 60: 985-995.

Stretton, A., Donmoyer, J., Davis, R., Meade, J., Cowden, C., & Sithigorngul, P. (1992) Motor behavior and motor nervous system function in the nematode *Ascaris suum*. J.Parasitol. 78: 206-214.

Stretton, A. O., Cowden, C., Sithigorngul, P., & Davis, R. E. (1991) Neuropeptides in the nematode *Ascaris suum*. Parasitology 102 Suppl: S107-S116.

Stretton, A. O. W., Davis, R. E., Angstadt, J. D., Donmoyer, J. E., & Johnson, C. D. (1985) Neural control of behavior in *Ascaris*. Trends Neurosci. 8, 294-300.

Stretton, A. O., Fishpool, R. M., Southgate, E., Donmoyer, J. E., Walrond, J. P., Moses, J. E., & Kass, I. S. (1978) Structure and physiological activity of the motoneurons of the nematode Ascaris. Proc.Natl.Acad.Sci.U.S.A 75: 3493-3497.

Stringfellow, F. (1986) Cultivation of *Haemonchus contortus* (Nematoda: Trichostrongylidae) from infective larvae to the adult male and the egg-laying female. J.Parasitol. 72: 339-345.

Strong, L., & Wall, R. (1990) The chemical control of livestock parasites: problems and alternatives. Parasitology Today 6: 291-296.

Supavilai, P., & Karobath, M. (1981) In vitro modulation by avermectin B1a of the GABA/benzodiazepine receptor complex of rat cerebellum. J.Neurochem. 36: 798-803.

Tabara, H., Grishok, A., & Mello, C. C. (1998) RNAi in *C. elegans*: soaking in the genome sequence. Science 282: 430-431.

Taylor, P. M., Connolly, C. N., Kittler, J. T., Gorrie, G. H., Hosie, A., Smart, T. G., & Moss, S. J. (2000) Identification of residues within GABA-A receptor a subunits that mediate specific assembly with receptor β subunits. J.Neurosci. 20: 1297-1306.

The *C. elegans* Sequencing Consortium (1998) Genome sequence of the nematode *C. elegans*: a platform for investigating biology. Science 282: 2012-2018.

Thompson, D. P., Klein, R. D., & Geary, T. G. (1996) Prospects for rational approaches to anthelmintic discovery. Parasitology 113 Suppl: S217-S238.

Timmons, L., & Fire, A. (1998) Specific interference by ingested dsRNA. Nature 395: 854.

Troemel, E. R., Chou, J. H., Dwyer, N. D., Colbert, H. A., & Bargmann, C. I. (1995) Divergent seven transmembrane receptors are candidate chemosensory receptors in *C. elegans*. Cell 83: 207-218.

Troemel, E. R., Kimmel, B. E., & Bargmann, C. I. (1997) Reprogramming chemotaxis responses: sensory neurons define olfactory preferences in *C. elegans*. Cell 91: 161-169.

Vassilatis, D. K., Elliston, K. O., Paress, P. S., Hamelin, M., Arena, J. P., Schaeffer, J. M., Van der Ploeg, L. H., & Cully, D. F. (1997a) Evolutionary relationship of the ligand-gated ion channels and the avermectin-sensitive, glutamate-gated chloride channels. J.Mol.Evol. 44: 501-508.

Vassilatis, D. K., Arena, J. P., Plasterk, R. H., Wilkinson, H. A., Schaeffer, J. M., Cully, D. F., & Van der Ploeg, L. H. (1997b) Genetic and biochemical evidence for a novel avermectin-sensitive chloride channel in *Caenorhabditis elegans*. Isolation and characterization. J.Biol.Chem. 272: 33167-33174.

Veglia, F. (1915) The anatomy and life history of *Haemonchus contortus*. Third and Fourth Reports of the Director of Veterinary Research, Ondeerstepoort, South Africa. 13, 347-500.

Wafford, K. A., & Whiting, P. J. (1992) Ethanol potentiation of GABA-A receptors requires phosphorylation of the alternatively spliced variant of the γ2 subunit. FEBS Lett. 313: 113-117.

Waller, P. J., & Faedo, M. (1993) The potential of nematophagous fungi to control the free-living stages of nematode parasites of sheep: screening studies. Vet.Parasitol. 49: 285-297.

Waller, P. J., & Larsen, M. (1993) The role of nematophagous fungi in the biological control of nematode parasites of livestock. Int.J.Parasitol. 23: 539-546.

Walrond, J. P., Kass, I. S., Stretton, A. O., & Donmoyer, J. E. (1985) Identification of excitatory and inhibitory motoneurons in the nematode *Ascaris* by electrophysiological techniques. J.Neurosci. 5: 1-8.

Walrond, J. P., & Stretton, A. O. (1985) Excitatory and inhibitory activity in the dorsal musculature of the nematode *Ascaris* evoked by single dorsal excitatory motonerons. J.Neurosci. 5: 16-22.

Ward, S. (1973) Chemotaxis by the nematode *C. elegans*: identification of attractants and analysis of the response by use of mutants. Proc. Natl. Acad. Sci. 70: 817-821.

Ward, S., Thomson, N., White, J. G., & Brenner, S. (1975) Electron microscopical reconstruction of the anterior sensory anatomy of the nematode *C. elegans*. J. Comp. Neurol. 160: 313-337.

White, J. G., Southgate, E., Thomson, J. N. & Brenner, S. (1986) The structure of the nervous system of the nematode *C. elegans*. Philosophical Transactions of the Royal Society of London. 314: 1-340.

Wood, W. B. (1988) The nematode *C. elegans* (Ed. Wood, W. B.), pp. 1-16. Cold Spring Harbor Laboratory Press, New York.

Yassin, L., Gillo, B., Kahan, T., Halevi, S., Eshel, M., & Treinin, M. (2001) Characterization of the deg-3/des-2 receptor: a nicotinic acetylcholine receptor that mutates to cause neuronal degeneration. Mol.Cell Neurosci. 17: 589-599.

Zheng, Y., Hirschberg, B., Yuan, J., Wang, A. P., Hunt, D. C., Ludmerer, S. W., Schmatz, D. M., & Cully, D. F. (2002) Identification of two novel *Drosophila melanogaster* histamine-gated chloride channel subunits expressed in the eye. J.Biol.Chem. 277: 2000-2005.